7th JOINT STUDENT SEMINAR on CIVIL INFRASTRUCTURE

August 19-20, 2015

7th Joint Student Seminar on Civil Infrastructure

19-20 August 2015
Bangkok, Thailand

Co-Organized by

School of Engineering and Technology,
Asian Institute of Technology (AIT), Thailand

International Center for Urban Safety Engineering
(ICUS)
Institute of Industrial Science
The University of Tokyo, Japan

Sirindhorn International Institute of Technology (SIIT),
Thammasat University

Chulalongkorn University

Myongji University, Korea

and

Hanyang University, Korea

Edited by

Dr. Yudai Honma, Dr. Kunnawee Kanipong,
Dr. Hyunmyung Kim and Dr. Withit Pansuk

Organization Teams

Prof. Worsak Kanok-Nukulchai (AIT, Thailand)
Dr. Pennung Warnitchai (AIT, Thailand)
Dr. Kunnawee Kanipong (AIT, Thailand)
Dr. Pakawat Sancharoen (SIIT, Thailand)
Assoc. Prof. Thavivongse Sriburi (Chulalongkorn U, Thailand)
Dr. Withit Pansuk (Chulalongkorn U, Thailand)

Dr. Hyunmyung Kim (Myongji U, Korea)
Dr. Wonho Suh (Hanyang Univ., Korea)

Prof. Kimiro Meguro (UT, Japan)
Dr, Yudai Honma (UT, Japan)
Dr. Wataru Takeuchi (UT, Japan)
Dr. Akiyuki Kawasaki (UT, Japan)

7th JOINT STUDENT SEMINAR ON CIVIL INFRASTRUCTURE

August 2015

PREFACE

In this era of rapid globalization, having an international sense and broad human resource network is essential. In particular, building up a good relationship with various communities during young school days will be of advantage in the future. To give such an opportunity to students from Asian countries, we held the 1st, 2nd 3rd, 4th, 5th, 6th and joint student seminar in July 2008, July 2009, July 2010, August 2011, August 2012, and August 2013 respectively, and following this success the "7th Joint Student Seminar on Civil Infrastructures" was held on 19 August, 2015.

The objectives of this seminar are:

1) to experience the international seminar,
2) to improve the presentation skill,
3) to share the research information and friendships.

The number of participants was 40, consisting of 3 faculties and 15 students from Myong Ji University, Hanyang University, Chulalongkorn University, Thammasat University (SIIT), Srinakharinwirot University and The University of Tokyo.

We had a presentation session, having 3 faculties (Chulalongkorn University and The University of Tokyo) lectures and 15 students' presentation. The topics covered wide range areas of civil engineering and every student did their best in his/her presentation. During the seminar, students and faculties had lively exchange of views beyond their specialty, culture and nationality. At the end of the seminar, excellent presentation awards were given to the following 3 students.

1. Mr. Yuto Tokumitsu from University of Tokyo, Japan
2. Mr. Yuki Munemasa from University of Tokyo, Japan
3. Mr. Tanakorn Sritarapipat from University of Tokyo, Japan

Although the seminar was quite successful and fruitful: this seminar gave not only knowledge and information but also a lot of other stimuli to the students. We hope to continue to hold this kind of interchange activities in the coming years.

Finally, we would like to express our sincere gratitude for those who kindly supported and contributed to the success of this seminar.

YUDAI HONMA, KUNNAWEE KANIPONG,
HYUNMYUNG KIM AND WITHIT PANSUK

Table of Contents

Page

Opening Session

SECTION 1 Invited Lectures

Introduction to mathematical analysis for next-generation vehicle 1
Yudai Honma

Water leak prevention at connections of precast concrete panels with butyl rubber 27
Withit Pansuk

Near-real time meteorological drought monitoring and early warning system for croplands in Asia 55
Wataru Takeuchi

SECTION 2 Student Presentations

Building classification in urban area in Yangon, Myanmar using stereo high resolution images and night time light data 81
Tanakorn Sritarapipat

Experiment and simulation study on flexural behavior of reinforced concrete slab before and after fire 91
Nguyen Thi Cao

The key index for rational bridge maintenance by municipalities in Japan 101
Riko SAKATA

Effect of free LIME content on mechanical properties of cement-fly ash mixtures 109
Adnan Nawaz

SECTION 3 Student Presentations

The relationship between the rainfall intensity and the subway passenger ridership in the Seoul metropolitan subway system 117
Kyoung-seon Park

Factors affecting the severity of motorcycles accidents and casualties in Thailand by using probit and logit model 125
Santosh Baral

Optimum assignment of housings and jobs with constrained capacity considering discomfort and travel costs 143
Yuki Munemasa

Factors influencing red light running behavior: a study of socio-economic characteristics and geometry of intersections 155
Auearree Jensupakarn

The optimum traffic volume survey locations for the travel demand analysis in Korea 173
Seong-min Kang

Site selection of potential railway route for supporting dawei deep-sea port Case study : Tambon Ban Kao Amphoe Mueang of Kanchanaburi province 181
Rattanawadee Dutsadeesuntornsakun

Numerical evaluation of road disconnection risk focusing on road collapsing after a large earthquake in Chigasaki city, Kanagawa 189
Yuto Tokumitsu

Image processing techniques for vehicle and pedestrian safety evaluation 199
Jinwoo Park

SECTION 4 Student Presentations

Ageing effect induced by particle movement 205
Koji Tanaka

An analysis of network throughputs for different origin-destination patterns 213
Koki Satsukawa

Water retainability and basic properties of coal bottom ash used as fine aggregate replacing material in concrete 225
Noulananh Lathsoulin

Experimental study on in-plane and out-of-plane behavior of masonry wallettes retrofitted with special fiber reinforced paint 233
Kenjiro Yamamoto

Knowledge based IT evacuation facility management system "COCOA" 241
Satoshi Takatsu

SECTION 5 Student Presentations

Report from Student Participation on 7th Joint Student Seminar on Civil Infrastructure 253
Koki Satsukawa, Satoshi Takatsu, Kenjiro Yamamoto, Riko Sakata, Yuto Tokumitsu, Yuki Munemasa, Tanakorn Sritarapipat, Koji Tanaka, Cao Nguyên Thi, Noulananh Lathsolulin, Jinwoo Park

Seminar Venue

Committee (Dr. Wonho Suh)

Dr. Yudai Honma

Dr. Withit Pansuk

Dr. Wataru Takeuchi

Mr. Tanakorn Sritarapipat

Mr. Nguyen Thi Cao

Ms. Riko Sakata

Mr. Adnan Nawaz

Ms. Kyoung Seon Park

Mr. Yuki Munemasa

Mr. Seong Min Kang

Ms. Rattanawadee Dutsadeesuntornsakun

Mr. Yuto Tokumitsu

Mr. Jinwoo Park

Mr. Koji Tanaka

Mr. Koki Satsukawa

Mr. Noulananh Lathsoulin

Mr. Kenjiro Yamamoto

Mr. Satoshi Takatsu

Closing ceremony (Dr. Hyunmyung Kim)

During Seminar

During Welcome Dinner

Excellence Presenter Mr. Yuto Tokumitsu *Excellence Presenter Mr. Tanakorn Sritarapipat*

Excellence Presenter Mr. Yuki Munemasa

Welcome Dinner & Close seminar

Seminar: Group Photo at Chulalongkorn University

Invited Lectures

INTRODUCTION TO MATHEMATICAL ANALYSIS FOR NEXT-GENERATION VEHICLE

Yudai Honma
The University of Tokyo, Japan
yudai@iis.u-tokyo.ac.jp

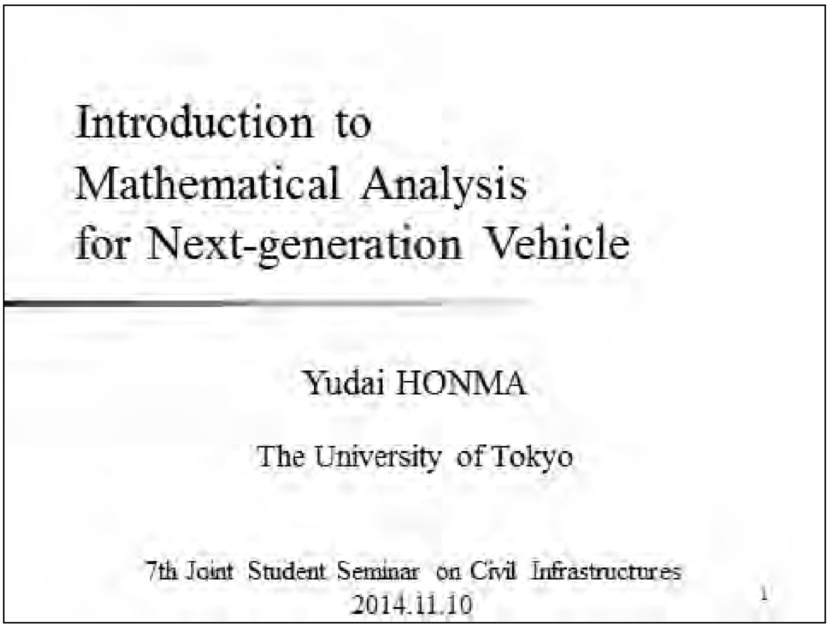

Introduction to
Mathematical Analysis
for Next-generation Vehicle

Yudai HONMA

The University of Tokyo

7th Joint Student Seminar on Civil Infrastructures
2014.11.10

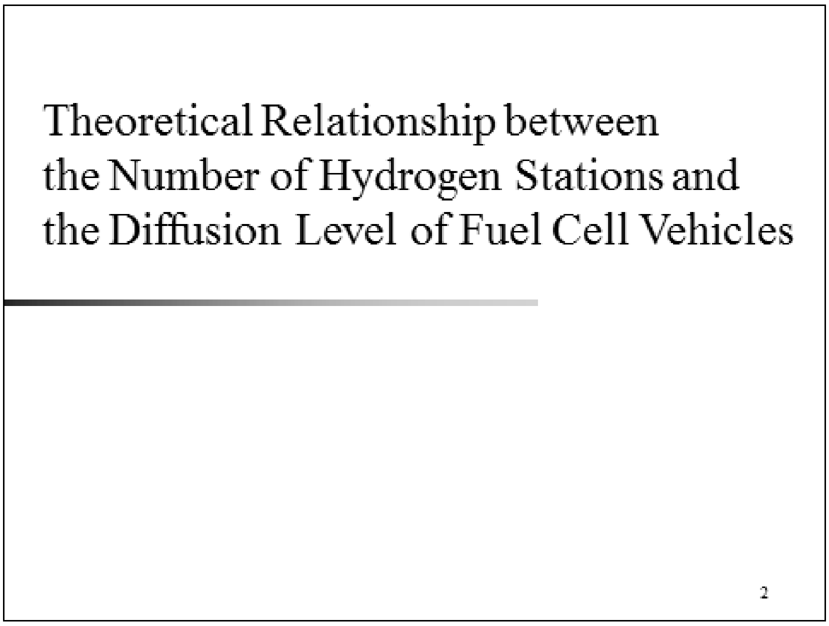

Theoretical Relationship between
the Number of Hydrogen Stations and
the Diffusion Level of Fuel Cell Vehicles

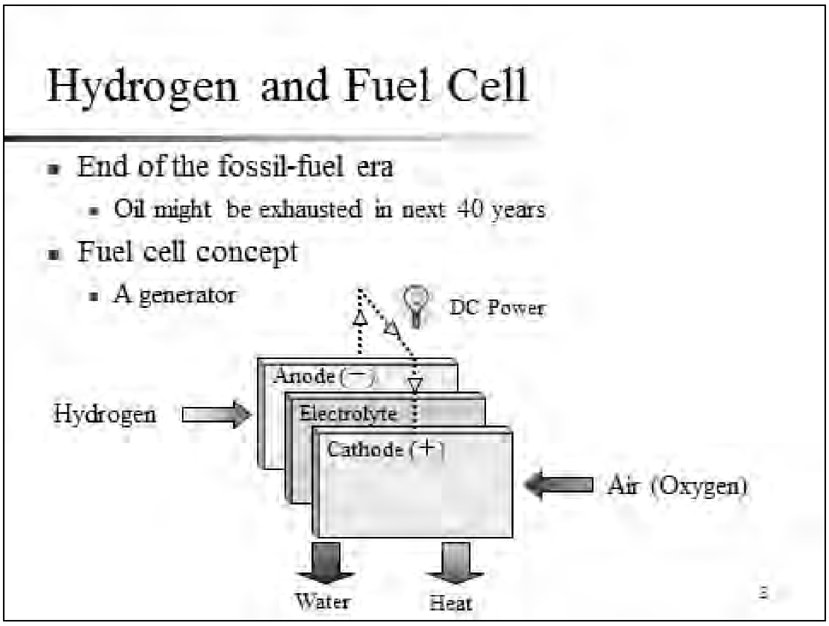

Hydrogen and Fuel Cell

- End of the fossil-fuel era
    - Oil might be exhausted in next 40 years
- Fuel cell concept
    - A generator

DC Power
Anode (−)
Electrolyte
Cathode (+)
Hydrogen
Air (Oxygen)
Water
Heat

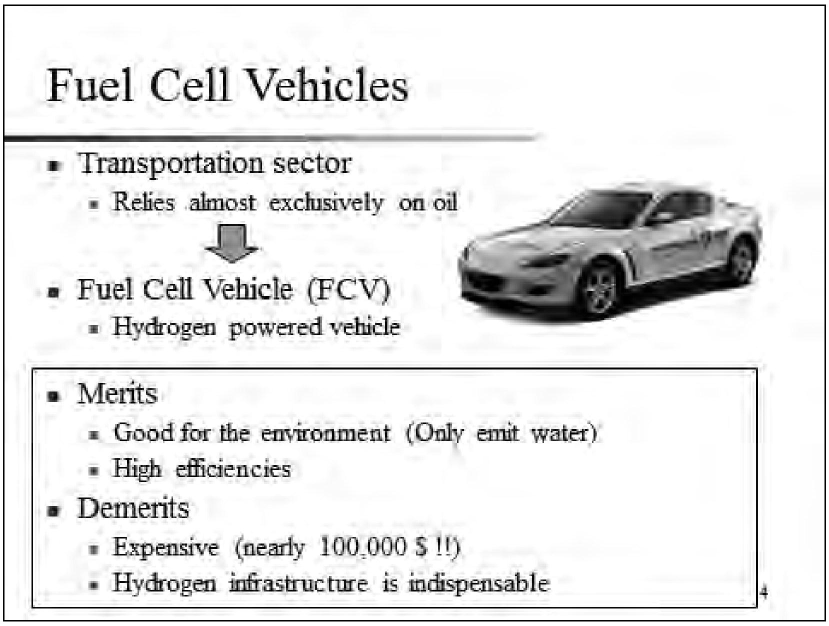

Fuel Cell Vehicles

- Transportation sector
    - Relies almost exclusively on oil
- Fuel Cell Vehicle (FCV)
    - Hydrogen powered vehicle

- Merits
    - Good for the environment (Only emit water)
    - High efficiencies
- Demerits
    - Expensive (nearly 100,000 $!!)
    - Hydrogen infrastructure is indispensable

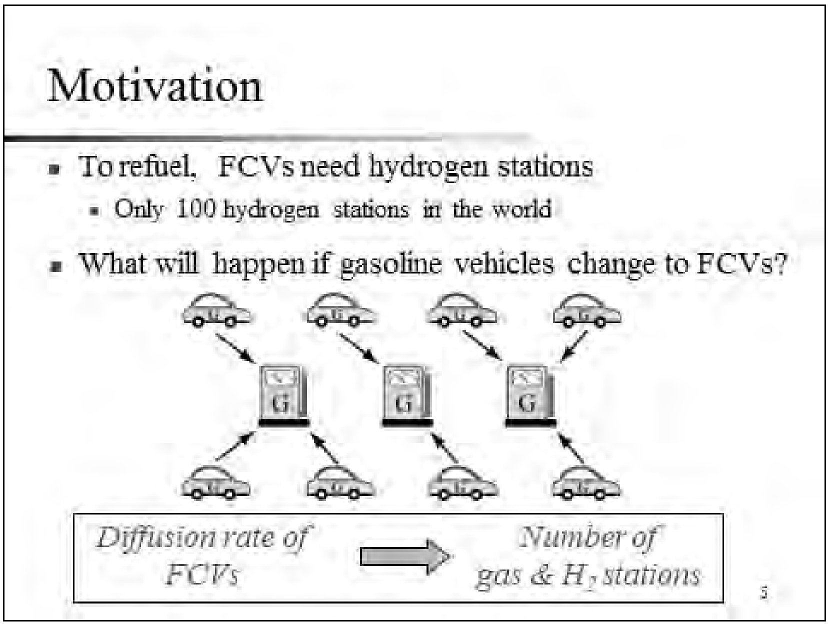

Motivation

- To refuel, FCVs need hydrogen stations
  - Only 100 hydrogen stations in the world
- What will happen if gasoline vehicles change to FCVs?

Diffusion rate of FCVs → *Number of gas & H_2 stations*

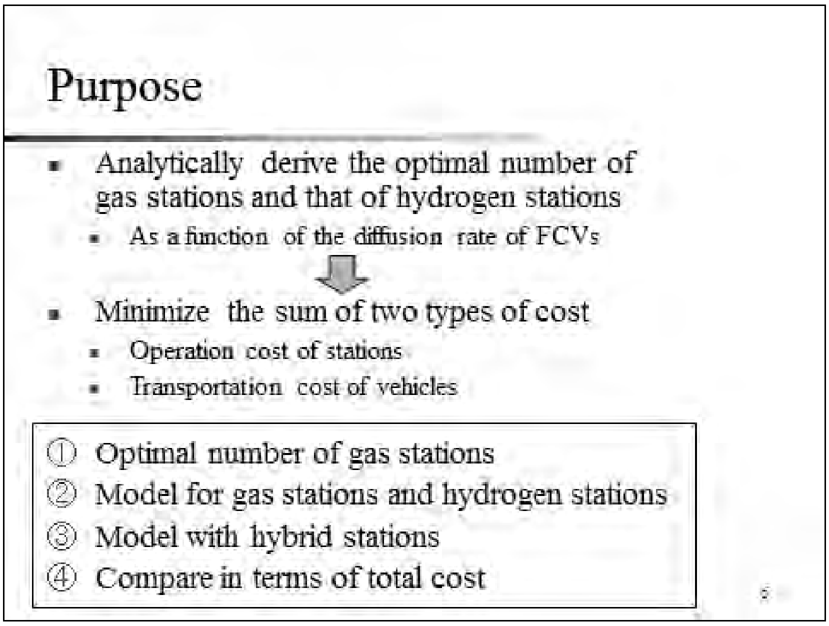

Purpose

- Analytically derive the optimal number of gas stations and that of hydrogen stations
  - As a function of the diffusion rate of FCVs
- Minimize the sum of two types of cost
  - Operation cost of stations
  - Transportation cost of vehicles

① Optimal number of gas stations
② Model for gas stations and hydrogen stations
③ Model with hybrid stations
④ Compare in terms of total cost

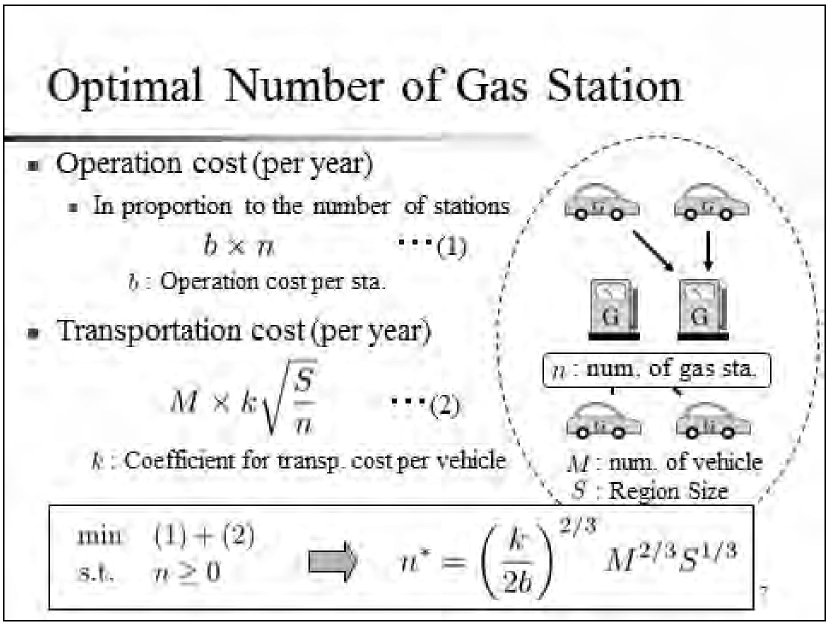

Optimal Number of Gas Station

- Operation cost (per year)
  - In proportion to the number of stations

$$b \times n \quad \cdots(1)$$

b : Operation cost per sta.

- Transportation cost (per year)

$$M \times k\sqrt{\frac{S}{n}} \quad \cdots(2)$$

k : Coefficient for transp. cost per vehicle

n : num. of gas sta.

M : num. of vehicle
S : Region Size

$$\begin{array}{ll} \min & (1)+(2) \\ \text{s.t.} & n \geq 0 \end{array} \Rightarrow n^* = \left(\frac{k}{2b}\right)^{2/3} M^{2/3} S^{1/3}$$

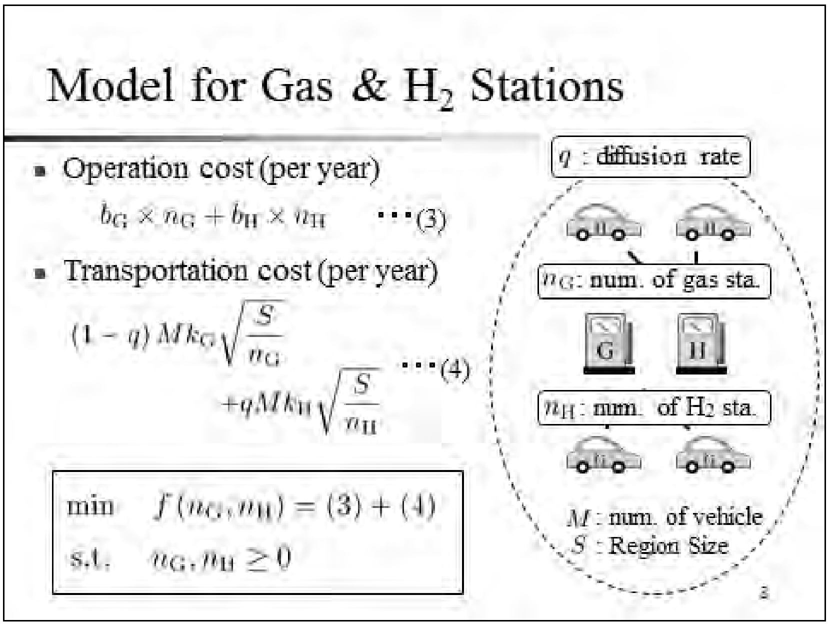

Model for Gas & H_2 Stations

- Operation cost (per year)

$$b_G \times n_G + b_H \times n_H \quad \cdots(3)$$

- Transportation cost (per year)

$$(1-q)Mk_G\sqrt{\frac{S}{n_G}} + qMk_H\sqrt{\frac{S}{n_H}} \quad \cdots(4)$$

$$\begin{array}{ll} \min & f(n_G, n_H) = (3)+(4) \\ \text{s.t.} & n_G, n_H \geq 0 \end{array}$$

q : diffusion rate

n_G: num. of gas sta.

n_H : mm. of H_2 sta.

M : num. of vehicle
S : Region Size

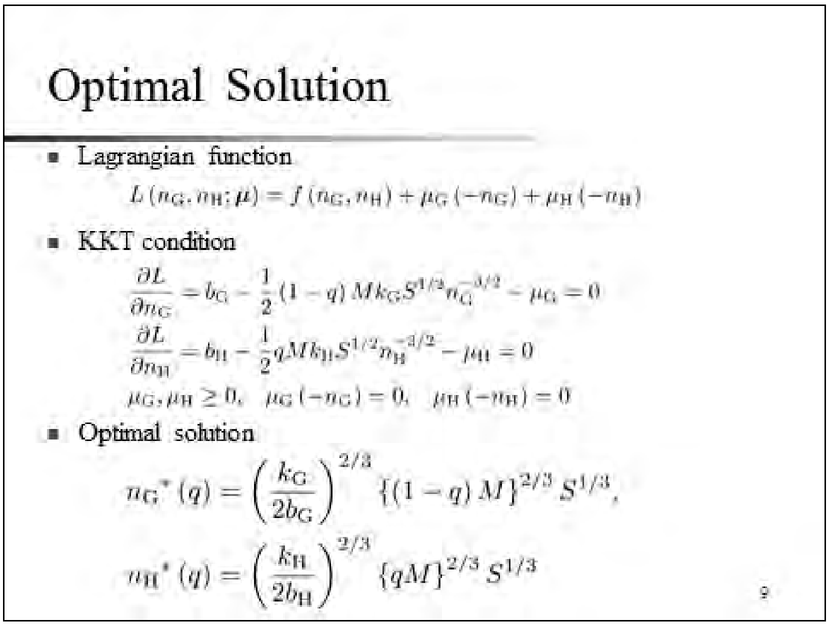

Optimal Solution

- Lagrangian function

$$L(n_G, n_H; \mu) = f(n_G, n_H) + \mu_G(-n_G) + \mu_H(-n_H)$$

- KKT condition

$$\frac{\partial L}{\partial n_G} = b_G - \frac{1}{2}(1-q)Mk_G S^{1/2} n_G^{-3/2} - \mu_G = 0$$

$$\frac{\partial L}{\partial n_H} = b_H - \frac{1}{2}qMk_H S^{1/2} n_H^{-3/2} - \mu_H = 0$$

$$\mu_G, \mu_H \geq 0, \quad \mu_G(-n_G) = 0, \quad \mu_H(-n_H) = 0$$

- Optimal solution

$$n_G^*(q) = \left(\frac{k_G}{2b_G}\right)^{2/3} \{(1-q)M\}^{2/3} S^{1/3},$$

$$n_H^*(q) = \left(\frac{k_H}{2b_H}\right)^{2/3} \{qM\}^{2/3} S^{1/3}$$

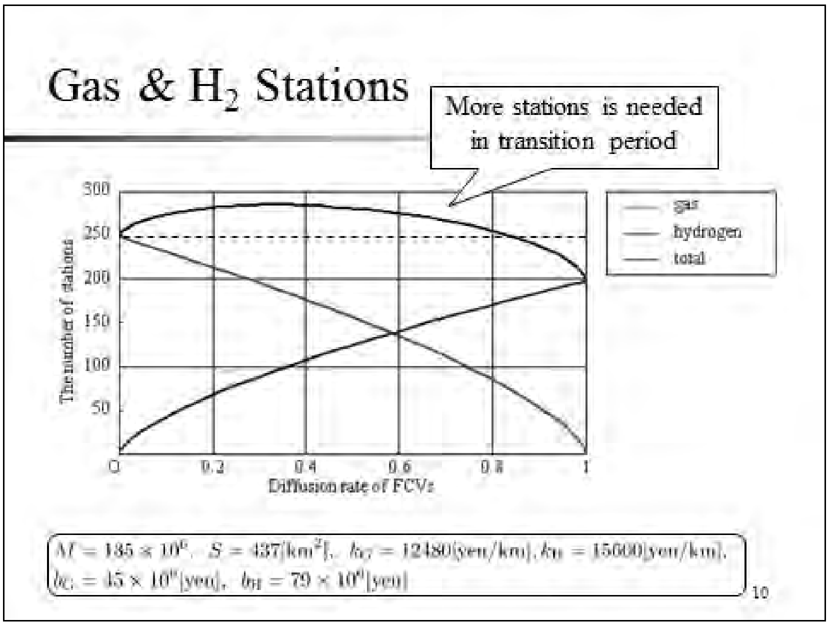

Gas & H_2 Stations

More stations is needed in transition period

$M = 135 \times 10^6$, $S = 437[\mathrm{km}^2]$, $k_G = 12480[\mathrm{yen/km}]$, $k_H = 15000[\mathrm{yen/km}]$,
$b_G = 45 \times 10^6[\mathrm{yen}]$, $b_H = 79 \times 10^6[\mathrm{yen}]$

Constraint of Total Number

- Total number of stations is less than
  (i) optimal num. of gas sta. before transition $n_G^*(0)$
  or
  (ii) optimal num. of H_2 sta. after transition $n_H^*(1)$
  - Site, Authorization, Replacing, etc.

⇩

$$\begin{aligned} \min \quad & f(n_G, n_H) \\ \text{s.t.} \quad & n_G, n_H \geq 0 \\ & n_G + n_H \leq N_{\text{high}} \\ & N_{\text{high}} = \max\left[n_G^*(0), n_H^*(1)\right] \end{aligned}$$

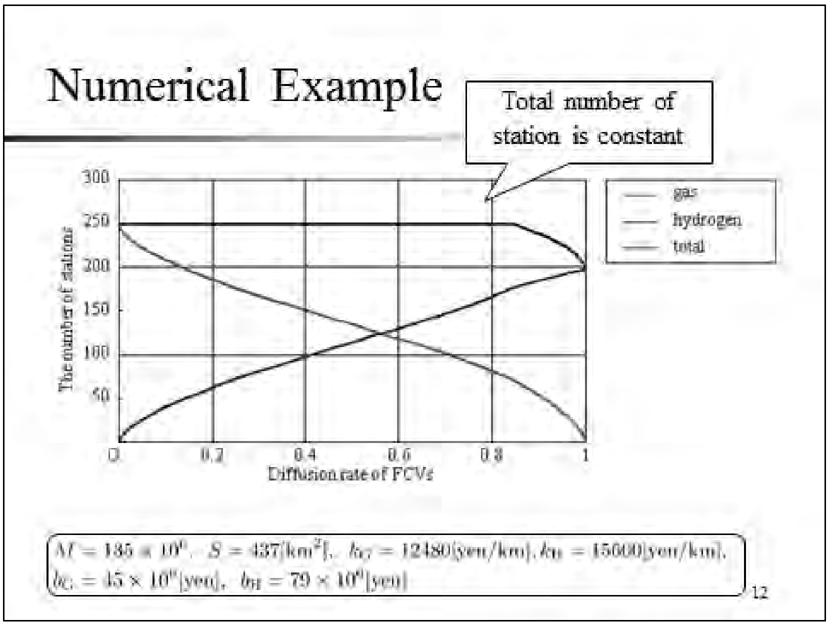

Numerical Example

Total number of station is constant

$M = 135 \times 10^6$, $S = 437[\text{km}^2]$, $k_G = 12480[\text{yen/km}]$, $k_H = 15000[\text{yen/km}]$,
$b_G = 45 \times 10^6[\text{yen}]$, $b_H = 79 \times 10^6[\text{yen}]$

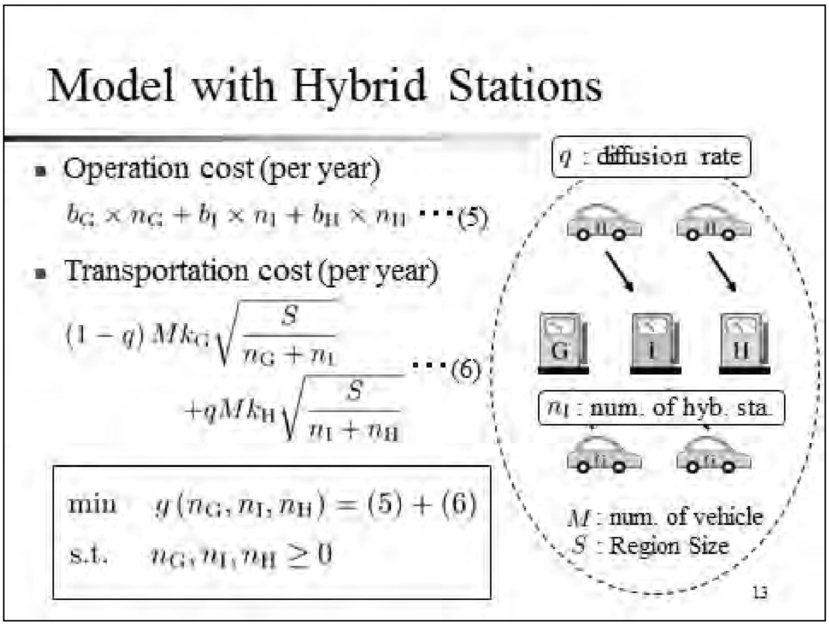

Model with Hybrid Stations

- Operation cost (per year)

$$b_{\mathrm{G}} \times n_{\mathrm{G}} + b_{\mathrm{I}} \times n_{\mathrm{I}} + b_{\mathrm{H}} \times n_{\mathrm{H}} \cdots (5)$$

- Transportation cost (per year)

$$(1-q)\, M k_{\mathrm{G}} \sqrt{\frac{S}{n_{\mathrm{G}} + n_{\mathrm{I}}}} + q M k_{\mathrm{H}} \sqrt{\frac{S}{n_{\mathrm{I}} + n_{\mathrm{H}}}} \cdots (6)$$

$$\begin{array}{ll} \min & g\left(n_{\mathrm{G}}, n_{\mathrm{I}}, n_{\mathrm{H}}\right) = (5) + (6) \\ \text{s.t.} & n_{\mathrm{G}}, n_{\mathrm{I}}, n_{\mathrm{H}} \geq 0 \end{array}$$

q : diffusion rate

n_{I} : num. of hyb. sta.

M : num. of vehicle

S : Region Size

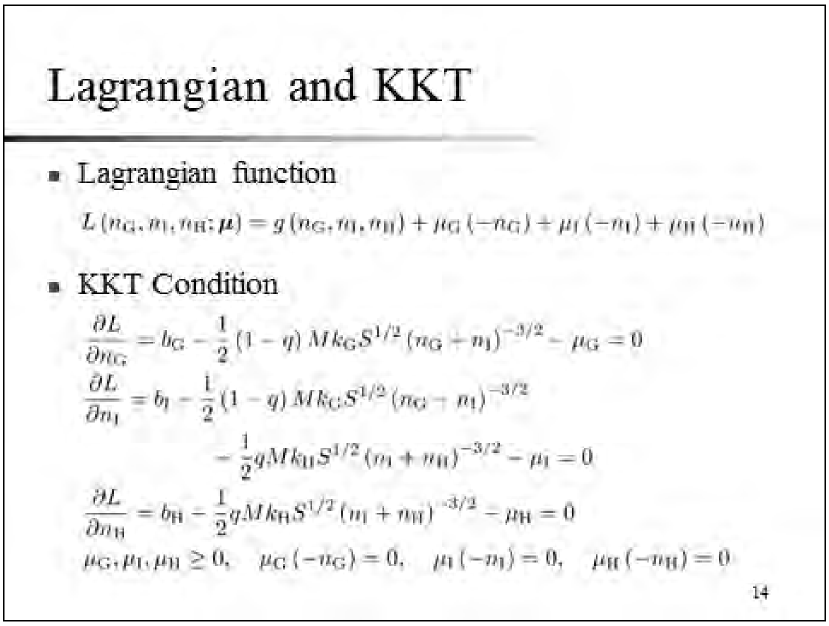

Lagrangian and KKT

- Lagrangian function

$$L\left(n_{\mathrm{G}}, n_{\mathrm{I}}, n_{\mathrm{H}}; \boldsymbol{\mu}\right) = g\left(n_{\mathrm{G}}, n_{\mathrm{I}}, n_{\mathrm{H}}\right) + \mu_{\mathrm{G}}\left(-n_{\mathrm{G}}\right) + \mu_{\mathrm{I}}\left(-n_{\mathrm{I}}\right) + \mu_{\mathrm{H}}\left(-n_{\mathrm{H}}\right)$$

- KKT Condition

$$\frac{\partial L}{\partial n_{\mathrm{G}}} = b_{\mathrm{G}} - \frac{1}{2}(1-q)\, M k_{\mathrm{G}} S^{1/2} \left(n_{\mathrm{G}} + n_{\mathrm{I}}\right)^{-3/2} - \mu_{\mathrm{G}} = 0$$

$$\frac{\partial L}{\partial n_{\mathrm{I}}} = b_{\mathrm{I}} - \frac{1}{2}(1-q)\, M k_{\mathrm{G}} S^{1/2} \left(n_{\mathrm{G}} + n_{\mathrm{I}}\right)^{-3/2} - \frac{1}{2} q M k_{\mathrm{H}} S^{1/2} \left(n_{\mathrm{I}} + n_{\mathrm{H}}\right)^{-3/2} - \mu_{\mathrm{I}} = 0$$

$$\frac{\partial L}{\partial n_{\mathrm{H}}} = b_{\mathrm{H}} - \frac{1}{2} q M k_{\mathrm{H}} S^{1/2} \left(n_{\mathrm{I}} + n_{\mathrm{H}}\right)^{-3/2} - \mu_{\mathrm{H}} = 0$$

$$\mu_{\mathrm{G}}, \mu_{\mathrm{I}}, \mu_{\mathrm{H}} \geq 0, \quad \mu_{\mathrm{G}}\left(-n_{\mathrm{G}}\right) = 0, \quad \mu_{\mathrm{I}}\left(-n_{\mathrm{I}}\right) = 0, \quad \mu_{\mathrm{H}}\left(-n_{\mathrm{H}}\right) = 0$$

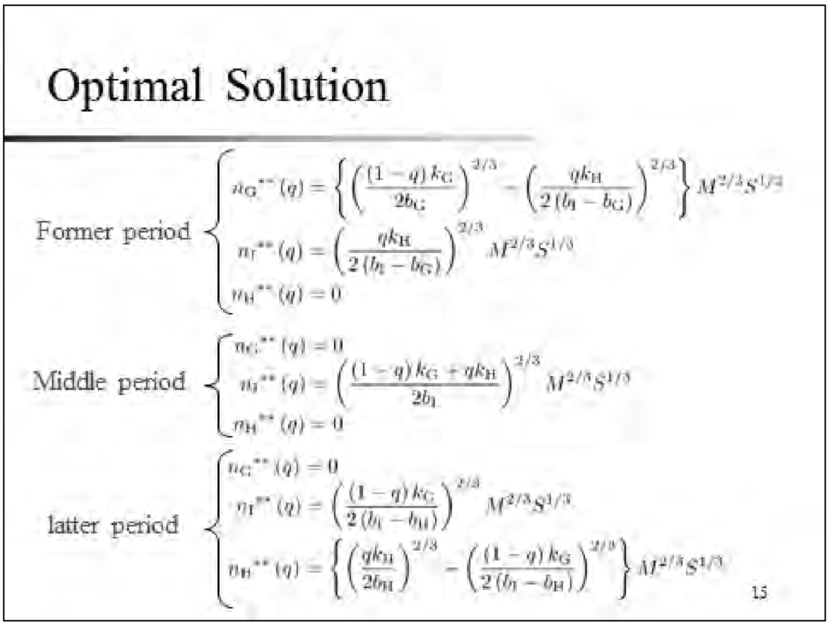

Optimal Solution

Former period
$$\begin{cases} n_{\mathrm{G}}^{**}(q) = \left\{ \left(\dfrac{(1-q)\,k_{\mathrm{G}}}{2b_{\mathrm{G}}} \right)^{2/3} - \left(\dfrac{qk_{\mathrm{H}}}{2\,(b_{\mathrm{I}} - b_{\mathrm{G}})} \right)^{2/3} \right\} M^{2/3} S^{1/3} \\ n_{\mathrm{I}}^{**}(q) = \left(\dfrac{qk_{\mathrm{H}}}{2\,(b_{\mathrm{I}} - b_{\mathrm{G}})} \right)^{2/3} M^{2/3} S^{1/3} \\ n_{\mathrm{H}}^{**}(q) = 0 \end{cases}$$

Middle period
$$\begin{cases} n_{\mathrm{G}}^{**}(q) = 0 \\ n_{\mathrm{I}}^{**}(q) = \left(\dfrac{(1-q)\,k_{\mathrm{G}} + qk_{\mathrm{H}}}{2b_{\mathrm{I}}} \right)^{2/3} M^{2/3} S^{1/3} \\ n_{\mathrm{H}}^{**}(q) = 0 \end{cases}$$

latter period
$$\begin{cases} n_{\mathrm{G}}^{**}(q) = 0 \\ n_{\mathrm{I}}^{**}(q) = \left(\dfrac{(1-q)\,k_{\mathrm{G}}}{2\,(b_{\mathrm{I}} - b_{\mathrm{H}})} \right)^{2/3} M^{2/3} S^{1/3} \\ n_{\mathrm{H}}^{**}(q) = \left\{ \left(\dfrac{qk_{\mathrm{H}}}{2b_{\mathrm{H}}} \right)^{2/3} - \left(\dfrac{(1-q)\,k_{\mathrm{G}}}{2\,(b_{\mathrm{I}} - b_{\mathrm{H}})} \right)^{2/3} \right\} M^{2/3} S^{1/3} \end{cases}$$

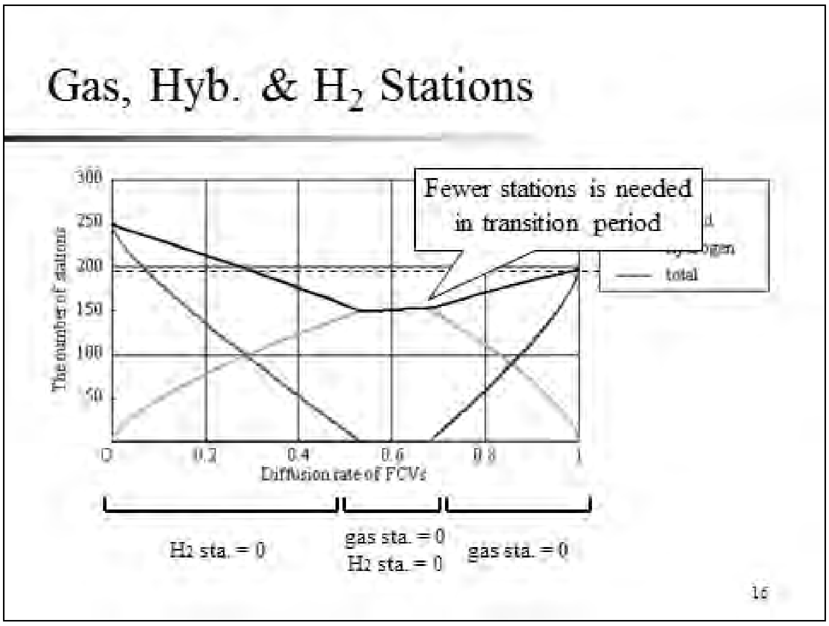

Gas, Hyb. & H_2 Stations

Fewer stations is needed in transition period

H_2 sta. = 0

gas sta. = 0
H_2 sta. = 0

gas sta. = 0

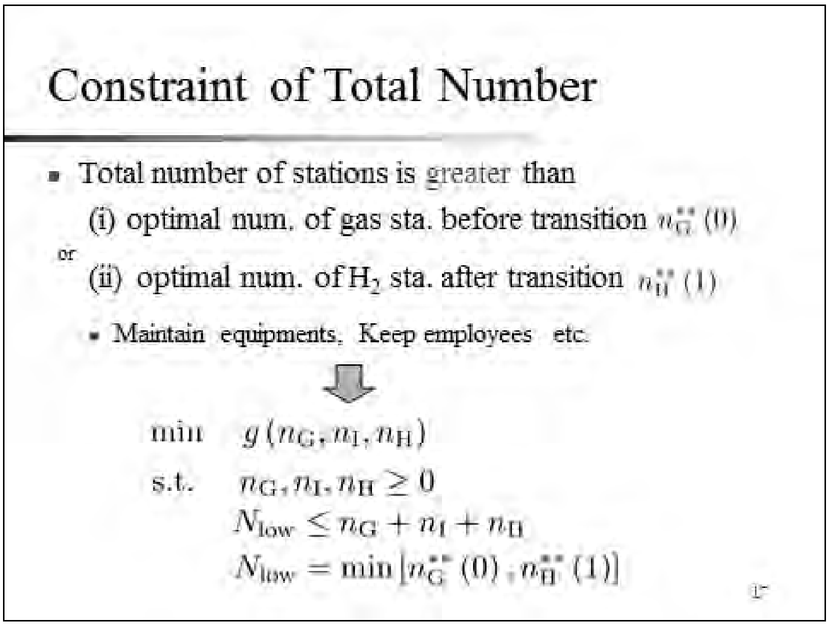

Constraint of Total Number

- Total number of stations is greater than

  (i) optimal num. of gas sta. before transition $n_G^{**}(0)$

  or

  (ii) optimal num. of H_2 sta. after transition $n_H^{**}(1)$

  - Maintain equipments, Keep employees etc.

$$\begin{aligned} \min \quad & g(n_G, n_I, n_H) \\ \text{s.t.} \quad & n_G, n_I, n_H \geq 0 \\ & N_{\text{low}} \leq n_G + n_I + n_H \\ & N_{\text{low}} = \min\left[n_G^{**}(0), n_H^{**}(1)\right] \end{aligned}$$

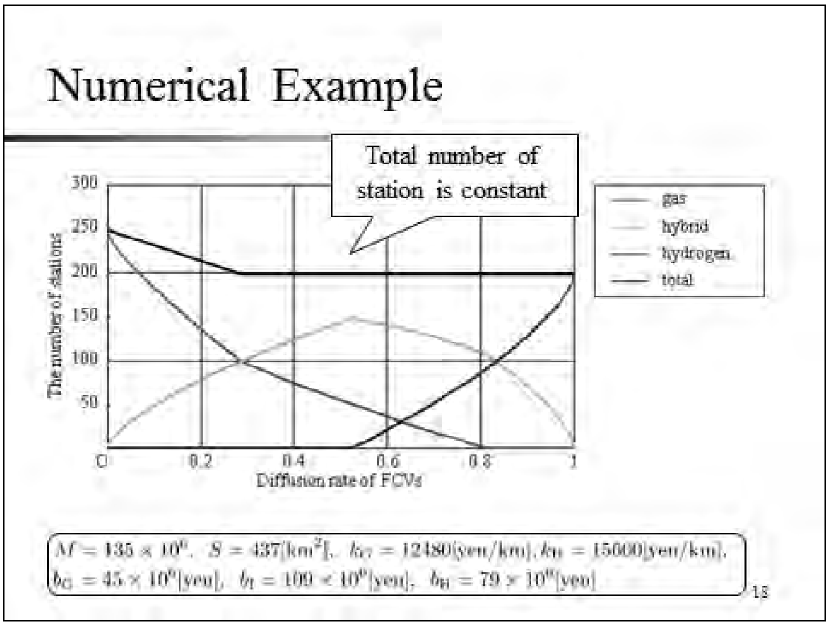

Numerical Example

Total number of station is constant

$M = 135 \times 10^6$, $S = 437[\mathrm{km}^2]$, $k_G = 12480[\mathrm{yen/km}]$, $k_H = 15000[\mathrm{yen/km}]$,
$b_G = 45 \times 10^6[\mathrm{yen}]$, $b_I = 109 \times 10^6[\mathrm{yen}]$, $b_H = 79 \times 10^6[\mathrm{yen}]$

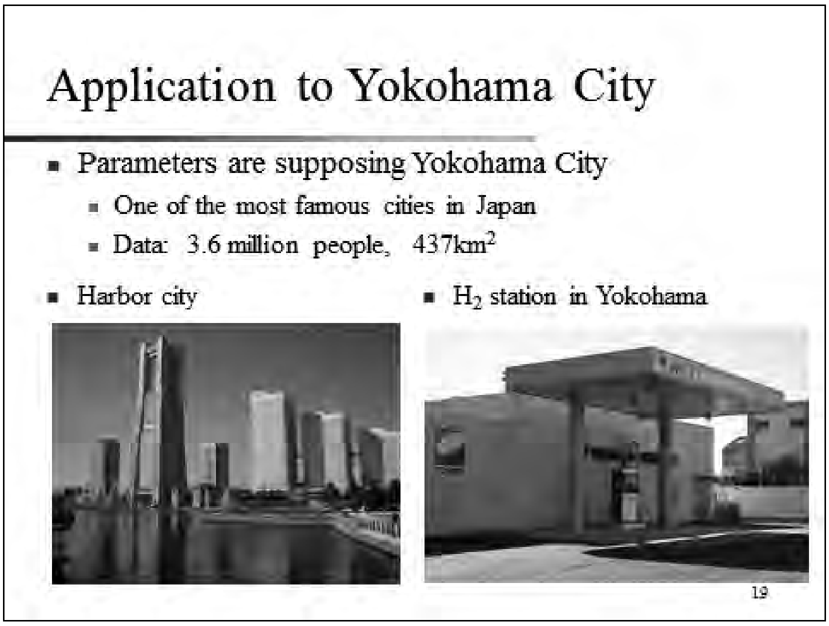

Application to Yokohama City

- Parameters are supposing Yokohama City
  - One of the most famous cities in Japan
  - Data: 3.6 million people, 437km^2
- Harbor city
- H_2 station in Yokohama

19

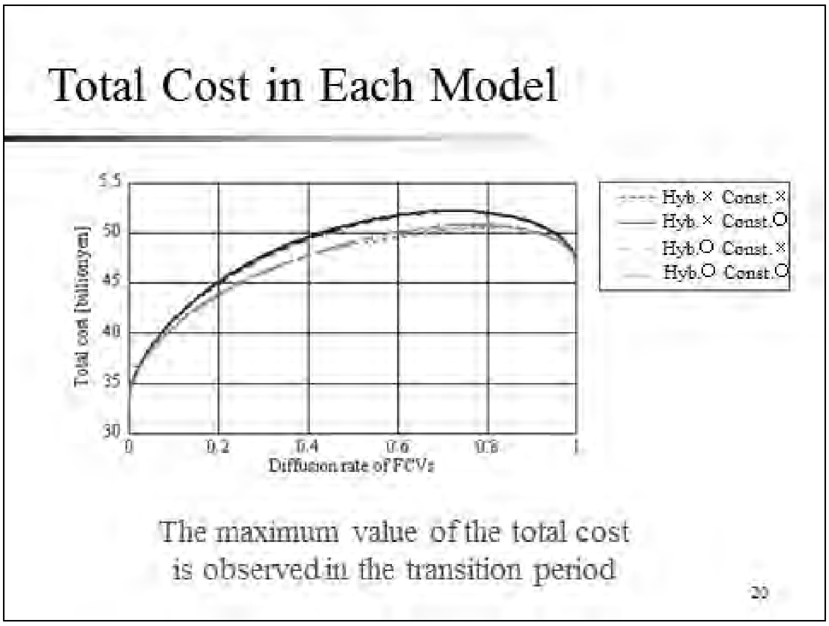

Total Cost in Each Model

The maximum value of the total cost is observed in the transition period

20

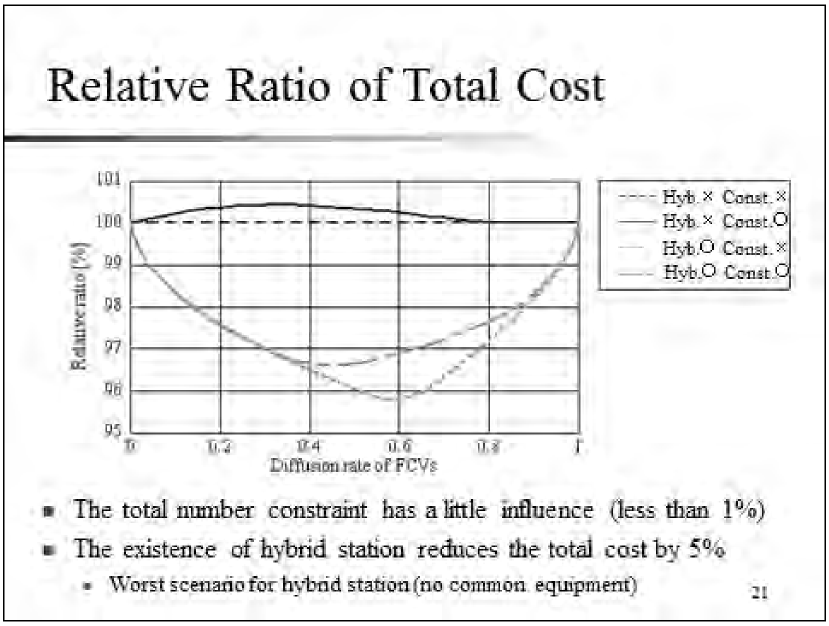

Relative Ratio of Total Cost

- The total number constraint has a little influence (less than 1%)
- The existence of hybrid station reduces the total cost by 5%
  - Worst scenario for hybrid station (no common equipment)

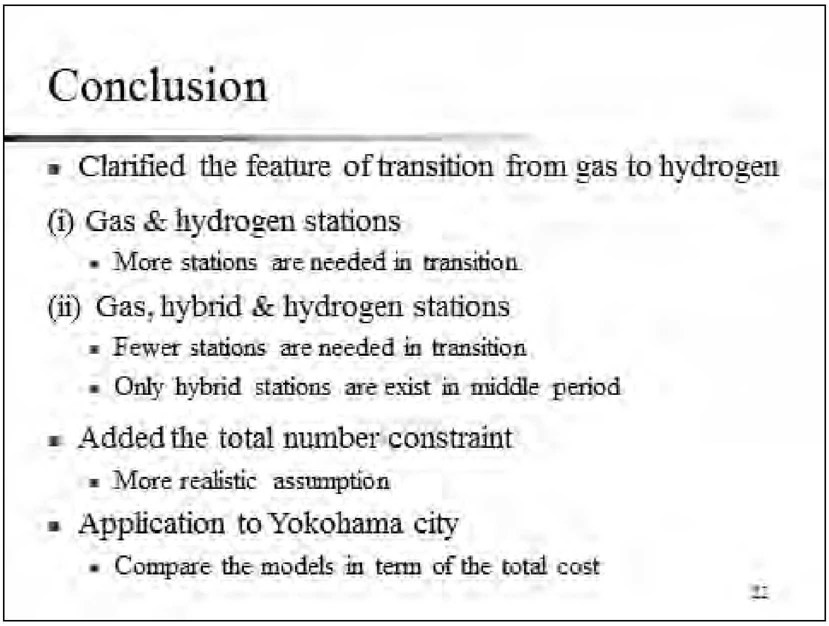

Conclusion

- Clarified the feature of transition from gas to hydrogen

(i) Gas & hydrogen stations
  - More stations are needed in transition

(ii) Gas, hybrid & hydrogen stations
  - Fewer stations are needed in transition
  - Only hybrid stations are exist in middle period

- Added the total number constraint
  - More realistic assumption
- Application to Yokohama city
  - Compare the models in term of the total cost

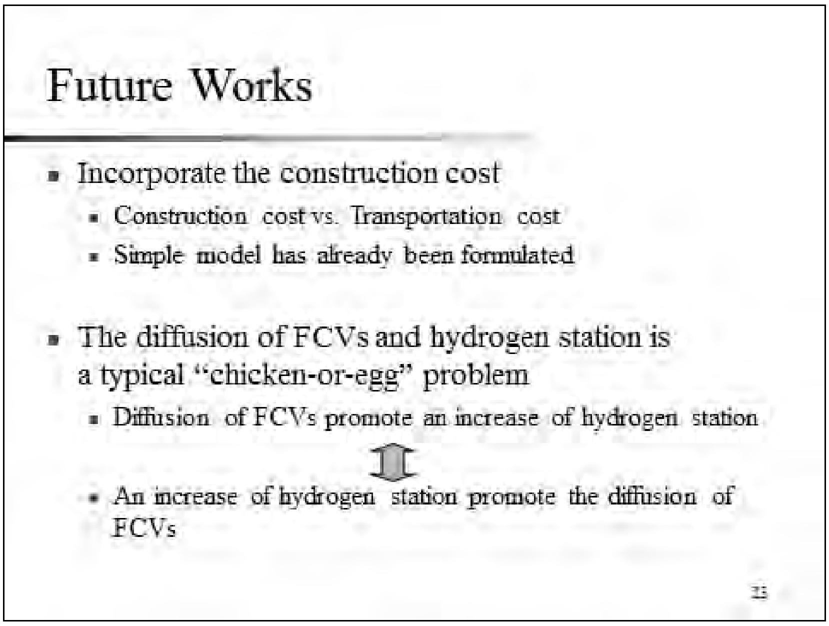

Future Works

- Incorporate the construction cost
  - Construction cost vs. Transportation cost
  - Simple model has already been formulated
- The diffusion of FCVs and hydrogen station is a typical "chicken-or-egg" problem
  - Diffusion of FCVs promote an increase of hydrogen station

⇕

  - An increase of hydrogen station promote the diffusion of FCVs

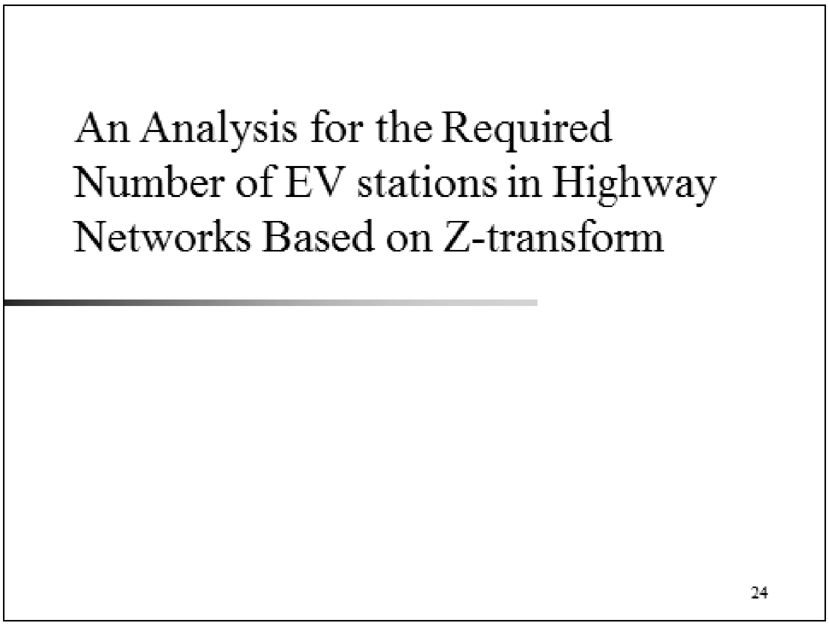

An Analysis for the Required Number of EV stations in Highway Networks Based on Z-transform

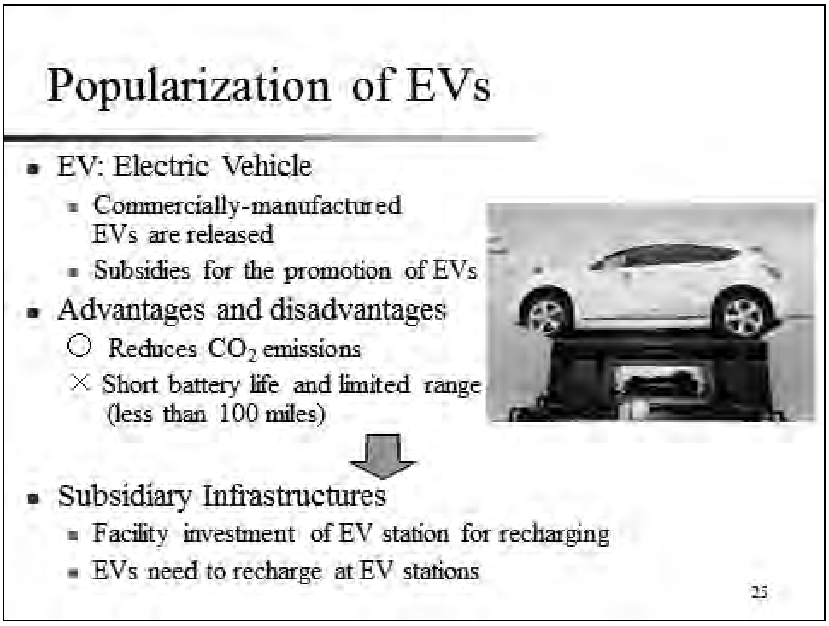

Popularization of EVs

- EV: Electric Vehicle
  - Commercially-manufactured EVs are released
  - Subsidies for the promotion of EVs
- Advantages and disadvantages

  ○ Reduces CO_2 emissions

  × Short battery life and limited range (less than 100 miles)

- Subsidiary Infrastructures
  - Facility investment of EV station for recharging
  - EVs need to recharge at EV stations

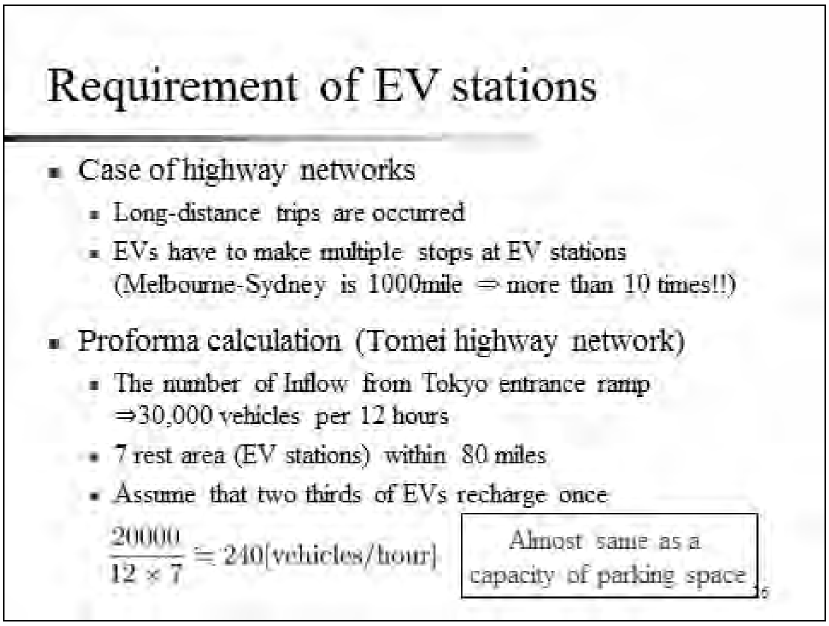

Requirement of EV stations

- Case of highway networks
  - Long-distance trips are occurred
  - EVs have to make multiple stops at EV stations (Melbourne-Sydney is 1000mile ⇒ more than 10 times!!)
- Proforma calculation (Tomei highway network)
  - The number of Inflow from Tokyo entrance ramp ⇒30,000 vehicles per 12 hours
  - 7 rest area (EV stations) within 80 miles
  - Assume that two thirds of EVs recharge once

$$\frac{20000}{12 \times 7} \fallingdotseq 240[\text{vehicles/hour}]$$

Almost same as a capacity of parking space

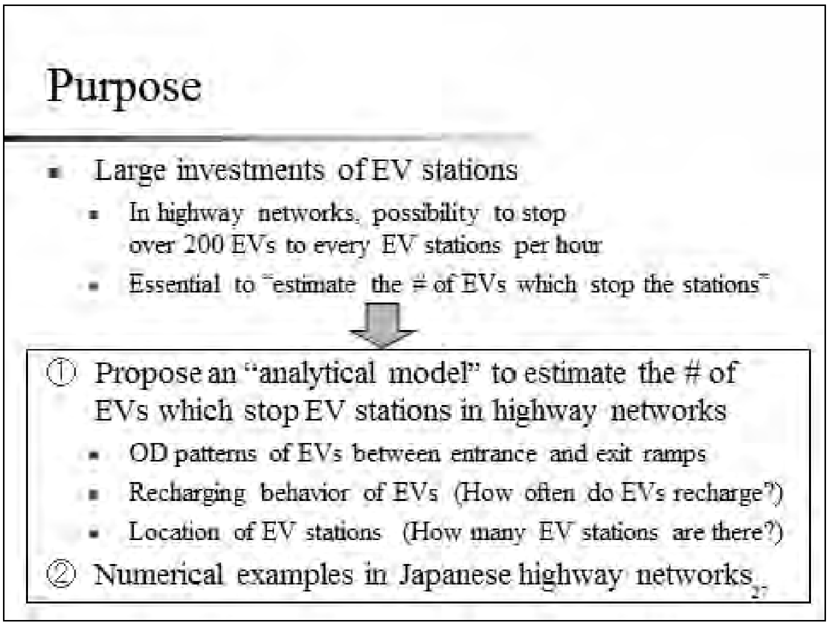

Purpose

- Large investments of EV stations
  - In highway networks, possibility to stop over 200 EVs to every EV stations per hour
  - Essential to "estimate the # of EVs which stop the stations"

① Propose an "analytical model" to estimate the # of EVs which stop EV stations in highway networks
  - OD patterns of EVs between entrance and exit ramps
  - Recharging behavior of EVs (How often do EVs recharge?)
  - Location of EV stations (How many EV stations are there?)

② Numerical examples in Japanese highway networks

27

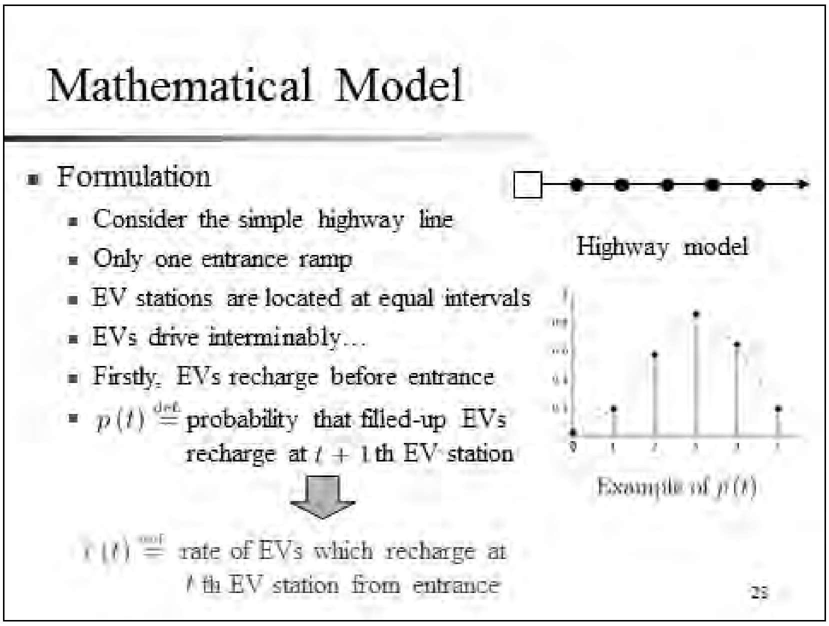

Mathematical Model

- Formulation
  - Consider the simple highway line
  - Only one entrance ramp
  - EV stations are located at equal intervals
  - EVs drive interminably…
  - Firstly, EVs recharge before entrance
  - $p(t) \overset{\text{def}}{=}$ probability that filled-up EVs recharge at $t+1$th EV station

$r(t) \overset{\text{def}}{=}$ rate of EVs which recharge at t th EV station from entrance

Highway model

Example of $p(t)$

28

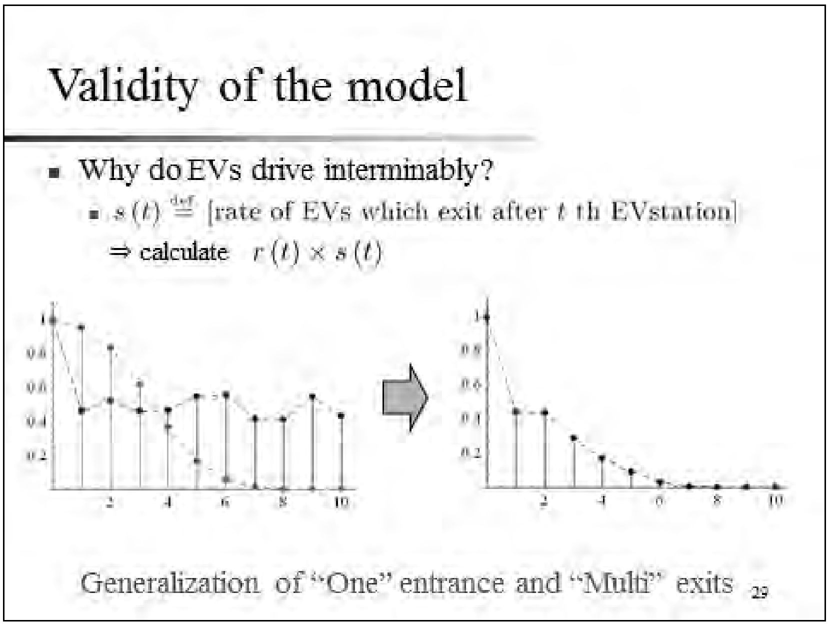

Validity of the model

- Why do EVs drive interminably?
  - $s(t) \overset{\text{def}}{=}$ [rate of EVs which exit after t th EVstation]

    ⇒ calculate $r(t) \times s(t)$

Generalization of "One" entrance and "Multi" exits

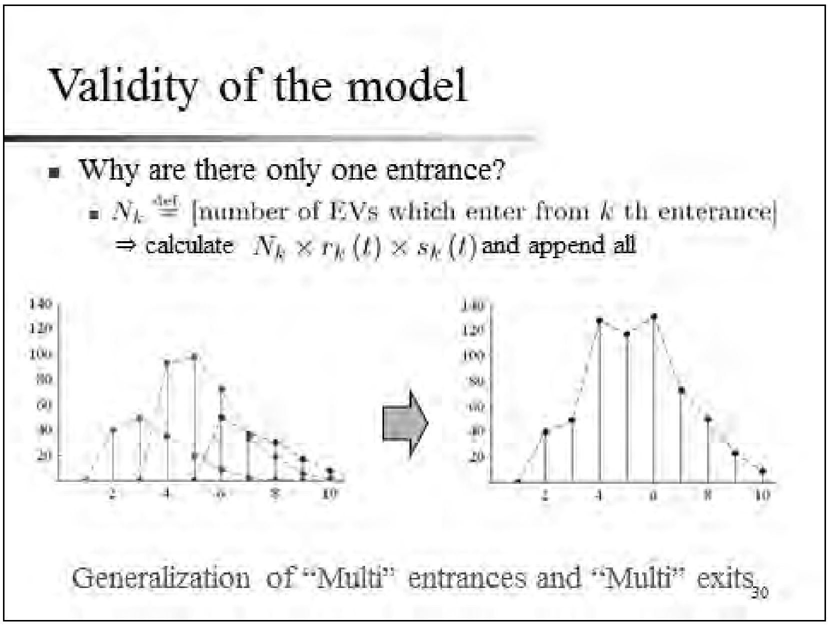

Validity of the model

- Why are there only one entrance?
  - $N_k \overset{\text{def}}{=}$ [number of EVs which enter from k th enterance]

    ⇒ calculate $N_k \times r_k(t) \times s_k(t)$ and append all

Generalization of "Multi" entrances and "Multi" exits

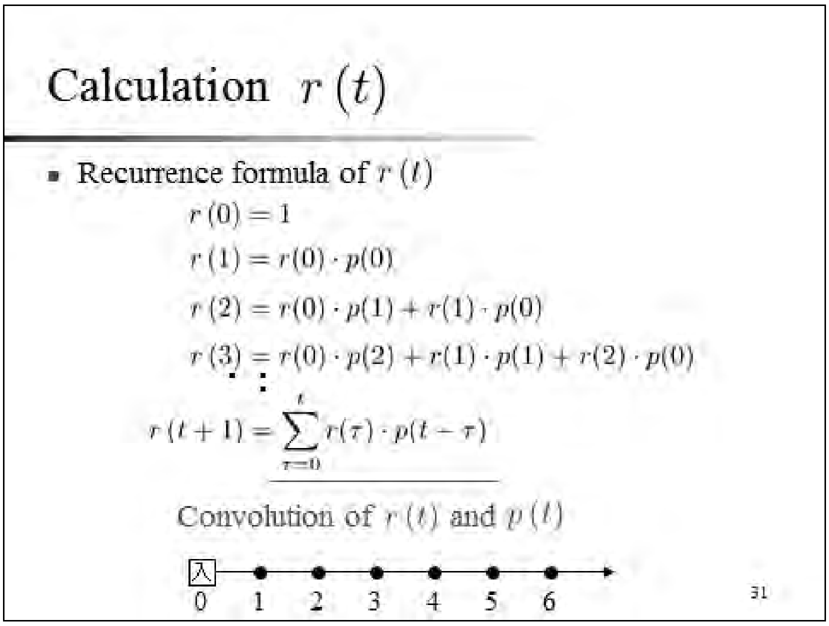

Calculation $r\,(t)$

- Recurrence formula of $r\,(t)$

$$r\,(0) = 1$$
$$r\,(1) = r(0)\cdot p(0)$$
$$r\,(2) = r(0)\cdot p(1) + r(1)\cdot p(0)$$
$$r\,(3) = r(0)\cdot p(2) + r(1)\cdot p(1) + r(2)\cdot p(0)$$
$$\vdots$$
$$r\,(t+1) = \underline{\sum_{\tau=0}^{t} r(\tau)\cdot p(t-\tau)}$$

Convolution of $r\,(t)$ and $p\,(t)$

31

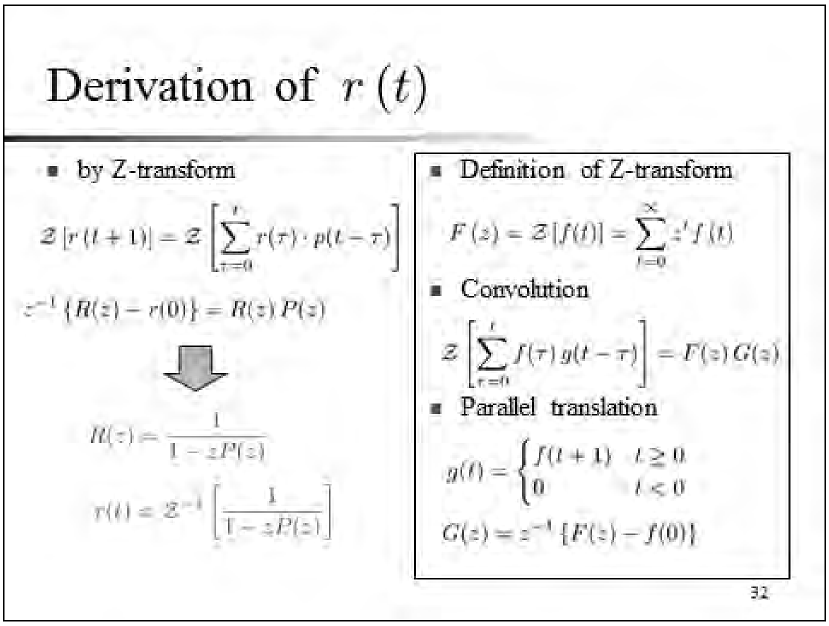

Derivation of $r\,(t)$

- by Z-transform

$$\mathcal{Z}\,[r\,(t+1)] = \mathcal{Z}\left[\sum_{\tau=0}^{t} r(\tau)\cdot p(t-\tau)\right]$$

$$z^{-1}\,\{R(z) - r(0)\} = R(z)\,P(z)$$

$$R(z) = \frac{1}{1 - zP(z)}$$

$$r(t) = \mathcal{Z}^{-1}\left[\frac{1}{1 - zP(z)}\right]$$

- Definition of Z-transform

$$F\,(z) = \mathcal{Z}\,[f(t)] = \sum_{t=0}^{\infty} z^{t} f\,(t)$$

- Convolution

$$\mathcal{Z}\left[\sum_{\tau=0}^{t} f(\tau)\,g(t-\tau)\right] = F(z)\,G(z)$$

- Parallel translation

$$g(t) = \begin{cases} f(t+1) & t \geq 0 \\ 0 & t < 0 \end{cases}$$

$$G(z) = z^{-1}\,\{F(z) - f(0)\}$$

32

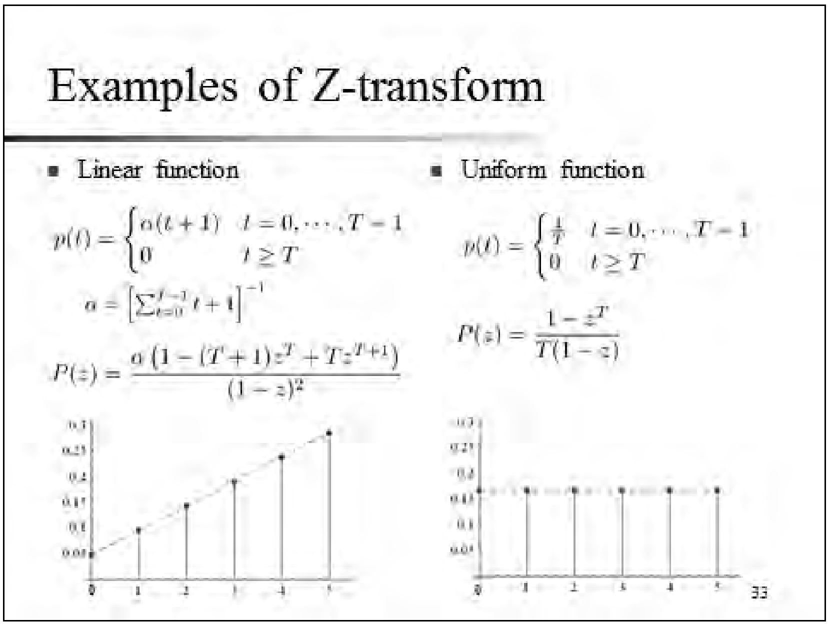

Examples of Z-transform

- Linear function

$$p(t) = \begin{cases} a(t+1) & t = 0, \cdots, T-1 \\ 0 & t \geq T \end{cases}$$

$$a = \left[\sum_{t=0}^{T-1} t+1\right]^{-1}$$

$$P(z) = \frac{a\left(1-(T+1)z^{T}+Tz^{T+1}\right)}{(1-z)^2}$$

0.3
0.25
0.2
0.15
0.1
0.05
0
1
2
3
4
5

- Uniform function

$$p(t) = \begin{cases} \frac{1}{T} & t = 0, \cdots, T-1 \\ 0 & t \geq T \end{cases}$$

$$P(z) = \frac{1-z^{T}}{T(1-z)}$$

0.3
0.25
0.2
0.15
0.1
0.05
0
1
2
3
4
5

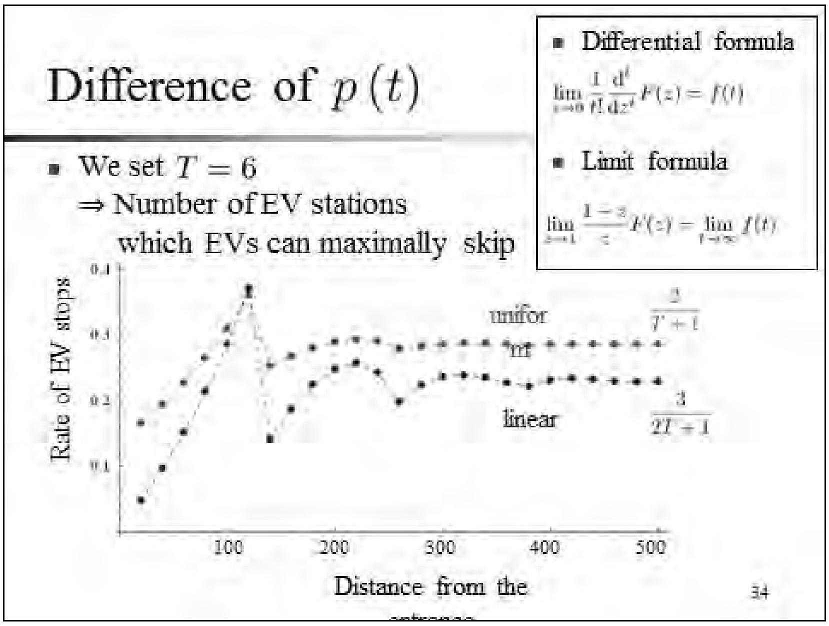

Difference of $p\,(t)$

- We set $T = 6$
  ⇒ Number of EV stations
  which EVs can maximally skip

- Differential formula

$$\lim_{z \to 0} \frac{1}{t!} \frac{\mathrm{d}^t}{\mathrm{d}z^t} F(z) = f(t)$$

- Limit formula

$$\lim_{z \to 1} \frac{1-z}{z} F(z) = \lim_{t \to \infty} f(t)$$

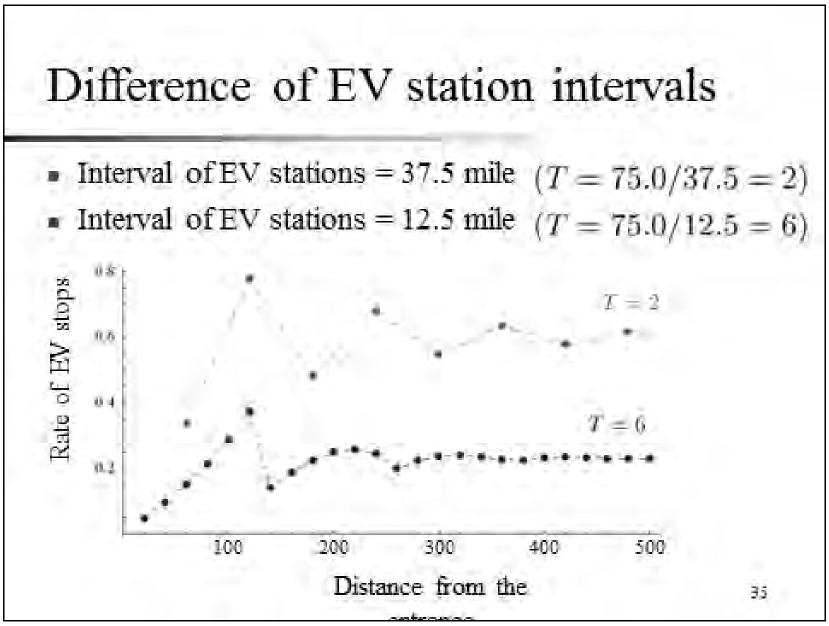

Difference of EV station intervals

- Interval of EV stations = 37.5 mile $(T = 75.0/37.5 = 2)$
- Interval of EV stations = 12.5 mile $(T = 75.0/12.5 = 6)$

35

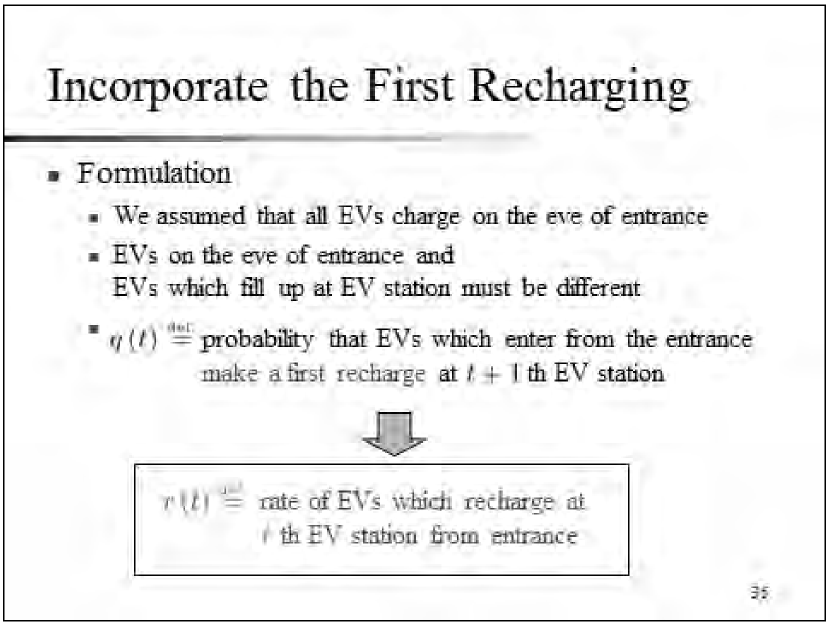

Incorporate the First Recharging

- Formulation
  - We assumed that all EVs charge on the eve of entrance
  - EVs on the eve of entrance and
    EVs which fill up at EV station must be different
  - $q(t) \overset{\text{def}}{=}$ probability that EVs which enter from the entrance
    make a first recharge at $t+1$ th EV station

$r(t) \overset{\text{def}}{=}$ rate of EVs which recharge at
t th EV station from entrance

35

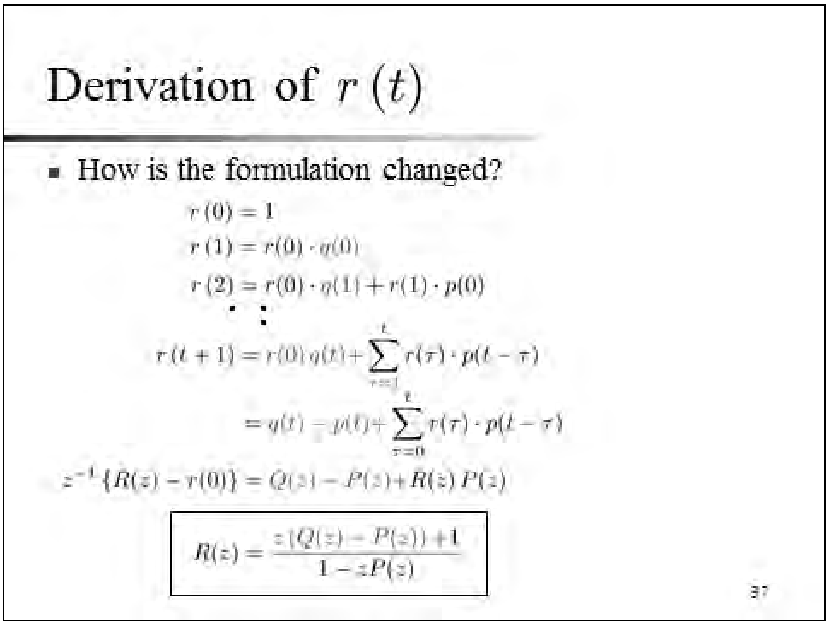

Derivation of $r\ (t)$

- How is the formulation changed?

$$r\,(0) = 1$$
$$r\,(1) = r(0)\cdot q(0)$$
$$r\,(2) = r(0)\cdot q(1) + r(1)\cdot p(0)$$
$$\vdots$$
$$r\,(t+1) = r(0)\,q(t) + \sum_{\tau=1}^{t} r(\tau)\cdot p(t-\tau)$$
$$= q(t) - p(t) + \sum_{\tau=0}^{t} r(\tau)\cdot p(t-\tau)$$
$$z^{-1}\{R(z) - r(0)\} = Q(z) - P(z) + R(z)\,P(z)$$
$$\boxed{R(z) = \frac{z\,(Q(z) - P(z)) + 1}{1 - zP(z)}}$$

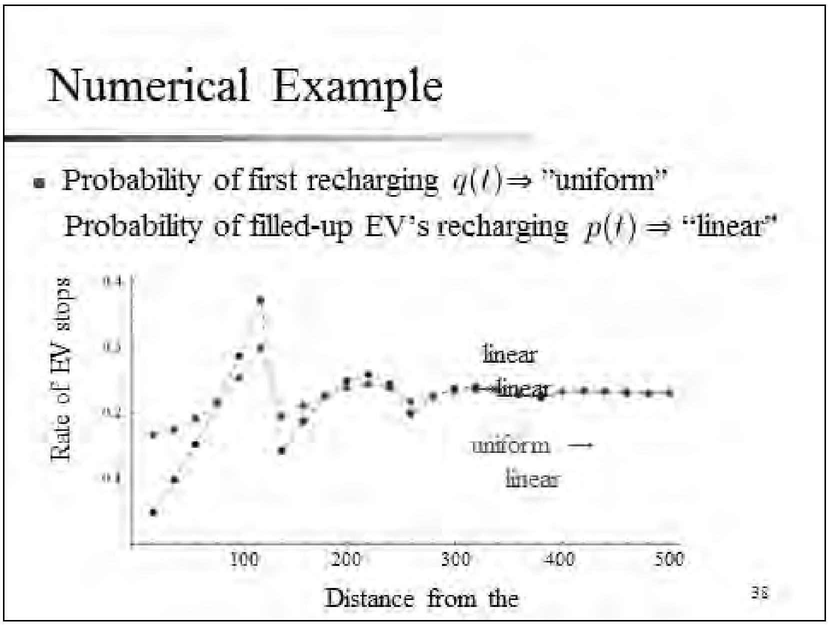

Numerical Example

- Probability of first recharging $q(t)$⇒ "uniform"
  Probability of filled-up EV's recharging $p(t)$ ⇒ "linear"

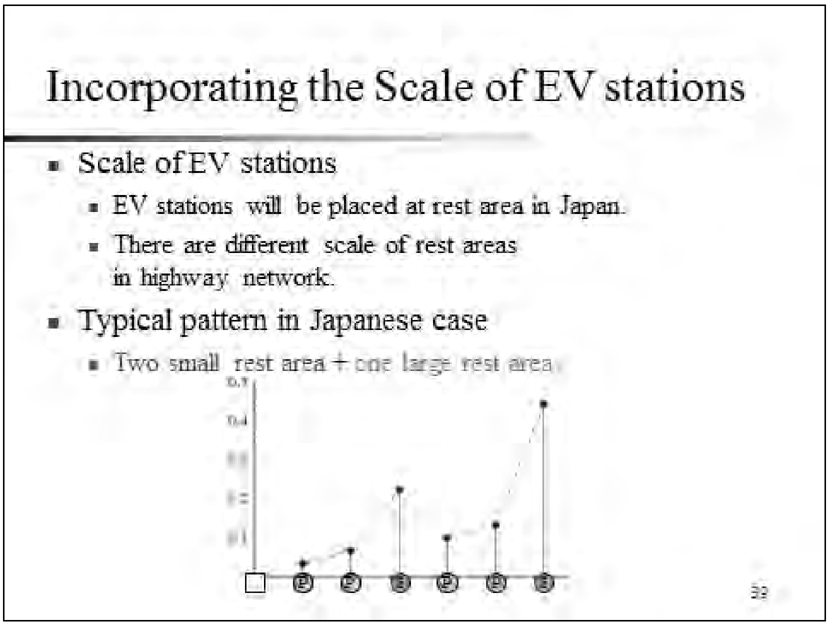

Incorporating the Scale of EV stations

- Scale of EV stations
  - EV stations will be placed at rest area in Japan.
  - There are different scale of rest areas in highway network.
- Typical pattern in Japanese case
  - Two small rest area + one large rest area

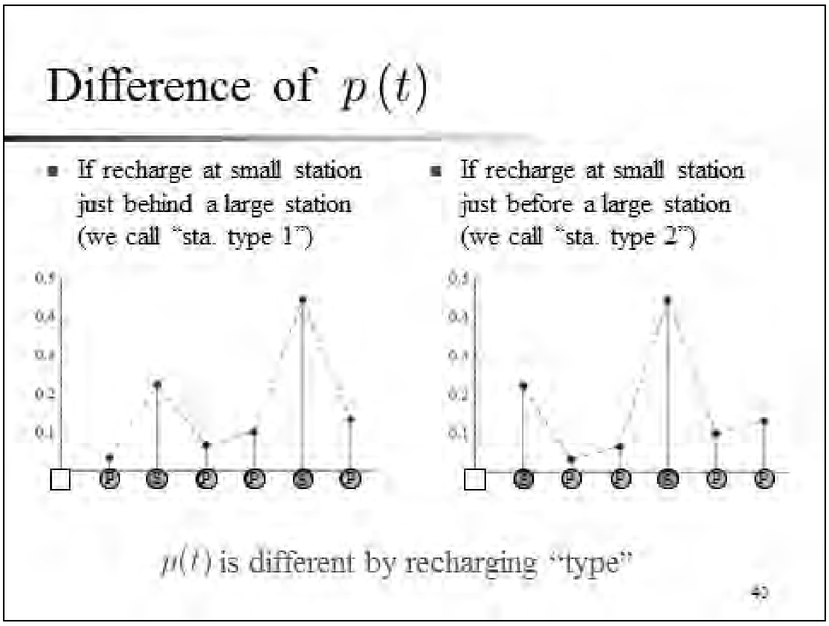

Difference of $p(t)$

- If recharge at small station just behind a large station (we call "sta. type 1")
- If recharge at small station just before a large station (we call "sta. type 2")

$p(t)$ is different by recharging "type"

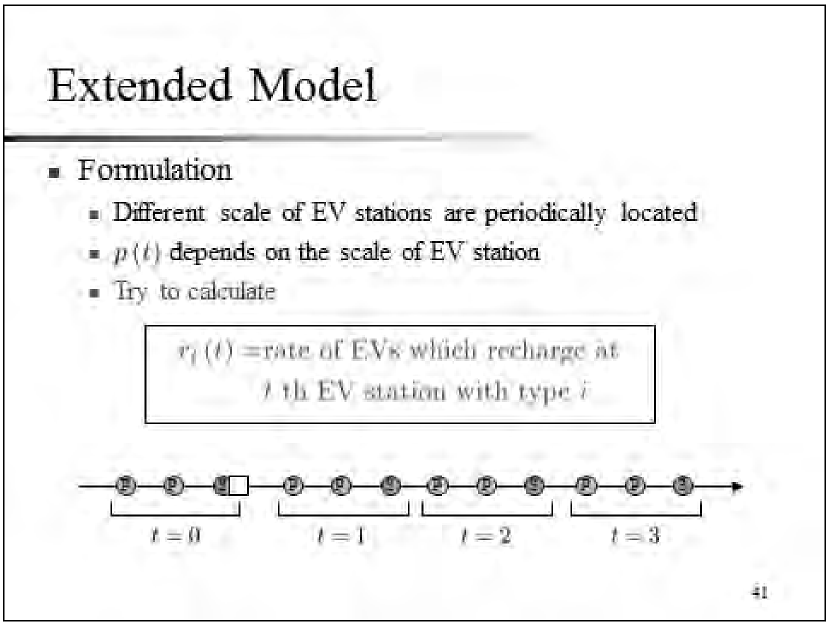

Extended Model

- Formulation
  - Different scale of EV stations are periodically located
  - $p(t)$ depends on the scale of EV station
  - Try to calculate

$r_i(t)$ =rate of EVs which recharge at
t th EV station with type i

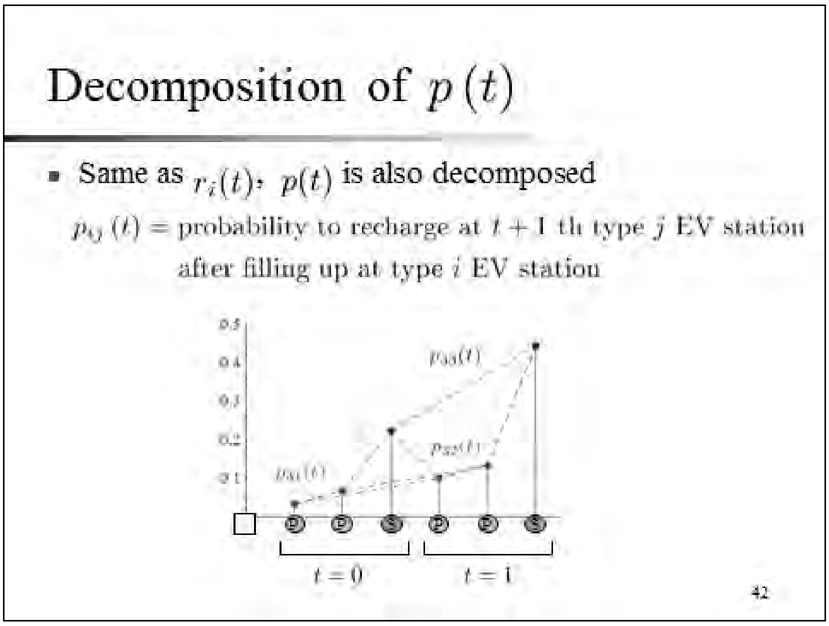

Decomposition of $p(t)$

- Same as $r_i(t)$, $p(t)$ is also decomposed

$p_{ij}(t)$ = probability to recharge at $t+1$ th type j EV station
after filling up at type i EV station

0.5
0.4
0.3
0.2
0.1
$p_{33}(t)$
$p_{22}(t)$
$p_{11}(t)$
$t=0$
$t=1$

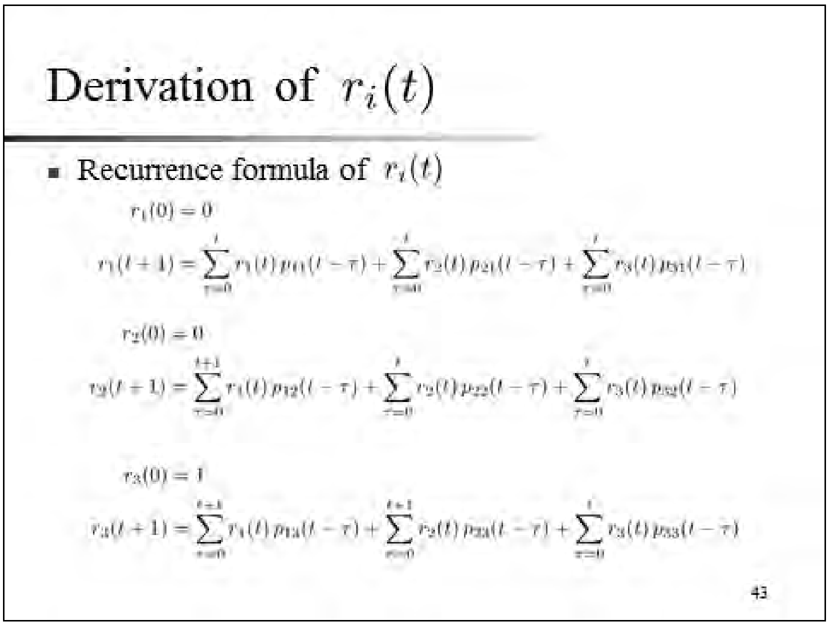

Derivation of $r_i(t)$

- Recurrence formula of $r_i(t)$

$$r_1(0)=0$$

$$r_1(t+1)=\sum_{\tau=0}^{t} r_1(t)\,p_{11}(t-\tau)+\sum_{\tau=0}^{t} r_2(t)\,p_{21}(t-\tau)+\sum_{\tau=0}^{t} r_3(t)\,p_{31}(t-\tau)$$

$$r_2(0)=0$$

$$r_2(t+1)=\sum_{\tau=0}^{t+1} r_1(t)\,p_{12}(t-\tau)+\sum_{\tau=0}^{t} r_2(t)\,p_{22}(t-\tau)+\sum_{\tau=0}^{t} r_3(t)\,p_{32}(t-\tau)$$

$$r_3(0)=1$$

$$r_3(t+1)=\sum_{\tau=0}^{t+1} r_1(t)\,p_{13}(t-\tau)+\sum_{\tau=0}^{t+1} r_2(t)\,p_{23}(t-\tau)+\sum_{\tau=0}^{t} r_3(t)\,p_{33}(t-\tau)$$

43

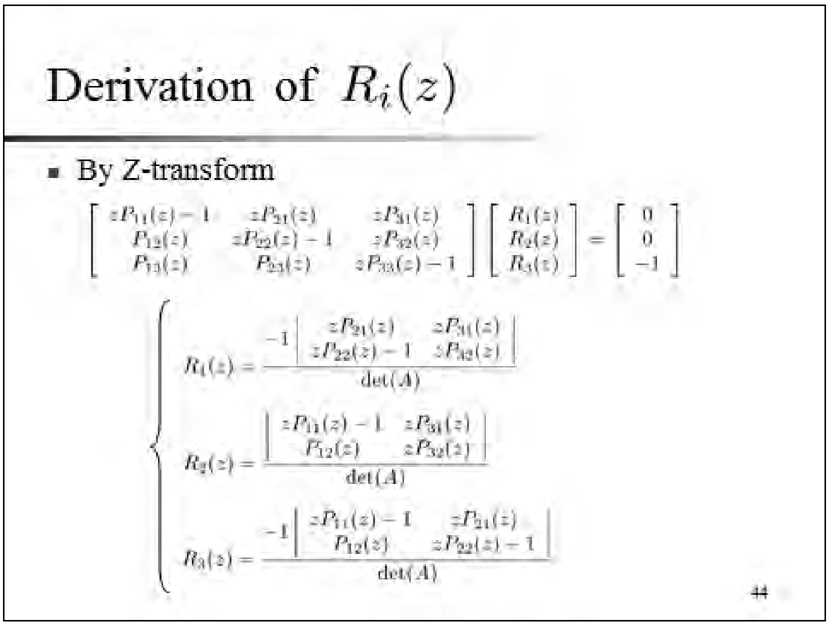

Derivation of $R_i(z)$

- By Z-transform

$$\begin{bmatrix} zP_{11}(z)-1 & zP_{21}(z) & zP_{31}(z) \\ P_{12}(z) & zP_{22}(z)-1 & zP_{32}(z) \\ P_{13}(z) & P_{23}(z) & zP_{33}(z)-1 \end{bmatrix}\begin{bmatrix} R_1(z) \\ R_2(z) \\ R_3(z) \end{bmatrix}=\begin{bmatrix} 0 \\ 0 \\ -1 \end{bmatrix}$$

$$\begin{cases} R_1(z)=\dfrac{-1\begin{vmatrix} zP_{21}(z) & zP_{31}(z) \\ zP_{22}(z)-1 & zP_{32}(z) \end{vmatrix}}{\det(A)} \\ R_2(z)=\dfrac{\begin{vmatrix} zP_{11}(z)-1 & zP_{31}(z) \\ P_{12}(z) & zP_{32}(z) \end{vmatrix}}{\det(A)} \\ R_3(z)=\dfrac{-1\begin{vmatrix} zP_{11}(z)-1 & zP_{21}(z) \\ P_{12}(z) & zP_{22}(z)-1 \end{vmatrix}}{\det(A)} \end{cases}$$

44

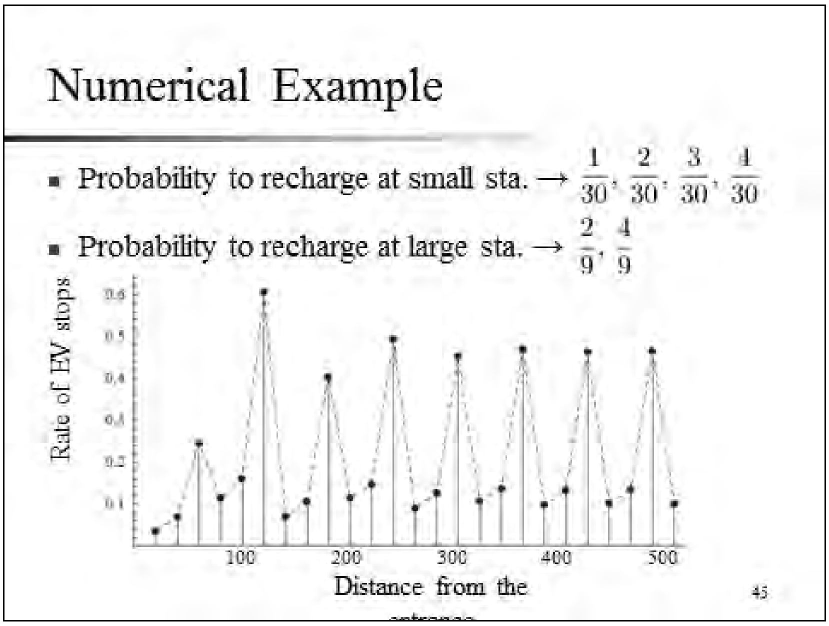

Numerical Example

- Probability to recharge at small sta. → $\frac{1}{30}, \frac{2}{30}, \frac{3}{30}, \frac{4}{30}$
- Probability to recharge at large sta. → $\frac{2}{9}, \frac{4}{9}$

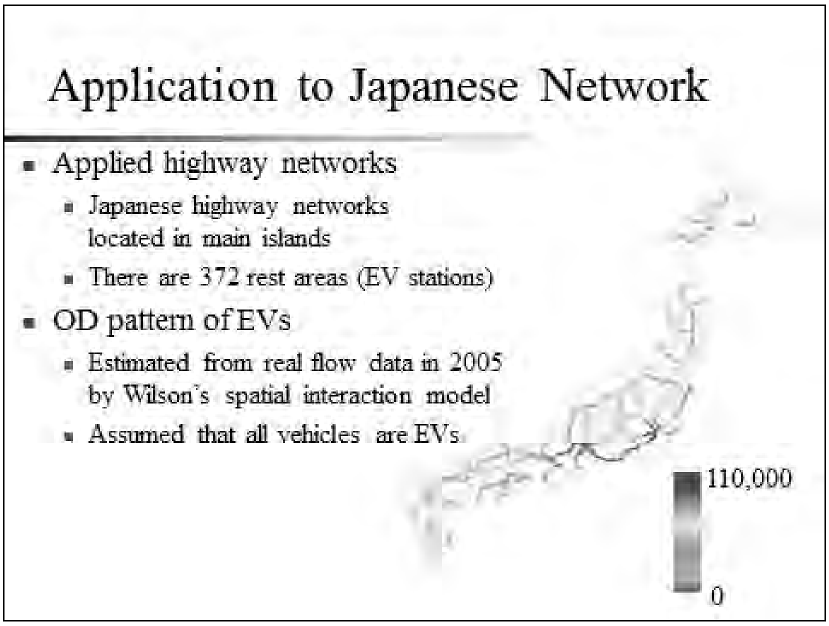

Application to Japanese Network

- Applied highway networks
  - Japanese highway networks located in main islands
  - There are 372 rest areas (EV stations)
- OD pattern of EVs
  - Estimated from real flow data in 2005 by Wilson's spatial interaction model
  - Assumed that all vehicles are EVs

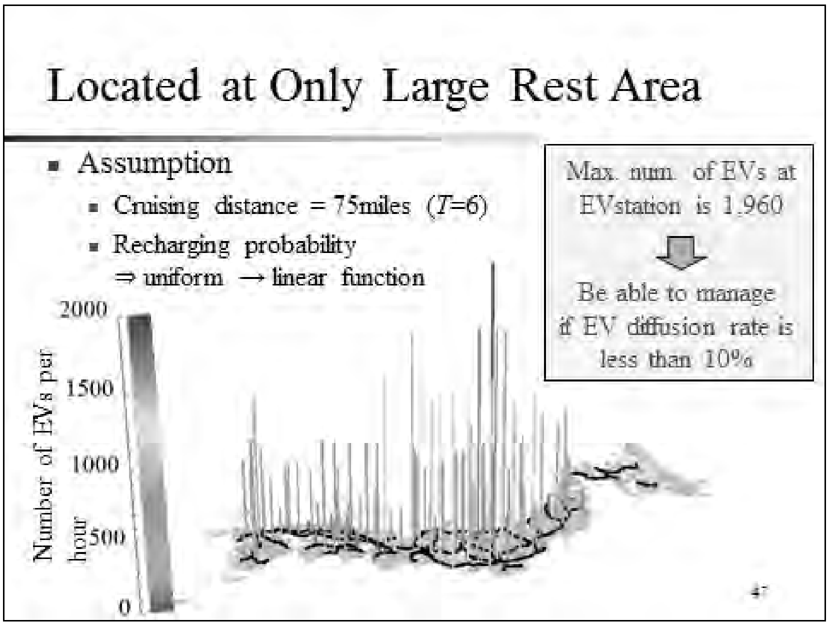

Located at Only Large Rest Area

- Assumption
  - Cruising distance = 75miles (*T*=6)
  - Recharging probability
    ⇒ uniform → linear function

Max. num. of EVs at EVstation is 1,960

⇩

Be able to manage if EV diffusion rate is less than 10%

2000
1500
1000
500
0
Number of EVs per hour

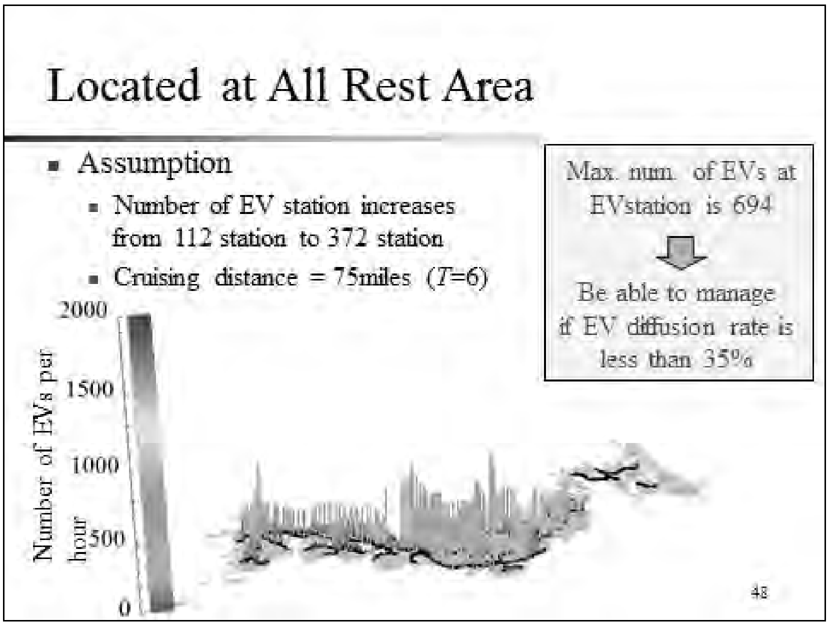

Located at All Rest Area

- Assumption
  - Number of EV station increases from 112 station to 372 station
  - Cruising distance = 75miles (*T*=6)

Max. num. of EVs at EVstation is 694

⇩

Be able to manage if EV diffusion rate is less than 35%

2000
1500
1000
500
0
Number of EVs per hour

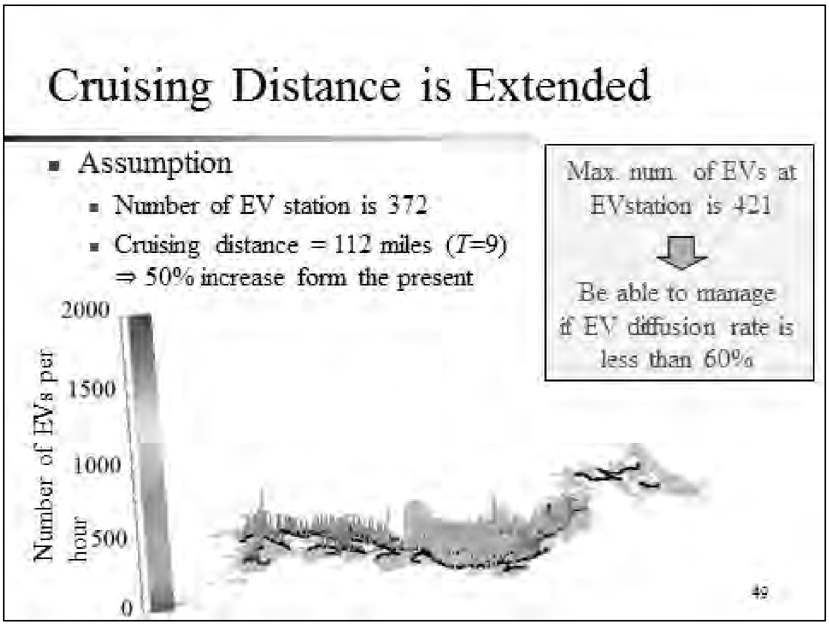

Cruising Distance is Extended

- Assumption
  - Number of EV station is 372
  - Cruising distance = 112 miles (T=9) ⇒ 50% increase form the present

Max. num. of EVs at EVstation is 421

⇩

Be able to manage if EV diffusion rate is less than 60%

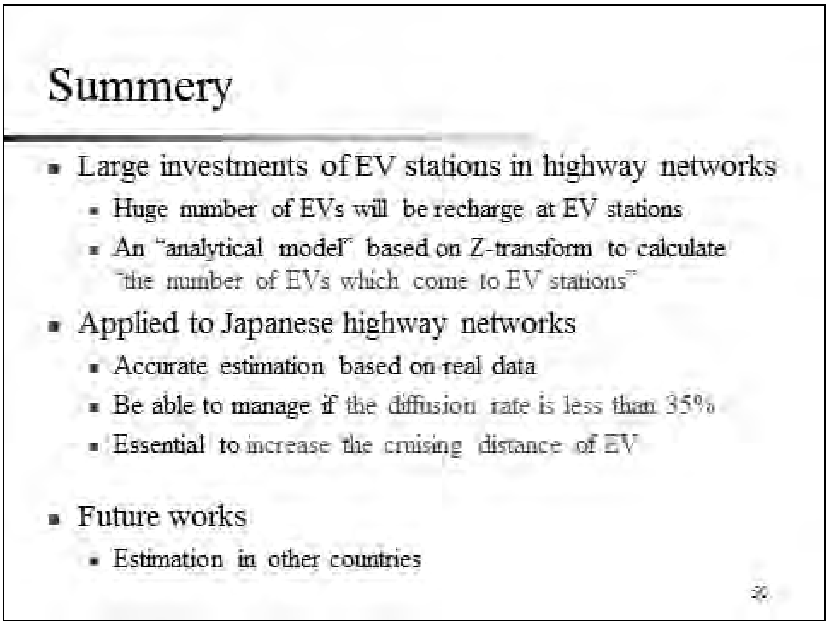

Summery

- Large investments of EV stations in highway networks
  - Huge number of EVs will be recharge at EV stations
  - An "analytical model" based on Z-transform to calculate "the number of EVs which come to EV stations"
- Applied to Japanese highway networks
  - Accurate estimation based on real data
  - Be able to manage if the diffusion rate is less than 35%
  - Essential to increase the cruising distance of EV
- Future works
  - Estimation in other countries

WATER LEAK PREVENTION AT CONNECTIONS OF PRECAST CONCRETE PANELS WITH BUTYL RUBBER

Withit PANSUK[1], Penpitcha KRITTAYANUPONG[2] and
Phongsak WIWATTANADATE[3]
[1] Assistant Professor, Department of Civil Engineering,
Chulalongkorn University, Thailand
Withit.P@chula.ac.th
[2] Graduate Student, Department of Civil Engineering,
Chulalongkorn University, Thailand
[3] Lecturer, Department of Materials Science,
Chulalongkorn University, Thailand

ABSTRACT

Construction technologies have been growing continuously. Many projects are trying to develop technical construction with minimum time. Precast concretes are defined as technologies that provide efficient strategy to prepare products with time-competing approach. It includes prefabricated methods, off-site productions, and offset manufacturing for buildings. The most common applications which have been widely used as members associated with building constructions are walls. Precast concrete walls provide excellent functions of durability and desirability. However, one of the biggest challenges of precast concrete walls is leakage between precast connections due to loss of strain on the walls and strength of reinforcing materials through connections. In Thailand, the most famous prevention is application of backing rod with sealant and grouting with non-shrink grout cement. Backing rods are usually made from extruded polyethylene foam with different diameters and lengths available. It is used as a backup material for cold applied sealants to give the sealant a proper thickness. Backing rod with sealant are a lot of advantages such as compatibility with cold applied sealants (e.g. polyurethane and silicone) and highly flexible and compressible. However, installation of backing rod must be done with care. During installation, the surface of the backing rod shall not be cut or punctuated and excessive longitudinal stretching of the rod is to be avoided. Also, it cannot work when the sealant is heated and applied at a temperature above 70 °C. Joint width is affected by backing rod diameter. The limitations of sealant are effects from environment and time cyclic. If the sealant cannot work capably, it will be considered as a weak point and leakage will occur. From previous researches about butyl rubber, its performance to prevent leakage has been widely reported. Therefore, substitution of the previous prevention between precast connections is promising by the possibility to substitute butyl rubber as backing rod with sealant. The common types of precast concrete connection in Thailand which were modeled and tested had been studied and inferred. In this study, *the 3-dimentional finite element model of precast concrete connection and its interaction with two adjusted concrete panels were simulated. Laboratory experiment of precast concrete panel connections was also conducted. The studying parameter was the critical crack width at the connections resulted from the differential loadings acting on the panels. The suitable position of butyl rubber installed at the connections was also one of the test parameter. The critical crack widths were induced on the real specimens to ex-amine possible application of three proposed connection types. Then, water permeability test was performed at specimens' connections. The water pressure was adjusted to maximum of 5 kgf/cm2 (water-head height: 50 m). The butyl rubber was found to have superior water leak prevention capability. The most suitable installation pattern was shown.*

Keywords: *water leak, connections, precast concrete, butyl rubber, water permeability*

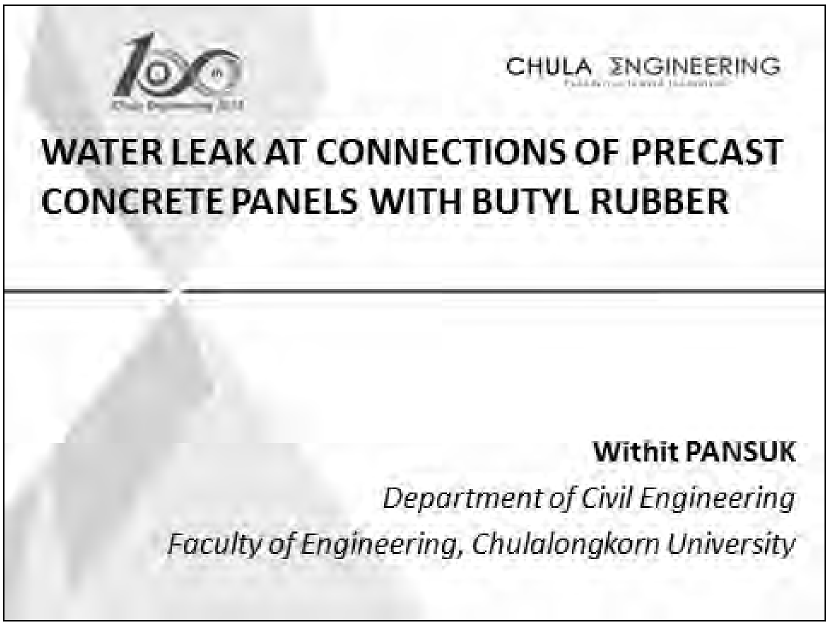

CHULA ΣNGINEERING

WATER LEAK AT CONNECTIONS OF PRECAST CONCRETE PANELS WITH BUTYL RUBBER

Withit PANSUK
Department of Civil Engineering
Faculty of Engineering, Chulalongkorn University

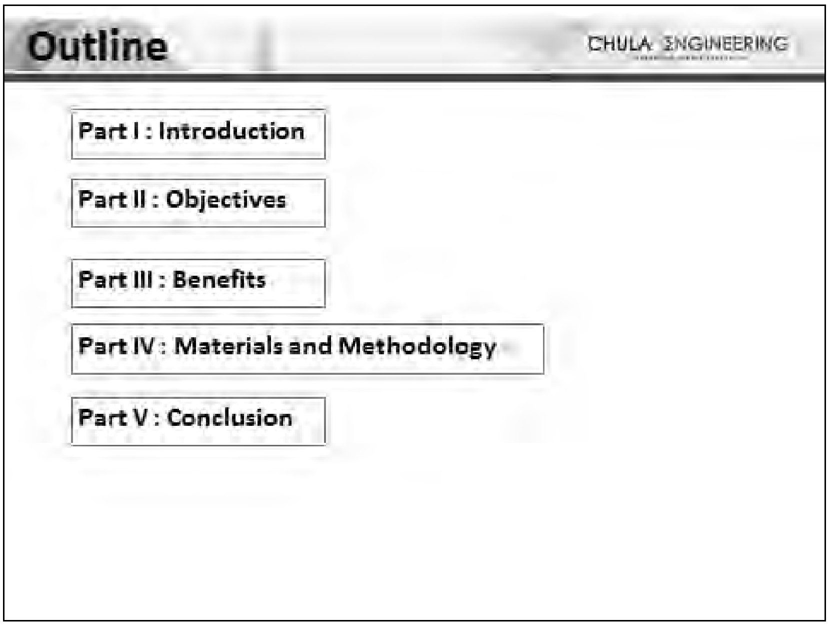

Outline

CHULA ΣNGINEERING

- Part I : Introduction
- Part II : Objectives
- Part III : Benefits
- Part IV : Materials and Methodology
- Part V : Conclusion

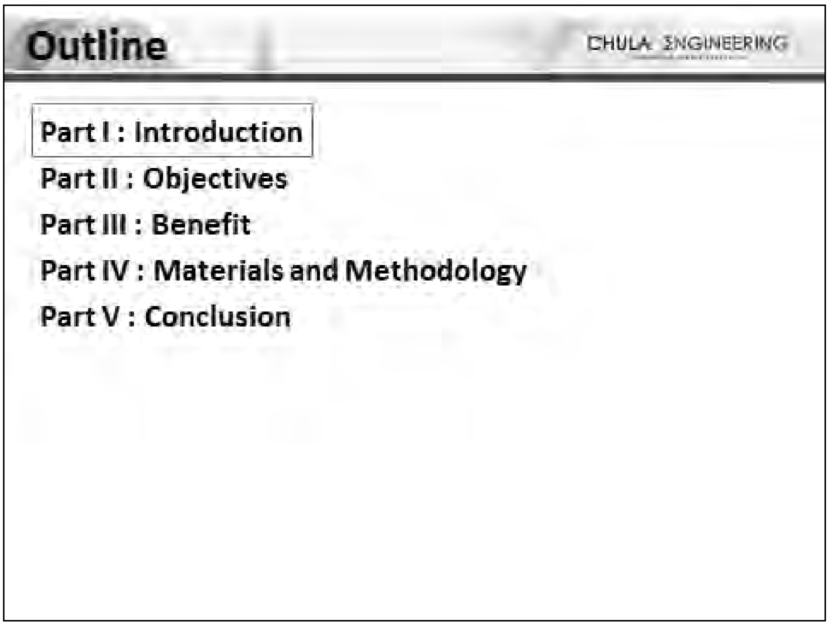

Outline

CHULA ENGINEERING

Part I : Introduction

Part II : Objectives

Part III : Benefit

Part IV : Materials and Methodology

Part V : Conclusion

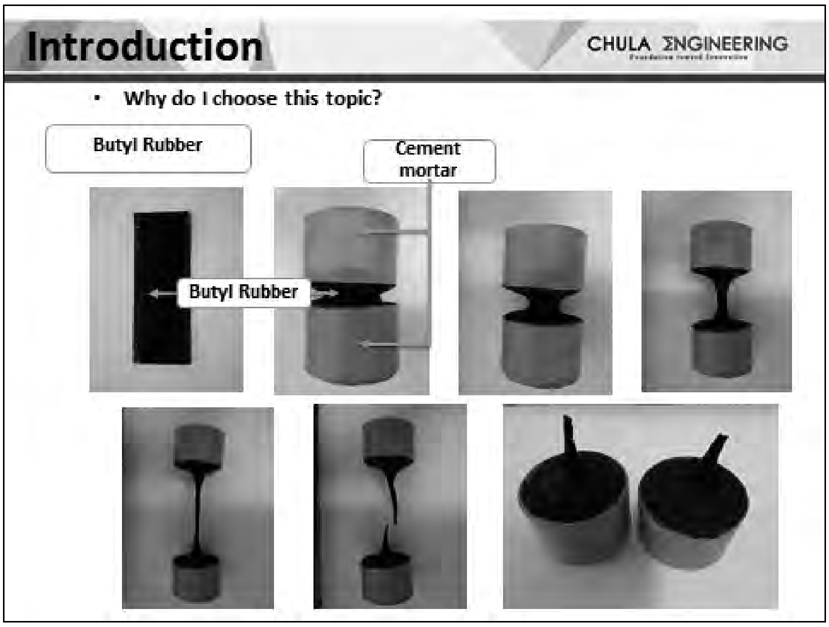

Introduction

CHULA ENGINEERING

- Why do I choose this topic?

Butyl Rubber

Cement mortar

Butyl Rubber

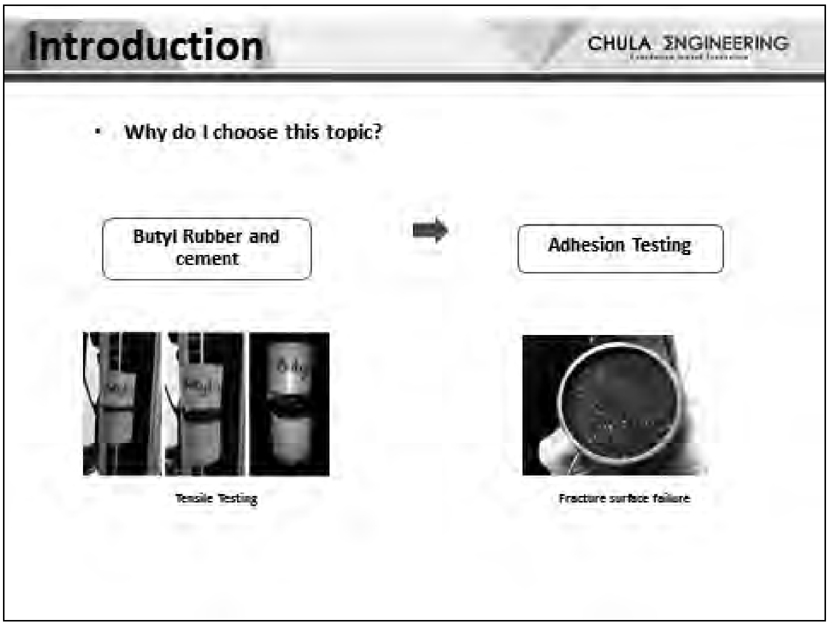

Introduction

CHULA ΣNGINEERING

- **Why do I choose this topic?**

Butyl Rubber and cement ➡ Adhesion Testing

Tensile Testing

Fracture surface failure

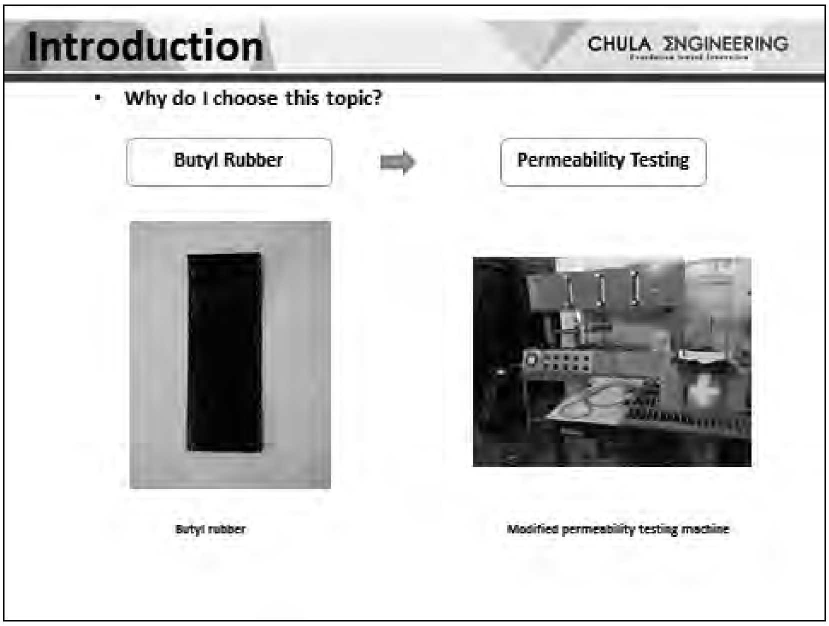

Introduction

CHULA ΣNGINEERING

- **Why do I choose this topic?**

Butyl Rubber ➡ Permeability Testing

Butyl rubber

Modified permeability testing machine

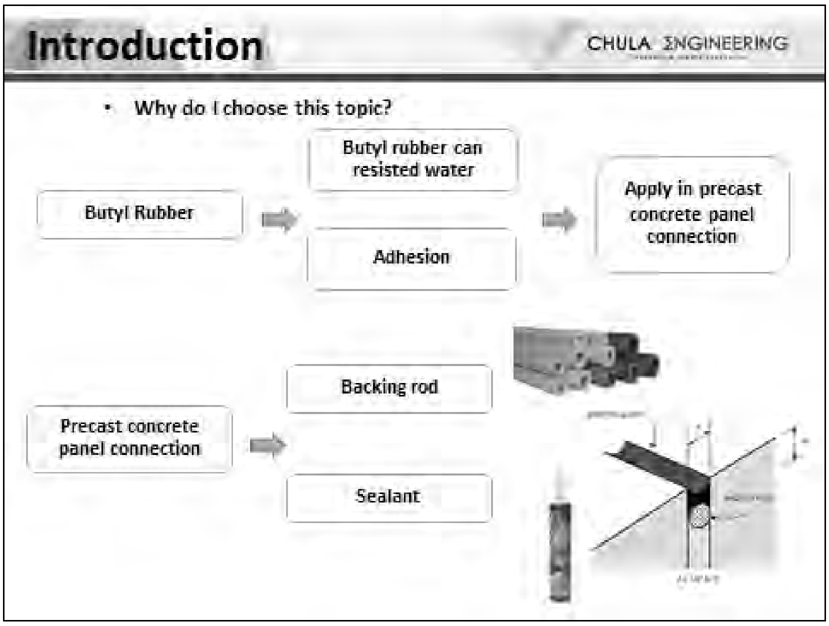

Introduction

CHULA ENGINEERING

- Why do I choose this topic?

Butyl Rubber → Butyl rubber can resisted water / Adhesion → Apply in precast concrete panel connection

Precast concrete panel connection → Backing rod / Sealant

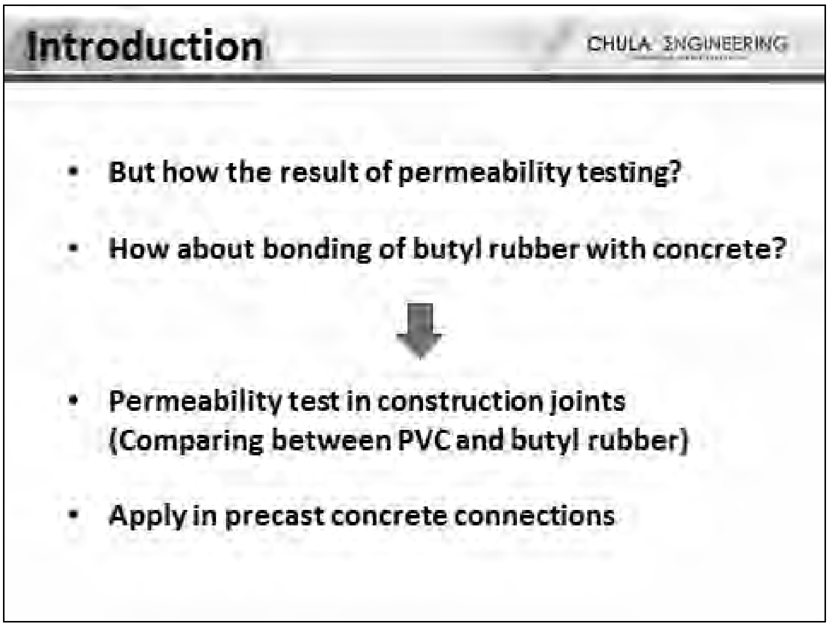

Introduction

CHULA ENGINEERING

- **But how the result of permeability testing?**
- **How about bonding of butyl rubber with concrete?**

↓

- **Permeability test in construction joints (Comparing between PVC and butyl rubber)**
- **Apply in precast concrete connections**

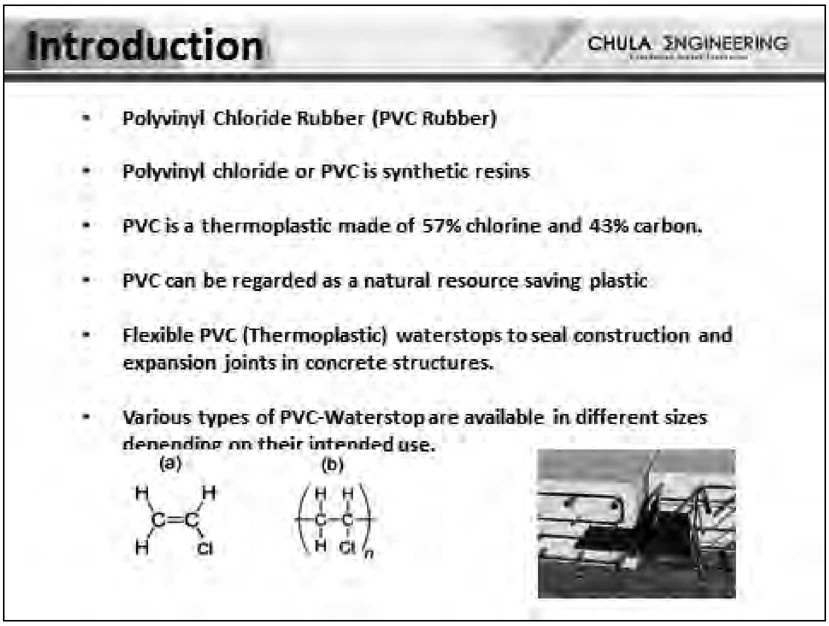

Introduction

CHULA ENGINEERING

- Polyvinyl Chloride Rubber (PVC Rubber)
- Polyvinyl chloride or PVC is synthetic resins
- PVC is a thermoplastic made of 57% chlorine and 43% carbon.
- PVC can be regarded as a natural resource saving plastic
- Flexible PVC (Thermoplastic) waterstops to seal construction and expansion joints in concrete structures.
- Various types of PVC-Waterstop are available in different sizes depending on their intended use.

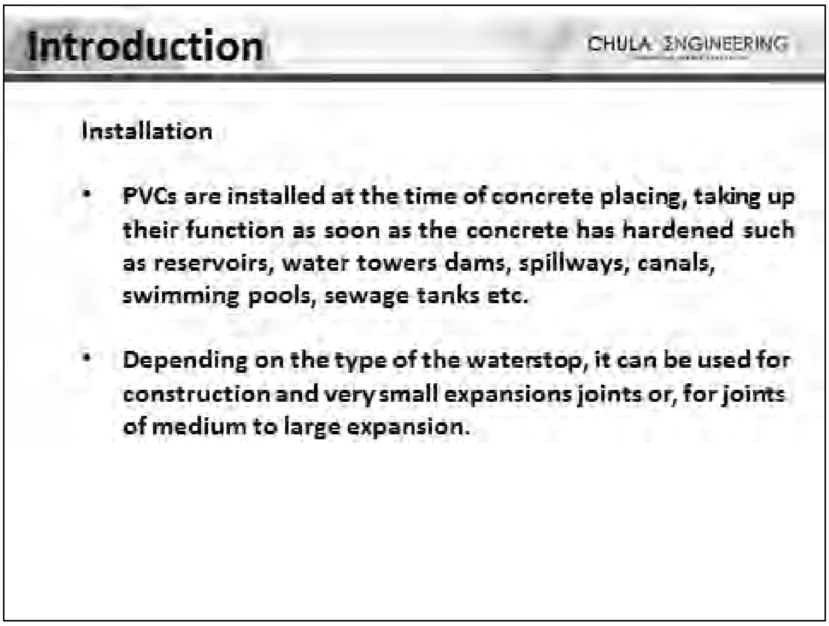

Introduction

CHULA ENGINEERING

Installation

- PVCs are installed at the time of concrete placing, taking up their function as soon as the concrete has hardened such as reservoirs, water towers dams, spillways, canals, swimming pools, sewage tanks etc.
- Depending on the type of the waterstop, it can be used for construction and very small expansions joints or, for joints of medium to large expansion.

Introduction

CHULA ΣNGINEERING

Tank construction
At Chonburi

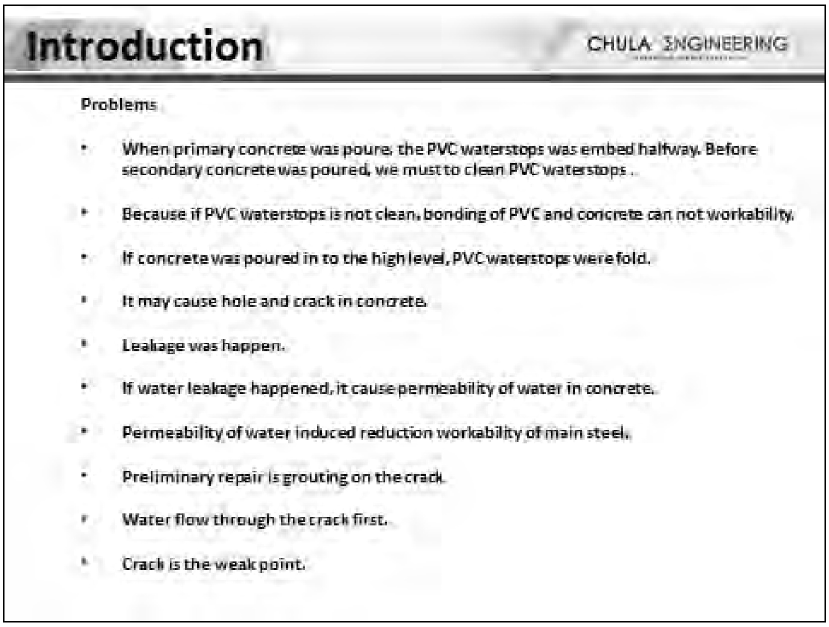

Introduction

CHULA ΣNGINEERING

Problems

- When primary concrete was poure, the PVC waterstops was embed halfway. Before secondary concrete was poured, we must to clean PVC waterstops .
- Because if PVC waterstops is not clean, bonding of PVC and concrete can not workability.
- If concrete was poured in to the high level, PVC waterstops were fold.
- It may cause hole and crack in concrete.
- Leakage was happen.
- If water leakage happened, it cause permeability of water in concrete.
- Permeability of water induced reduction workability of main steel.
- Preliminary repair is grouting on the crack.
- Water flow through the crack first.
- Crack is the weak point.

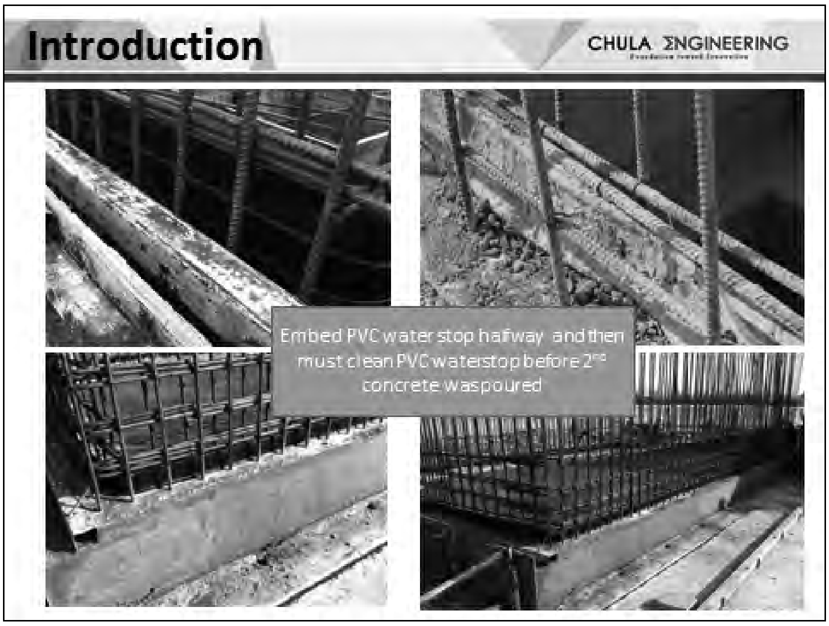

Introduction

CHULA ΣNGINEERING

Embed PVC water stop halfway and then must clean PVC waterstop before 2nd concrete was poured

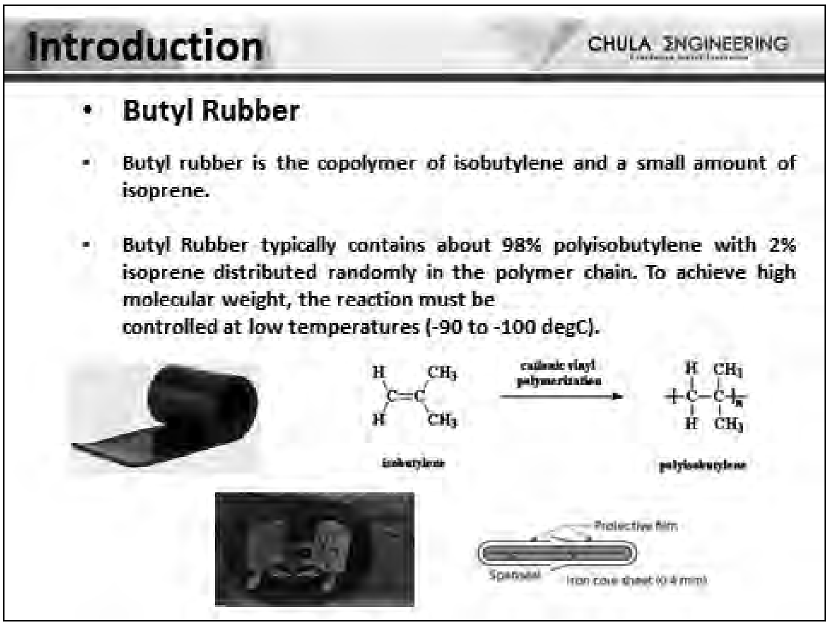

Introduction

CHULA ΣNGINEERING

- **Butyl Rubber**
- Butyl rubber is the copolymer of isobutylene and a small amount of isoprene.
- Butyl Rubber typically contains about 98% polyisobutylene with 2% isoprene distributed randomly in the polymer chain. To achieve high molecular weight, the reaction must be controlled at low temperatures (-90 to -100 degC).

cationic vinyl polymerization
isobutylene
polyisobutylene
Protective film
Spanseal
Iron core sheet (0.4 mm)

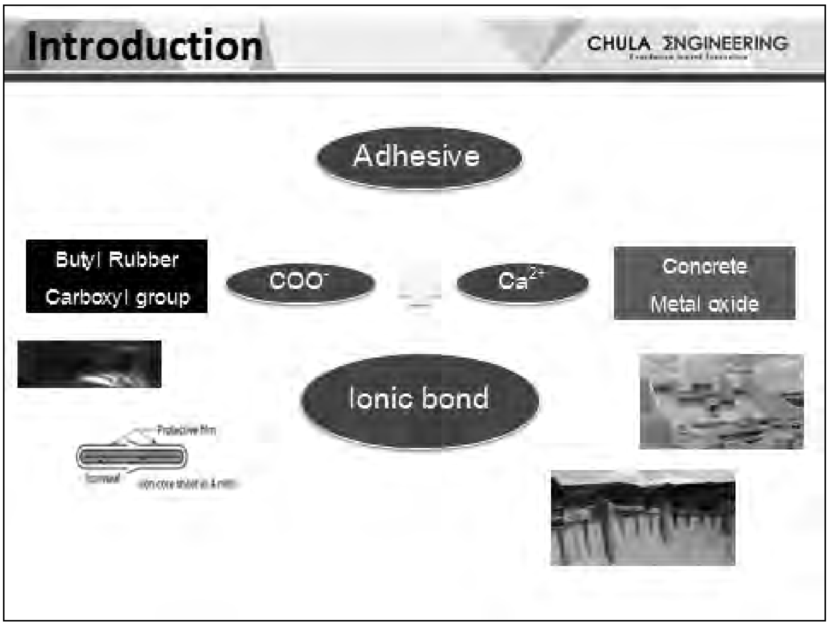

Introduction

CHULA ΣNGINEERING

Adhesive

Butyl Rubber
Carboxyl group

COO⁻

Ca²⁺

Concrete
Metal oxide

Ionic bond

Protective film

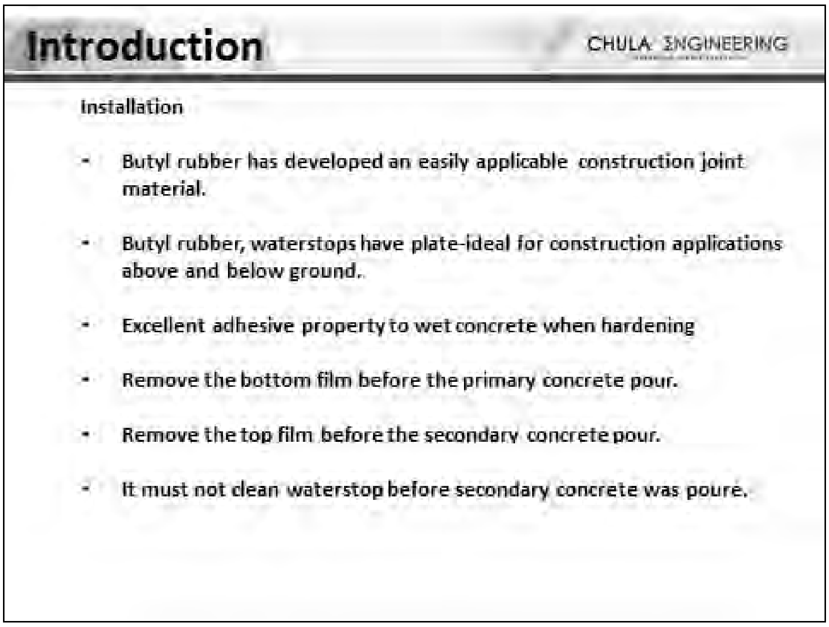

Introduction

CHULA ΣNGINEERING

Installation

- Butyl rubber has developed an easily applicable construction joint material.
- Butyl rubber, waterstops have plate-ideal for construction applications above and below ground.
- Excellent adhesive property to wet concrete when hardening
- Remove the bottom film before the primary concrete pour.
- Remove the top film before the secondary concrete pour.
- It must not clean waterstop before secondary concrete was poure.

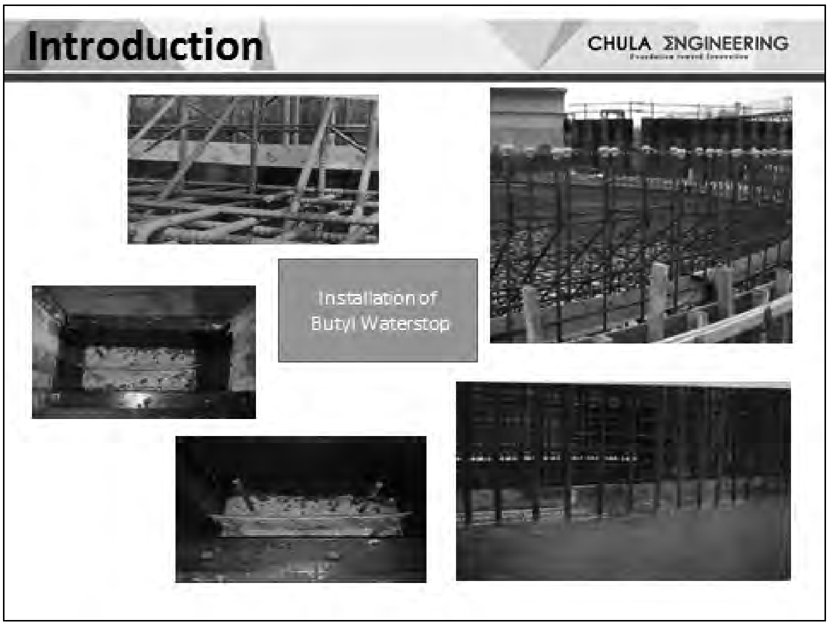

Introduction

CHULA ΣNGINEERING

Installation of Butyl Waterstop

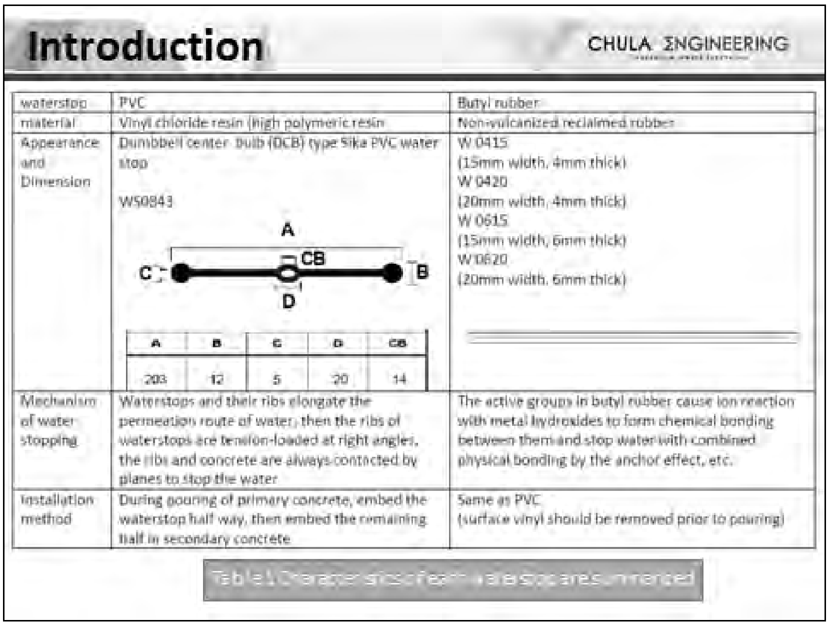

Introduction

CHULA ΣNGINEERING

waterstop	PVC	Butyl rubber
material	Vinyl chloride resin (high polymeric resin	Non-vulcanized reclaimed rubber
Appearance and Dimension	Dumbbell center Bulb (DCB) type Sika PVC water stop WS0843 A: 203, B: 12, C: 5, D: 20, CB: 14	W 0415 (15mm width, 4mm thick) W 0420 (20mm width, 4mm thick) W 0615 (15mm width, 6mm thick) W 0620 (20mm width, 6mm thick)
Mechanism of water stopping	Waterstops and their ribs elongate the permeation route of water, then the ribs of waterstops are tension-loaded at right angles, the ribs and concrete are always contacted by planes to stop the water	The active groups in butyl rubber cause ion reaction with metal hydroxides to form chemical bonding between them and stop water with combined physical bonding by the anchor effect, etc.
Installation method	During pouring of primary concrete, embed the waterstop half way, then embed the remaining half in secondary concrete	Same as PVC (surface vinyl should be removed prior to pouring)

Table 1 Characteristics of each waterstops are summarized

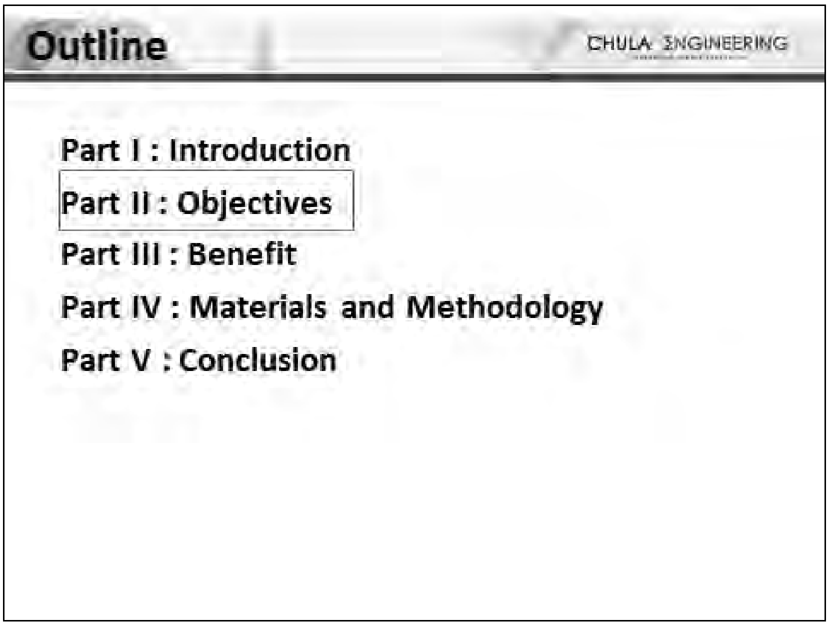

Outline

CHULA ENGINEERING

Part I : Introduction

Part II : Objectives

Part III : Benefit

Part IV : Materials and Methodology

Part V : Conclusion

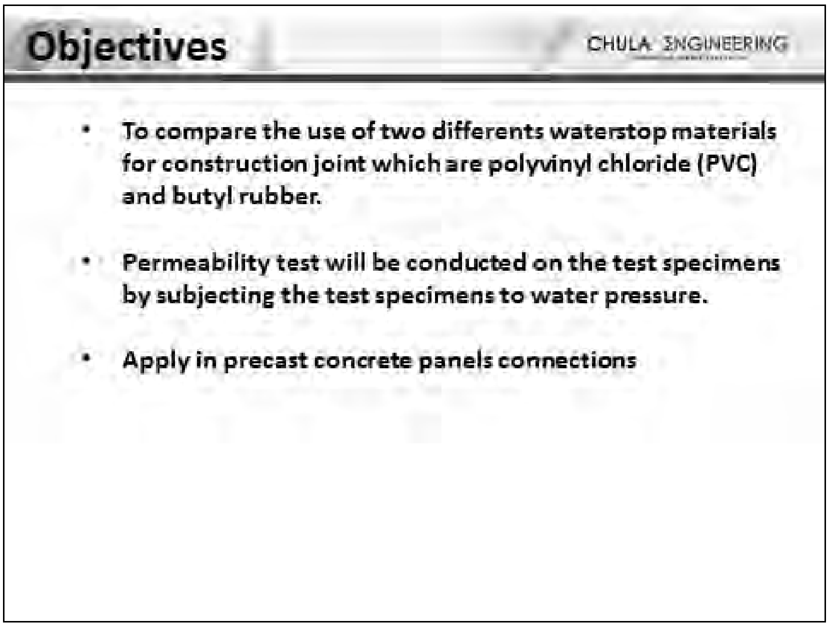

Objectives

CHULA ENGINEERING

- To compare the use of two differents waterstop materials for construction joint which are polyvinyl chloride (PVC) and butyl rubber.
- Permeability test will be conducted on the test specimens by subjecting the test specimens to water pressure.
- Apply in precast concrete panels connections

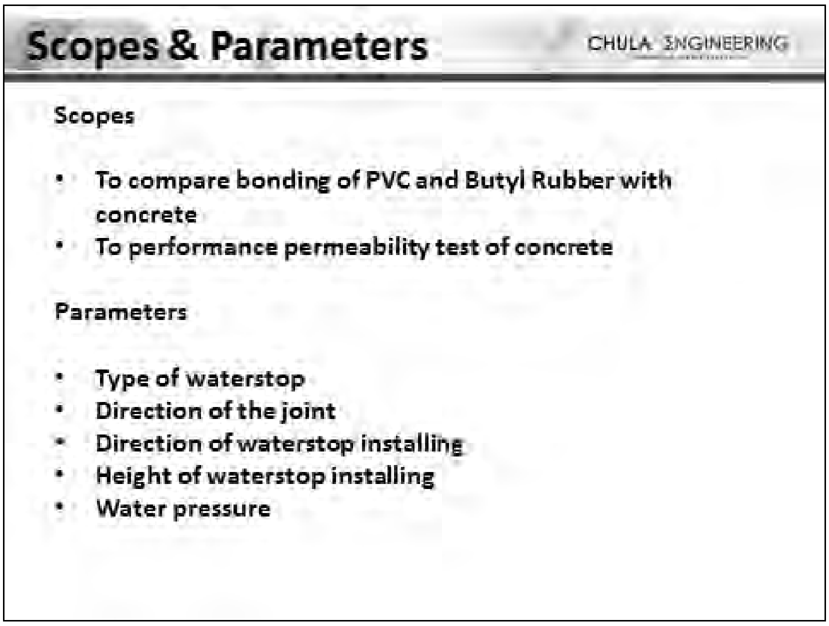

Scopes & Parameters

CHULA ENGINEERING

Scopes

- To compare bonding of PVC and Butyl Rubber with concrete
- To performance permeability test of concrete

Parameters

- Type of waterstop
- Direction of the joint
- Direction of waterstop installing
- Height of waterstop installing
- Water pressure

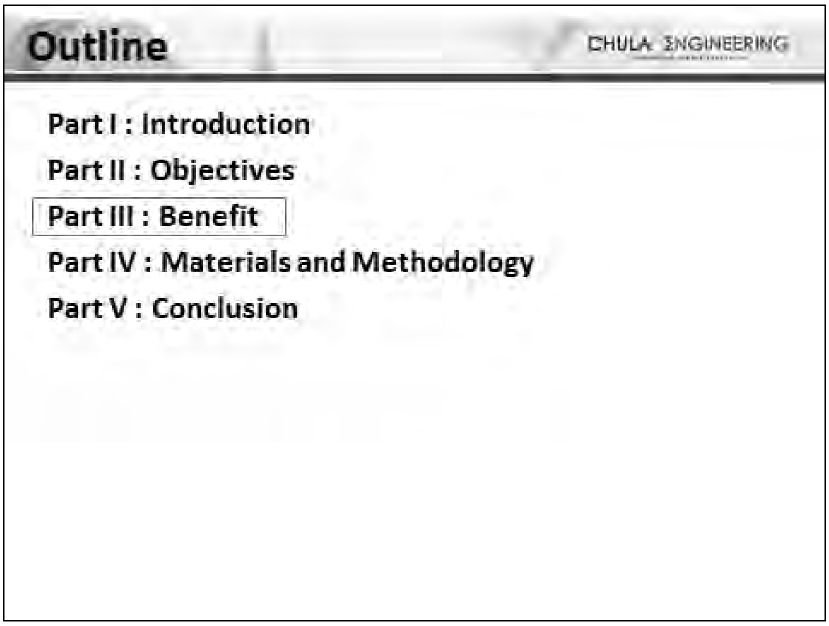

Outline

CHULA ENGINEERING

Part I : Introduction

Part II : Objectives

Part III : Benefit

Part IV : Materials and Methodology

Part V : Conclusion

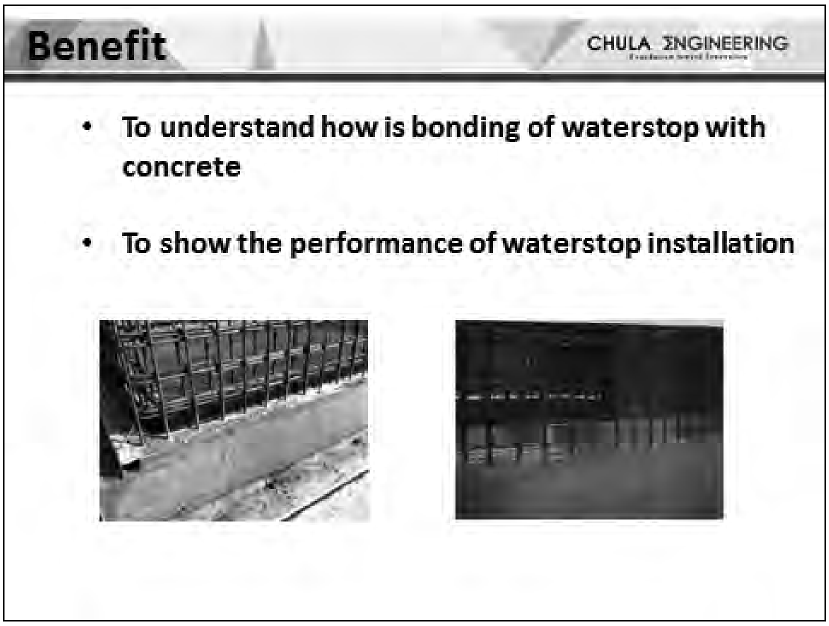

Benefit

CHULA ENGINEERING

- To understand how is bonding of waterstop with concrete
- To show the performance of waterstop installation

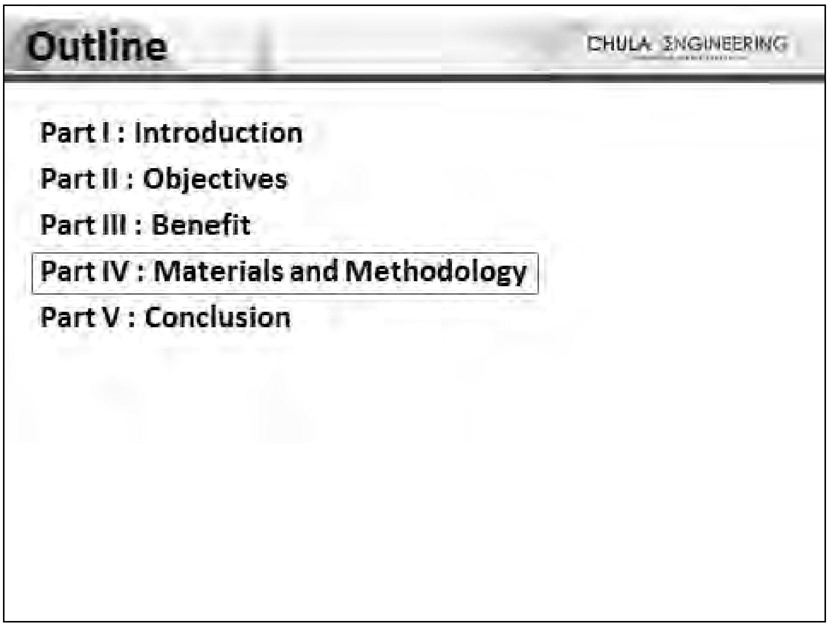

Outline

CHULA ENGINEERING

Part I : Introduction
Part II : Objectives
Part III : Benefit
Part IV : Materials and Methodology
Part V : Conclusion

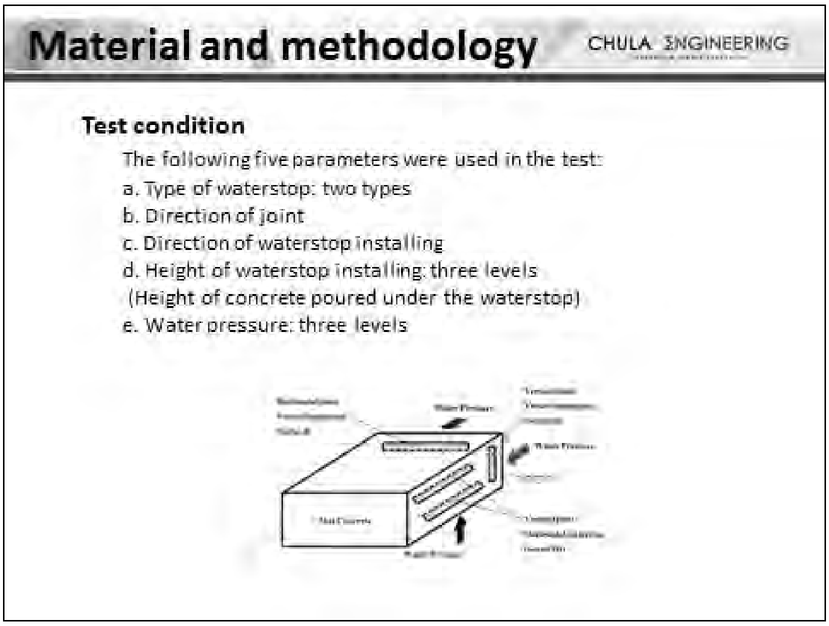

Material and methodology

CHULA ENGINEERING

Test condition

The following five parameters were used in the test:
a. Type of waterstop: two types
b. Direction of joint
c. Direction of waterstop installing
d. Height of waterstop installing: three levels
(Height of concrete poured under the waterstop)
e. Water pressure: three levels

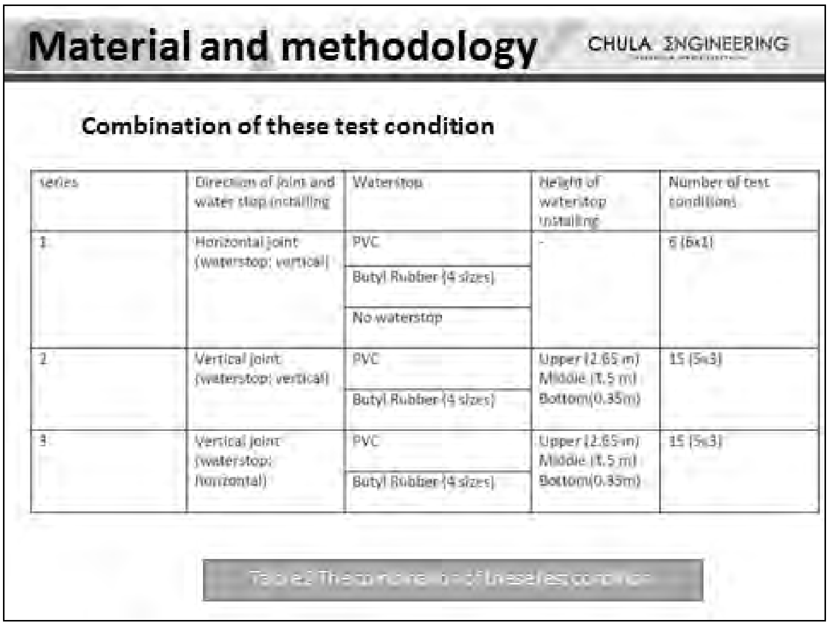

Material and methodology

CHULA ENGINEERING

Combination of these test condition

series	Direction of joint and water stop installing	Waterstop	Height of waterstop installing	Number of test condition
1	Horizontal joint (waterstop: vertical)	PVC Butyl Rubber (4 sizes) No waterstop	-	6 (6x1)
2	Vertical joint (waterstop: vertical)	PVC Butyl Rubber (4 sizes)	Upper (2.65 m) Middle (1.5 m) Bottom(0.35m)	15 (5x3)
3	Vertical joint (waterstop: horizontal)	PVC Butyl Rubber (4 sizes)	Upper (2.65 m) Middle (1.5 m) Bottom(0.35m)	15 (5x3)

Table2 The combination of the series condition

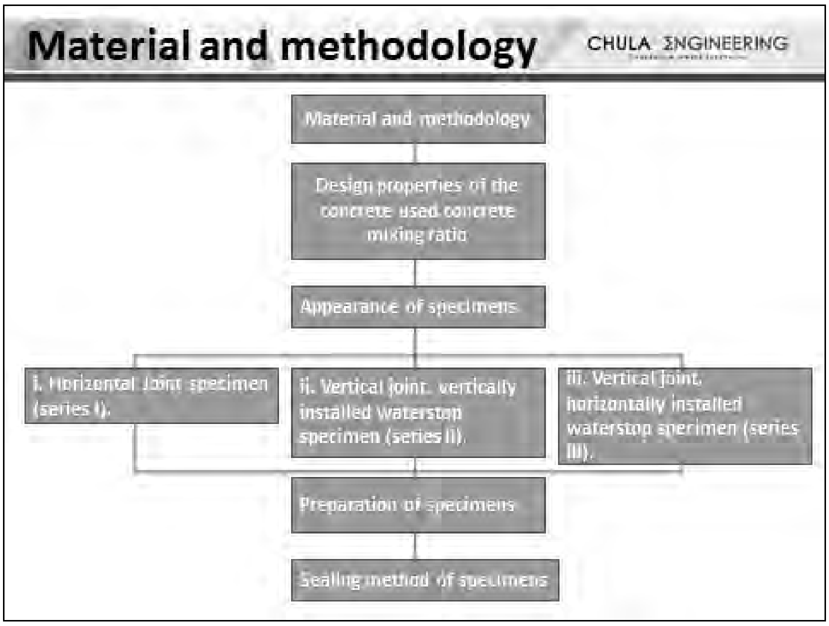

Material and methodology

Material and methodology

Design properties of the concrete used concrete mixing ratio

Appearance of specimens

i. Horizontal Joint specimen (series I).

ii. Vertical joint, vertically installed Waterstop specimen (series II).

iii. Vertical joint, horizontally installed waterstop specimen (series III).

Preparation of specimens

Sealing method of specimens

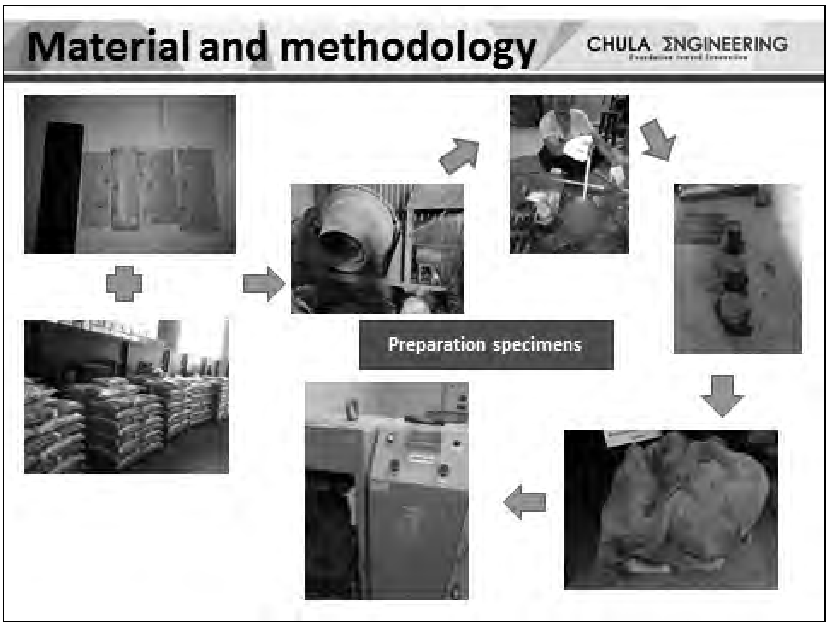

Material and methodology

Preparation specimens

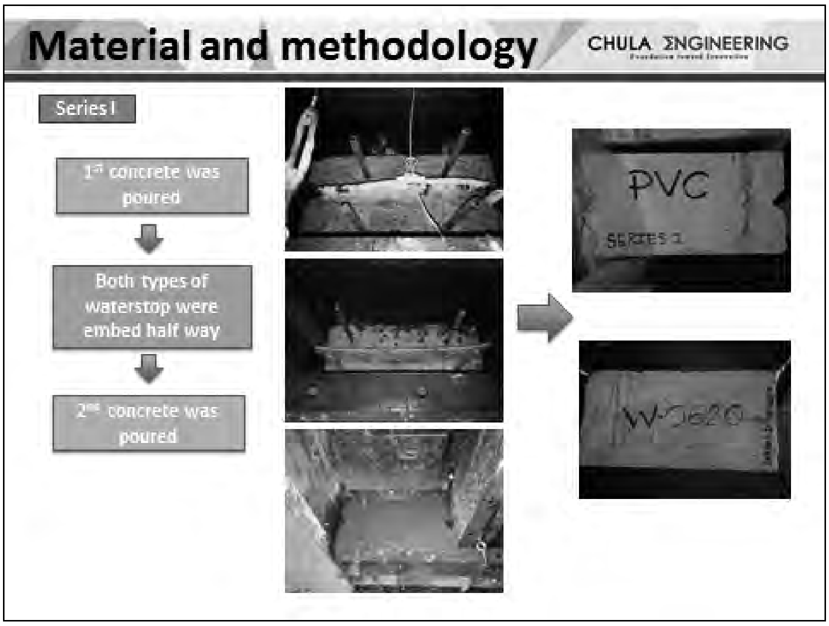

Material and methodology

Series I

1st concrete was poured

Both types of waterstop were embed half way

2nd concrete was poured

PVC
SERIES 1
W-3620

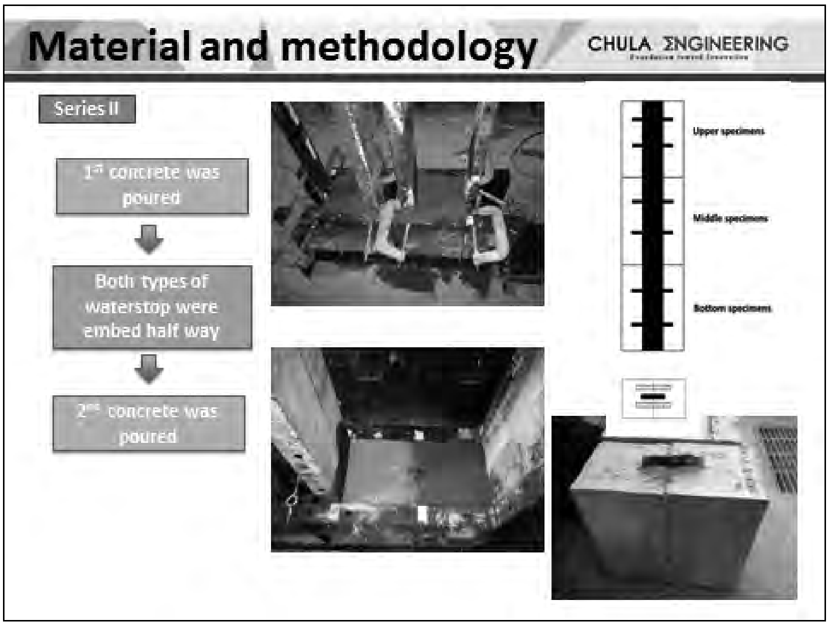

Material and methodology

Series II

1st concrete was poured

Both types of waterstop were embed half way

2nd concrete was poured

Upper specimens
Middle specimens
Bottom specimens

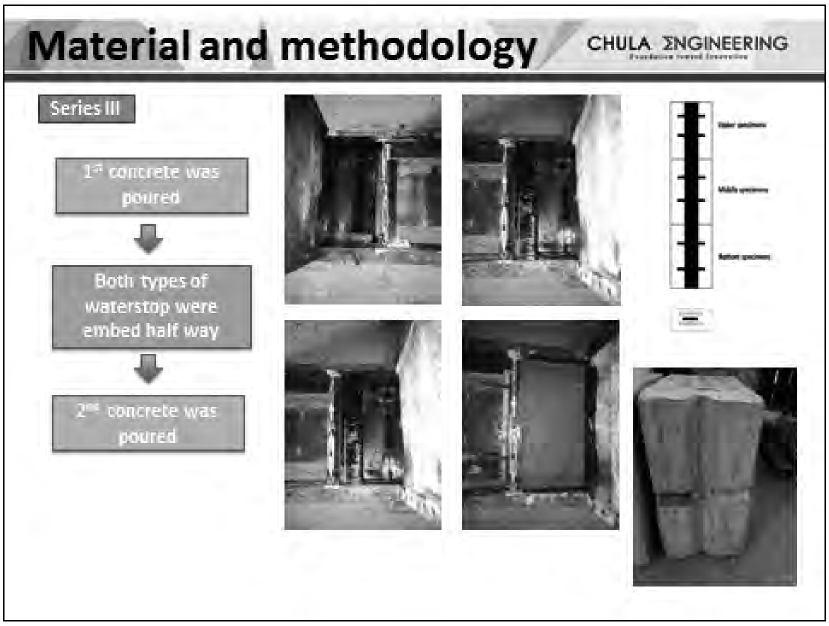

Material and methodology

CHULA ΣNGINEERING

Series III

1st concrete was poured

Both types of waterstop were embed half way

2nd concrete was poured

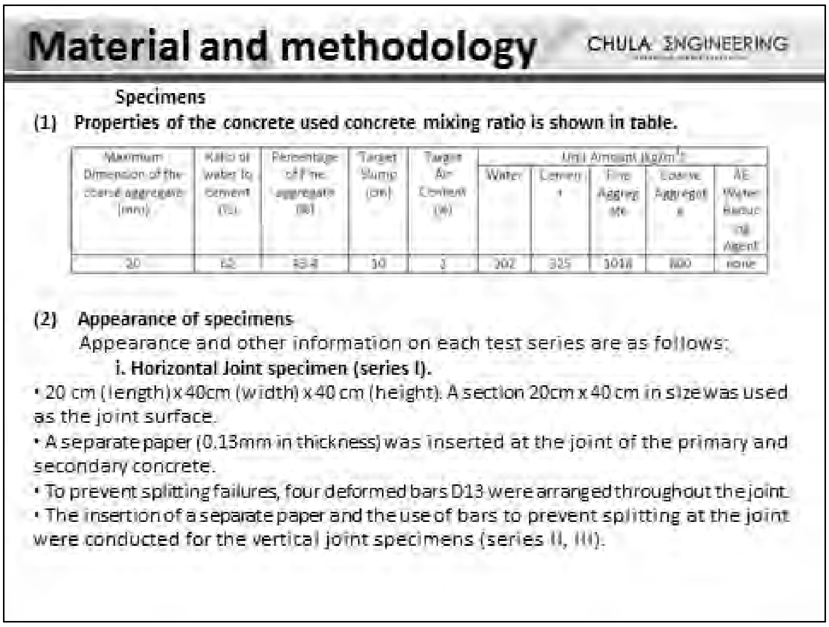

Material and methodology

CHULA ΣNGINEERING

Specimens

(1) Properties of the concrete used concrete mixing ratio is shown in table.

Maximum Dimension of the coarse aggregate (mm)	Ratio of water to cement (%)	Percentage of Fine aggregate (%)	Target Slump (cm)	Target Air Content (%)	Unit Amount (kg/m³)				
					Water	Cement	Fine Aggregate	Coarse Aggregate	AE Water Reducing Agent
20	62	43.4	10	2	202	325	1018	800	none

(2) Appearance of specimens

Appearance and other information on each test series are as follows:

i. Horizontal Joint specimen (series I).

- 20 cm (length) x 40cm (width) x 40 cm (height). A section 20cm x 40 cm in size was used as the joint surface.
- A separate paper (0.13mm in thickness) was inserted at the joint of the primary and secondary concrete.
- To prevent splitting failures, four deformed bars D13 were arranged throughout the joint.
- The insertion of a separate paper and the use of bars to prevent splitting at the joint were conducted for the vertical joint specimens (series II, III).

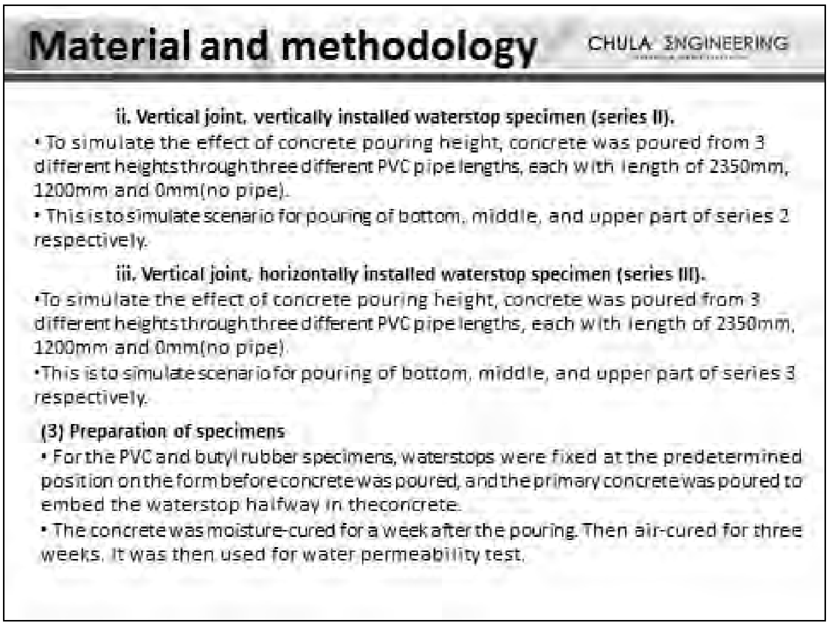

Material and methodology

CHULA ENGINEERING

ii. Vertical joint, vertically installed waterstop specimen (series II).

- To simulate the effect of concrete pouring height, concrete was poured from 3 different heights through three different PVC pipe lengths, each with length of 2350mm, 1200mm and 0mm(no pipe).
- This is to simulate scenario for pouring of bottom, middle, and upper part of series 2 respectively.

iii. Vertical joint, horizontally installed waterstop specimen (series III).

- To simulate the effect of concrete pouring height, concrete was poured from 3 different heights through three different PVC pipe lengths, each with length of 2350mm, 1200mm and 0mm(no pipe).
- This is to simulate scenario for pouring of bottom, middle, and upper part of series 3 respectively.

(3) Preparation of specimens

- For the PVC and butyl rubber specimens, waterstops were fixed at the predetermined position on the form before concrete was poured, and the primary concrete was poured to embed the waterstop halfway in the concrete.
- The concrete was moisture-cured for a week after the pouring. Then air-cured for three weeks. It was then used for water permeability test.

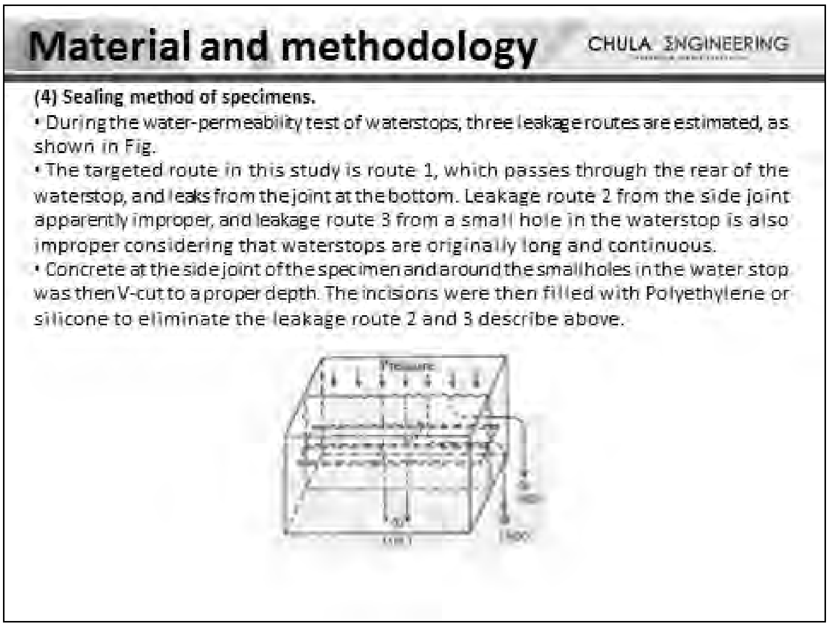

Material and methodology

CHULA ENGINEERING

(4) Sealing method of specimens.

- During the water-permeability test of waterstops, three leakage routes are estimated, as shown in Fig.
- The targeted route in this study is route 1, which passes through the rear of the waterstop, and leaks from the joint at the bottom. Leakage route 2 from the side joint apparently improper, and leakage route 3 from a small hole in the waterstop is also improper considering that waterstops are originally long and continuous.
- Concrete at the side joint of the specimen and around the small holes in the water stop was then V-cut to a proper depth. The incisions were then filled with Polyethylene or silicone to eliminate the leakage route 2 and 3 describe above.

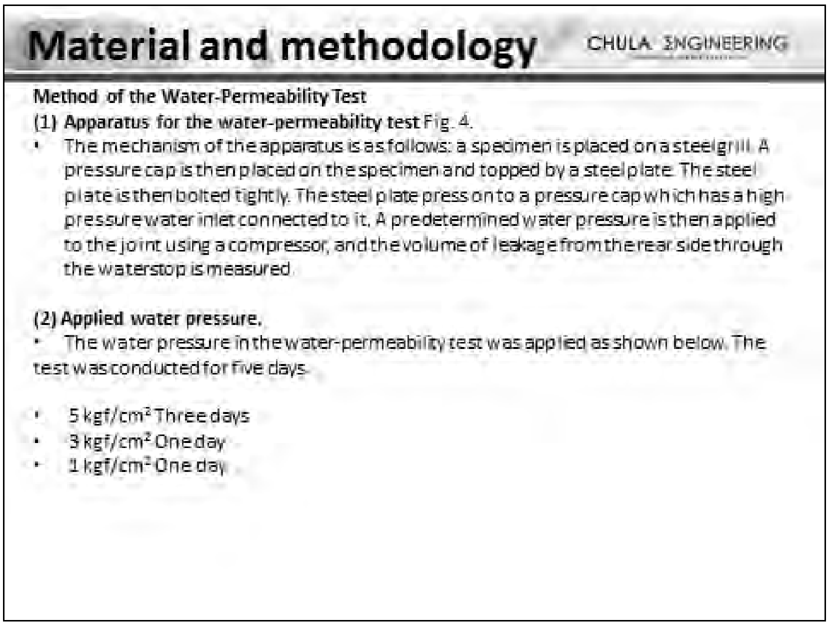

Material and methodology

CHULA ENGINEERING

Method of the Water-Permeability Test

(1) Apparatus for the water-permeability test Fig. 4.

- The mechanism of the apparatus is as follows: a specimen is placed on a steel grill. A pressure cap is then placed on the specimen and topped by a steel plate. The steel plate is then bolted tightly. The steel plate press on to a pressure cap which has a high pressure water inlet connected to it. A predetermined water pressure is then applied to the joint using a compressor, and the volume of leakage from the rear side through the waterstop is measured.

(2) Applied water pressure.

- The water pressure in the water-permeability test was applied as shown below. The test was conducted for five days.

- 5 kgf/cm² Three days
- 3 kgf/cm² One day
- 1 kgf/cm² One day

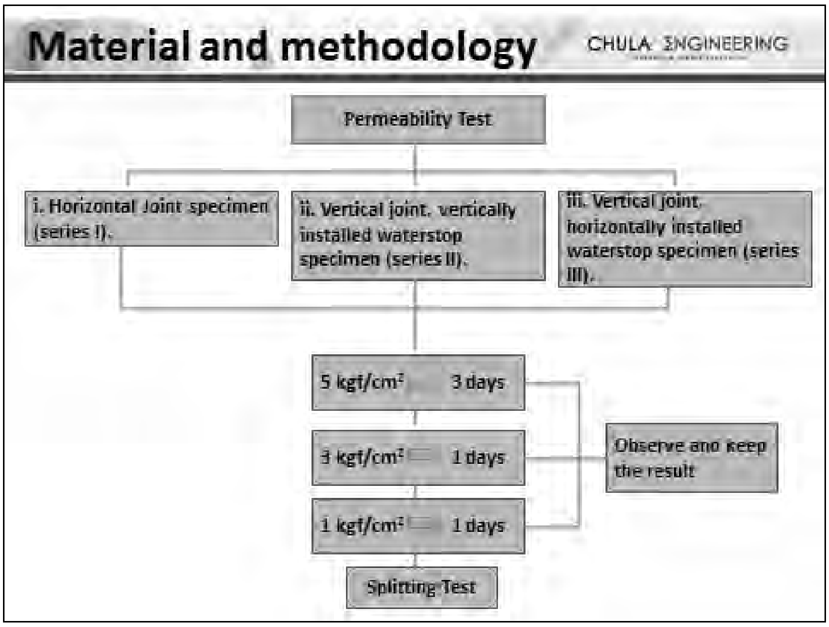

Material and methodology

CHULA ENGINEERING

Permeability Test
i. Horizontal Joint specimen (series I).
ii. Vertical joint, vertically installed waterstop specimen (series II).
iii. Vertical joint, horizontally installed waterstop specimen (series III).
5 kgf/cm² 3 days
3 kgf/cm² 1 days
1 kgf/cm² 1 days
Observe and keep the result
Splitting Test

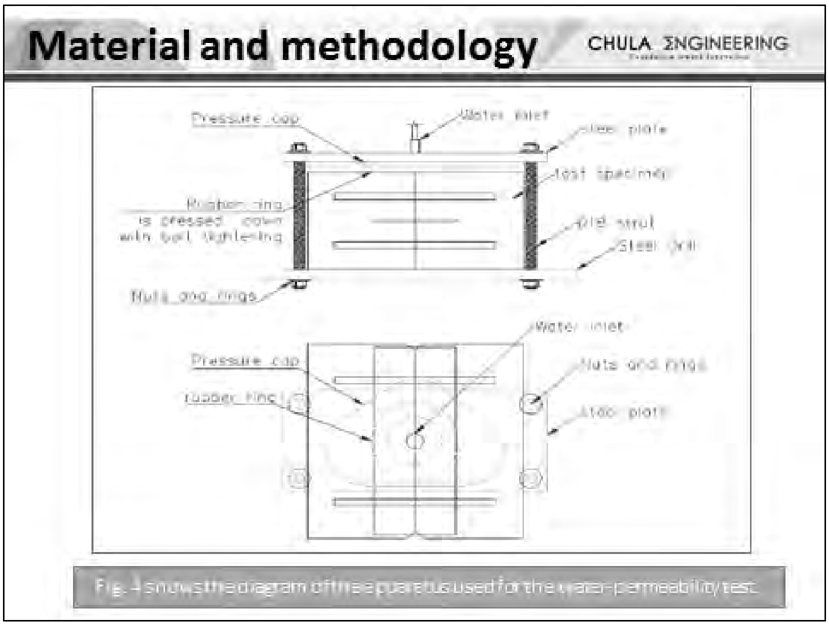

Material and methodology

CHULA ΣNGINEERING

Pressure cap
Water inlet
Steel plate
Test specimen
Rubber ring is pressed down with bolt tightening
Grid strut
Steel grill
Nuts and rings
Water inlet
Pressure cap
Nuts and rings
Rubber ring
Steel plate

Fig. 4 shows the diagram of the apparatus used for the water-permeability test.

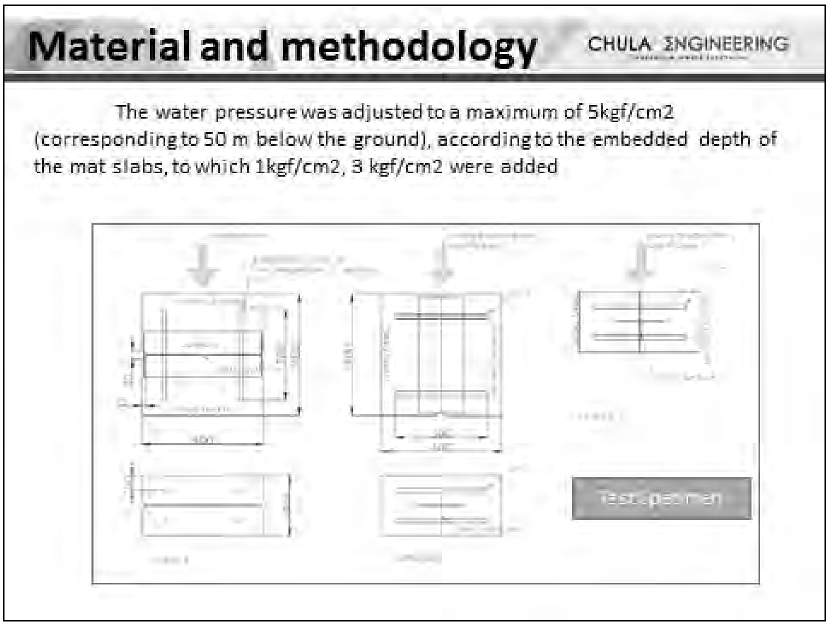

Material and methodology

CHULA ΣNGINEERING

The water pressure was adjusted to a maximum of 5kgf/cm2 (corresponding to 50 m below the ground), according to the embedded depth of the mat slabs, to which 1kgf/cm2, 3 kgf/cm2 were added

400
Test specimen

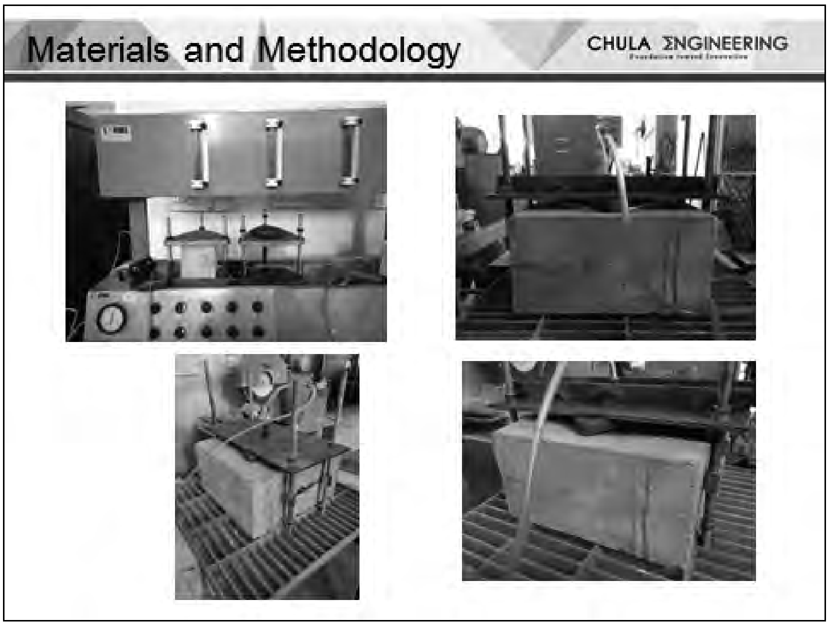
Materials and Methodology

CHULA ΣNGINEERING

Materials and Methodology

CHULA ΣNGINEERING
W 0620
PVC
SERIES II

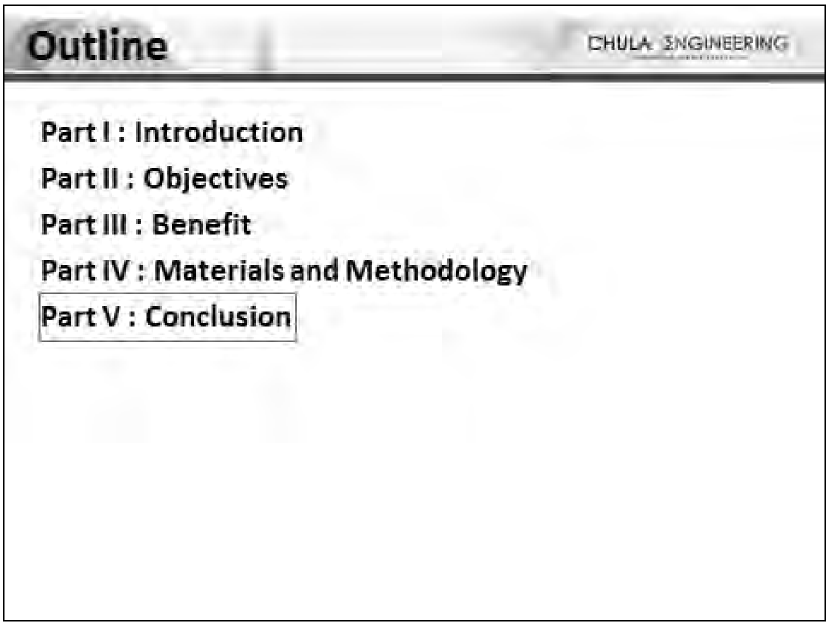

Outline

CHULA ΣNGINEERING

Part I : Introduction

Part II : Objectives

Part III : Benefit

Part IV : Materials and Methodology

Part V : Conclusion

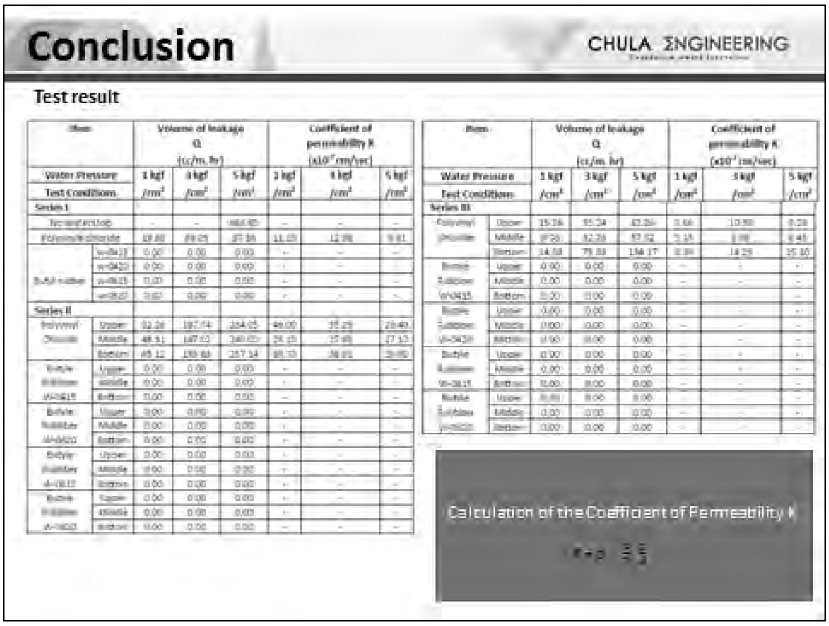

Conclusion

CHULA ΣNGINEERING

Test result

Calculation of the Coefficient of Permeability K

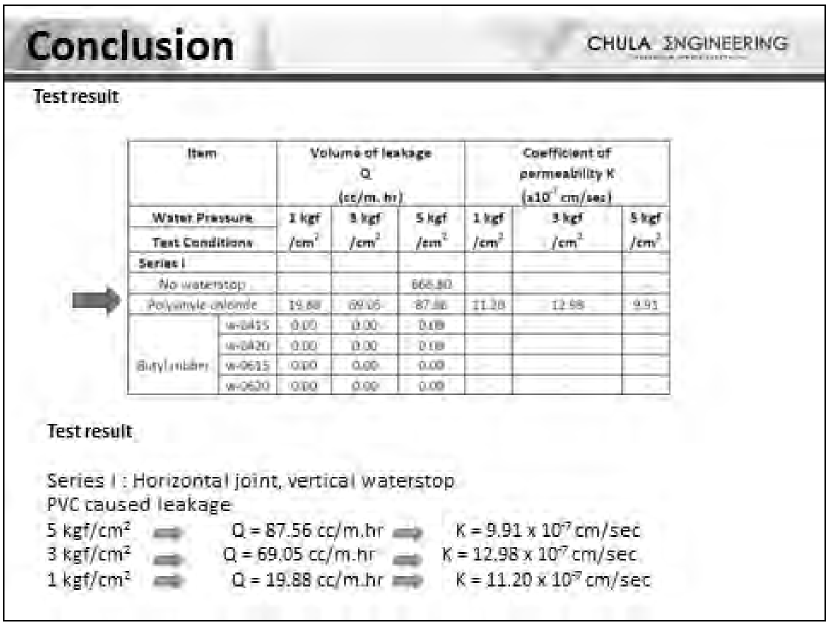

Conclusion

CHULA ΣNGINEERING

Test result

Item		Volume of leakage Q (cc/m. hr)			Coefficient of permeability K ($x10^{-7}$ cm/sec)		
Water Pressure Test Conditions		1 kgf /cm^2	3 kgf /cm^2	5 kgf /cm^2	1 kgf /cm^2	3 kgf /cm^2	5 kgf /cm^2
Series I							
No waterstop				666.80			
Polyvinyle chloride		19.88	69.05	87.56	11.20	12.98	9.91
Butyl rubber	w-0415	0.00	0.00	0.00	-		-
	w-0420	0.00	0.00	0.00	-		-
	w-0615	0.00	0.00	0.00	-		-
	w-0620	0.00	0.00	0.00	-		-

Test result

Series I : Horizontal joint, vertical waterstop
PVC caused leakage
5 kgf/cm^2 ⇒ Q = 87.56 cc/m.hr ⇒ K = 9.91 x 10^{-7} cm/sec
3 kgf/cm^2 ⇒ Q = 69.05 cc/m.hr ⇒ K = 12.98 x 10^{-7} cm/sec
1 kgf/cm^2 ⇒ Q = 19.88 cc/m.hr ⇒ K = 11.20 x 10^{-7} cm/sec

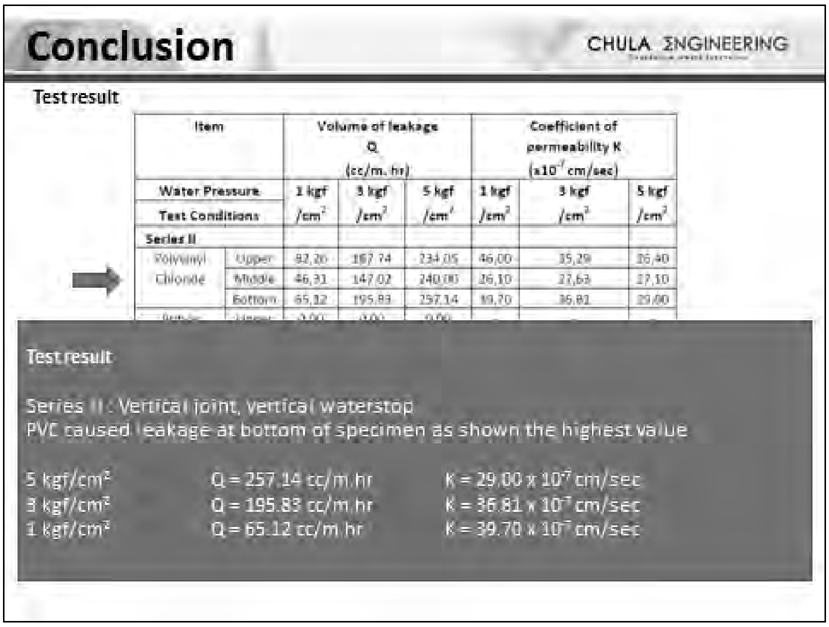

Conclusion

CHULA ΣNGINEERING

Test result

Item		Volume of leakage Q (cc/m. hr)			Coefficient of permeability K ($x10^{-7}$ cm/sec)		
Water Pressure Test Conditions		1 kgf /cm^2	3 kgf /cm^2	5 kgf /cm^2	1 kgf /cm^2	3 kgf /cm^2	5 kgf /cm^2
Series II							
Polyvinyl Chloride	Upper	82.20	167.74	234.05	46.00	35.29	26.40
	Middle	46.31	147.02	240.00	26.10	27.63	27.10
	Bottom	65.12	195.83	257.14	39.70	36.81	29.00
[illegible]	Upper	0.00	0.00	0.00	-	-	-

Test result

Series II : Vertical joint, vertical waterstop
PVC caused leakage at bottom of specimen as shown the highest value

5 kgf/cm^2 Q = 257.14 cc/m.hr K = 29.00 x 10^{-7} cm/sec
3 kgf/cm^2 Q = 195.83 cc/m.hr K = 36.81 x 10^{-7} cm/sec
1 kgf/cm^2 Q = 65.12 cc/m.hr K = 39.70 x 10^{-7} cm/sec

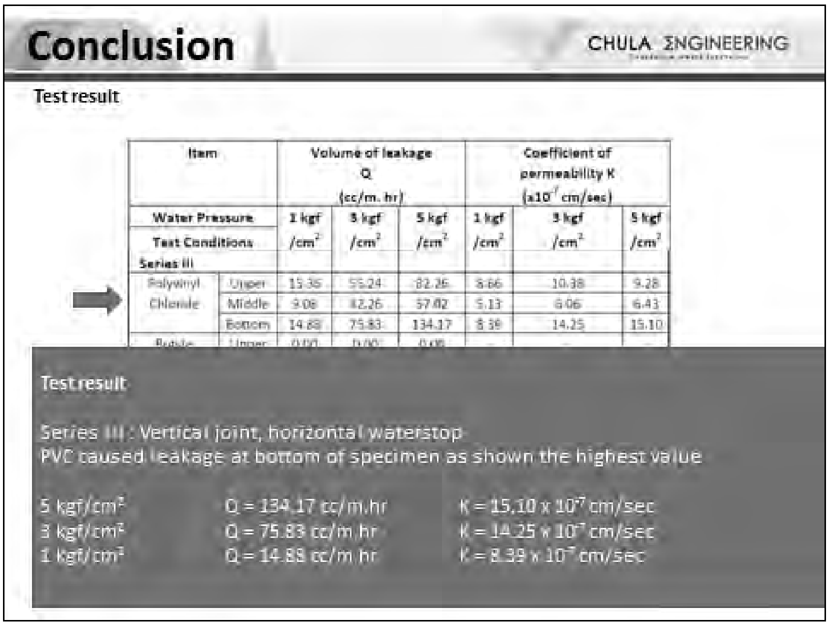

Conclusion

CHULA ΣNGINEERING

Test result

Item		Volume of leakage Q (cc/m. hr)			Coefficient of permeability K (x10^{-7} cm/sec)		
Water Pressure Test Conditions		1 kgf /cm^2	3 kgf /cm^2	5 kgf /cm^2	1 kgf /cm^2	3 kgf /cm^2	5 kgf /cm^2
Series III							
Polyvinyl Chloride	Upper	15.36	55.24	82.26	8.66	10.38	9.28
	Middle	9.08	32.26	57.02	5.13	6.06	6.43
	Bottom	14.88	75.83	134.17	8.39	14.25	15.10
Butyle	Upper	0.00	0.00	0.00	-	-	-

Test result

Series III : Vertical joint, horizontal waterstop
PVC caused leakage at bottom of specimen as shown the highest value

5 kgf/cm^2 Q = 134.17 cc/m.hr K = 15.10 x 10^{-7} cm/sec
3 kgf/cm^2 Q = 75.83 cc/m.hr K = 14.25 x 10^{-7} cm/sec
1 kgf/cm^2 Q = 14.88 cc/m.hr K = 8.39 x 10^{-7} cm/sec

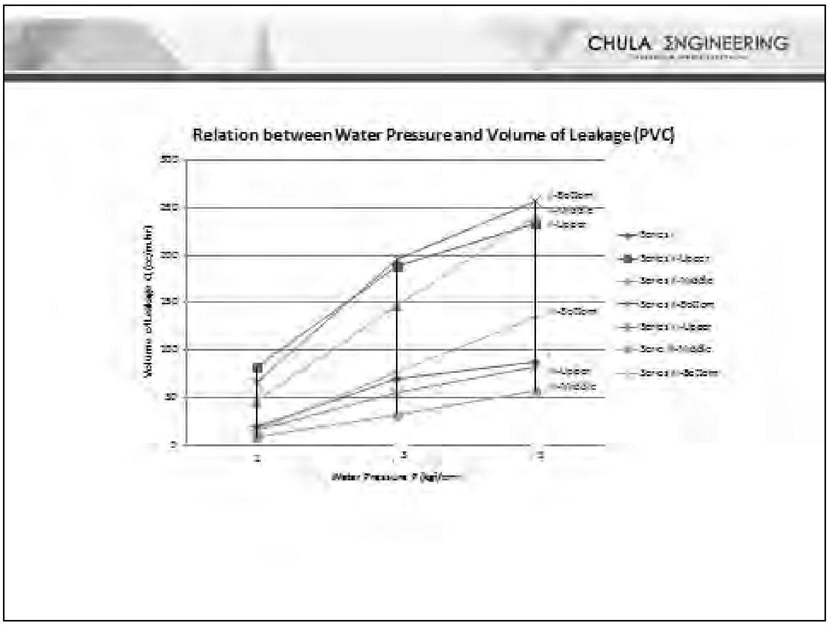

CHULA ΣNGINEERING

Relation between Water Pressure and Volume of Leakage (PVC)

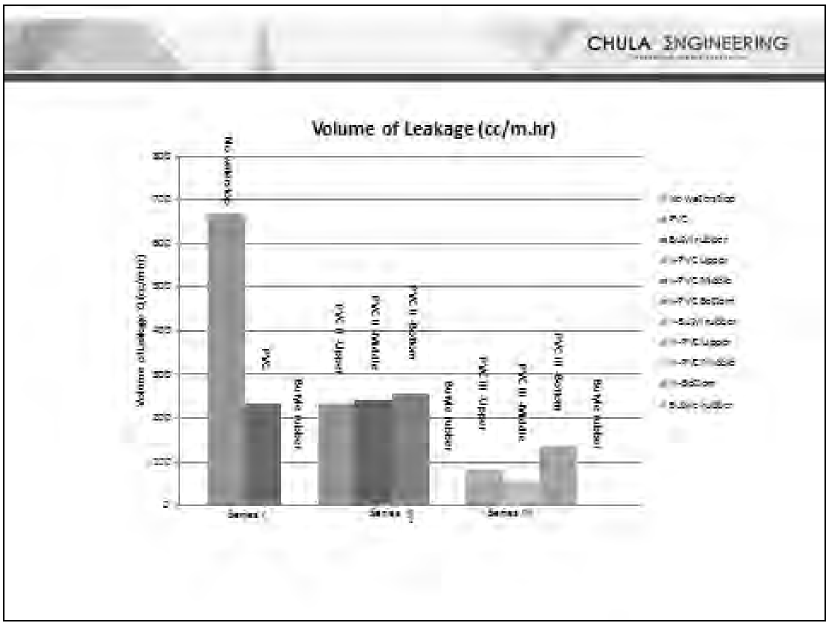
CHULA ƎNGINEERING

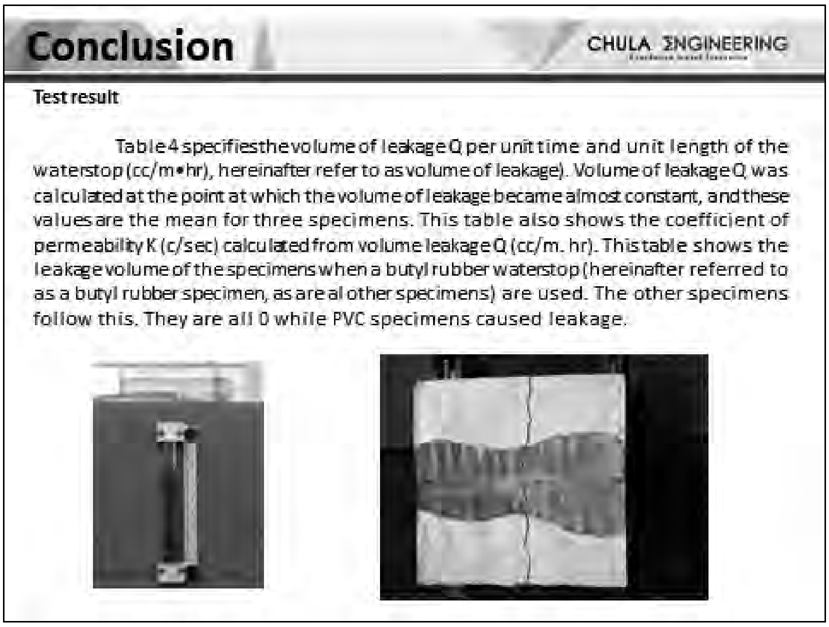
Conclusion

CHULA ƎNGINEERING

Test result

Table 4 specifies the volume of leakage Q per unit time and unit length of the waterstop (cc/m•hr), hereinafter refer to as volume of leakage). Volume of leakage Q was calculated at the point at which the volume of leakage became almost constant, and these values are the mean for three specimens. This table also shows the coefficient of permeability K (c/sec) calculated from volume leakage Q (cc/m. hr). This table shows the leakage volume of the specimens when a butyl rubber waterstop (hereinafter referred to as a butyl rubber specimen, as are al other specimens) are used. The other specimens follow this. They are all 0 while PVC specimens caused leakage.

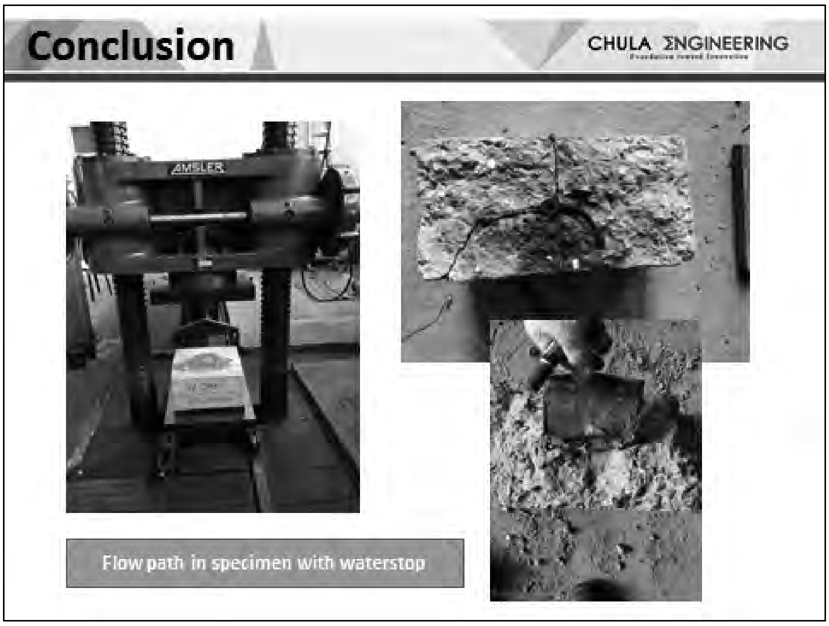

Conclusion

CHULA ΣNGINEERING
AMSLER

Flow path in specimen with waterstop

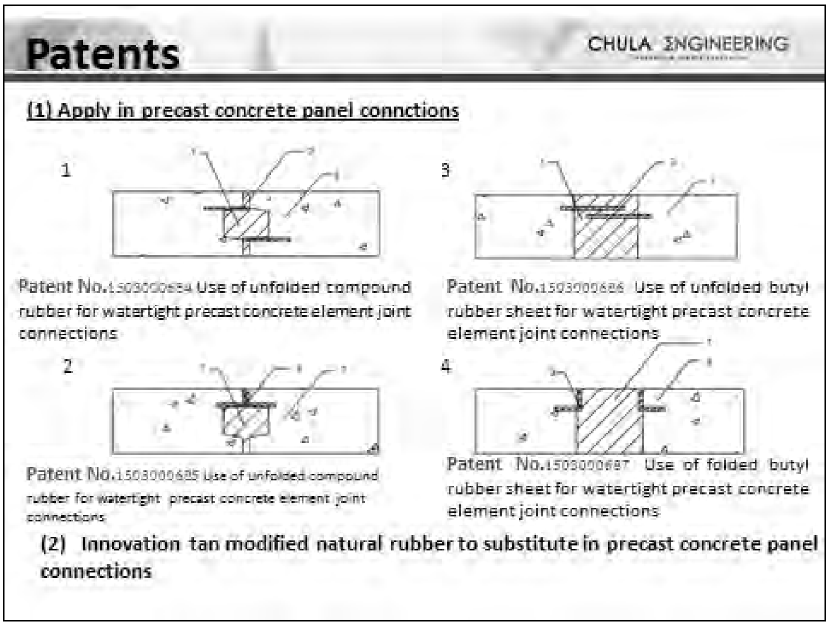

Patents

CHULA ΣNGINEERING

(1) Apply in precast concrete panel connctions

1

Patent No.1503000684 Use of unfolded compound rubber for watertight precast concrete element joint connections

2

Patent No.1503000685 Use of unfolded compound rubber for watertight precast concrete element joint connections

3

Patent No.1503000686 Use of unfolded butyl rubber sheet for watertight precast concrete element joint connections

4

Patent No.1503000687 Use of folded butyl rubber sheet for watertight precast concrete element joint connections

(2) Innovation tan modified natural rubber to substitute in precast concrete panel connections

CHULA ΣNGINEERING

Any Question ???

THANK YOU
FOR YOUR ATTENTION

NEAR-REAL TIME METEOROLOGICAL DROUGHT MONITORING AND EARLY WARNING SYSTEM FOR CROPLANDS IN ASIA

Wataru Takeuchi[1], Soni Darmawan[1,2], Rizatus Shofiyati[3], Mai Van Khiem[4], Kyaw San Oo[5], Uday Pimple[6] and Suthy Heng[7]

[1]Institute of Industrial Science, The University of Tokyo
6-1, Komaba 4-chome, Meguro, Tokyo 153-8505 JAPAN
E-mail:wataru@iis.u-tokyo.ac.jp

[2]Center for Remote Sensing, Institut Teknologi Bandung (ITB), Indonesia

[3]Indonesian Center for Agricultural Land Resources Research and Development (ICALRD), Indonesia

[4]Institute of Meteorology, Hydrology and Environment (IMHEN), Vietnam

[5]Myanmar Geospatial and Resource Program (MGRP),
Myanmar Peace Center (MPC), Myanmar

[6]King Mongkut's University of Technology (KMUTT), Thailand

[7]Mekong River Commission (MRC), Cambodia

ABSTRACT

This research focuses on a development of satellite-based drought monitoring warning system for croplands in Asian countries. Drought condition of cropland is evaluated by using Keeth- Byram Drought Index (KBDI) computed from rainfall measurements with GSMaP product, land surface temperature by MTSAT product and vegetation phenology by MODIS NDVI product at daily basis. The derived information is disseminated as a system for an application of space based technology (SBT) in the implementation of the Core Agriculture Support Program. The benefit of this system are to develop satellite-based drought monitoring and early warning system in Asian counties using freely available data, and to develop capacity of policy makers in those countries to apply the developed system in policy making. A series of training program has been carried out in 2013 and 2014 to officers and researchers of ministry of agriculture and relevant agencies in Greater Mekong Subregion countries including Cambodia, China, Myanmar, Laos, Thailand, Vietnam and Indonesia. This system is running as fully operational and can be accessed at http://wtlab.iis.u-tokyo.ac.jp/DMEWS/.

Keywords: *KBDI, yield estimation, land surface temperature, rainfall*

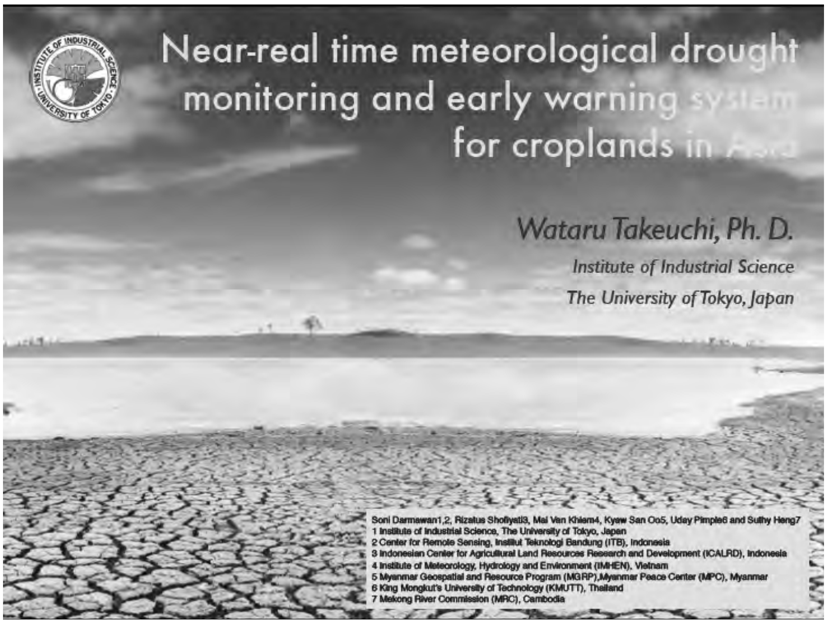

Near-real time meteorological drought monitoring and early warning system for croplands in Asia

Wataru Takeuchi, Ph. D.

Institute of Industrial Science
The University of Tokyo, Japan

Soni Darmawan1,2, Rizatus Shofiyati3, Mai Van Khiem4, Kyaw San Oo5, Uday Pimple6 and Suthy Heng7
1 Institute of Industrial Science, The University of Tokyo, Japan
2 Center for Remote Sensing, Institut Teknologi Bandung (ITB), Indonesia
3 Indonesian Center for Agricultural Land Resources Research and Development (ICALRD), Indonesia
4 Institute of Meteorology, Hydrology and Environment (IMHEN), Vietnam
5 Myanmar Geospatial and Resource Program (MGRP),Myanmar Peace Center (MPC), Myanmar
6 King Mongkut's University of Technology (KMUTT), Thailand
7 Mekong River Commission (MRC), Cambodia

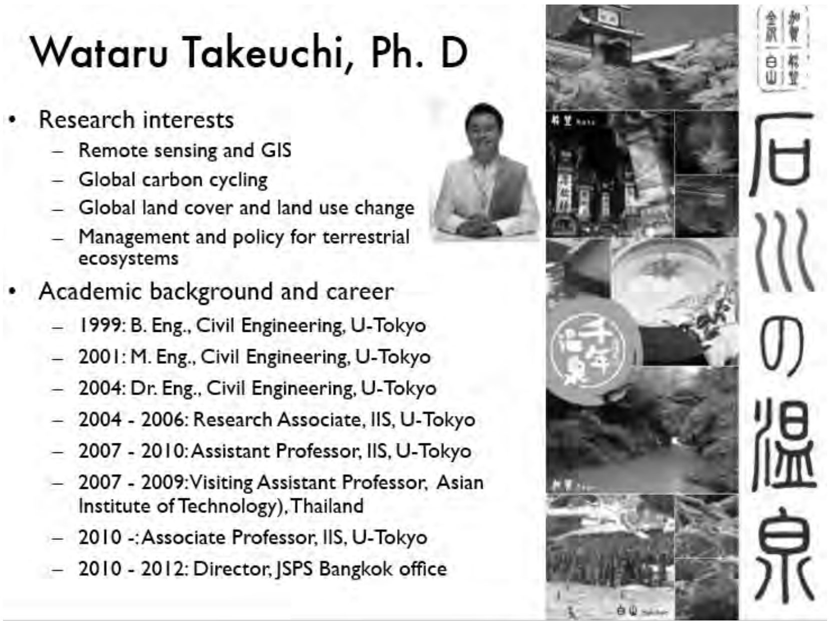

Wataru Takeuchi, Ph. D

- Research interests
    - Remote sensing and GIS
    - Global carbon cycling
    - Global land cover and land use change
    - Management and policy for terrestrial ecosystems
- Academic background and career
    - 1999: B. Eng., Civil Engineering, U-Tokyo
    - 2001: M. Eng., Civil Engineering, U-Tokyo
    - 2004: Dr. Eng., Civil Engineering, U-Tokyo
    - 2004 - 2006: Research Associate, IIS, U-Tokyo
    - 2007 - 2010: Assistant Professor, IIS, U-Tokyo
    - 2007 - 2009: Visiting Assistant Professor, Asian Institute of Technology), Thailand
    - 2010 -: Associate Professor, IIS, U-Tokyo
    - 2010 - 2012: Director, JSPS Bangkok office

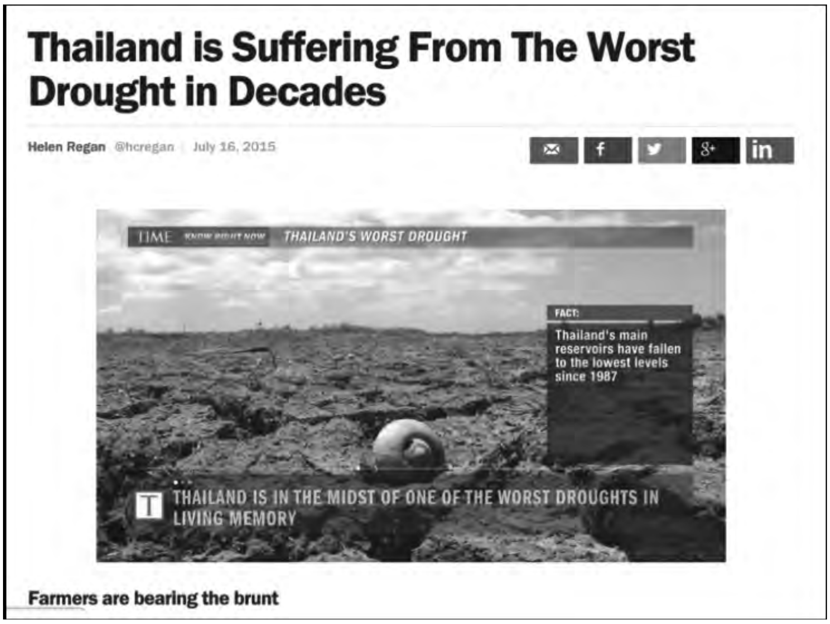

Thailand is Suffering From The Worst Drought in Decades

Helen Regan @hcregan | July 16, 2015

TIME
KNOW RIGHT NOW
THAILAND'S WORST DROUGHT
FACT:
Thailand's main reservoirs have fallen to the lowest levels since 1987
THAILAND IS IN THE MIDST OF ONE OF THE WORST DROUGHTS IN LIVING MEMORY

Farmers are bearing the brunt

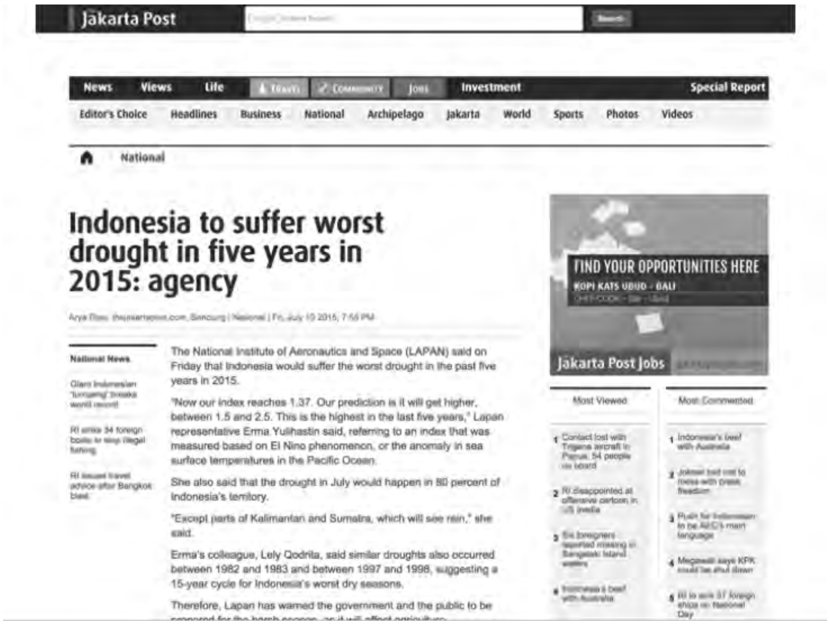

Jakarta Post
Search
News
Views
Life
Travel
Community
Jobs
Investment
Special Report
Editor's Choice
Headlines
Business
National
Archipelago
Jakarta
World
Sports
Photos
Videos
National
National News
FIND YOUR OPPORTUNITIES HERE
KOPI KATS UBUD - BALI
Jakarta Post Jobs
Most Viewed
Most Commented

Indonesia to suffer worst drought in five years in 2015: agency

The National Institute of Aeronautics and Space (LAPAN) said on Friday that Indonesia would suffer the worst drought in the past five years in 2015.

"Now our index reaches 1.37. Our prediction is it will get higher, between 1.5 and 2.5. This is the highest in the last five years," Lapan representative Erma Yulihastin said, referring to an index that was measured based on El Nino phenomenon, or the anomaly in sea surface temperatures in the Pacific Ocean.

She also said that the drought in July would happen in 80 percent of Indonesia's territory.

"Except parts of Kalimantan and Sumatra, which will see rain," she said.

Erma's colleague, Lely Qodrita, said similar droughts also occurred between 1982 and 1983 and between 1997 and 1998, suggesting a 15-year cycle for Indonesia's worst dry seasons.

Therefore, Lapan has warned the government and the public to be

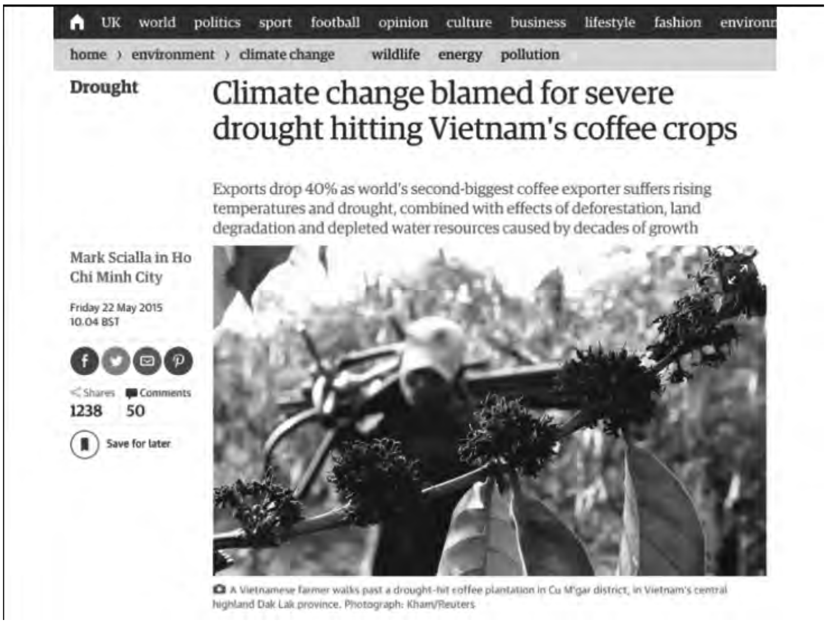
UK
world
politics
sport
football
opinion
culture
business
lifestyle
fashion
environm
home › environment › climate change
wildlife
energy
pollution
f
P
Shares
Comments
Save for later

Drought

Climate change blamed for severe drought hitting Vietnam's coffee crops

Exports drop 40% as world's second-biggest coffee exporter suffers rising temperatures and drought, combined with effects of deforestation, land degradation and depleted water resources caused by decades of growth

Mark Scialla in Ho Chi Minh City

Friday 22 May 2015
10.04 BST

Shares 1238 Comments 50

A Vietnamese farmer walks past a drought-hit coffee plantation in Cu M'gar district, in Vietnam's central highland Dak Lak province. Photograph: Kham/Reuters

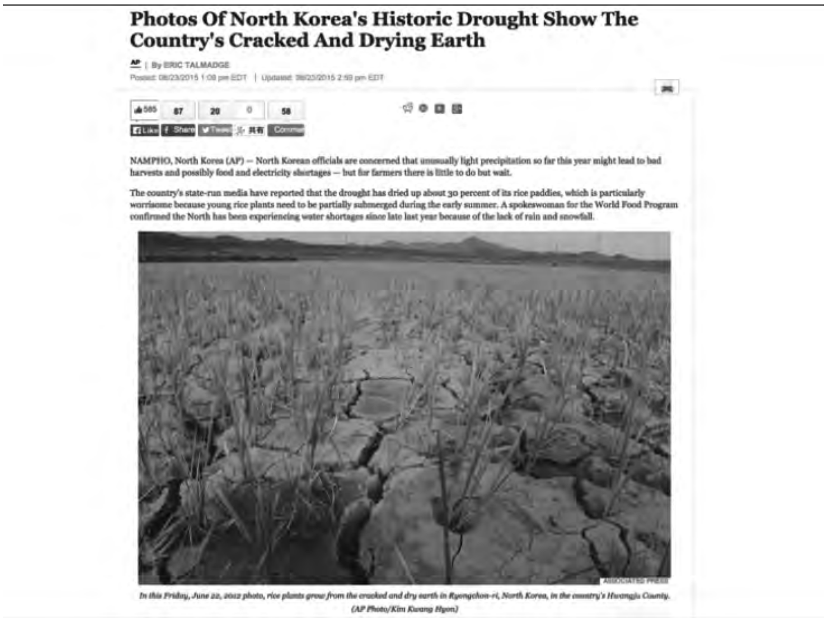
AP
585
87
20
0
58
Like
Share
Tweet
共有
Comme
ASSOCIATED PRESS

Photos Of North Korea's Historic Drought Show The Country's Cracked And Drying Earth

By ERIC TALMADGE

Posted: 08/23/2015 1:08 pm EDT | Updated: 08/23/2015 2:59 pm EDT

NAMPHO, North Korea (AP) — North Korean officials are concerned that unusually light precipitation so far this year might lead to bad harvests and possibly food and electricity shortages — but for farmers there is little to do but wait.

The country's state-run media have reported that the drought has dried up about 30 percent of its rice paddies, which is particularly worrisome because young rice plants need to be partially submerged during the early summer. A spokeswoman for the World Food Program confirmed the North has been experiencing water shortages since late last year because of the lack of rain and snowfall.

In this Friday, June 22, 2012 photo, rice plants grow from the cracked and dry earth in Ryongchon-ri, North Korea, in the country's Hwangju County. (AP Photo/Kim Kwang Hyon)

Asia and Africa are very prone to natural disasters

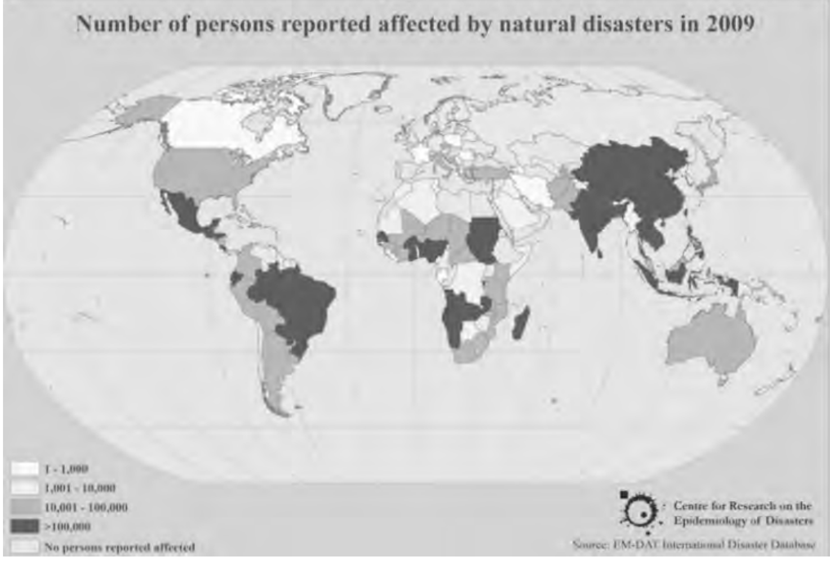
Number of persons reported affected by natural disasters in 2009
1 - 1,000
1,001 - 10,000
10,001 - 100,000
>100,000
No persons reported affected
Centre for Research on the Epidemiology of Disasters

Source: EM-DAT International Disaster Database

Rapid population increase in Asia and Africa

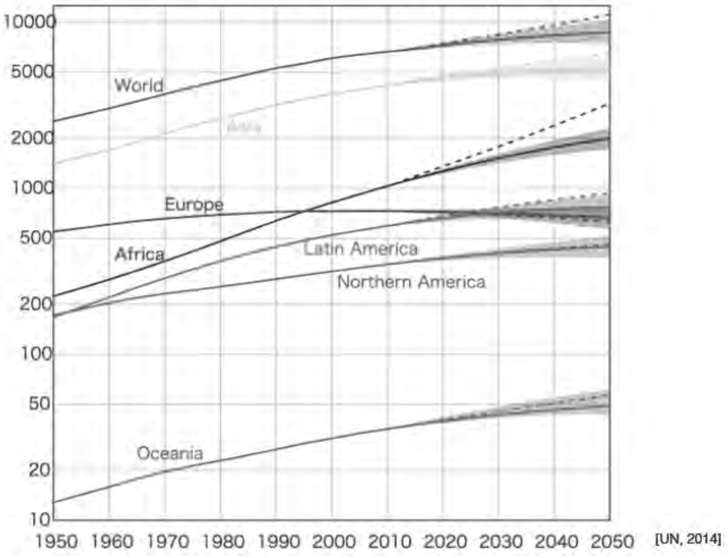

[UN, 2014]

Natural disaster classification

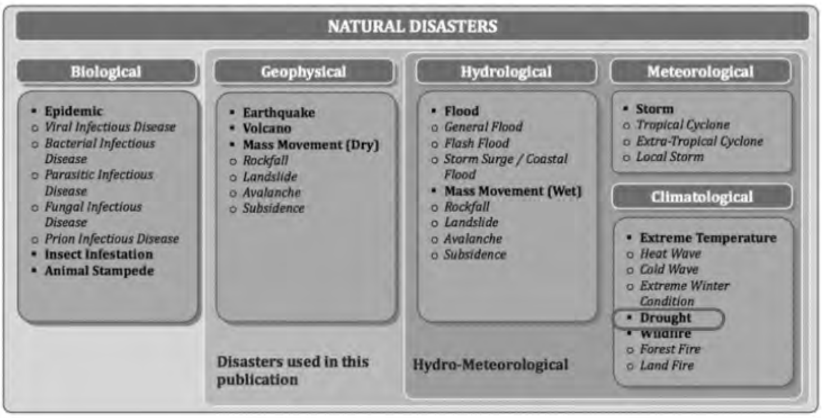

NATURAL DISASTERS

Biological

- **Epidemic**
  - *Viral Infectious Disease*
  - *Bacterial Infectious Disease*
  - *Parasitic Infectious Disease*
  - *Fungal Infectious Disease*
  - *Prion Infectious Disease*
- **Insect Infestation**
- **Animal Stampede**

Geophysical

- **Earthquake**
- **Volcano**
- **Mass Movement (Dry)**
  - *Rockfall*
  - *Landslide*
  - *Avalanche*
  - *Subsidence*

Hydrological

- **Flood**
  - *General Flood*
  - *Flash Flood*
  - *Storm Surge / Coastal Flood*
- **Mass Movement (Wet)**
  - *Rockfall*
  - *Landslide*
  - *Avalanche*
  - *Subsidence*

Meteorological

- **Storm**
  - *Tropical Cyclone*
  - *Extra-Tropical Cyclone*
  - *Local Storm*

Climatological

- **Extreme Temperature**
  - *Heat Wave*
  - *Cold Wave*
  - *Extreme Winter Condition*
- **Drought**
- **Wildfire**
  - *Forest Fire*
  - *Land Fire*

Disasters used in this publication

Hydro-Meteorological

[EMDAT, 2009]

Types of droughts

Meteorological Drought

Agricultural Drought

Hydrological Drought

Socioeconomic Drought

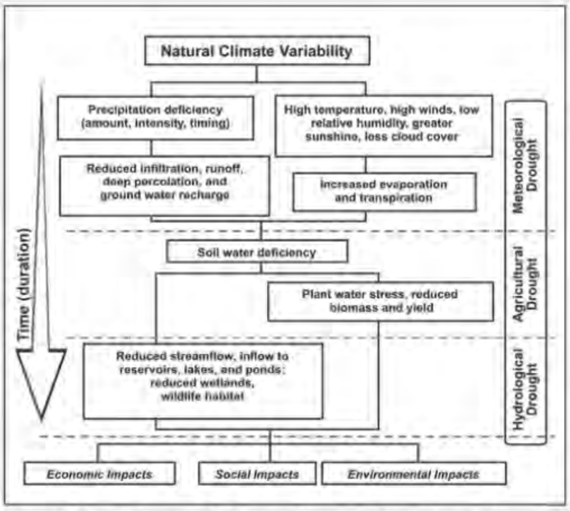
Natural Climate Variability
Precipitation deficiency (amount, intensity, timing)
High temperature, high winds, low relative humidity, greater sunshine, less cloud cover
Reduced infiltration, runoff, deep percolation, and ground water recharge
Increased evaporation and transpiration
Soil water deficiency
Plant water stress, reduced biomass and yield
Reduced streamflow, inflow to reservoirs, lakes, and ponds; reduced wetlands, wildlife habitat
Economic Impacts
Social Impacts
Environmental Impacts
Time (duration)
Meteorological Drought
Agricultural Drought
Hydrological Drought

Sequence of drought occurrence and impacts for commonly accepted drought types. All droughts originate from a deficiency of precipitation or meteorological drought but other types of drought and impacts cascade from this deficiency. (*Source*: National Drought Mitigation Center, University of Nebraska-Lincoln, U.S.A.)

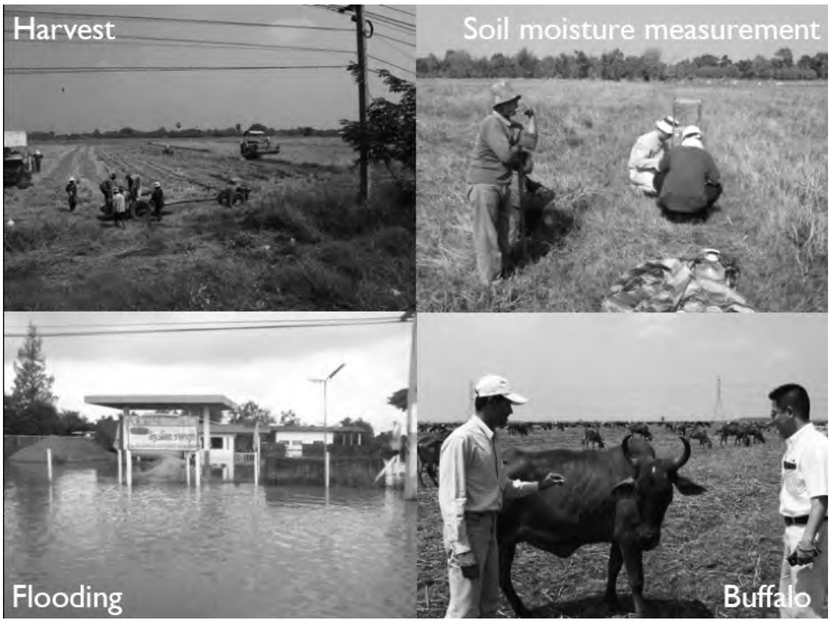
Harvest
Soil moisture measurement
Flooding
Buffalo

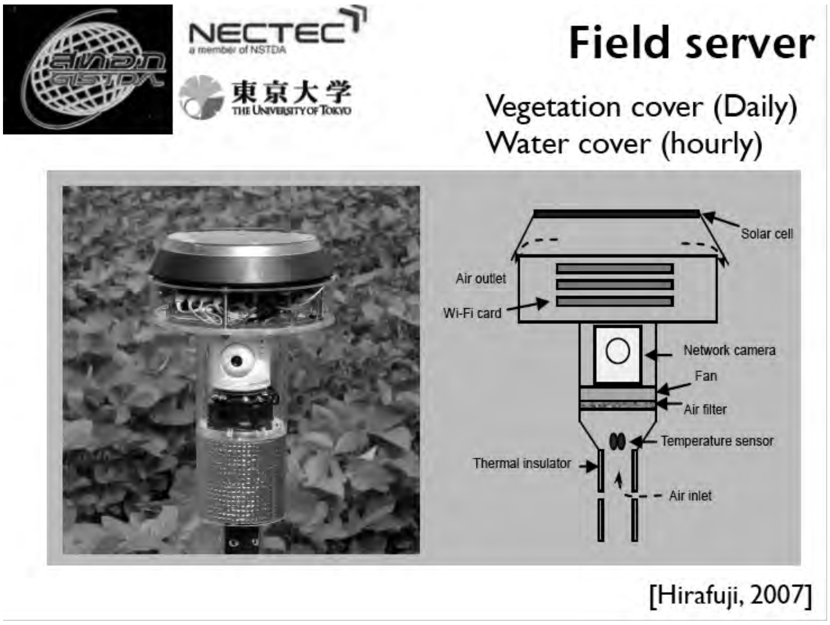
NECTEC
a member of NSTDA
東京大学
THE UNIVERSITY OF TOKYO
Solar cell
Air outlet
Wi-Fi card
Network camera
Fan
Air filter
Temperature sensor
Thermal insulator
Air inlet

Field server

Vegetation cover (Daily)
Water cover (hourly)

[Hirafuji, 2007]

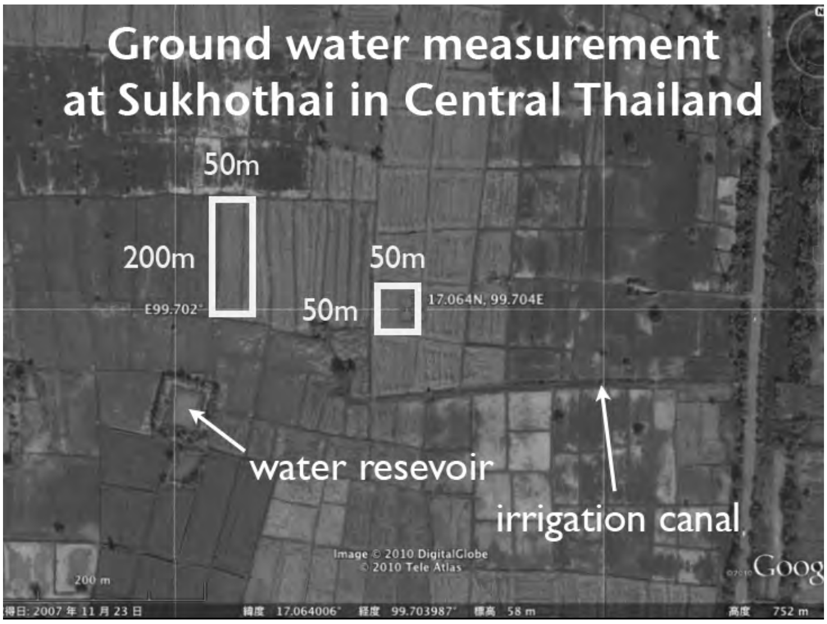

Ground water measurement at Sukhothai in Central Thailand

50m
200m
50m
50m
E99.702°
17.064N, 99.704E
water resevoir
irrigation canal
Image © 2010 DigitalGlobe
© 2010 Tele Atlas
200 m
©2010 Goog
得日: 2007 年 11 月 23 日
緯度 17.064006°
経度 99.703987°
標高 58 m
高度 752 m

Rice field in Khon Kaen
(Oct. 8, 2011 to Nov. 8, 2011)

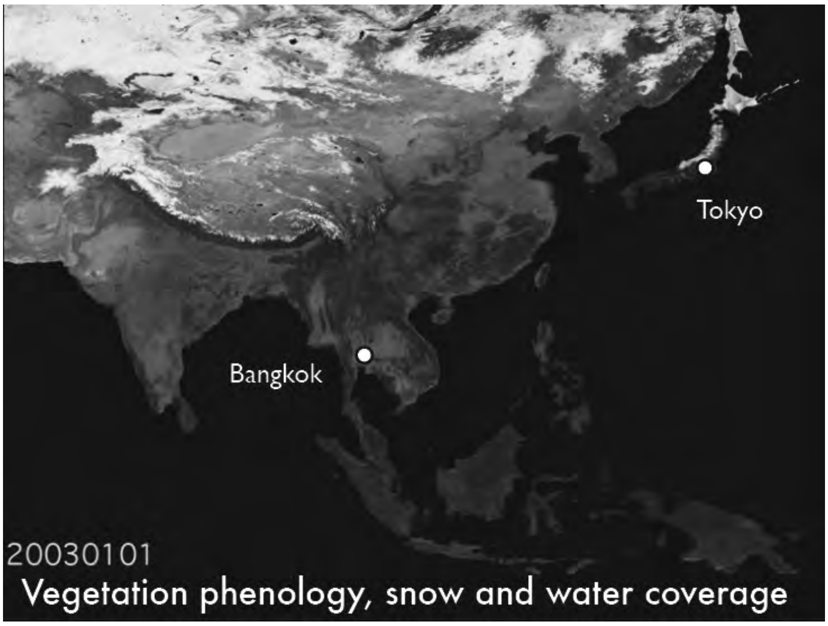

Vegetation phenology, snow and water coverage

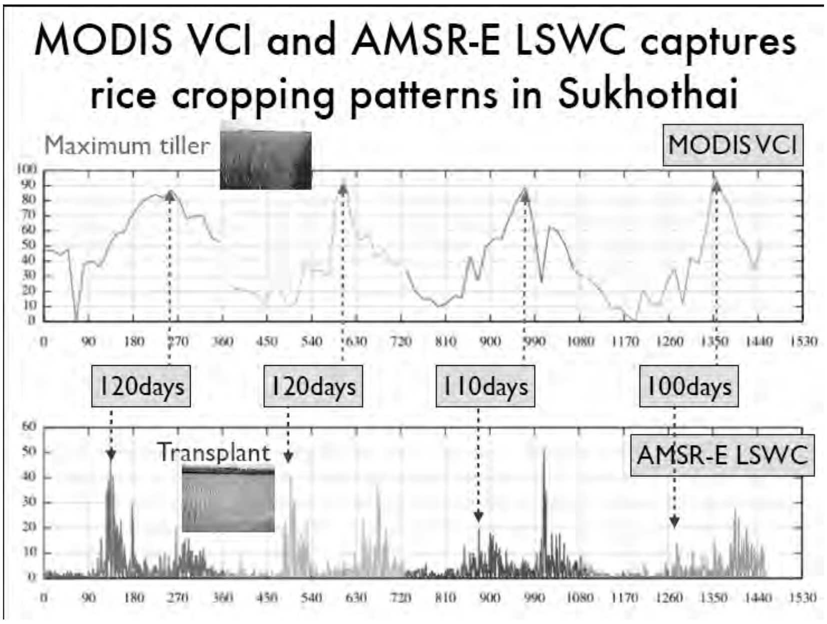

MODIS VCI and AMSR-E LSWC captures rice cropping patterns in Sukhothai

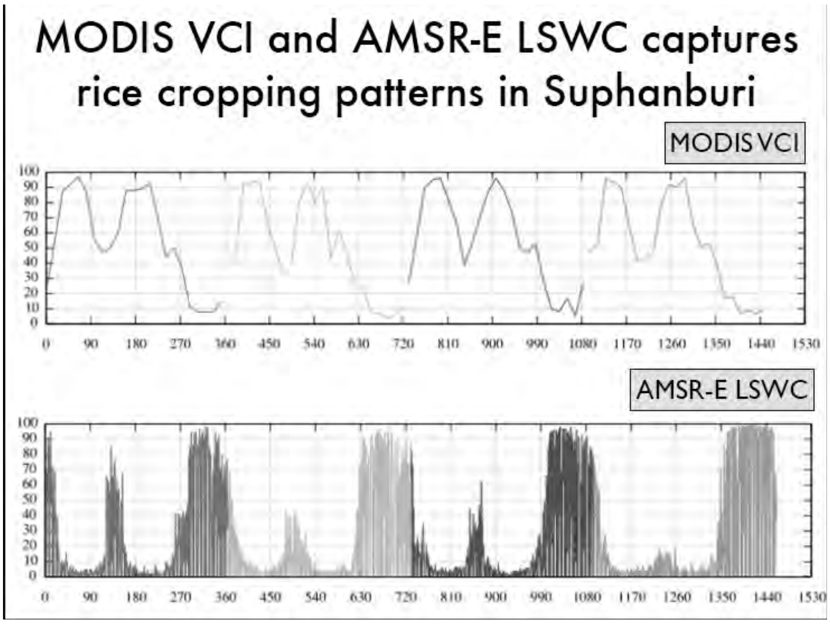

MODIS VCI and AMSR-E LSWC captures rice cropping patterns in Suphanburi

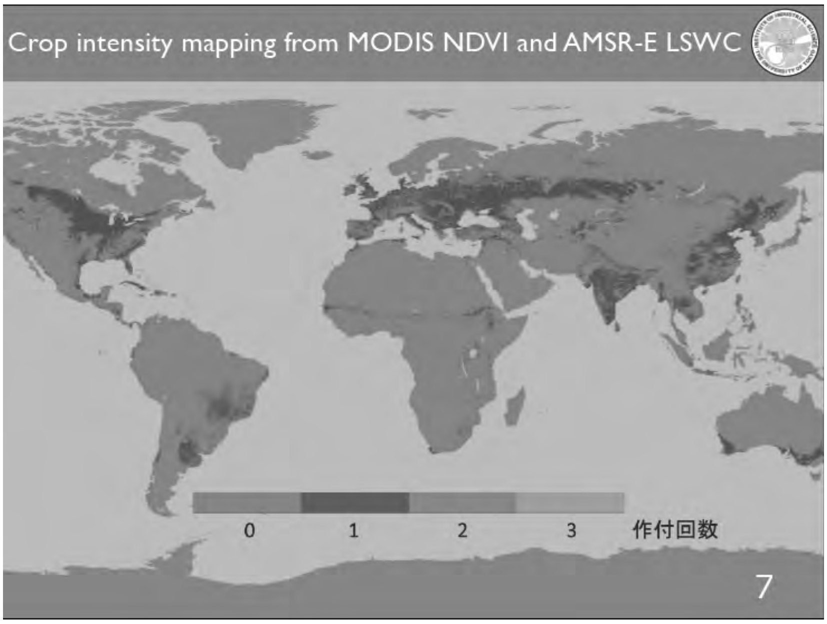

Crop intensity mapping from MODIS NDVI and AMSR-E LSWC

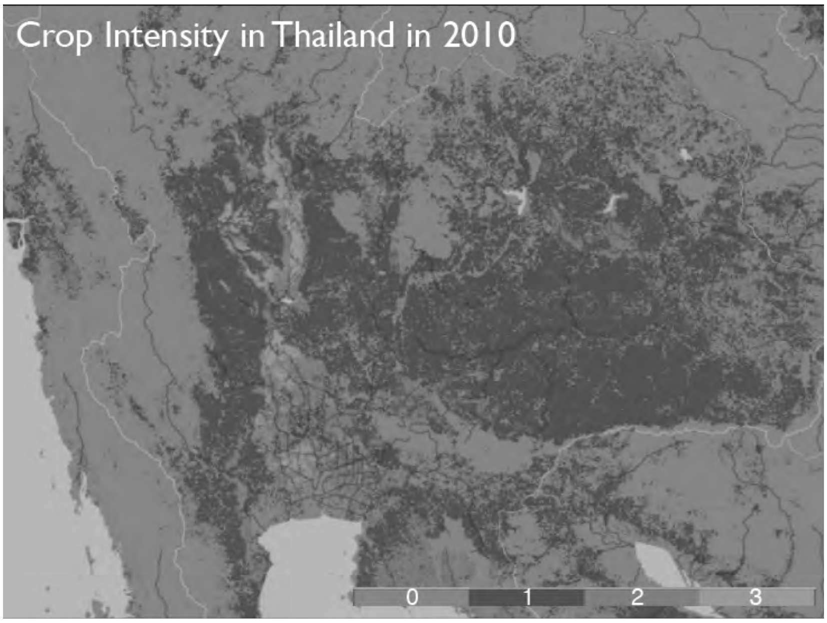

Crop Intensity in Thailand in 2010

Surface water storage and flow

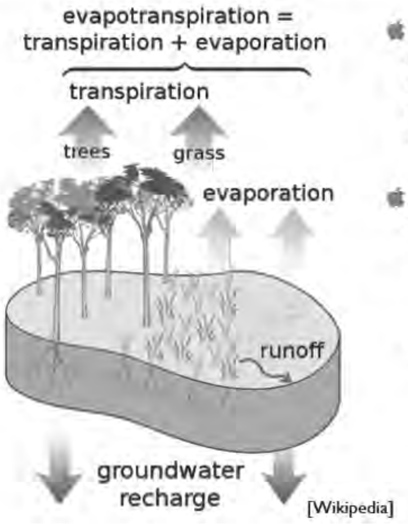
evapotranspiration =
transpiration + evaporation
transpiration
trees
grass
evaporation
runoff
groundwater
recharge

[Wikipedia]

- KBDI index are used to compute the balance between evapotranspiration and precipitation. [Keetch et. *al*, 1965]
- Presently, this index is derived from satellite observation:
  - land surface temperature (LST) from MTSAT received at IIS/U-Tokyo
  - rainfall from global satellite mapping (GSMaP) provided by JAXA EROC.

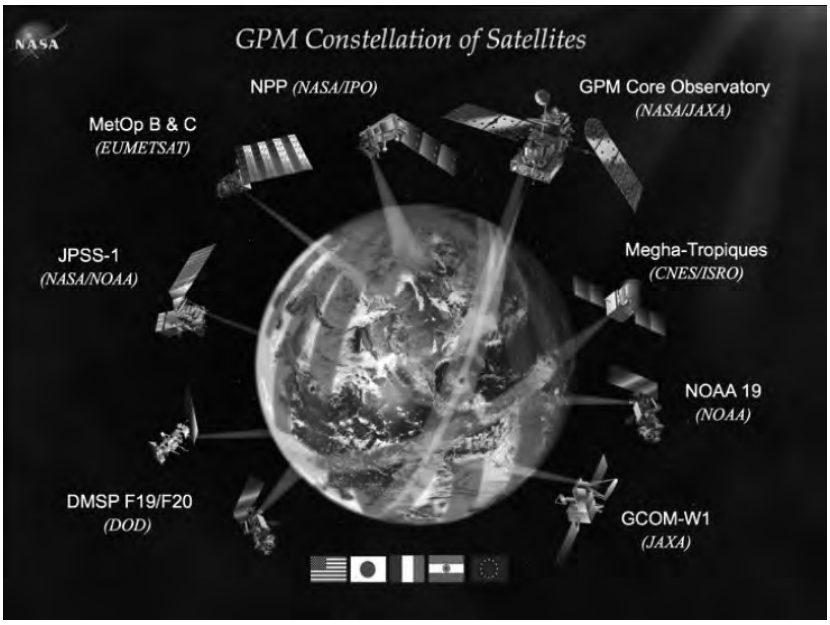

GPM Constellation of Satellites

NASA
NPP (NASA/IPO)
GPM Core Observatory (NASA/JAXA)
MetOp B & C (EUMETSAT)
JPSS-1 (NASA/NOAA)
Megha-Tropiques (CNES/ISRO)
NOAA 19 (NOAA)
DMSP F19/F20 (DOD)
GCOM-W1 (JAXA)

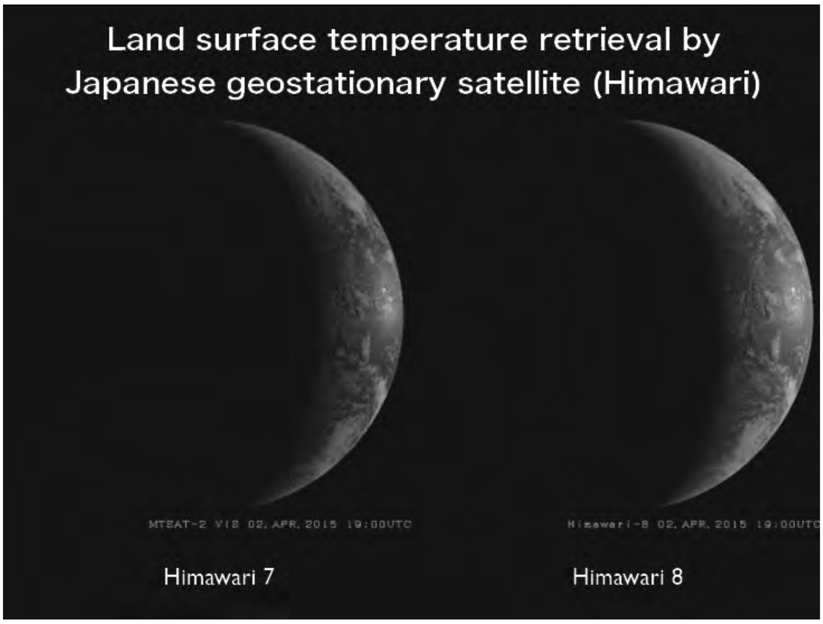

Land surface temperature retrieval by Japanese geostationary satellite (Himawari)

MTSAT-2 VIS 02.APR.2015 19:00UTC
Himawari-8 02.APR.2015 19:00UTC
Himawari 7
Himawari 8

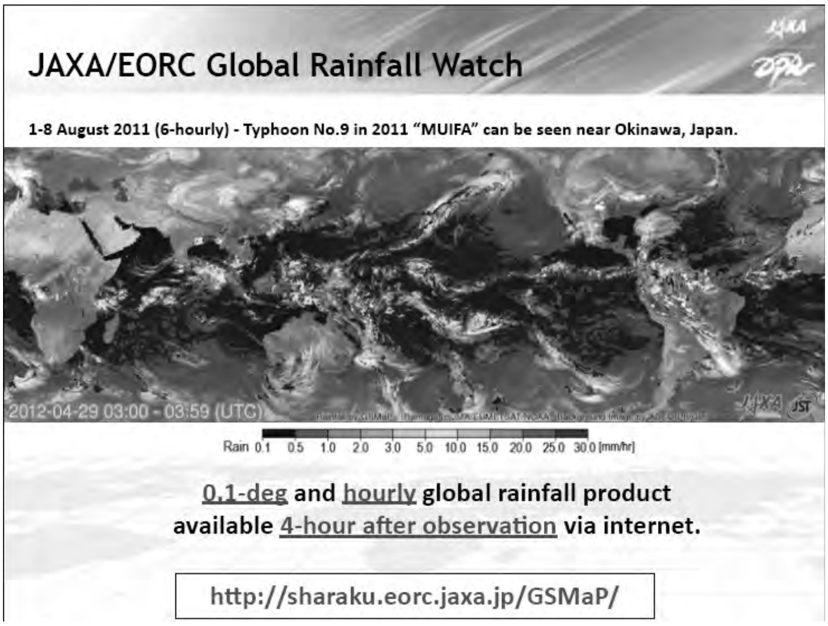

JAXA/EORC Global Rainfall Watch

1-8 August 2011 (6-hourly) - Typhoon No.9 in 2011 "MUIFA" can be seen near Okinawa, Japan.

2012-04-29 03:00 - 03:59 (UTC)
JAXA
JST
Rain 0.1 0.5 1.0 2.0 3.0 5.0 10.0 15.0 20.0 25.0 30.0 [mm/hr]

0.1-deg and hourly global rainfall product available 4-hour after observation via internet.

http://sharaku.eorc.jaxa.jp/GSMaP/

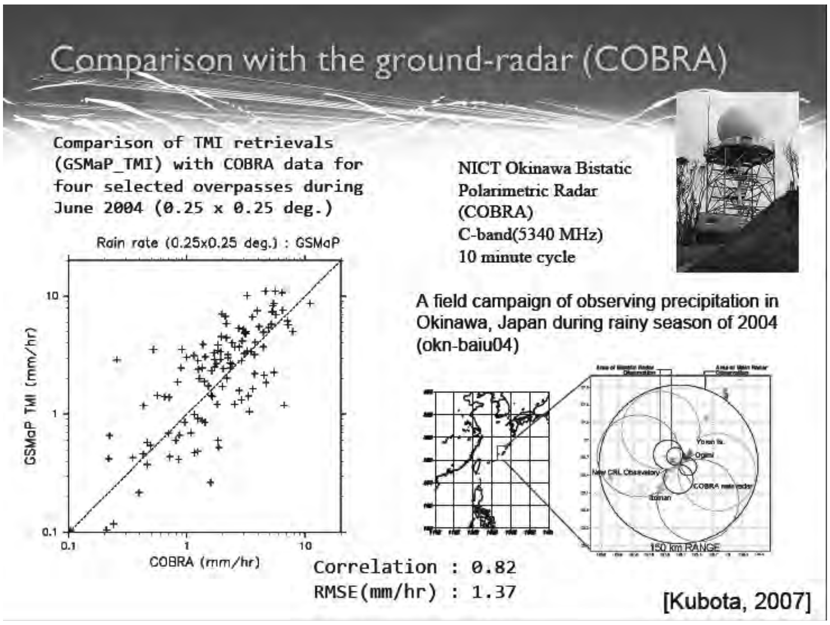

Comparison with the ground-radar (COBRA)

Comparison of TMI retrievals (GSMaP_TMI) with COBRA data for four selected overpasses during June 2004 (0.25 x 0.25 deg.)

NICT Okinawa Bistatic Polarimetric Radar (COBRA)
C-band(5340 MHz)
10 minute cycle

A field campaign of observing precipitation in Okinawa, Japan during rainy season of 2004 (okn-baiu04)

Correlation : 0.82
RMSE(mm/hr) : 1.37

[Kubota, 2007]

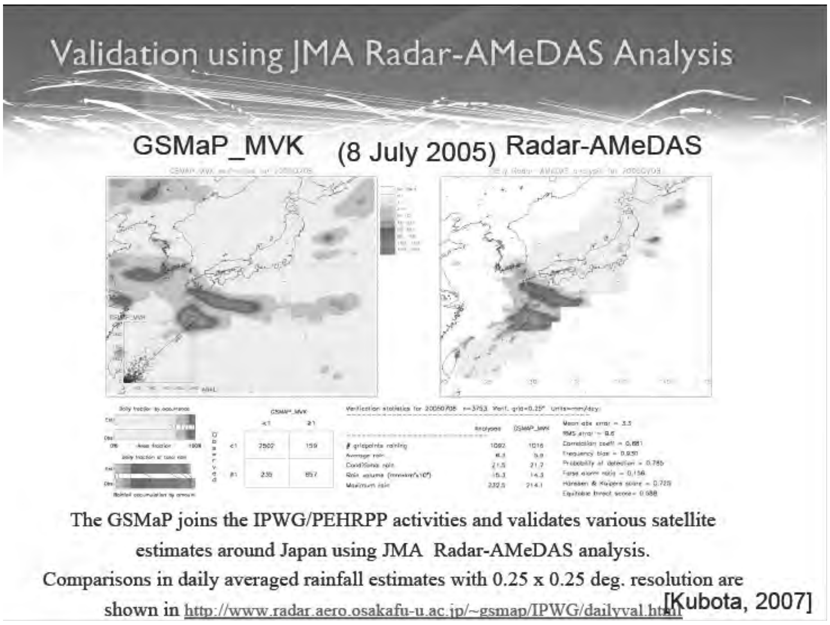

Validation using JMA Radar-AMeDAS Analysis

GSMaP_MVK (8 July 2005) Radar-AMeDAS

GSMaP_MVK
Verification statistics for 20050708 n=3753 Verif. grid=0.25° Units=mm/day
Analyses
GSMaP_MVK
# gridpoints raining 1092 1016
Average rain
Conditional rain 21.5 21.7
Rain volume
Maximum rain 232.5 214.1
Mean abs error = 3.5
RMS error = 9.6
Correlation coeff = 0.881
Frequency bias = 0.930
Probability of detection = 0.785
False alarm ratio = 0.156
Hanssen & Kuipers score = 0.725
Equitable threat score = 0.588
<1
≥1
2502
159
235
857
Observed

The GSMaP joins the IPWG/PEHRPP activities and validates various satellite estimates around Japan using JMA Radar-AMeDAS analysis.
Comparisons in daily averaged rainfall estimates with 0.25 x 0.25 deg. resolution are shown in http://www.radar.aero.osakafu-u.ac.jp/~gsmap/IPWG/dailyval.html

[Kubota, 2007]

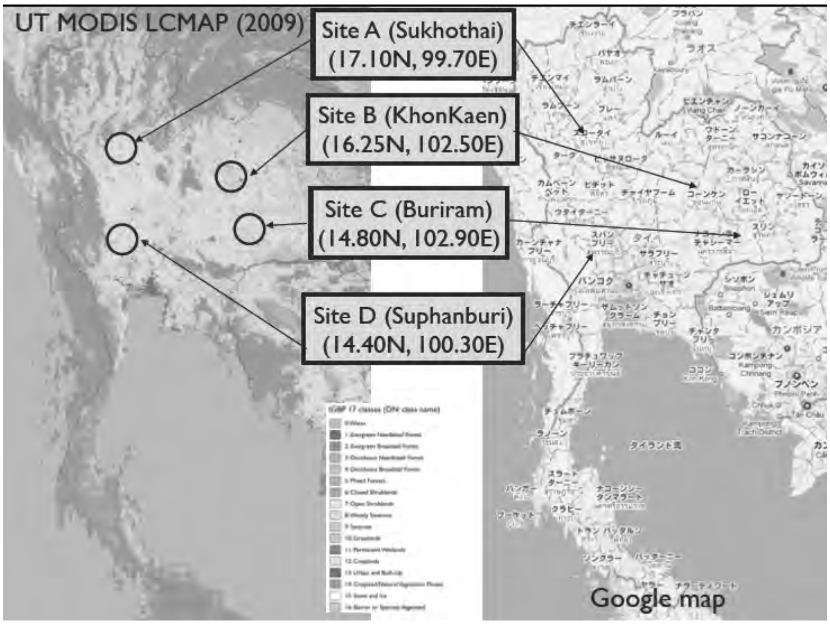

UT MODIS LCMAP (2009)

Site A (Sukhothai)
(17.10N, 99.70E)

Site B (KhonKaen)
(16.25N, 102.50E)

Site C (Buriram)
(14.80N, 102.90E)

Site D (Suphanburi)
(14.40N, 100.30E)

Google map

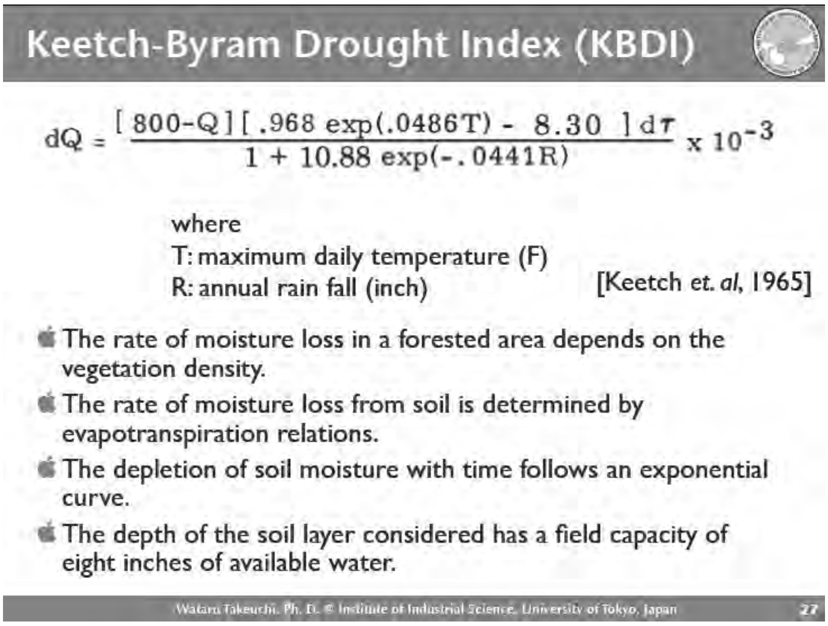

Keetch-Byram Drought Index (KBDI)

$$dQ = \frac{[800-Q][.968\exp(.0486T) - 8.30]\,d\tau}{1 + 10.88\exp(-.0441R)} \times 10^{-3}$$

where
T: maximum daily temperature (F)
R: annual rain fall (inch)

[Keetch *et. al*, 1965]

- The rate of moisture loss in a forested area depends on the vegetation density.
- The rate of moisture loss from soil is determined by evapotranspiration relations.
- The depletion of soil moisture with time follows an exponential curve.
- The depth of the soil layer considered has a field capacity of eight inches of available water.

Wataru Takeuchi, Ph. D. © Institute of Industrial Science, University of Tokyo, Japan 27

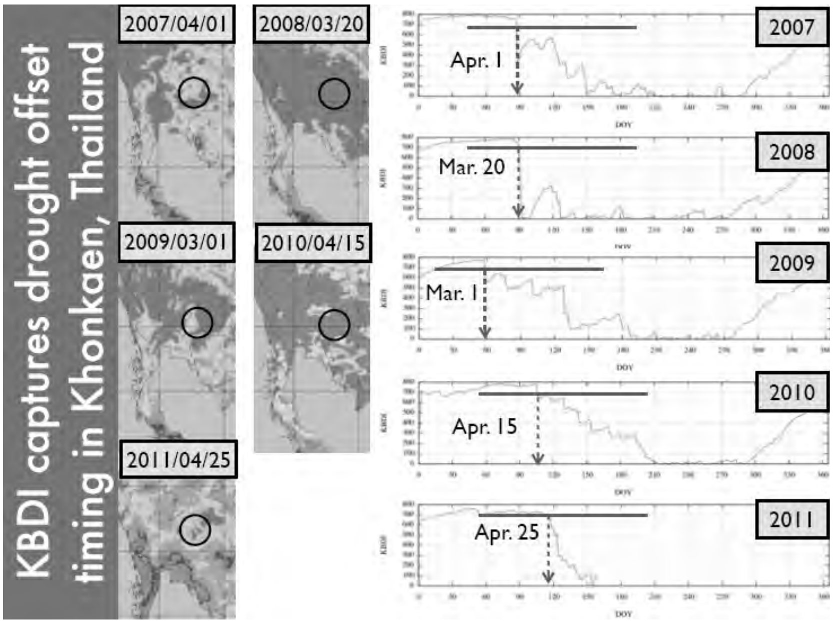

KBDI captures drought offset timing in Khonkaen, Thailand

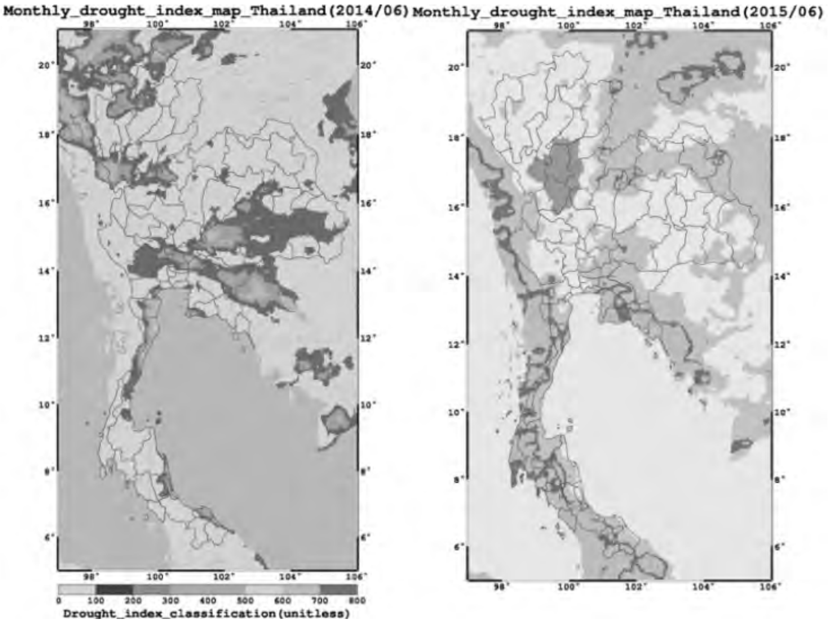
Monthly_drought_index_map_Thailand(2014/06)
Monthly_drought_index_map_Thailand(2015/06)
98°
100°
102°
104°
106°
20°
18°
16°
14°
12°
10°
8°
6°
0
100
200
300
400
500
600
700
800
Drought_index_classification(unitless)

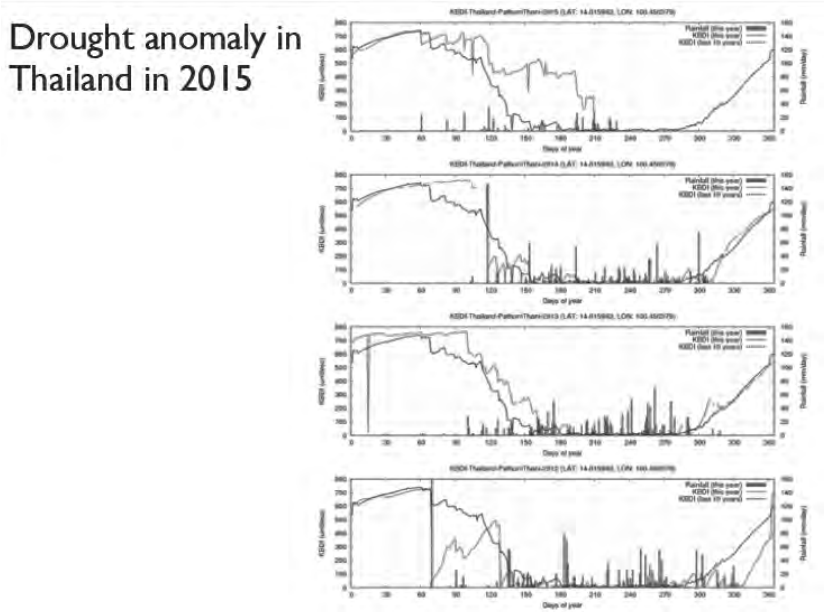

Drought anomaly in Thailand in 2015

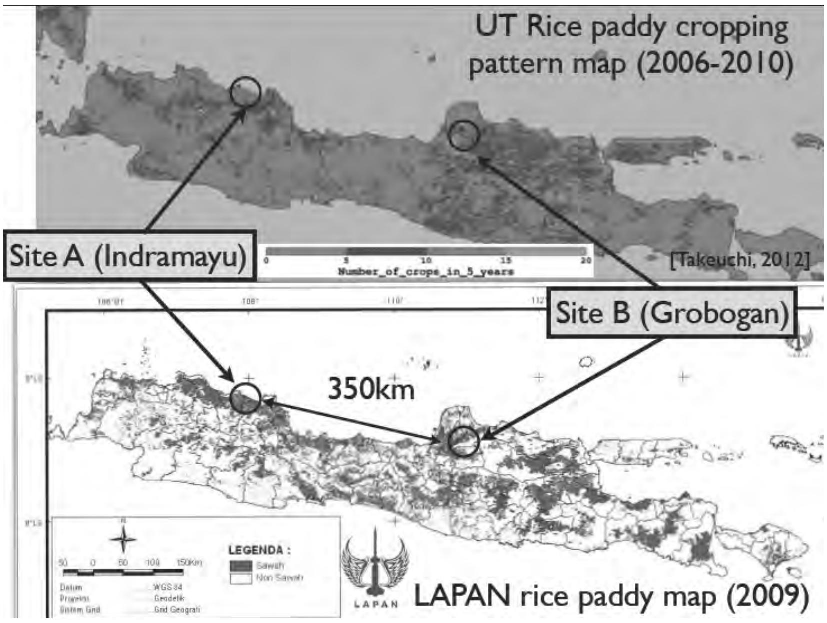
UT Rice paddy cropping pattern map (2006-2010)
Number_of_crops_in_5_years
0
5
10
15
20
[Takeuchi, 2012]
Site A (Indramayu)
Site B (Grobogan)
350km
LEGENDA :
Sawah
Non Sawah
50 0 50 100 150Km
Datum WGS 84
Projeksi Geodetik
Sistem Grid Grid Geografi
LAPAN
LAPAN rice paddy map (2009)

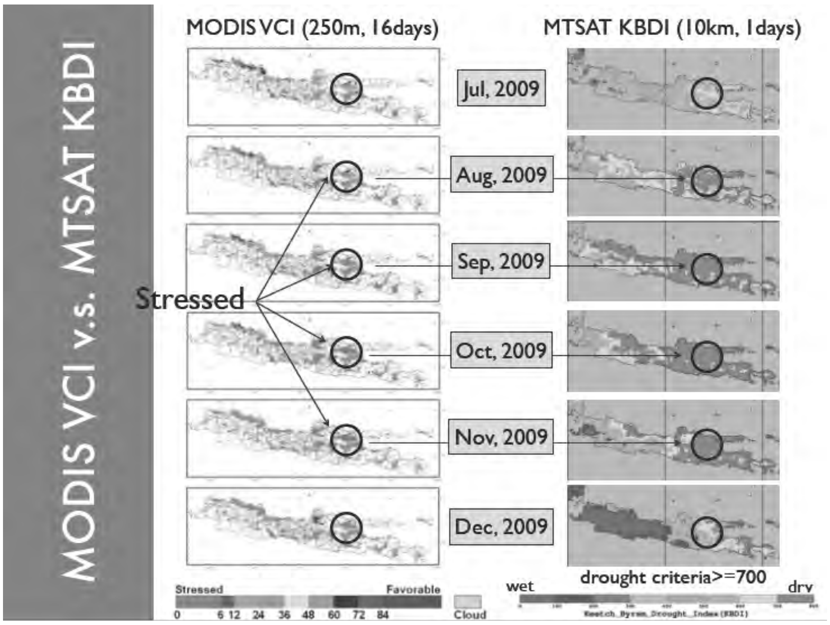
MODIS VCI v.s. MTSAT KBDI
MODIS VCI (250m, 16days)
MTSAT KBDI (10km, 1days)
Jul, 2009
Aug, 2009
Sep, 2009
Oct, 2009
Nov, 2009
Dec, 2009
Stressed
Stressed
Favorable
0
6
12
24
36
48
60
72
84
Cloud
wet
drought criteria>=700
dry
Keetch_Byram_Drought_Index(KBDI)

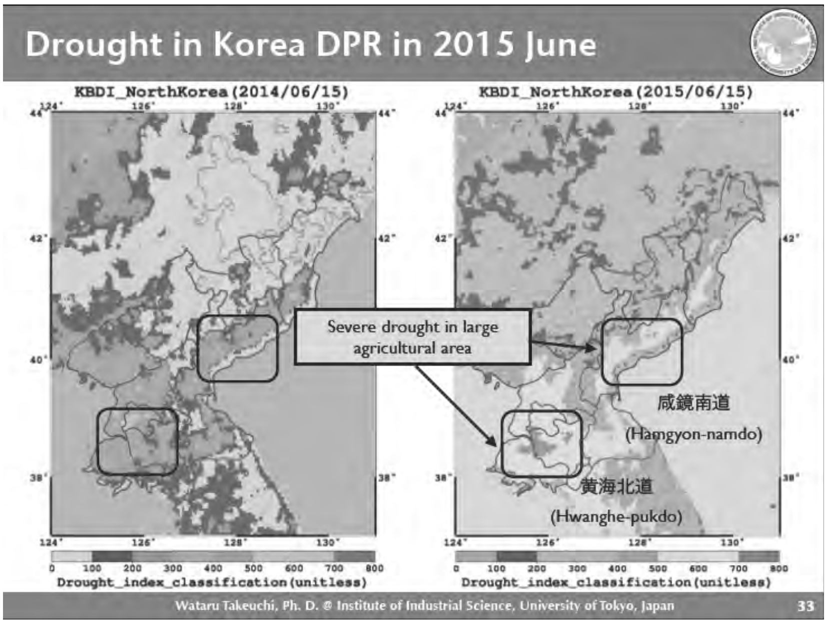

Drought in Korea DPR in 2015 June

KBDI_NorthKorea(2014/06/15)

KBDI_NorthKorea(2015/06/15)

Severe drought in large agricultural area

咸鏡南道 (Hamgyon-namdo)

黄海北道 (Hwanghe-pukdo)

Drought_index_classification(unitless)

Wataru Takeuchi, Ph. D. © Institute of Industrial Science, University of Tokyo, Japan

33

124°
126°
128°
130°
44°
42°
40°
38°
0
100
200
300
400
500
600
700
800

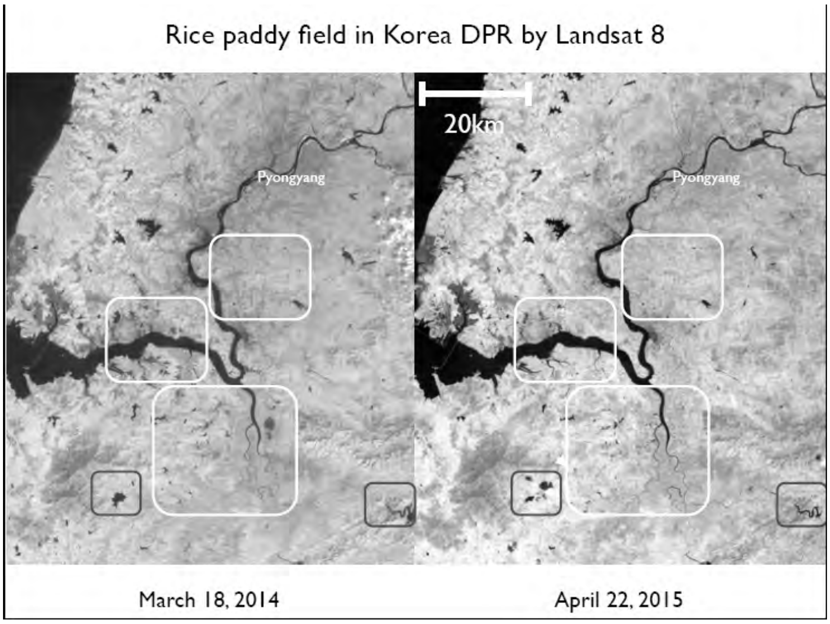

Rice paddy field in Korea DPR by Landsat 8

20km
Pyongyang
Pyongyang

March 18, 2014

April 22, 2015

Rice paddy field in Korea DPR by Landsat 8

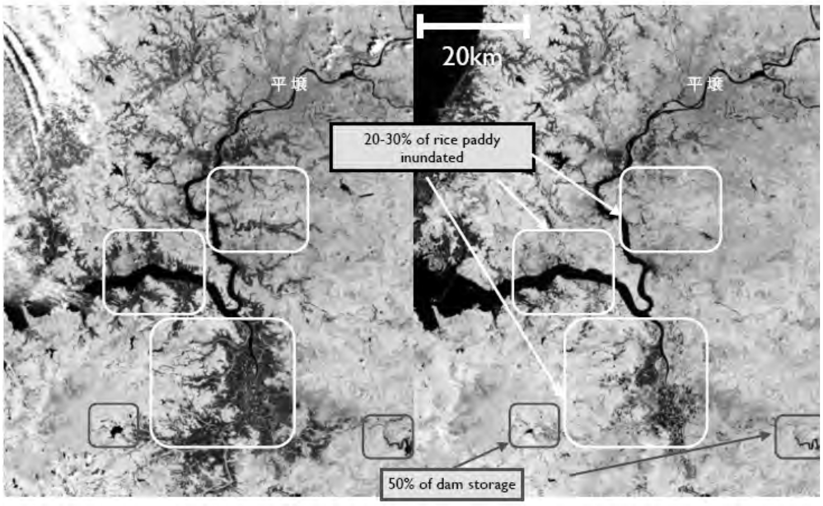
20km
平壌
平壌
20-30% of rice paddy inundated
50% of dam storage

May 21, 2014 May 24, 2015

Rice paddy field in Korea DPR by Landsat 8

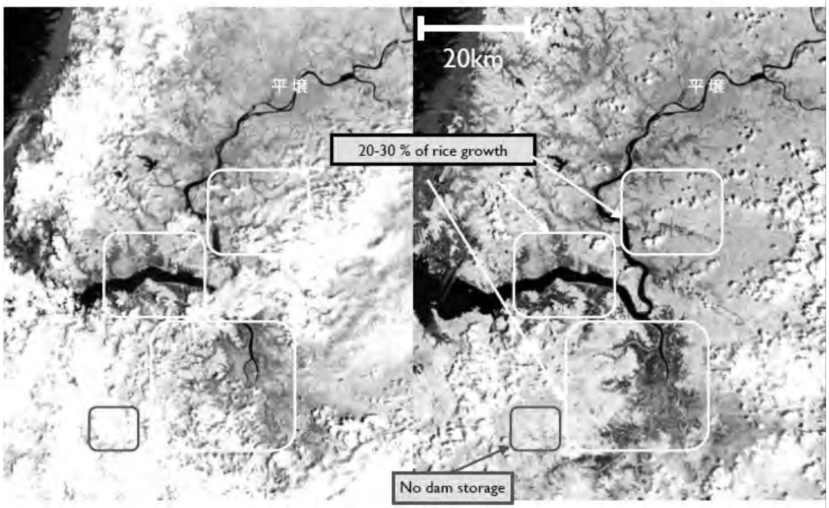
20km
平壌
平壌
20-30 % of rice growth
No dam storage

July 8, 2014 July 11, 2015

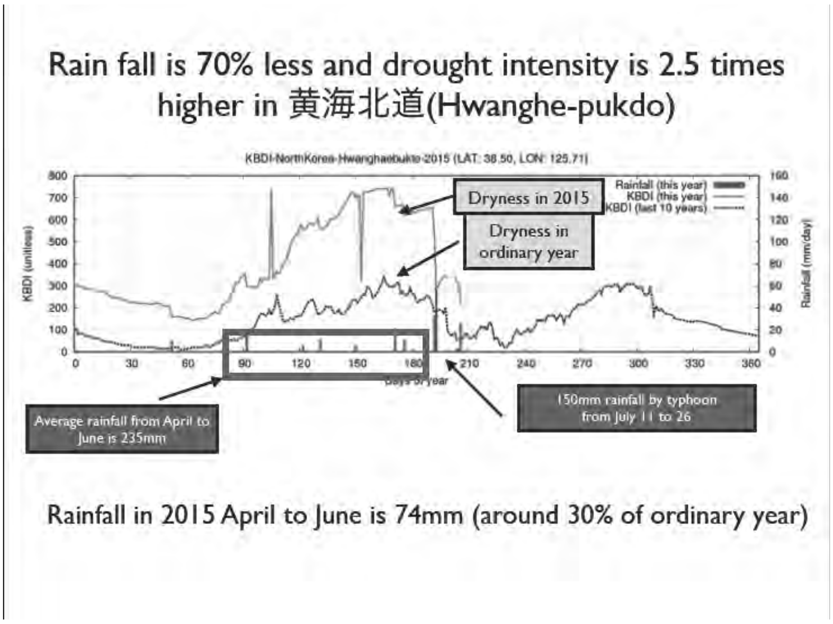

Rain fall is 70% less and drought intensity is 2.5 times higher in 黄海北道(Hwanghe-pukdo)

Dryness in 2015

Dryness in ordinary year

Average rainfall from April to June is 235mm

150mm rainfall by typhoon from July 11 to 26

Rainfall in 2015 April to June is 74mm (around 30% of ordinary year)

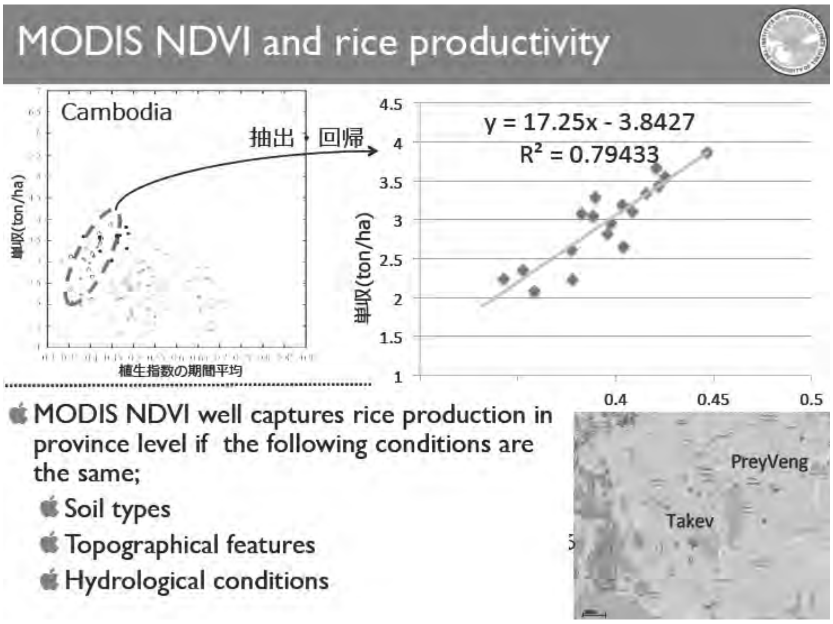

MODIS NDVI and rice productivity

- MODIS NDVI well captures rice production in province level if the following conditions are the same;
  - Soil types
  - Topographical features
  - Hydrological conditions

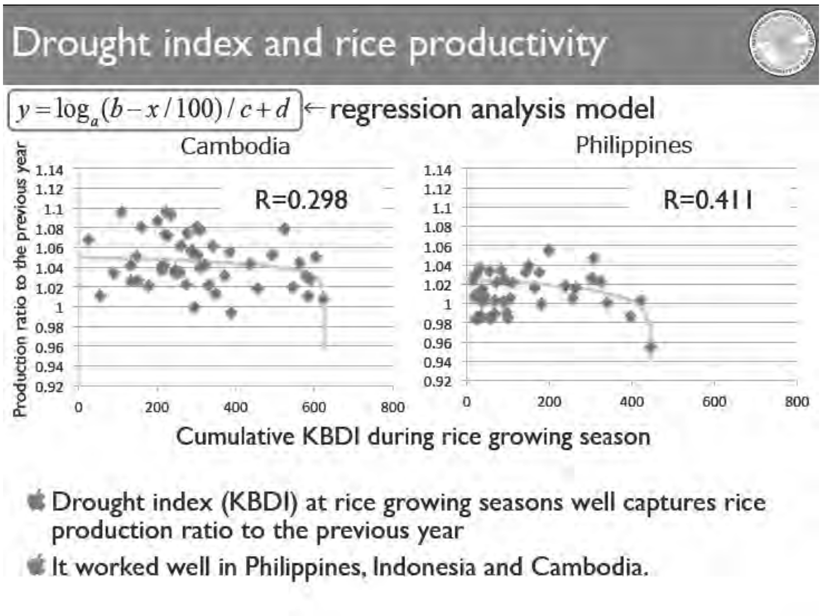

Drought index and rice productivity

$y = \log_a(b - x/100)/c + d$ ← regression analysis model

- Drought index (KBDI) at rice growing seasons well captures rice production ratio to the previous year
- It worked well in Philippines, Indonesia and Cambodia.

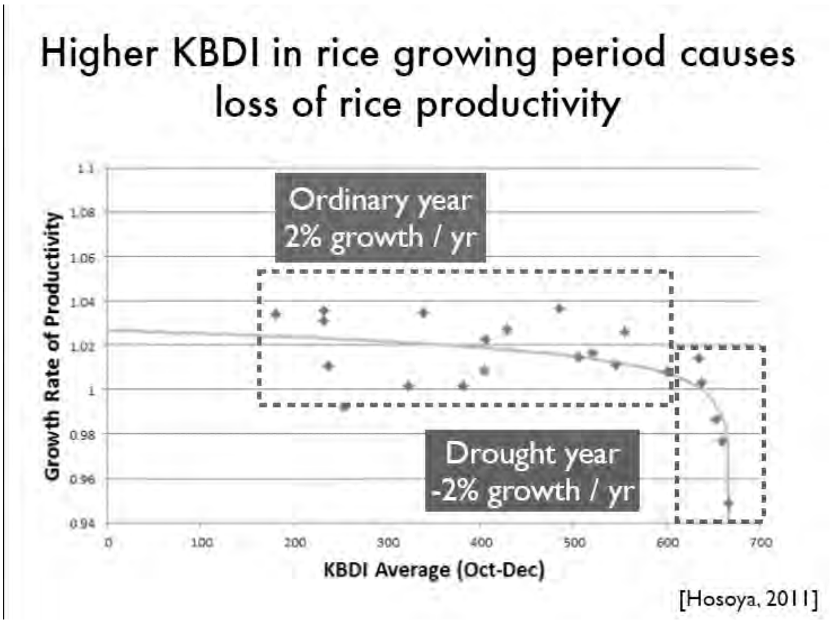

Higher KBDI in rice growing period causes loss of rice productivity

[Hosoya, 2011]

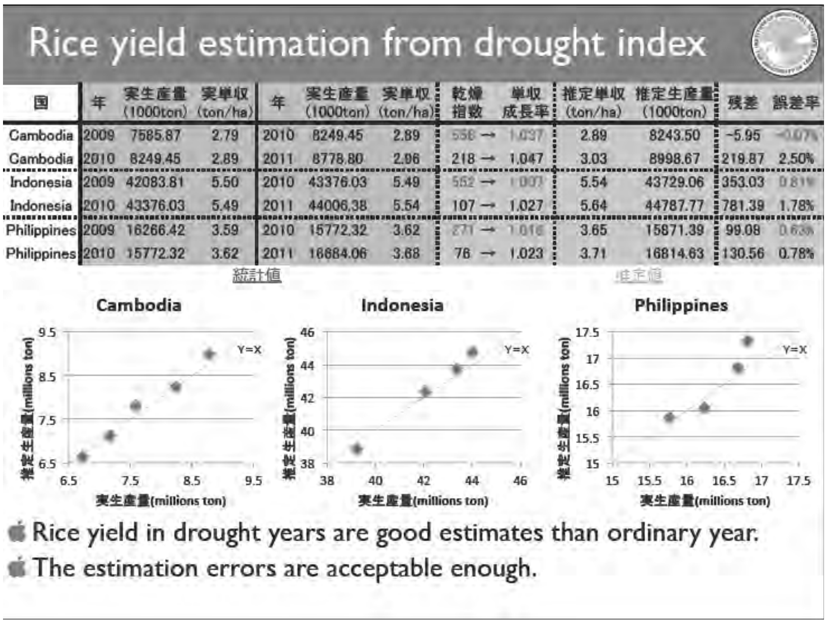

Rice yield estimation from drought index

国	年	実生産量 (1000ton)	実単収 (ton/ha)	年	実生産量 (1000ton)	実単収 (ton/ha)	乾燥指数	単収成長率	推定単収 (ton/ha)	推定生産量 (1000ton)	残差	誤差率
Cambodia	2009	7585.87	2.79	2010	8249.45	2.89	556 →	1.037	2.89	8243.50	-5.95	-0.07%
Cambodia	2010	8249.45	2.89	2011	8778.80	2.96	218 →	1.047	3.03	8998.67	219.87	2.50%
Indonesia	2009	42083.81	5.50	2010	43376.03	5.49	552 →	1.007	5.54	43729.06	353.03	0.81%
Indonesia	2010	43376.03	5.49	2011	44006.38	5.54	107 →	1.027	5.64	44787.77	781.39	1.78%
Philippines	2009	16266.42	3.59	2010	15772.32	3.62	271 →	1.016	3.65	15871.39	99.08	0.63%
Philippines	2010	15772.32	3.62	2011	16684.06	3.68	76 →	1.023	3.71	16814.63	130.56	0.78%

統計値

推定値

Cambodia
9.5
8.5
7.5
6.5
6.5
7.5
8.5
9.5
Y=X
推定生産量(millions ton)
実生産量(millions ton)
Indonesia
46
44
42
40
38
38
40
42
44
46
Y=X
推定生産量(millions ton)
実生産量(millions ton)
Philippines
17.5
17
16.5
16
15.5
15
15
15.5
16
16.5
17
17.5
Y=X
推定生産量(millions ton)
実生産量(millions ton)

- Rice yield in drought years are good estimates than ordinary year.
- The estimation errors are acceptable enough.

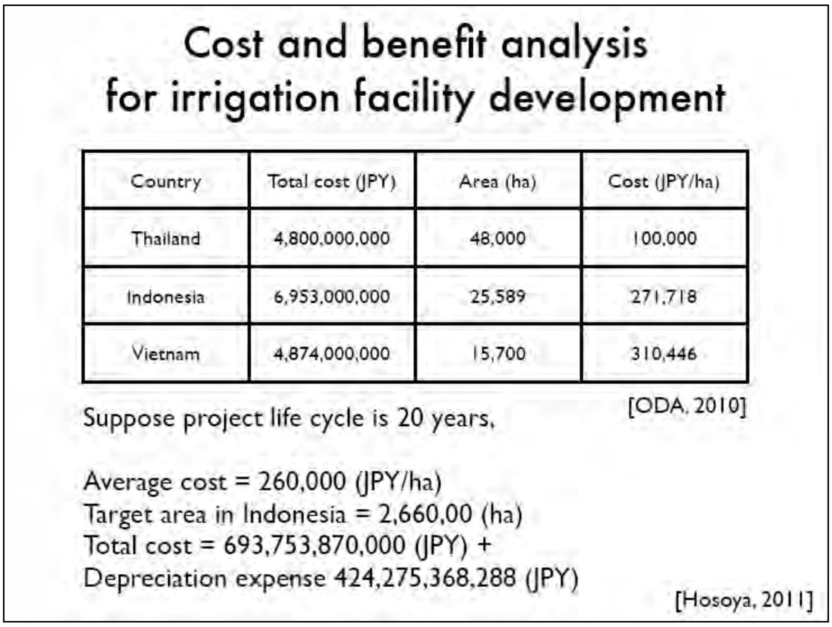

Cost and benefit analysis for irrigation facility development

Country	Total cost (JPY)	Area (ha)	Cost (JPY/ha)
Thailand	4,800,000,000	48,000	100,000
Indonesia	6,953,000,000	25,589	271,718
Vietnam	4,874,000,000	15,700	310,446

[ODA, 2010]

Suppose project life cycle is 20 years,

Average cost = 260,000 (JPY/ha)
Target area in Indonesia = 2,660,00 (ha)
Total cost = 693,753,870,000 (JPY) +
Depreciation expense 424,275,368,288 (JPY)

[Hosoya, 2011]

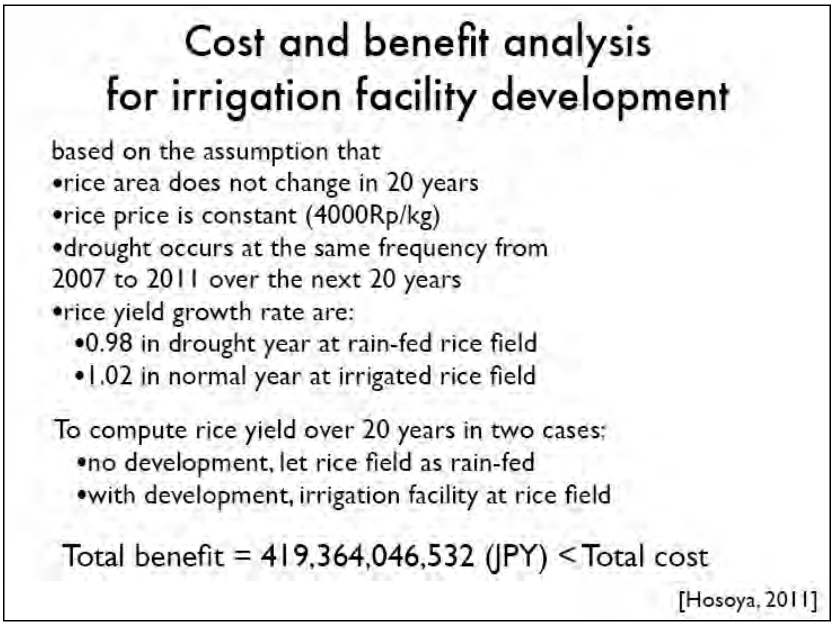

Cost and benefit analysis for irrigation facility development

based on the assumption that
- rice area does not change in 20 years
- rice price is constant (4000Rp/kg)
- drought occurs at the same frequency from 2007 to 2011 over the next 20 years
- rice yield growth rate are:
  - 0.98 in drought year at rain-fed rice field
  - 1.02 in normal year at irrigated rice field

To compute rice yield over 20 years in two cases:
- no development, let rice field as rain-fed
- with development, irrigation facility at rice field

Total benefit = 419,364,046,532 (JPY) < Total cost

[Hosoya, 2011]

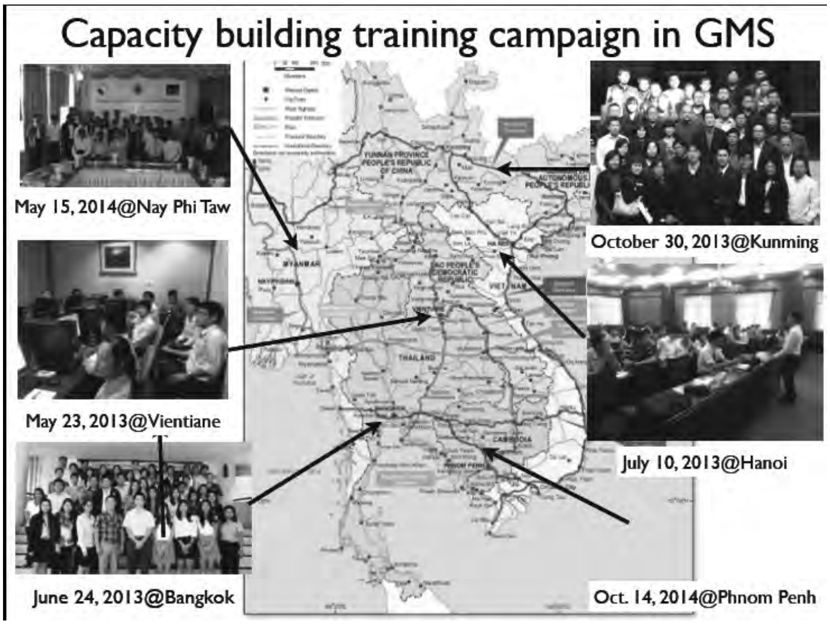

Capacity building training campaign in GMS

May 15, 2014@Nay Phi Taw

May 23, 2013@Vientiane

June 24, 2013@Bangkok

October 30, 2013@Kunming

July 10, 2013@Hanoi

Oct. 14, 2014@Phnom Penh

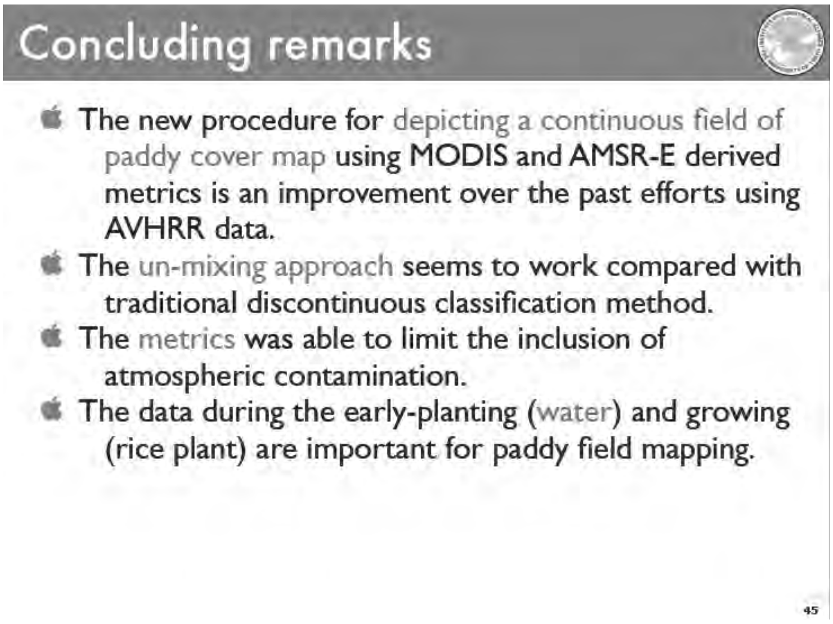

Concluding remarks

- The new procedure for depicting a continuous field of paddy cover map using MODIS and AMSR-E derived metrics is an improvement over the past efforts using AVHRR data.
- The un-mixing approach seems to work compared with traditional discontinuous classification method.
- The metrics was able to limit the inclusion of atmospheric contamination.
- The data during the early-planting (water) and growing (rice plant) are important for paddy field mapping.

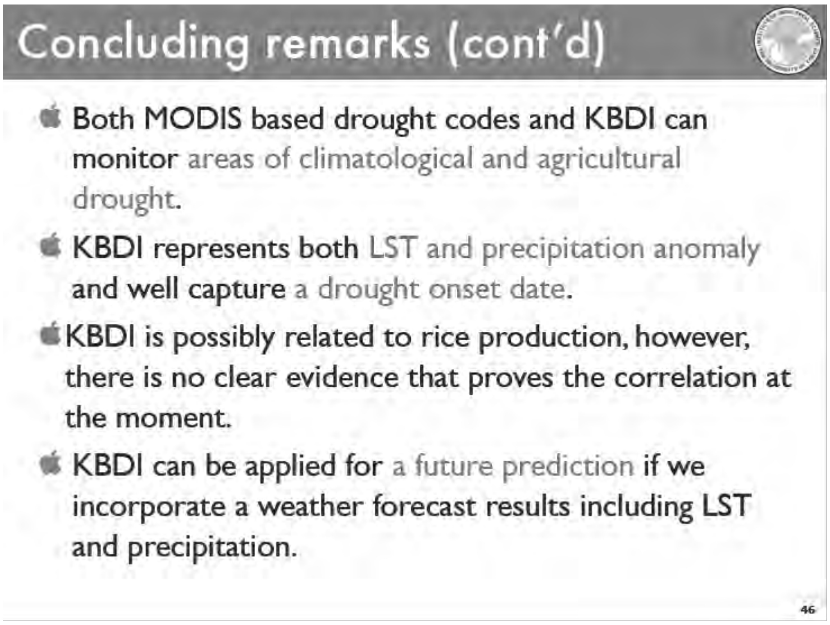

Concluding remarks (cont'd)

- Both MODIS based drought codes and KBDI can monitor areas of climatological and agricultural drought.
- KBDI represents both LST and precipitation anomaly and well capture a drought onset date.
- KBDI is possibly related to rice production, however, there is no clear evidence that proves the correlation at the moment.
- KBDI can be applied for a future prediction if we incorporate a weather forecast results including LST and precipitation.

Thank you

Wataru Takeuchi, Ph. D.
Institute of Industrial Science
University of Tokyo, Japan
URL: http://wtlab.iis.u-tokyo.ac.jp/~wataru/
E-mail: wataru@iis.u-tokyo.ac.jp

Student Presentation

BUILDING CLASSIFICATION IN URBAN AREA IN YANGON, MYANMAR USING STEREO HIGH RESOLUTION IMAGES AND NIGHT TIME LIGHT DATA

Tanakorn SRITARAPIPAT[1] and Wataru TAKEUCHI[2]
[1] Ph.D. Student, IIS, The University of Tokyo, Japan
tanakorn@iis.u-tokyo.ac.jp
[2] Associate Professor, IIS, The University of Tokyo, Japan

ABSTRACT

This research proposed a methodology to provide building type in urban area using remotely sensed data (that can observe in wide area) in Yangon, Myanmar. Stereo high-resolution satellite images acquired by GeoEye, medium-resolution images of Landsat 8 and low-resolution images of night time light of VIIRS (Visible Infrared Imaging Radiometer Suite) were used in this research. The high-resolution images was employed to provide land cover and digital elevation model (DEM), and medium-resolution image was classified as land cover. The height of building were generated by using land cover and DEM. Combining height of building with the night time light data, building type such as residential, commercial, industrial building were able to obtain. In our experiment, Yangon, former capital of Myanmar, was concentrated to classify since it is the country's largest city with five million people and is major economic country's center. Building type map using our proposed method was compared with local images in residential and commercial areas, and industrial zone map. The experimental result indicated the relationship between building type map and validate data is highly positive.

Keywords*: residential building, commercial building, industrial building*

1. INTRODUCTION

Understanding type of building in each area is an important information for urban planning and management in efficiency. Generally, building type information is provided by surveying that takes a number of workers, long process time and high budget. In urban area, there are various human-built features which is highly complicated. So it is quite difficult to collect this information by surveying in vast area.

Since remote sensing technology provides observation in large area. Many researchers have widely used remotely sensed data to detect building and classify type of building. For detecting building, Grigillo (2011) introduced building detection method using GeoEye Images. They applied segmentation method to extract building. Building extraction method was proposed by Turker (2015). They used support vector machine and hough transform also perception grouping to extract building as object-based classification. For building classification, Lu (2014) presented building type classification using LiDAR remote sensing data. They used LiDAR to provide the height of building. Then, height of building was segmented as building. Building classification method using very high resolution image and GIS was introduced by Du (2015). They extract the building form the image and related it to GIS data to provide building classification. Moreover, damage building detection by using high resolution oblique airborne images (Vetrivel, 2015). They detected anomaly segmentation of building.

We proposed a methodology to newly classify building types; residential, commercial, and industrial buildings using GeoEye, Landsat images and night time light data. In this research, Yangon (Morley, 2013), Myanmar was concentrated since it is major center of country’s economics. A methodology to classify building type was describe in section 2. In section 3, experimental result was compared with validated data also analyzed. Finally, Conclusion of this research was given in section 4.

2. METHODOLOGY

2.1 Factors to indicate building class

In this research, only three types of buildings classification were concentrated; commercial building, industrial building and residential building. Firstly, commercial building such as department store, shopping mall, hotel etc. has characteristics of high height of building. Also in the night time, this building has high consuming light energy due to various activities and crowded area. As result, it can indicate that these building has high night time light. Secondly, industrial building such as factory or plant has feature of high height of building as well. However, in the night time, this building has low consuming light energy. So, night time light data of this building is low. Finally, residential building has aspect of low building such as house and low night time light data.

2.2 Materials

We used three remotely sensed data sources; GeoEye, Landsat 8, NPP (National Polar-orbiting Partnership) – VIIRS (Visible Infrared Imaging Radiometer Suite). Stereo images of GeoEye Satellite were used to provide height of building. Landsat-8 multispectral image was employed to classify land cover area. NPP-VIIRS has capability to obtain day/night band composite data (DNB). The radiance of DNB has a number in order of magnitude of 10^{-9} and the unit of $W/(cm^2\text{-}sr)$. The details of these images was displayed in table 1. Figure 1 shows satellite dataset of this research.

Table 1: Details of satellite images

Satellite	Resolution	Bands	Acquisition Date
GeoEye-1	0.5 m.	3	2013/11/16
Landsat-8	30 m.	11	2015/02/26
NPP-VIIRS DNB	460 m.	1	2012/04/18-2012/04/26 2012/10/11-2012/10/23

(a) (Red: Red, Green: Green, Blue: Blue)

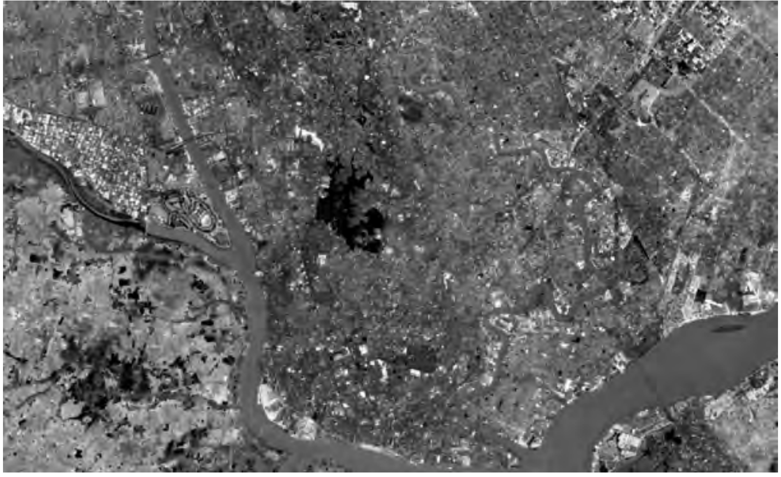

(b) (Red:NIR, Green:Green, Blue:Blue)

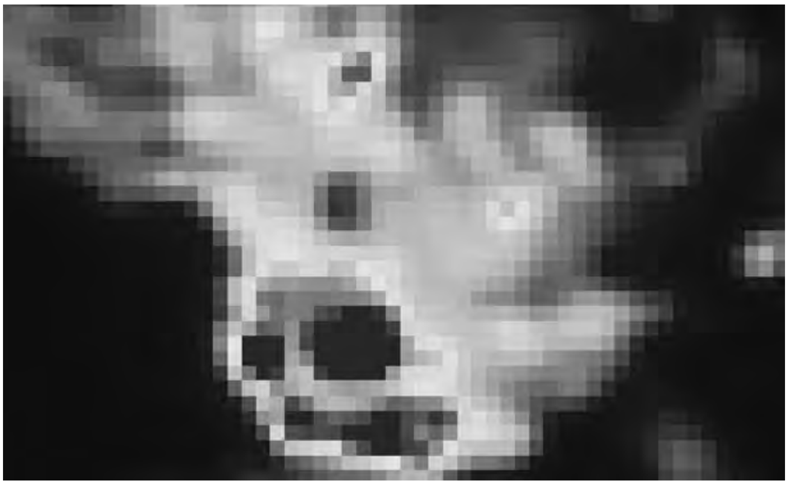

(c) (Red:High, Blue:Low)

Figure 1: (a) GeoEye Image, (b) Landsat Image, (c) NPP-VIIRS DNB

Firstly, the stereo images of GeoEye were extracted to provide Digital Surface Model (DSM), Digital Terrain Model (DTM) and Digital Building Model (DBM). The multispectral images of Landsat 8 was classified as land cover areas. Using urban area in land cover and DBM, Building class such as residential building (low building) and commercial and industrial buildings (high building) was obtain based on height of building. The night time light data from NPP-VIIRS DNB was taken exploit to separate between commercial and industrial buildings. The mapping of building classification was illustrated.

2.3 Classifications

The stereo images of GeoEye were used to provide DSM. Using DSM, orthorectified images from GeoEye was obtain. Then DSM was applied by using morphological filtering to provide DTM. DBM was generated by using the equation that DBM equals to DSM minus DTM. Orthorectified images with RGB bands was classified by using Mahalanobis distance method (supervised classification) into 2 classes; vegetation and non-vegetation. Using non-vegetation area and DBM, the height of building was able to obtain without effect of trees or forest areas. We separate height of building using manual threshloding into two groups; low building from 2 to 10 meters height (1-2 floors) and high buildings more than 10 meters height (more than 2 floors). In general, 1 floor of residential building is 3.1 meters and 1 floor of commercial building is 3.9 meters

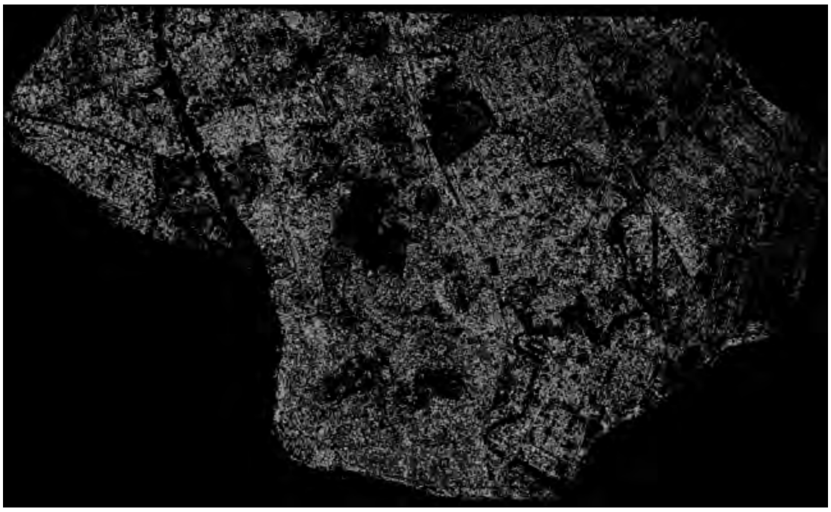

Figure 2: Building classification
(Blue: High building, Green: Low building)

The Landsat image was classified by using Mahalanobis distance (Supervised Classification). Land cover classes were separated into 3 class; Urban, Vegetation, Water. Training samples were selected more than 1000 samples per class.

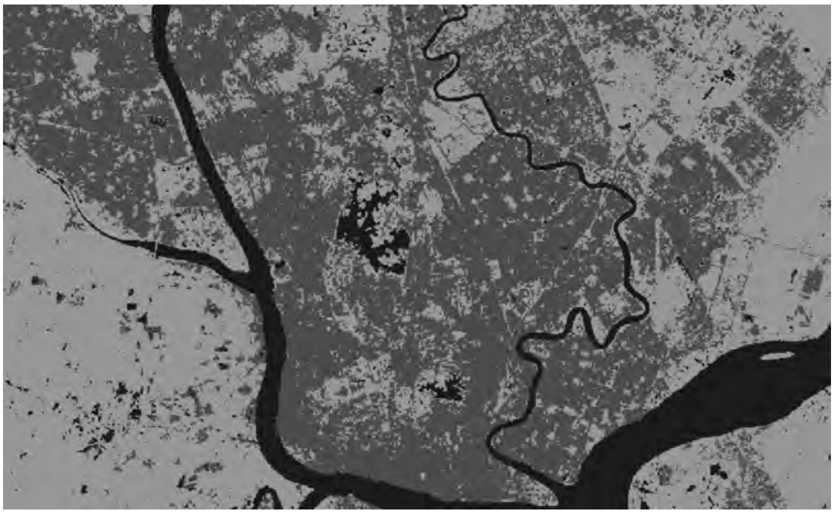

Figure 3: Land cover classification
(Red: Urban, Green: Vegetation, Blue: Water)

We separated night time light data into 3 classes by using K-means (Unsupervised classification). Three classes of night time light data are low night time light class with mean of 1.83 (Digital number, DN), medium night time light class with mean of 8.69 (DN) and high night time light class with mean of 24.13 (DN).

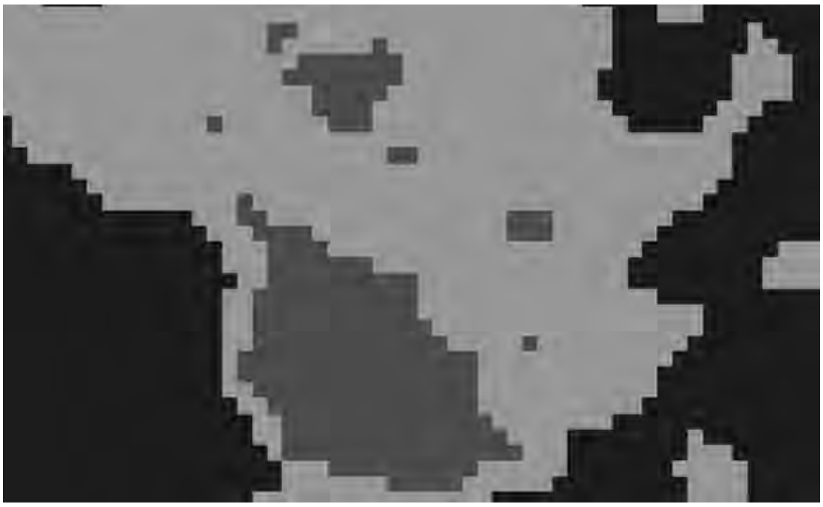

Figure 4: Night time light (NLT) classification
(Red: High NTL, Green: Middle NTL, Blue: Low NTL)

2.3 Hierarchy classification

After three resultant of each classification; height of building, land cover, night time light, were already obtain. The hierarchy classification was used to classify the building type; (1) residential, (2) commercial, (3) industrial buildings.

Firstly, height of building; low and high buildings, was provided without any errors of tree. However, since the spectral resolution in GeoEye image was poor (just RGB), some errors of height of building from vegetation and water areas are still remain. Hence, integrating between building areas and land cover classification; urban, vegetation, water was applied. Using only urban area from land cover with area of height of building, more accurate resultant of height of building was provides without any errors from vegetation and water areas. Separating between low building that indicate residential building and high building was provided. However, high buildings were mixed between commercial and industrial buildings. Combining height of building with night time light data, commercial building that has high night time light intensity and industrial building that has medium night time light intensity are separated. In this case, the group of low night time light generally indicates non-urban area. Thus, it does not include in consideration for building classification.

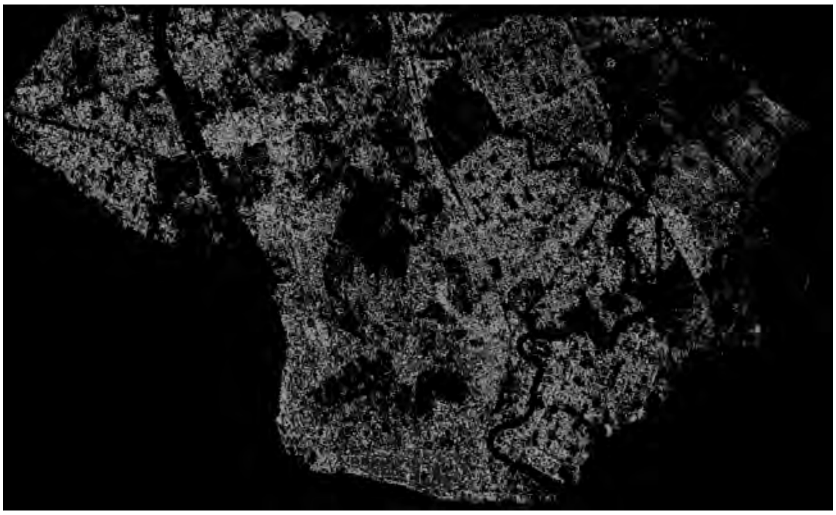

Figure 5: Result of classification building
(Green: Residential Buildings, Blue: Commercial Buildings, Red: Industrial Buildings)

2.4 Improving classification result

Since the spatial resolution of night time light data from NPP-VIIRS DNB is quite low (approximately 460 meters). The edge areas between two classifications are still errors. In order to solve such problem, spatial relationship between commercial and industrial areas was introduced. Commonly, industrial area such as factory and plant that probably makes loud noise or some pollution should be located in isolation from commercial area such as shopping center and hotel that intensive human’s activities. As a result, the rule of distance between commercial and industrial areas were defined that the building that located near the commercial buildings must be residential or commercial building.

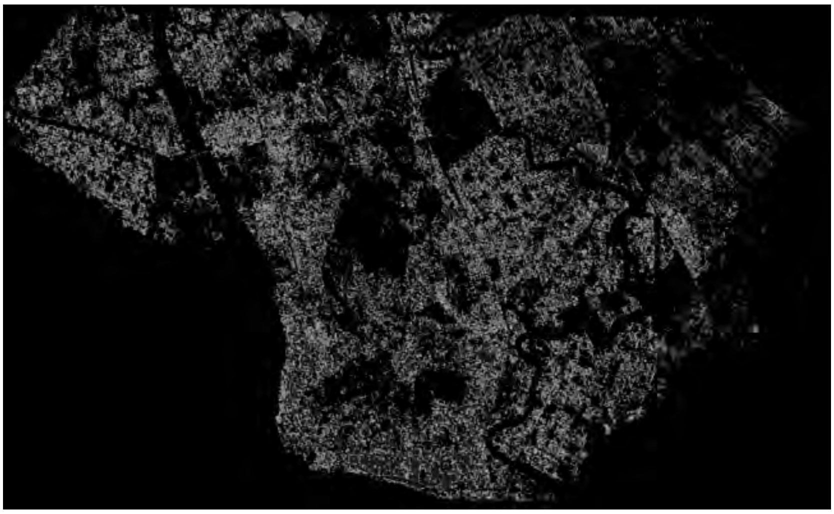

Figure 6: improved result of classification building
(Green: Residential Buildings, Blue: Commercial Buildings, Red: Industrial Buildings)

3. EXPERIMENTAL RESULT

In our experiment, Yangon, former capital of Myanmar, was concentrated to classify since it is the country's largest city with five million people and is major economic country's center. The statistical of building classification area in urban area in Yangon with 238.48 km^2 (focused area) using our methodology was shown in table 2.

Table 2: The statistical of building classification area using our method (total area is about 238.48 km^2)

Type of Building	**Area (km^2)**	**Area (%)**
Residential Buildings	45.85	84.19
Commercial Buildings	6.69	12.28
Industrial Buildings	1.92	3.53
Total Buildings	54.46	100.00

In order to validate the result, the map of building classification using our proposed method was compare with the local images with two types; residential and commercial buildings in urban area in Yangon.

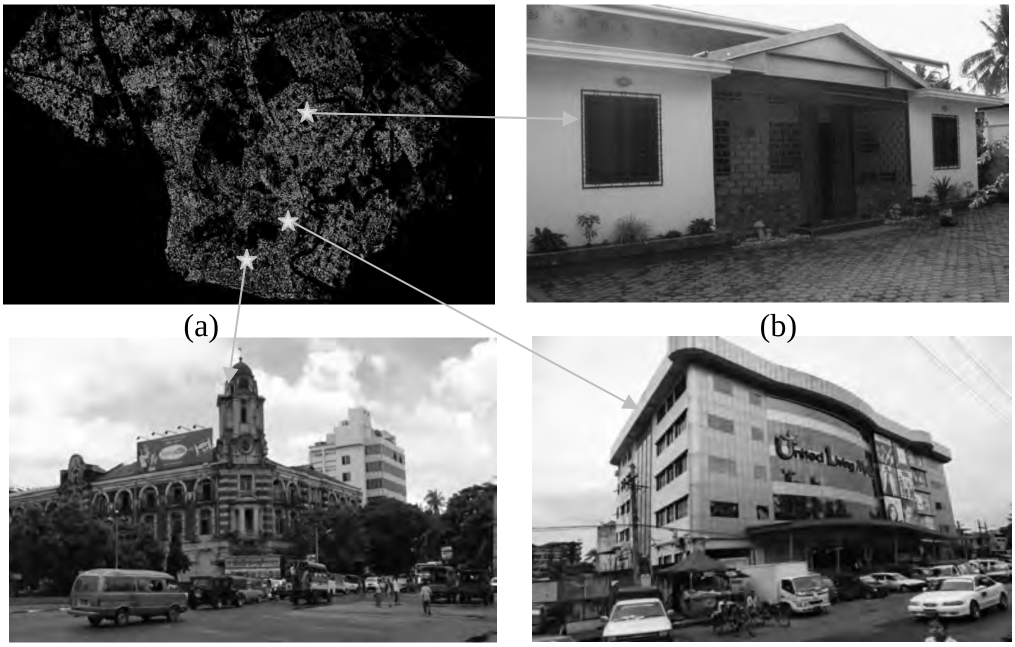

(a) (b)

(c) (d)

Figure 7: Comparison between the building type map (a) and local images; (b) residential building, (c and d) commercial building

The comparative result between the building class map and local images is a very high relationship.

Also the resultant map was compared with industrial zone map from Myanmar Industries Association (http://myanmarindustries.org).

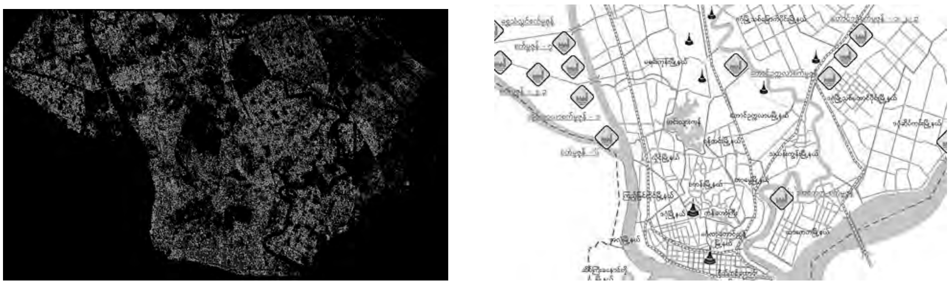

(a) (b)

Figure 8: Comparison between (a) the building type map and (b) industrial zone map

The resultant map is highly related to the industrial zone map.

However, the result of residential buildings looks overestimated. Since some commercial and industrial buildings are low building especially industrial buildings. Thus, low buildings of commercial and industrial were classified as residential buildings that are incorrect. To correct this problem, the spatial analysis is highly recommended.

4. CONCLUSION

We proposed a novel methodology to classify building type in urban area using remotely sensed data in Yangon, Myanmar. Stereo images of GeoEye was used to provide the height of building. Based on height of building, building class was obtain. Landsat-8 image was applied to provide land cover area. Using land cover, result of building class was improved. We combined building class with night time light data. Three building classes; residential, commercial, industrial buildings, were obtain. The rule of distance between commercial and industrial areas were defined to improve classification result. To validate the map of building classification, local images in residential and commercial buildings were compared as well as the industrial zone map in Yangon. The comparison between resultant map and validated data has high relationship.

REFERENCES

Du, S., Zhang, F., Zhang, X., 2015. Semantic classification of urban buildings combining VHR image and GIS data: An improved random forest approach

ISPRS Journal of Photogrammetry and Remote Sensing 105, 107–119.

Grigillo, D., Fras, M.K., 2011. Classification Based Building Detection From GeoEye-1 Images. *Joint Urban Remote Sensing Event*, 381–384, Munich, Germany.

Lu, Z., Im, J., Rhee, J., Hodgson, M., 2014. Building type classification using spatial and landscape attributes derived from LiDAR remote sensing data. *Landscape and Urban Planning* 130, 134–148.

Morley, I., 2013. Rangoon, *Cities* 31, 601–614.

Turker, M., Koc-San, D., 2015. Building extraction from high-resolution optical spaceborne imagesusing the integration of support vector machine (SVM) classification, Hough transformation and perceptual grouping. *International Journal of Applied Earth Observation and Geoinformation* 34, 58–69.

Vetrivel, A., Gerke, M., Kerle, N., Vosselman, G., 2015. Identification of damage in buildings based on gaps in 3D point clouds from very high resolution oblique airborne images. *ISPRS Journal of Photogrammetry and Remote Sensing* 105, 61–78

EXPERIMENT AND SIMULATION STUDY ON FLEXURAL BEHAVIOR OF REINFORCED CONCRETE SLAB BEFORE AND AFTER FIRE

Nguyen Thi CAO[1], Withit PANSUK[2] and Lluis TORRES[3]
[1] PhD Student, Department of Civil Engineering, Faculty of Engin eering, Bangkok, Thailand
caonguyenthi@tgu.edu.vn
[2] Assistant Professor, Department of Civil Engineering, Faculty of Engineering, Bangkok, Thailand
[3] Professor, AMADE, Polytechnic School, University of Girona, Campus Montilivi, Girona, Spain

ABSTRACT

After exposure to fire, the decrease in load capacity of reinforced concrete (RC) structure occurs and the building can be damaged or collapsed. In order to assess the state of fire-damaged structure for reusing or replacing, it is essential to estimate the residual behavior of RC member after exposure to fire. This paper will report an experiment to evaluate the load-deflection behavior of RC slabs before and after fire as a part of a study in repairing and strengthening fire-damaged RC slabs. Besides, a simple numerical investigation utilizing non-linear finite element (FE) analysis was carried out using ABAQUS software and verified with experimental data. It is concluded that the developed FE model was suitable to predict the flexural behavior of unheated and heated RC slabs.

Keywords: Reinforced concrete slab, fire-damaged concrete, ABAQUS

1. INTRODUCTION

As it is well known, the deterioration in the properties of reinforced concrete (RC) structure occurs when it is subjected to a fire. Of particular importance are loss in compressive strength, loss of elastic modulus, cracking and spalling of the concrete; reduce yield strength, ductility and tensile strength of the steel, and the loss of bond between them (Short et al. 2001). Although the concrete structure is damaged during the fire, it may retain a residual load bearing capacity (Annerel & Taerwe 2013). Due to its low thermal conductivity, concrete can be considered as a good fire resistance structural material (fib 2007). It can protect reinforcing steel against the fire by the concrete cover layers (Ünlüoğlu et al. 2007). Therefore it is possible to reuse after repairing and retrofitting reinforced concrete structures that have been exposed to fire.

In order to supply the necessary data for retrofitting the structure, it is essential to estimate the residual behavior of RC member after exposure to fire. The properties of the constituent materials of RC member, concrete and steel, in terms of strength and stiffness are progressively reduced by the increasing temperature (Hsu & Lin 2006). The stress-strain curve of concrete is strongly effected under fire and a number of stress-strain relation models for concrete have been suggested such as Chang et al. 2006; EN1994-1-2 2005; Nechnech et al. 2002; Youssef & Moftah 2007. After exposure to elevated temperature, concrete cannot recover its initially mechanical properties. With respect to steel rebar, the effect are also significantly by the temperature increase, the yield strength and the modulus of elasticity will be reduced. But it can recover almost the original mechanical properties after cooling to room temperature (fib 2008). However, in a report of stress-strain curves for steel bars after cooling from various elevated temperatures to room temperature (Qiang et al. 2012), the reduction in yield and ultimate strengths become notable when heating temperature are 500°C and above.

This paper carries out an experiment work as a part of a study for repairing and retrofitting reinforced concrete slab after exposure to fire (Thi et al. 2015). The research aims to evaluate the flexural behavior of RC slabs through of the bending test. The experiment conducts on the specimens before and after fire whereby the load-displacement curves can be compared for both of cases. The experimental data will be useful for an evaluation to propose the effective method for repairing fire-damaged RC slab. Besides, a simple numerical investigation utilizing non-linear finite element (FE) analysis is carried out using ABAQUS software and verified with experimental data. The model can be used to predict the state of RC slab after fire and also will be possible to develop for making a simulation that can predict the flexural behavior of fire-damaged RC slab after repairing.

2. EPERIMENTAL SET-UP

Two RC slabs were designed under standard ACI 318-95 (ACI 1995) as shown in Fig. 1. The slabs were casted by using ready mixed concrete with the concrete strength of 240 Kg/cm^2. They had the dimension of 1000x900x150 mm and were reinforced longitudinally in flexure with 10 mm diameter steel bars. The specimens had been cured for 28 days before conducting fire test in a furnace. The installation and process of fire test were operated under ASTM E119 standard (ASTM 2000). These slabs had been fired for 1 hour and 30 minutes to reach the peak point of the time-temperature curve of about 1000°C by using a furnace (Fig. 2). Moreover, the thermocouples also were installed at 4 different depths (0, 25, 75 and 125 mm) from the exposure surface to record the temperature during the test. The details of slabs are reported in Table 1.

Table 1: The details of specimens

Specimens	**Slab SC1**	**Slab SF1**
Concrete strength (MPa)	24	24
Fire time (minute)	00	90

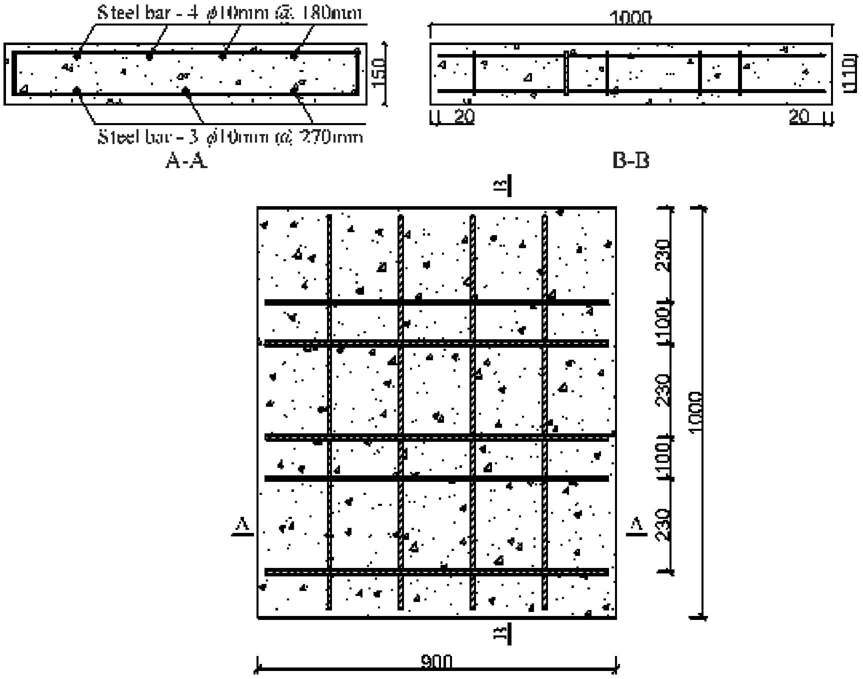
Steel bar - 4 ϕ10mm @ 180mm
150
Steel bar - 3 ϕ10mm @ 270mm
A-A
1000
110
20
20
B-B
B
230
100
230
100
230
1000
A
A
B
900

Figure 1: The design of reinforced concrete slab

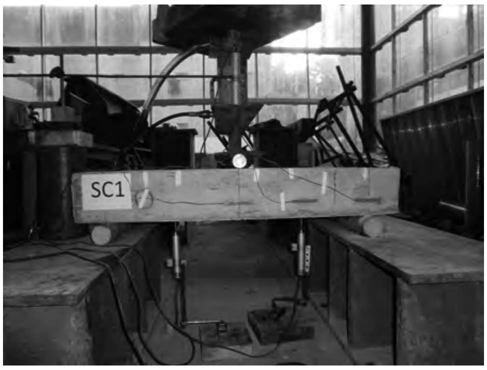

Figure 2: The furnace used for the fire test

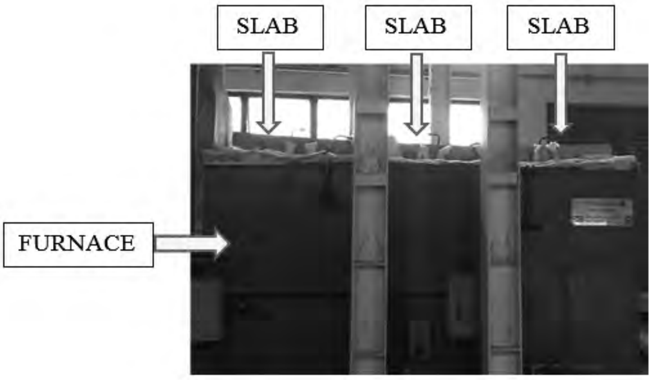
SLAB
SLAB
SLAB
FURNACE

Figure 3: The set-up of flexural test on slab

After fire test, the slab would be cured in room temperature for one month then move to the flexural test. The simply supported slabs were tested under three-point bending test to determine the load-deflection curves (Fig. 3). The applied load was controlled by a hand-operated hydraulic jack with a maximum capacity of 500 KN under a loading rate of 700 Kg/min and was monitored by load cell. An LVDT was installed at the middle point of the top of the slab and two other LVDTs were placed at 1/4 point of the span to obtain the deflection profiles.

3. FINITE ELEMENT MODELLING

3.1 Element description

The developed three-dimensional (3D) FE models were created using the finite element code ABAQUS/Explicit (Simulia 2014). The concrete was simulated using a solid element that was defined by eight nodes (3D 8-Node) and each node had three translational degrees of freedom in x, y and z directions. Besides, the 3D 2-Node truss element was used to simulate the steel reinforcement bars. The steel reinforcement bars were fully embedded in the concrete. The 3D 8-Node element also was used to simulate the steel support and loading for slab.

3.2. Geometry of the developed FE model

As part of the research presented in this paper, 2 FE models of RC slabs before and after fire were developed and the numerical solutions had been correlated with the experimental data. The models had the same geometry and boundary conditions of the tested simply supported slabs. Two steel supports and one steel loading bars were modeled. The details of model are shown in Figure 4.

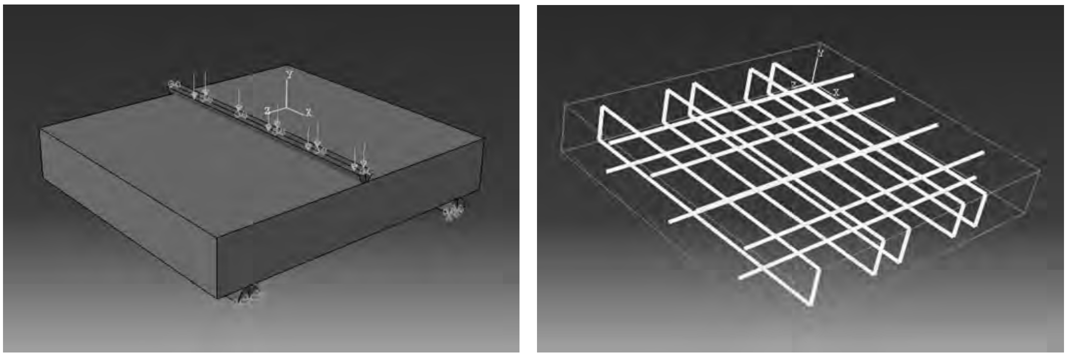

(a) (b)

Figure 4: The model of RC slab
(a) FE model with applied loading and boundary conditions.
(b) The reinforcement bars of slab model.

3.3. Constitutive models for concrete

The Concrete Damaged Plasticity (CDP) model was used in FE code ABAQUS to define the concrete behavior (Simulia 2014). It assumes that the main two failures mechanisms are tensile cracking and compressive crushing of the concrete material. The evolution of the yield surface is controlled by two hardening variables, $\tilde{\varepsilon}_t^{pl}$ and $\tilde{\varepsilon}_c^{pl}$ (tensile and compressive equivalent plastic strain), linked to failure mechanism under tension and compression loading respectively. The model is based on the assumption of scalar (isotropic) damage and is designed for applications in which the concrete is subjected to arbitrary loading condition, including cyclic loading. The model takes into consideration the degradation of the elastic stiffness induced by plastic straining both in tension and compression.

In the present study, the Model Code (fib 2010) is adopted to define the uniaxial compressive stress-strain relationship of concrete. The compressive response of concrete is assumed to be linear elastic until reaches the uniaxial yield stress and follows by a strain-hardening curve up to the peak compressive stress, then a descending branch represents the post-peak softening behavior of concrete.

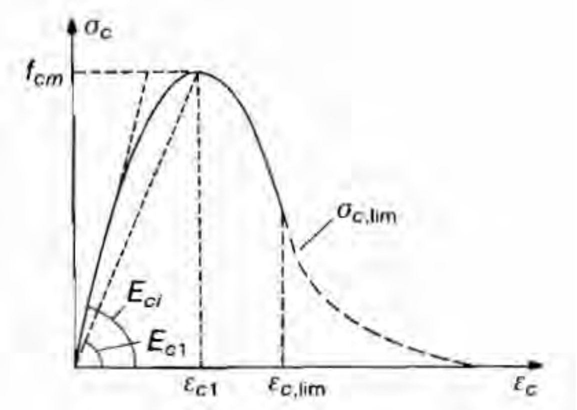

Figure 5: Stress-strain diagram for uniaxial compression (fib 2010)

where σ_c = compression stress; ε_c = compression strain; f_{cm} = maximum compressive stress; E_{c1} = secant modulus from the origin to the peak compressive stress f_{cm}; E_{ci} = tangent modulus; $\varepsilon_{c1} = 0.0022$; $\sigma_{c,lim} = 0.5f_{cm}$; $\varepsilon_{c,lim}$ = the compression strain at the stress $\sigma_{c,lim}$.

Regarding to the tensile behavior of concrete, it is assumed to be linear elastic before cracking then follows by a descending branch. A tension model proposed by Hsu is used in this study (Wang & Hsu 2001) as shown in Fig. 6 where the ascending and descending branches are given as:

$$\sigma_1 = E_C \varepsilon_1 \qquad \varepsilon_1 \le \varepsilon_{cr} \tag{01}$$

$$\sigma_1 = f_{cr}\left(\frac{\varepsilon_{cr}}{\varepsilon_1}\right)^{0.4} \qquad \varepsilon_1 \ge \varepsilon_{cr} \tag{02}$$

where σ_1 = tension stress; ε_1 = tension strain; E_c = modulus of elasticity of concrete; f_{cr} = cracking stress of concrete; εcr = cracking strain of concrete.

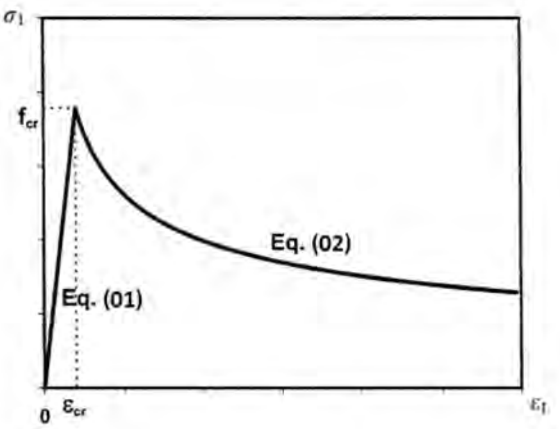

Figure 6: Tensile stress-strain curve of concrete (Wang & Hsu 2001)

When concrete expose to elevated temperatures, its stress-strain behavior will change due to the decrease of modulus of elasticity, compressive strength and tensile strength. The tensile strength at temperature θ is taken as 0.1 of the compressive strength at temperature θ (Dai et al. 2014). A stress-strain diagram of concrete under compression at elevated temperatures can be obtained based on the Eurocode model (EN1994-1-2 2005):

$$\sigma_{c,\theta} = f_{c,\theta}\left[3\left(\frac{\varepsilon_{c,\theta}}{\varepsilon_{cu,\theta}}\right)/\left\{2+\left(\frac{\varepsilon_{c,\theta}}{\varepsilon_{cu,\theta}}\right)^3\right\}\right] \tag{03}$$

$$f_{c,\theta} = k_{c,\theta} f_c \tag{04}$$

where $\sigma_{c,\theta}$ = compression stress at temperature θ, $f_{c,\theta}$ = compression strength at temperature θ; $\varepsilon_{c,\theta}$ = compression strain at temperature θ; $\varepsilon_{cu,\theta}$ = the strain corresponding to $f_{c,\theta}$; k = the reduction factor; f_c = compression strength at ambient temperature.

With respect to simulate the fire-damaged slab, the temperature distribution from the exposure surface is considered. The maximum temperatures measured versus the cross section concrete depth during a fire test are reported in Table 2. In this paper, a simple method is used to model the slab after fire by dividing the slab to be many layers. At each layers, the stress-strain relation of concrete will change corresponding to the temperature distribution versus the depth of cross section. The detail is shown in Figure 7.

Table 2: The maximum temperatures measured versus the cross section concrete depth

Distance from exposure surface (mm)	Max. Temperature
0	949
25	358.4
75	131
125	130.7

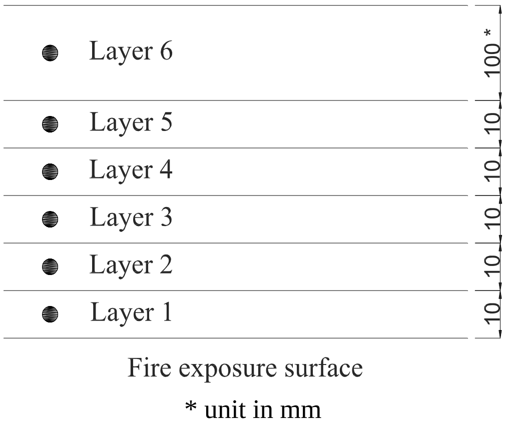

Figure 7: Stress-strain application range for each layers

3.4. Constitutive models for steel

The typical stress-strain relationships for steel bar is shown in Fig. 8. The steel bar has approximately linear elastic behavior at low strain magnitudes. At higher strain magnitudes, it begins to have nonlinear, which is referred to as plasticity. The shift from elastic to plastic behavior occur at a yield point. Once the stress in the steel exceeds the yield stress, plastic deformation begins to occur. The stiffness of the steel decreases once the material yields. After heating and cooling to the temperature, it may have a notable decrease in yield strength but the influence on the modulus of elasticity is generally less significant (Tao et al. 2012). In general, the shape of the stress-strain curve of steel remains the same as before heated.

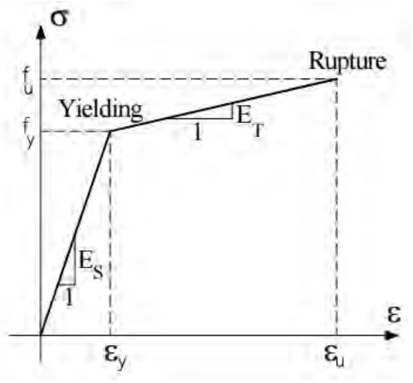

Figure 8: Stress-strain curve for steel (Neale et al. 2005)

4. RESULTS AND DISCUSSION

4.1. Experimental results

After fire test, the crack and spalling could be observed on the fire exposure surface but the damaged level was not much. Only 12% of the surface area was spalling. Then the flexural test on control specimen and heated slab was conducted and the results are shown in Fig. 9.

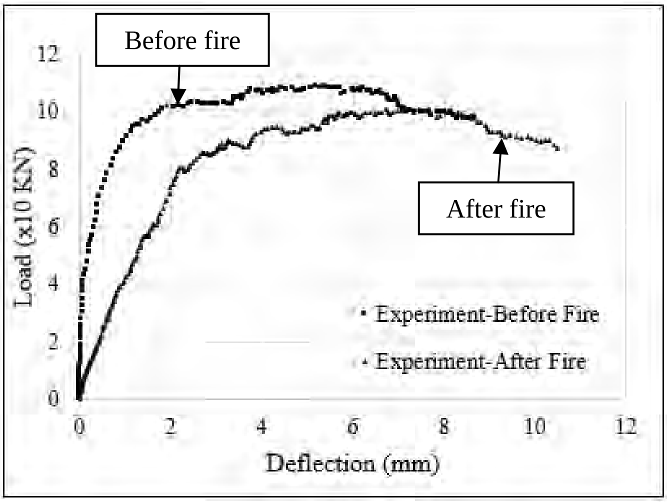

Figure 9: The load-deflection curve of slabs SC1 and SF1

In regard to the control slab SC1 after bending test, its failure patterns were typical bending cracks that located in the maximum moment zone. This type of failure can be observed with respect to any normal flexural reinforced concreted members. In case of the fire-damaged slab SF1, the bending cracks were also observed similar to the failure pattern of specimen SC1. However, the cracks appeared early due to the loss of load capacity of the slab after fire.

4.2. Modelling results

The results from the FE analysis program are shown in Fig 10 in a comparison with experimental data. As it can be seen in the figure, the result of modelling in case of unheated slab is in a good agreement with the experimental curve. After cracking both modelling and experimental curves have rather the same inclinations until yielding of steel bars and they show the same cracking plateau after that. In order to the stress-strain relation of fire-damaged slab, the curve of modelling shows an approximate shape with the curve of experimental results. This indicates that the modelling method as mentioned above can be acceptable with respect to simulate the fire-damaged slab.

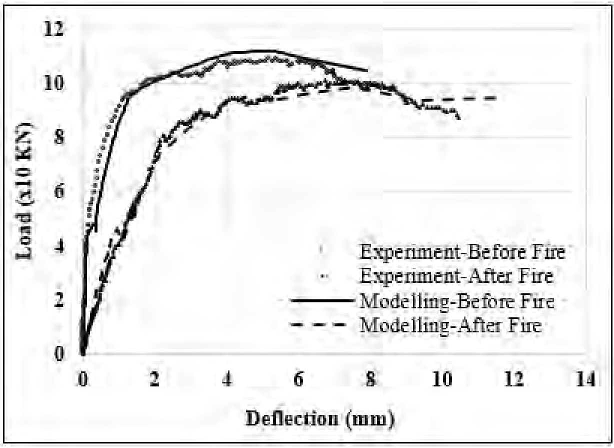

Figure 10: The results of modelling and experiment of RC slabs

5. CONCLUSION

In this paper, the remaining strength of reinforced concrete slab after the thermal loading is evaluated at the room temperature and compare with the unheated slab. The simulation on flexural behavior of unheated and heated slabs are performed by using 3D finite element analysis program ABAQUS. The stress-strain-temperature relation for concrete is applied and the following conclusions are made:

- Due to the effect of thermal loading, the loading capacity of fire-damaged slab reduced and is lower the maximum value of control specimen. Besides, its stiffness was less than the value obtained for unheated slab.
- The results of modelling indicated a good agreement with the experimental curves in both of cases.

Therefore the stress-strain-temperature relation models corresponding to the temperature distribution on cross section depth of slab is suitable to develop a model for the prediction of flexural behavior on RC slab exposure to fire.

REFERENCES

ACI, 1995. "*Building Code Requirements for Reinforced Concrete*." American Concrete Institute, Farmington Hills, Mich.

Annerel E.V. and Taerwe L.R., (2013). "Assessment techniques for the evaluation of concrete structures after fire." *Journal of structural fire engineering*, 4, 123-130.

ASTM, 2000. "*ASTM E119: Standard Test Methods for Fire Tests of Building Construction and Materials*." West Conshohocken, America: American Society for Testing and Materials.

Chang Y.-F., Chen Y.-H., Sheu M.-S. and Yao G.C., (2006). "Residual stress–strain relationship for concrete after exposure to high temperatures." *Cement and Concrete Research*, 36, 1999-2005.

Dai J.-G., Gao W.-Y. and Teng J., (2014). "Finite Element Modeling of Insulated FRP-Strengthened RC Beams Exposed to Fire." *Journal of Composites for Construction*,

EN1994-1-2, 2005. "*Eurocode 4: Design of composite steel and concrete structures - Part 1-2: General Rules - Structural Fire Design*." London, UK: British Standards Institution.

fib, 2007. "Fire design of concrete structures - materials, structures and modelling."

fib, 2008. "Fire design of concrete structures - structural behaviour and assessment." Switzerland: the International Federation for Structural Concrete (fib).

fib, 2010. "*Model Code 2010*." Fédération Internationale du Béton fib/International Federation for Structural Concrete.

Hsu J.H. and Lin C., 2006. "Residual bearing capabilities of fire-exposed reinforced concrete beams." *International Journal of Applied Science and Engineering*, 4, 151-163.

Neale K., Ebead U., Abdel Baky H., Elsayed W. and Godat A., (2005). "Modelling of debonding phenomena in FRP-strengthened concrete beams and slabs." *International Institute for FRP in Construction,*

Nechnech W., Meftah F. and Reynouard J., 2002. "An elasto-plastic damage model for plain concrete subjected to high temperatures." *Engineering structures*, 24, 597-611.

Qiang X., Bijlaard F.S. and Kolstein H., 2012. "Post-fire mechanical properties of high strength structural steels S460 and S690." *Engineering structures*, 35, 1-10.

Short N., Purkiss J. and Guise S., 2001. "Assessment of fire damaged concrete using colour image analysis." *Construction and Building Materials*, 15, 9-15.

Simulia, 2014. " ABAQUS Version 6.13-4 and ABAQUS user’s manual." Hibbitt Karlsson & Sorensen Inc:

Tao Z., Wang X.-Q. and Uy B., 2012. "Stress-strain curves of structural and reinforcing steels after exposure to elevated temperatures." *Journal of Materials in Civil Engineering*, 25, 1306-1316.

Thi C.N., Pansuk W. and Torres L., 2015. "Flexural Behavior of Fire-Damaged Reinforced Concrete Slabs Repaired with Near-Surface Mounted (NSM) Carbon Fiber Reinforced Polymer (CFRP) Rods." *Journal of Advanced Concrete Technology*, 13, 15-29.

Ünlüoğlu E., Topcu I.B. and Yalaman B., 2007. "Concrete cover effect on reinforced concrete bars exposed to high temperatures." *Construction and Building Materials*, 21, 1155-1160.

Wang T. and Hsu T.T., 2001. "Nonlinear finite element analysis of concrete structures using new constitutive models." *Computers & structures*, 79, 2781-2791.

Youssef M. and Moftah M., 2007. "General stress–strain relationship for concrete at elevated temperatures." *Engineering structures*, 29, 2618-2634

THE KEY INDEX FOR RATIONAL BRIDGE MAINTENANCE BY MUNICIPALITIES IN JAPAN

Riko Sakata
Bachelor's 4th grade student, Nagai lab, ICUS, IIS,
The University of Tokyo, Japan
sakata@iis.u-tokyo.ac.jp

ABSTRACT

Japan has almost 700,000 bridges over 2m spans. Many of them were constructed in high economic growth period around 1970s, and damaged due to severe environment, fatigue loading, inappropriate maintenance etc. It becomes important to establish the rational and feasible maintenance strategy considering the damaged condition of bridges, social condition and capability of managers.

Most bridges are managed by municipalities in Japan. Thinking about their efficient maintenance, there are 4 steps; specify the bridges we should care, decide the management level we need, how we improve it, and consider how we implement it in practice. The management level means how well the municipalities responsible for their bridge maintenance, and it was evaluated by the interview in rural municipalities in Niigata, Japan. It was found that situation in each municipalities is totally different as well as the population, area, number of brides so that the rational maintenance method should be established corresponding to the situation. For it, indexation of the factors to be considered is useful to evaluate the rationality of the maintenance framework.

This study focuses on 1st and 2nd steps above. For the first step, indexation of condition of bridges, basic data of bridges such as number, length, bridge type, damage level etc. are selected because municipalities usually have their data. Then, the number of important bridges to be cared is calculated. Through the comparison it with the management level, ideal level of maintenance by referring some good municipalities are proposed.

Keywords: *road bridge deterioration, maintenance, municipalities, management level, important bridge*

1. INTRODUCTION

We Japan have almost 700,000 bridges over 2m spans. Since many of them are constructed during high economic growth by early 1970s, almost 70% will be over 50 years old in 20 years, which is said to be the life span of the bridge. (Figures 1 and 2) So the cost of the bridge maintenance will increase dramatically due to the damaged from chloride attach or long-time fatigue loading, and other aren’t managed appropriately. In order to manage them effectively and keep the bridge safety, we need to think about the rational and feasible maintenance strategy.

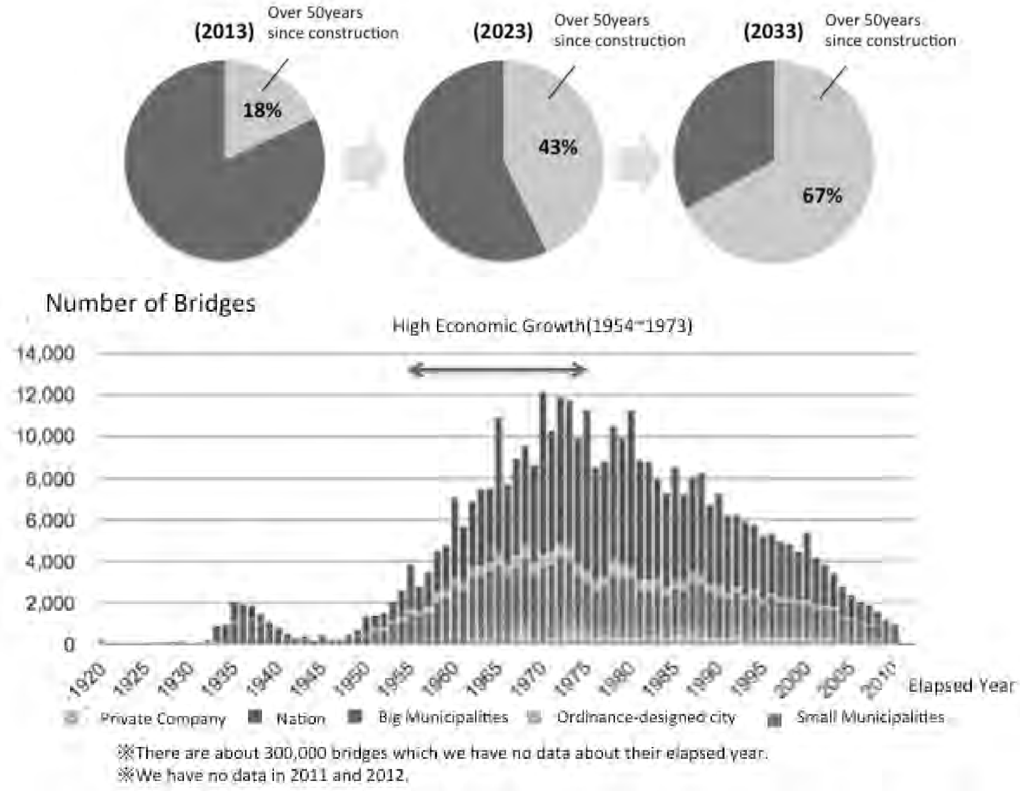

※There are about 300,000 bridges which we have no data about their elapsed year.
※We have no data in 2011 and 2012.

Figure 1: Number and the age of bridges in Japan (MLIT, 2013)

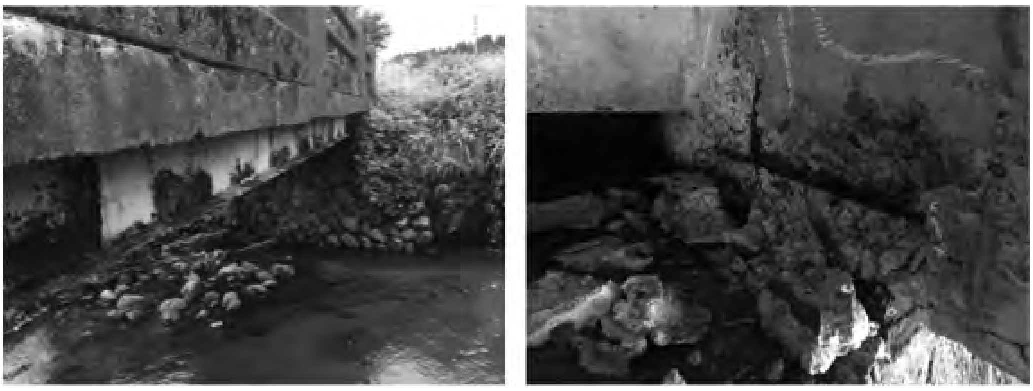

Figure 2: Deterioration of bridge

2. MANAGEMENT OF BREDGES BY SMALL MUNICIPALITIES

About 70% bridges are managed by small municipalities in Japan as Figure 3 shows, but they don’t have enough experts. In many small municipalities, some staff deal with both technical work and deskwork, and no one have enough technical knowledge or skill. It is necessary to consider this situation in thinking about bridge maintenance.

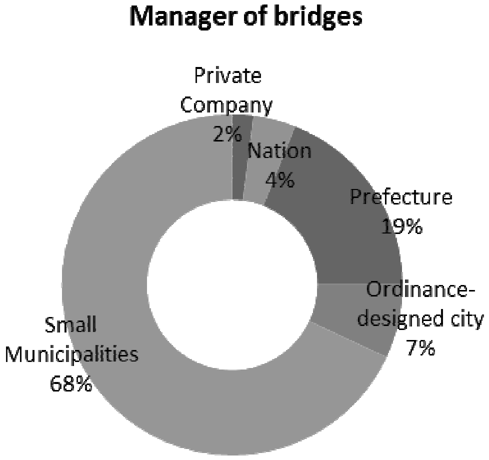

Figure 3: Manager of Bridges in Japan (MLIT, 2013)

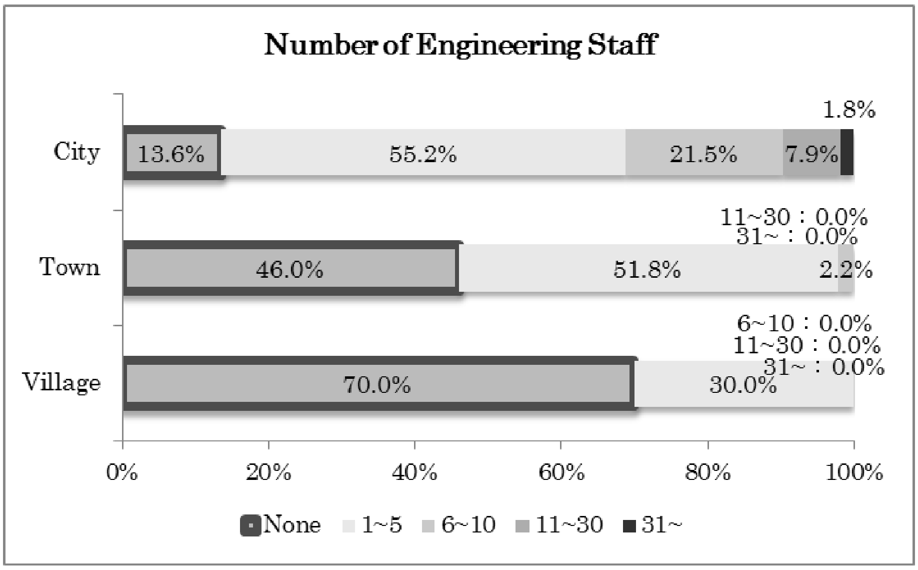

Figure 4: Manager of Bridges in Japan (MLIT, 2013)

In the near future, more and more bridges have the deterioration with aging, and much more cost will be needed to repair them. In order to deal with this situation efficiently, each municipality has established the bridge maintenance plan by 2013. And as of 2015 they have mostly finished the inspection of their bridges over 2m span and some of them start repairing them based on the plan.

In previous research, Nakashima (2013) inquired the situation about how small municipalities in Niigata prefecture manage bridges. Through the investigation, each municipality is scored the management level in terms of how they can judge to meet the actual situation in the 4 steps shown in Figure 5, although the system outputs some strategy automatically. Higher score means that municipalities can judge by themselves in each step and it was found the management level varies depending on the population and the number of bridge.

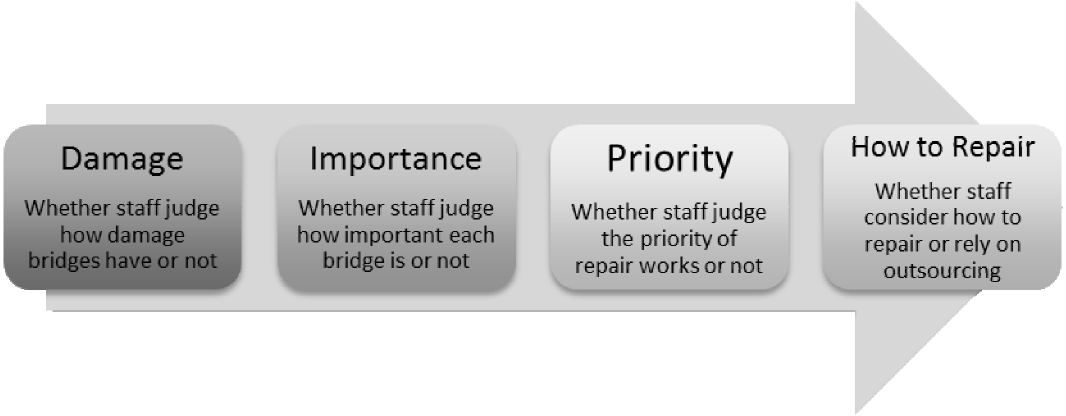
Damage
Whether staff judge how damage bridges have or not
Importance
Whether staff judge how important each bridge is or not
Priority
Whether staff judge the priority of repair works or not
How to Repair
Whether staff consider how to repair or rely on outsourcing

Figure 5: Flow of judgment (Nakashima, 2013)

Management level		A Damage	B Importance	C Priority	D How to repair
○	2	Inspection by staff	Change inspection depending on importance	Arrange among municipalities, judgment	Examine/ Design by staff
△	1	Inspection by staff	Intensify the system	Arrange only budget	Accept consultant's proposal （Some Action）
×	0	Don't check the results/Only check	The level in system	Order in system	Accept consultant's proposal （No action）

Figure 6: Management level (Nakashima, 2013)

3. METHOD OF THIS STUDY

3.1 Introduction

There are many varieties of factors, such as physical condition, potential manager and social condition, in thinking about the bridge maintenance. 4 steps are proposed here for the rational and feasible strategy: specify the bridges we should care, decide the management level we need, how we improve it, and consider how we implement it in practice. In this study the first 2 steps are treated. In Niigata prefecture, Niigata Construction

Technology Center collects the inspection data from small municipalities and supports them. The date is used to make a suggestion about the rational strategy of bridge maintenance through the data.

3.2 Importance of the bridge

In the bridge maintenance plan, bridge importance is divided in Division 1/2/3/4, based on physical and social condition, such as length, bridge type and the volume of traffic. Division 1 is the most important bridges, and municipalities should manage them with more cost. Municipalities usually judge which bridges need repair by next inspection in 5 years with the matrix in Figure 7. Figure 8 shows the number of these bridges in small municipalities in Niigata prefecture with the bridge need to be repaired.

		Damage Level					
		E	C3	C2	C1	B2	B1
Division	1	①	⑤	⑨	⑫	⑭	
	2	②	⑥	⑩	⑬		
	3	③	⑦	⑪			
	4	④	⑧				

Figure 7: Matrix for repair priority with Damage Level and Division

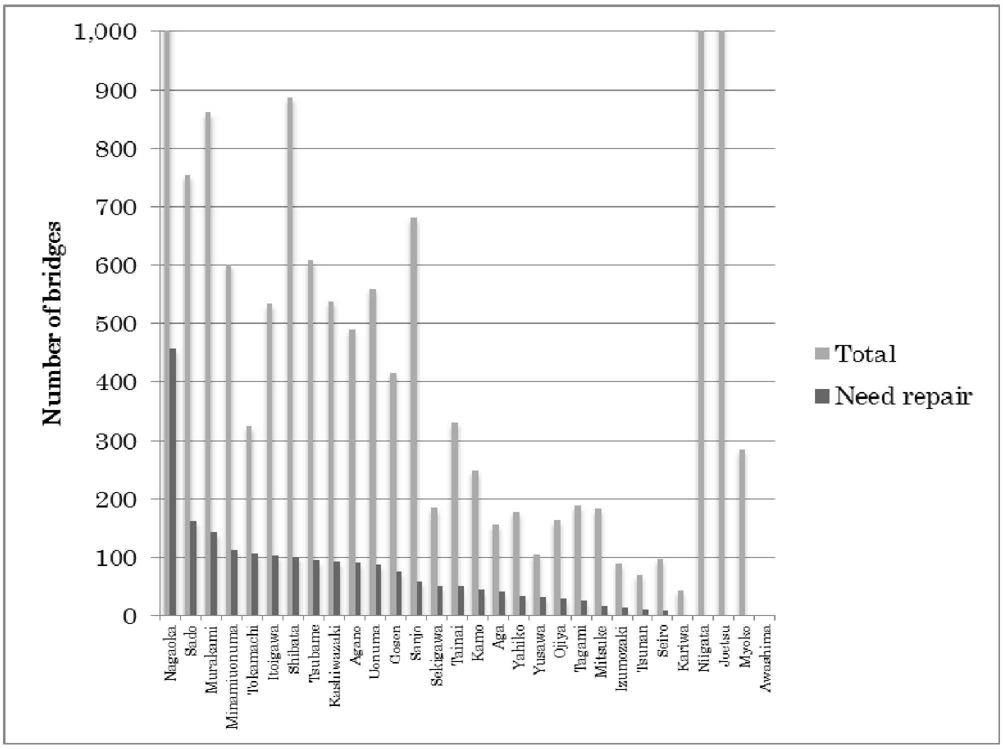

Figure 8: Number of bridges
(Total/Need repair by next inspection)

3.3 Management level and bridge in municipalities

Table 1 and Figure 9 show the relationship with the management level investigated by Nakashima and the number of the bridges which need repair by next inspection. It can be said that the more bridges municipalities have, the higher management level they need for maintenance. Each municipality has different situation, and smaller municipalities has limited staff and budget. So smaller municipalities should rely on outsourcing instead of gaining staff, while bigger ones should assign enough staff and improve technical skill so that they can manage inhouse.

	Population	Number of bridges		Management level				
		Total	Need repair	Damage	Importance	Priority	How to Repair	Total Score
Nagaoka	279,845	2,037	457	1	1	2	2	6
Sado	60,415	755	163	0	1	2	1	4
Murakami	64,730	862	143	0	–	–	–	0
Minamiuonuma	60,593	601	113	1	1	–	2	4
Tokamachi	57,358	325	106	0	2	2	2	6
Itoigawa	46,438	533	102	0	2	2	1	5
Shibata	100,035	888	100	2	2	2	2	8
Tsubame	81,183	609	95	1	1	2	2	6
Kashiwazaki	89,768	538	93	1	2	2	2	7
Agano	44,720	490	91	0	1	2	1	4
Uonuma	39,163	559	87	0	1	1	0	2
Gosen	53,316	415	76	0	0	2	0	2

Sanjo	100,844	681	58	1	0	0	0	1
Sekigawa	6,244	184	51	0	2	1	2	4
Tainai	30842	332	51	-	-	-	-	-
Kamo	29,085	248	44	2	1	−	1	4
Aga	12,723	155	40	2	1	−	1	4
Yahiko	8,404	178	34	0	1	0	0	1
Yusawa	8,351	104	32	0	0	1	0	1
Ojiya	37,712	163	30	0	0	1	0	1
Tagami	12,577	188	25	0	0	0	0	0
Mitsuke	41,294	183	15	0	0	2	1	3
Izumozaki	4,759	88	14	0	2	1	2	5
Tsunan	10,570	69	10	0	1	−	1	2
Seiro	13,914	96	8	0	0	0	0	0
Kariwa	4,781	42	3	0	1	1	0	2
Niigata	811,386	4,093	−	1	2	1	2	6
Joetsu	201,153	1,146	−	0	2	1	0	3
Myoko	34,545	285	−	1	0	2	2	5
Awashima	344	2	−	-	-	-	-	-

Table 1: Population/Number of bridges/Management level in small municipalities in Niigata prefecture

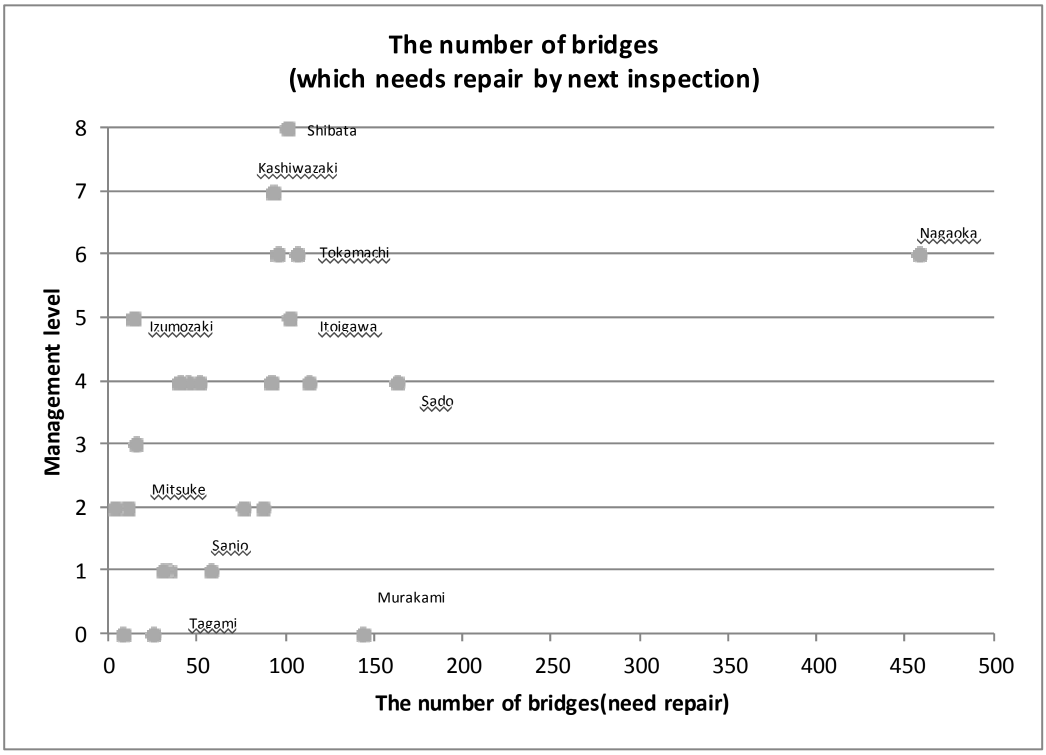

Figure 9: Management level with the number of bridges need to be repaired by next inspection

4. CONCLUSION

In municipalities, the management level is different depending on how many important bridge they have, and this seems the key index for the bridge maintenance by small municipalities. Each municipality has different situation so they need the different way of the maintenance. They should improve the management level as they can. And understanding their position compared with other municipalities helps them efficient bridge maintenance.

REFERENCES

Nakashima Mari, 2013, *The inquiry of the bridge maintenance by small municipalities and the analysis of the management level*

Ministry of Land, Infrastructure and Transport, 2013, *The maintenance of the road infrastructure(Bridge)*

http://www.mlit.go.jp/road/sisaku/yobohozen/yobo1_1.pdf

EFFECT OF FREE LIME CONTENT ON MECHANICAL PROPERTIES OF CEMENT-FLY ASH MIXTURES

Adnan NAWAZ [a], Parnthep JULNIPITAWONG [b],
Somnuk TANGTERMSIRIKUL [c]
[a]Doctoral student, School of Engineering and Technology,
Asian Institute of Technology
haveadnan@gmail.com
[b]Research faculty, Construction and Maintenance Technology Research Center, School of Civil Engineering and Technology,
Sirindhorn International Institute of Technology, Thammasat University
[c]Professor, School of Civil Engineering and Technology,
Sirindhorn International Institute of Technology, Thammasat University

ABSTRACT

This study highlights the effect of free lime content in fly ash on the mechanical properties of cement-fly ash. A detailed experimental program was carried out in order to evaluate the effect of free lime content in fly ashes with different SO_3 contents on the mechanical properties including initial and final setting times, water requirement and compressive strength of cement-fly ash mixtures. Four distinct types of fly ashes were obtained from two different sources, and free lime was added to obtain overall free lime contents of 5%, 7% and 10% for each type of fly ash. Tests were conducted with two fly ash replacement percentages (20% and 40%). Experimental results revealed that an increase in the free lime content resulted in reduced water requirement. Higher free lime content also resulted in faster setting times and improved compressive strength.

***Keywords**: Fly ash, Free lime, Mechanical Properties*

1. INTRODUCTION

In Thailand, one of the main production source of fly ash is Mae Moh power plant of the Electricity Generating Authority of Thailand (EGAT) which contributes around 90% of total national production. Recently, fly ash obtained from this source has shown increased content of free lime, which may affect the mechanical and durability properties of cement-fly ash mixtures. Kaewmanee et al. (2013) conducted a comprehensive study on properties of fly ash mixes, with various free lime contents and reported a set of experimental results to clarify the effect of free lime content on fly ash mixes. Results showed that basic properties (normal consistency and water demand) were not much affected by free lime added.

Moreover, fly ash obtained from the Mae Moh power plant has also shown higher sulfur trioxide (SO_3) content, which may ultimately result in compromised long-term properties. There are only a very few studies that simultaneously consider the effect of high free lime and high SO_3 content in fly ashes on mechanical properties of cement-fly ash mixtures. This study is an attempt to further explore the knowledge of the effect of high free lime content in different fly ashes of Thailand, particularly in the case of fly ashes with different sulfur trioxide (SO_3) contents, on the mechanical properties of the cement-fly ash mixtures.

Table 2 Chemical compositions of ordinary Portland cement type I, Mae Moh fly ashes A, B, C and Rayong fly ash R.

Table 1: Physical properties of ordinary Portland cement type I, Mae Moh fly ashes A, B, C, Rayong fly ash R and free lime.

Physical properties	OPC type I	Fly ash A	Fly ash B	Fly ash C	Fly ash R	Free lime
Specific gravity	3.15	2.21	2.57	2.57	2.17	2.96
Blaine fineness (cm^2/g)	3100	2867	2820	2722	2723	3749

2. EXPERIMENTAL PROGRAM

2.1 Materials

Four primary fly ashes F(A), F(B), F(C), and F(R) from two different sources and an ordinary Portland cement (OPC) type I, were used in this study. F(A), F(B), and F(C) were obtained from the Mae Moh power generating plant of the Electricity Generating Authority of Thailand (EGAT) in Lampang province (located in the north of Thailand), whereas F(R) was obtained from the Rayong coal burning thermal power plant in Rayong province (Eastern part of Thailand). **Tables 1 and 2** show the physical properties and chemical compositions of the materials utilized.

Based on chemical requirements of TIS 2135, F(R) was categorized as Class 2a (low CaO fly ash) whereas F(A), F(B) and F(C) were classified as Class 2b (high CaO fly ash). The amount of sulfur trioxide (SO_3) in F(B) and F(C) exceeded the maximum allowable limit of 5%, as specified by TIS 2135.

Free lime was added in F(A), F(B) and F(C) to prepare fly ashes having total free lime contents of 5%, 7% and 10%, respectively. River sand compatible with ASTM C33-92a, with a specific gravity of 2.60 was used as the fine aggregate.

Chemical compositions %	OPC type I	Fly ash A	Fly ash B	Fly ash C	Fly ash R
SiO_2	18.93	35.71	26.61	25.22	61.46
Al_2O_3	5.51	20.44	13.6	13.88	20.27
Fe_2O_3	3.31	15.54	18.34	17.39	5.56
CaO	65.53	16.52	24.97	26.25	1.73
MgO	1.24	2.00	2.33	2.38	0.96
Na_2O	0.15	1.15	1.75	1.40	0.73
K_2O	0.31	2.41	1.77	1.92	1.36
SO_3	2.88	4.26	8.53	9.44	0.38
LOI	-	0.49	0.53	0.56	5.38
Free lime	0.75	1.71	3.93	3.06	0.03
Equivalent sodium oxide ($Na_2O + 0.658\ K_2O$)	0.35	2.74	2.91	2.66	1.62

3. RESULTS AND DISCUSSION

3.1 Scanning electron microscope (SEM) images

It can be observed in **Figure 1a** that the particles of fly ash obtained from the Mae Moh electricity generating power plant are round or spherical shape while irregular particles of free lime can be seen, dispersed around fly ash particles. **Figure 1b** shows that the Rayong fly ash particles are relatively less spherical than those of the Mae Moh fly ash.

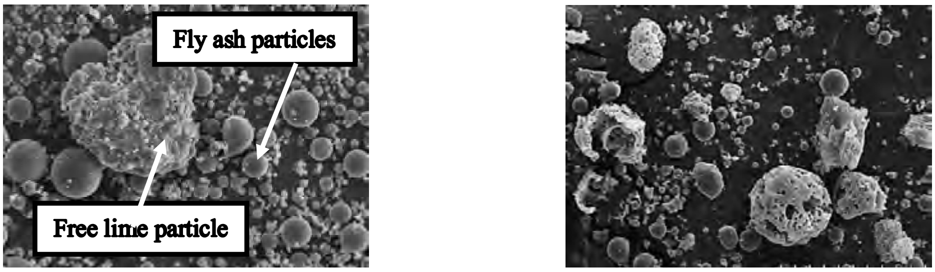

(a) Mae Moh fly ash (b) Rayong fly ash

Figure 1: SEM images

3.2 Water requirement

Water requirement results (**Figure 3a**) show that to attain same flow, mixtures of primary fly ashes from Mae Moh, F(A), F(B), and F(C) required a lower amount of water as compared to the cement-only mixtures, due to spherical particle shape**.** F(R) mixtures required more water than the cement-only mixtures in order to achieve the same flow. The water requirement of fly ash mixtures further reduced as the replacement percentage of fly ashes is increased from 20% to 40%, except for F(R) mixtures where 40% fly ash replacement showed higher water requirement than that of 20% replacement. **Figure 3b-d** show the effect of addition of free lime in fly ashes on the water requirement of mixtures. Mixtures with a higher amount of free lime required more water to attain the same flow.

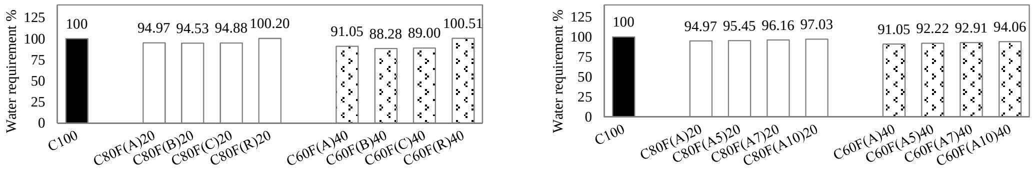

(a) Mixtures with primary fly ashes (b) Mixtures with F(A) based fly ashes

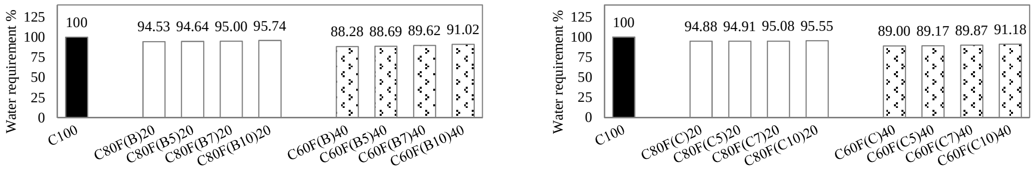

(c) Mixtures with F(B) based fly ashes (d) Mixtures with F(C) based fly ashes

Figure 3: Water requirement of mortar mixtures

3.3 Initial and final setting times

Figure 4a shows that primary fly ash mixtures of F(A), F(B), F(C), and F(R) exhibited longer setting times than the cement-only mix. Mixtures of F(B) as well as F(C), tend to set faster than F(A) mixtures because of the higher calcium oxide and free lime contents in F(B) and F(C). In contrast, F(R) mixtures set slower because of its lower calcium oxide (CaO) and free lime contents and higher water requirement. The increase of fly ash percentages from 20% to 40% resulted in longer setting times. The influence of free lime addition on setting time is obvious in **Figure 4b-d.** It can be seen that addition of free lime caused faster setting times.

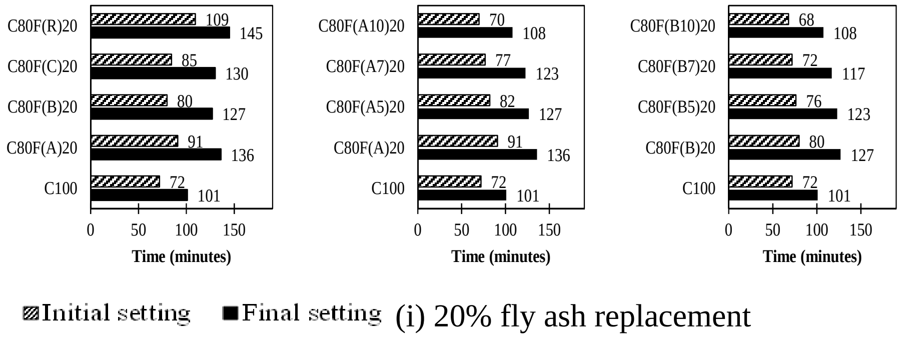

(i) 20% fly ash replacement

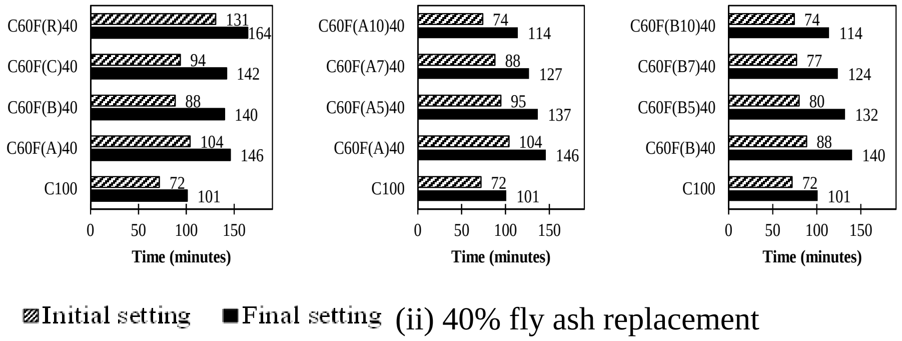

(ii) 40% fly ash replacement

(a) Primary fly ash mixtures (b) F(A) based fly ash mixtures (c) F(B) based fly ash mixtures

Figure 4: Initial and final setting times of different mixtures

3.4 Compressive strength

Figure 5 shows the comparison of compressive strength (at different ages) of cement-only mixtures and primary fly ash mixtures. Higher calcium oxide (CaO) and free lime contents and lower water requirement in F(B) and F(C) as compared to F(A) contributed to higher compressive strength than F(A) mixtures. F(R) mixtures showed lower compressive strengths at 1, 7, and 28 days than the mixtures with Mae Moh fly ashes. However F(R) mixtures showed higher 91-day strength because of higher SiO_2 content (61.4%) leading to more pozzolanic reaction in the long term.

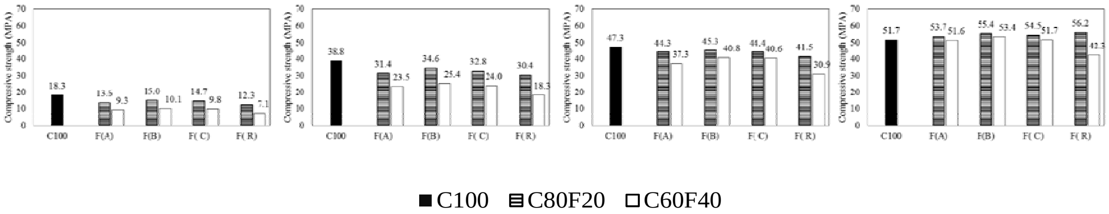

(a) 1 day (b) 7 days (c) 28 days (d) 91 days

Figure :5 Compressive strength of mortar specimens with primary fly ash mixes

Figure 6 indicates that in the case of F(A), an increase in free lime content resulted in improved compressive strength. The improvement is more obvious at an early age of 1-day. In the case of F(B), an increase in free lime content resulted in increased compressive strength at an early age of 1 day, as illustrated in **Figure 7**. At 7 and 28 days, the differences in the compressive strengths of mixtures, with and without added free lime, are not significant. At a later age of 91 days, the compressive strengths are relatively reduced. For F(C), an increase in free lime content caused improved compressive strength. However at 28 and 91 days, F(C10) mixture with 40% fly ash showed relatively lower compressive strength as compared to F(C) mixture, as shown in **Figure 8.**

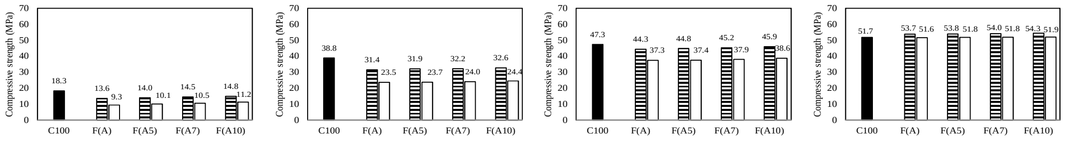

(a) 1 day (b) 7 days (c) 28 days (d) 91 days

■C100 ▤C80F20 □C60F40

Figure 6: Compressive strength of mortar specimens with F (A) based fly ash mixes

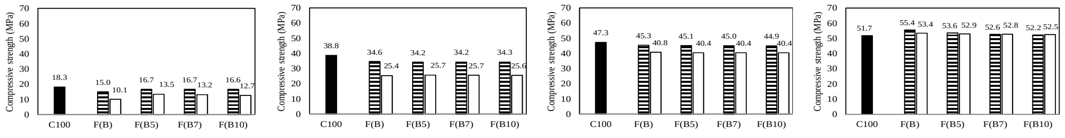

(a) 1 day (b) 7 days (c) 28 days (d) 91 days

■C100 ▤C80F20 □C60F40

Figure 7: Compressive strength of mortar specimens with F

(B) based fly ash mixes

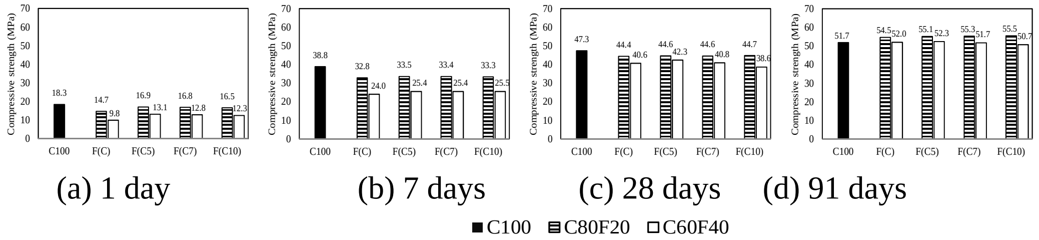

(a) 1 day (b) 7 days (c) 28 days (d) 91 days

■C100 ▤C80F20 □C60F40

Figure 8 Compressive strength of mortar specimens with F (C) based fly ash mixes

3.5 Strength activity index

Figure 9 shows that the strength activity indices of mixtures, containing Class 2a fly ash [F(R)] and Class 2b fly ashes [F(A), F(B), F(C)], are higher than 75%, and 85% of the strength of the reference cement-only mixture at 28, and 91 days, respectively. Thus, all tested fly ashes fulfilled the strength requirement of TIS 2135.

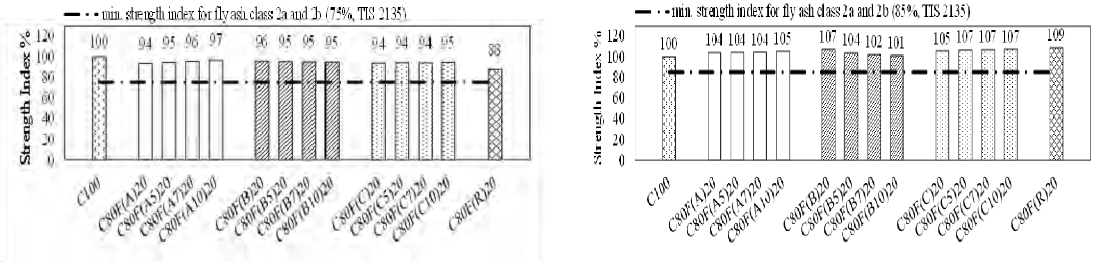

(b) 28 days (c) 91 days

Figure :9 Strength index of mortar specimens

4. CONCLUSIONS

This is a preliminary study to investigate and verify the effect of free lime content in fly ashes with different SO_3 contents and fly ash replacement ratios only on the mechanical properties of cement-fly ash mixtures. Further verification and durability testing is needed in the future. Conclusions drawn from this study are as follows:

i. Water requirement of Mae Moh fly ashes is lower than the Rayong fly ash because of the high LOI and relatively irregular particle shape of the Rayong fly ash.
ii. Water requirement of fly ash mixtures increases as the free lime content is increased,
iii. Fly ash mixtures containing higher free lime content tend to set earlier.
iv. Higher free lime content in fly ash results in improved compressive strength, particularly at early ages.
v. In the case of fly ashes with a naturally high free lime content, an increase in compressive strength due to the addition of free lime is less significant at a long age of 91 days.

vi. All the tested mixtures of fly ashes with free lime content up to 10% fulfill the compressive strength requirements of TIS 2135.

ACKNOWLEDGEMENTS

The authors would like to thank the Electricity Generating Authority of Thailand for providing research support and fly ash samples for this study. This research is also supported by Center of Excellence in Material Science, Construction and Maintenance Technology, Thammasat University, the Higher Education Research Promotion and National Research University Project, the Office of the Higher Education Commission of Thailand.

REFERENCES

Thai Industrial Standards. TIS 2135 standard Specification for coal fly ash; 2002.

Kaewmanee K., Krammart P., Sumranwanich T., Choktaweekarn P., Tangtermsirikul S. Effect of free lime content on properties of cement–fly ash mixtures. J Construction and Building Materials Res 2013;38:829-36.

Annual Book of ASTM Standards. ASTM C33 standard specification for concrete aggregates; 2003.

Annual Book of ASTM Standards. ASTM C187 standard test method for normal consistency of hydraulic cement; 1998.

Annual Book of ASTM Standards. ASTM C191 standard test method for time of setting of hydraulic cement by Vicat needle; 1999.

Annual Book of ASTM Standards. ASTM C109/C109M standard test method for compressive strength of hydraulic cement mortars (using 2-in. or [50-mm] cube specimens)

Annual Book of ASTM Standards. ASTM C311 standard test methods for sampling and testing fly ash or natural pozzolans for use in Portland-cement concrete; 2004

THE RELATIONSHIP BETWEEN THE RAINFALL INTENSITY AND THE SUBWAY PASSENGER RIDERSHIP IN THE SEOUL METROPOLITAN SUBWAY SYSTEM

Kyoung-seon PARK[1], Sung-hi AN[2], Chang-hyeon Joh[3]
and Hyun-myung KIM[4]
[1] Researcher/Transportation Planning Lab, Dept. of Transportation Eng.
College of Engineering, The MyongJi University, South Korea
seon3675@nate.com
[2] Graduate Student School of Eng., The MyongJi University, South Korea
[3] Ph.D., KyungHee University, South Korea
[4] Ph.D., Director, The MyongJi University, South Korea

ABSTRACT

The in-vehicle congestion of the urban railway is the most important indicator to reflect the operation state of the urban railway. To provide the good service quality of urban railway, the crowdedness of the urban railway should be managed appropriately. The weather is one of the critical factors for the crowdedness. That is because even though the crowdedness of the urban railway is the same, passengers feel more uncomfortable in rainy weather condition. Indeed if specific sections and stations suddenly are concentrated excessive demand, it will lead far more serious problem. Therefore, this study analysis the relationship between the number of urban railway passenger and rainfall intensity in Seoul and then conducts the space analysis to deduct passenger demand patterns.This study is expected to be useful base study in order to manage the congestion at the urban railway station effectively by considering the different rainfall intensity.

Keywords: *urban railway, crowdedness, rainfall, GIS spatial analysis, subway passenger ridership*

1. INTRODUCTION

The crowdedness of the urban railway is the most important indicator to reflect the operation state of the urban railway. To provide the good service quality of urban railway, the crowdedness of the urban railway should be managed appropriately. To evaluate the crowdedness in the urban railway, quantitative factors and qualitative factors are needed. The weather is one of the critical factors to influence the crowdedness. This is because even though the crowdedness of the urban railway is the same, passengers feel more uncomfortable in rainy weather condition. Indeed if specific sections and stations suddenly are concentrated excessive demand, it will lead far more serious problem.

However, few literatures had been studied to analyze the relationship between the weather and traffic demand. This is because collecting the traffic demand and weather data was difficult. However, these data have been opened to the public; it is possible as get detailed information such as Passenger data

Park et al. (2012) analyzed the passenger's transfer pattern during rainfall in Busan. This study showed that the ratio of the passenger's mode choice is different with the different amount of rain. This research also showed that the ratio of mode choice is more influenced by the rainfall on weekend.

Lee et al. (2014) conducted the relationship between the number of public transportation passenger and the weather, especially for rain with the smart card data. This study revealed that both the number of bus and urban railway passengers were reduced in the rain. With these results, Lee et al. (2014) pointed out that the public transportation passengers at Seodaemun-gu, Dongdaemun-gu, and Jung-gu were easily influenced by the rain intensity.

Lee et al., (2011) analyzed the rain intensity and the bus travel time to verify the quality of bus services. The study showed that the quality of the bus services was greatly influenced by rain start in the morning peak hours.

However, these researches focused on the specific regions so that it could not show a detail analysis.

Therefore, this study constructs the database set about the urban railway passenger with the rainfall intensity in Seoul and conducts the spatial analysis to deduct passenger demand patterns. This paper collects rainfall data which are collected from July to September and urban railway passenger data. With these data, this study analyzed the relationship between the number of urban railway passenger and rainfall intensity.

2. THE RELATIONSHIP BETWEEN THE RAINFALL INTENSITY AND THE SUBWAY PASSENGER RIDERSHIP

2.1 Data for analysis

Seoul is one of the biggest cities in the world and eight subway lines are connected so people can reach every single place in Seoul. So many people use subway for commuting and other travel purposes. According to the Kang et al. (2014) study, up to 36 % of people responded that they choose subway as a travel mode.

This paper analyzes the rainfall intensity to show its impact on demand of the Seoul urban railway with the urban railway passenger data. This study use railway passenger data which are collected from July to

September 2012 and 2013. Daily rainfall data which are used are collected from the Automatic Weather Stations (AWS). To analyze the relationship between the rainfall intensity and the subway passenger ridership, this study selects in that same period rainfall data and then conducts a spatial analysis.

Based on the Meteorological Agency data, this study categorizes rainfall intensity by 6 level (Table 1).

Table 1: Rainfall Analysis Database set

Level	Rainfall(mm)	Analysis days		Sum(days)
		2012(days)	2013(days)	
1	Less than 1	36	36	72
2	1~5	6	8	14
3	5~10	5	6	11
4	10~25	7	5	12
5	25~50	2	5	7
6	More than50	9	6	15
Sum (days)		65	66	131

Table 2 describes in detail the urban railway passenger dataset from Seoul metro (Line 1~4) and Seoul Metropolitan Rapid Transit Corporation (Line 5~8). Data are constructed total number of board passenger in July to September 2012, 2013. The total number of stations on line 1 to 4 in the 2012-2013 is 119 stations. However, total number of stations on line 5 to 8 is different. In 2012, there are 148 stations on line 5 to 8. However, 9 stations which are Gulpocheon station, Kkachiul station, Bucheon Cityhall Station, Bucheon Stadium station, Samsan Gymnasium station, Sangdong station, Sinjung-dong station, Chun-ui station data from October 2013 added.

Table 2: Urban Railway passengers Analysis Database set sample

(e.g. Passegner(person))

Line	Station	Date	06:00	07:00	08:00	…	23:00	24:00	Sum
5	Banghwa	20120701	139	250	347	…	30	1	4,808
5	Banghwa	20120702	670	1,239	591	…	66	16	8,495
5	Banghwa	…	…	…	…	…	…	…	…
5	Banghwa	20120930	124	178	178	…	57	18	3.670

2.2 Urban railway demand analysis

This study set the number of passenger data in level 1 as a standard. Based on this standard, this study compares each level' passenger number and standard and then calculates reduction ratio.

As a result, this study finds out that the number of passengers is decreased during the rainfall. In level 2, total number of passengers is increased by 0.53% than level 1. At level 3, total number of passengers is decreased by 1.84% and level 4, total number of passengers is decreased by 3.17%. Demand was reduced by 2.65% at Level 5. At the level 6, it was reduced by 5.39%. Detailed results are given in [Appendix A].

This study also conducted the passengers' ridership on each station. The results show that the ridership on Yeouinaru Station and Ttukseom

Resort Station is highly influenced by amount of the rain. This is because people visit these stations for leisure activities. On the other hand, the ridership on Samsung station, Gasan Digital Complex Station, and Gangnam Station does not have a significant difference by the rain. These stations are highly involved with work trip. Detailed results are given in [Appendix B].

Contrary to this pattern, Hangnyeoul station subway passenger rate is 47% increase from relationship. Regardless of the rainfall, It can imply that this is because of the close Hangnyeoul station event.

3. SPATIAL ANALYSIS ON SUBWAY NETWORK IN SEOUL METROPOLITAN AREA

A GIS software can be used to store, analyze and allows spatial data layers. First, this study analyzes the high number of the board and alight passenger station in Seoul.

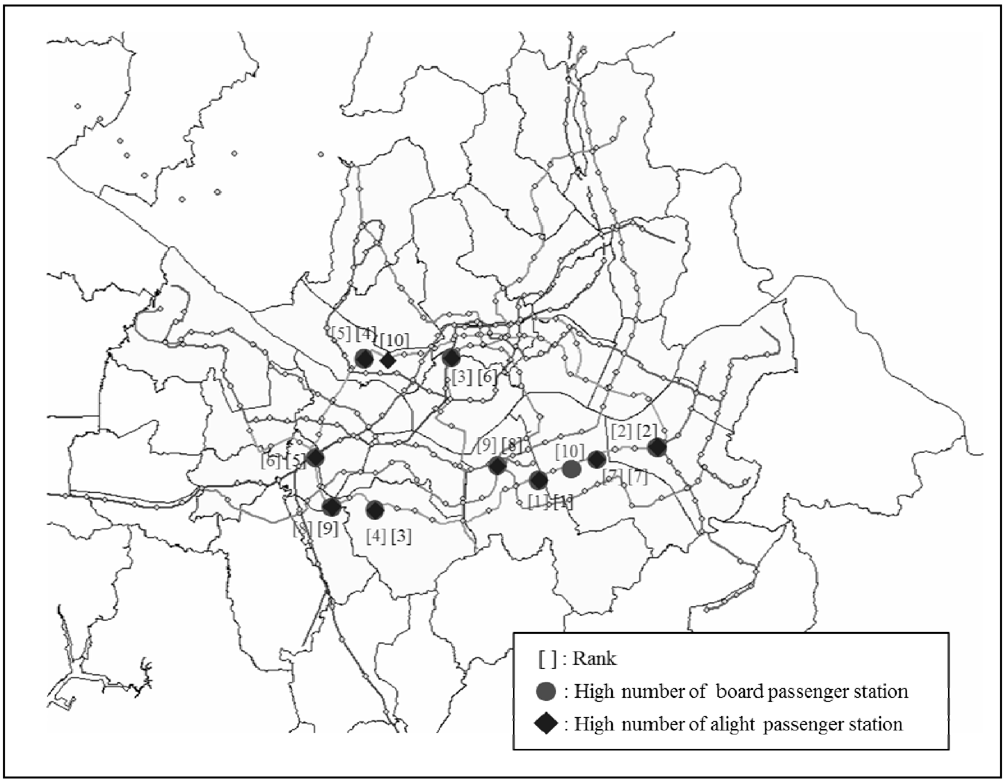
[5] [4]
[10]
[3] [6]
[2] [2]
[9] [8]
[10]
[6] [5]
[7] [7]
[1] [1]
[8] [9]
[4] [3]
[ ] : Rank
● : High number of board passenger station
◆ : High number of alight passenger station

Figure 1: The high number of the board and alight passenger station in Seoul

Figure 1 depicts the high total number of board passenger station analysis data from top 1 to top 10; Gang-nam station: 37,181,419persons, Jam-sil station: 27,974,601 persons, Seoul station: 26,244,942 persons, Sillim station: 26,201,372 persons, etc. Figure 1 also shows the high total number of alight passenger station: Gang-nam station: 38,498,150 persons, Jam-sil station: 25,588,647 persons, Sillim station: 25,491,673 persons, Hongik university station: 25,019,830 persons.

This study analyzes the high number of board and alight passenger station by GIS, in which multiple layers of information can be integrated in different combinations ([Appendix B]). Figure 2 visualizes the spatial analysis results on a map.

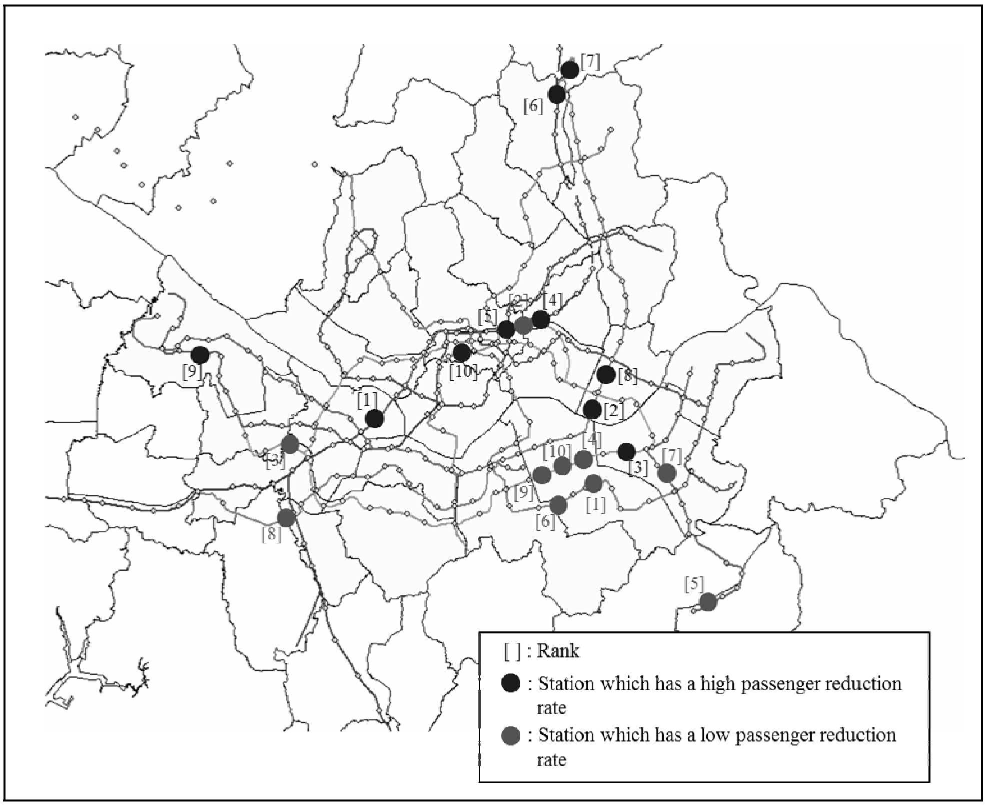
[7]
[6]
[5]
[2]
[4]
[9]
[10]
[8]
[1]
[2]
[3]
[10]
[4]
[3]
[7]
[9]
[1]
[6]
[8]
[5]
[ ] : Rank
● : Station which has a high passenger reduction rate
● : Station which has a low passenger reduction rate

Figure 2: Stations which have high or low passenger reduction rate

4. CONCLUSION

The crowdedness of the urban railway is the most important indicator to reflect the operation state of the urban railway. The weather is one of the critical factors to influence the crowdedness. That is because even though the crowdedness of the urban railway is the same, passengers feel more uncomfortable in rainy weather condition. Indeed if specific sections and stations suddenly are concentrated excessive demand, it will lead far more serious problem.

This study finds out that each station’s passenger is decreased by the rainfall level, except for level 2. The number of passengers in level 6 is decreased about 5.39%. The stations which are highly related to leisure activity are sensitive to the rainfall.

Also, we analyzed the sensitivity area of the rainfall level. The station was analyzed by using a high sensitivity for the station leisure activities such as Yeouinaru Station and Ttukseom Resort Station. On the other hand, Samsung station, Gasan Digital Complex Station, Gangnam Station was analyzed and the sensitivity is low.

With the GIS program, this study conducts the spatial analysis to show the relationship between the rainfall intensity and the subway passenger ridership in GIS map.

This study focuses on the entire date of data and passenger data. To conduct more accurate analysis, the study should consider peak-hour and non-peak hour data.

REFERENCES

Park Kun Young, Lee Si Bok, 2012. *A study on the effect of adverse weather conditions on public transportation mode choice*, Journal of Civil Engineering, Korean Society of Civil Engineers 32(1), 23-31.

Kwang Sub Lee, Jin Ki Eum, So Young You, Jae Hong Min, Keun Yul Yang, 2014. *The impact of rain on public transit ridership in Seoul*, The Korean Society for Railway.

Yi Chang, Ko Joon Ho, Kang Young Eun, Lee Tae Kyung, 2011. *The impact of rainfall on public transport service in Seoul – Focusing on the changes in punctuality and speed of bus service*, Journal of Korea Planners Association, 46(7), 73-87.

Kang Yeonggyeong, Yi Changhyo, Lee Seungil, 2014. A study on the factors affecting crowding degree in the subway train considering the Seoul Metropolitan subway network and the land use of its catchment area, Journal of Korea Planners Association, 203-218.

[Appendix A] Relationship of the reduction rate between the urban railway passengers in accordance with the rainfall

Station	Less than 1mm	1mm~5mm		5 mm ~10 mm	
	passenger	passenger	Reduction ratio(%)	passenger	Reduction ratio(%)
Yeouinaru	44,541.9	42,780.8	-3.95	42,050.5	-5.59
Ttukseom Resort	42,055.3	40,300.2	-4.17	39,574.1	-5.90
Stadium	77,243.1	71,697.9	-7.18	69,869.9	-9.55
Jegi-dong	88,168.2	85,418.2	-3.12	82,734.3	-6.16
Dongmyo	34,413.1	35,039.4	1.82	33,319.5	-3.18
Dobongsan	44,960.4	43,205.1	-3.90	42,102.7	-6.36
Jangam	8,280.9	7,895.9	-4.65	7,860.5	-5.08
Children’s Grand Park	66,480.0	63,312.0	-4.77	58,590.3	-11.87
Magok	3,993.4	3,940.6	0.18	3,643.0	-7.38
Myeongdong	173,761.3	173,369.7	-0.23	168,717.4	-2.90
Bokjeong	25,287.7	24,419.2	-3.43	22,643.6	-10.46
Hanyang Univ.	57,738.5	54,484.9	-5.64	46,208.0	-19.97

Cheongyangni	136,757.4	134,611.6	-1.57	131,683.6	-3.71
…	…	…	…	…	…
Hangnyeoul	10,812.0	10,618.7	-1.79	13,006.0	20.29
Sum	21,118,821.4	21082416.3	**0.53**	20,589,430.4	**-1.84**

Station	**10mm ~25mm**		**25 mm~50mm**		**More than 50mm**	
	passenger	**Reduction ratio(%)**	**passenger**	**Reduction ratio(%)**	**passenger**	**Reduction ratio(%)**
Yeouinaru	38,672.5	-13.18	37,378.8	-16.08	34,958.1	-21.52
Ttukseom Resort	37,105.7	-11.77	36,074.3	-14.22	34,158.7	-18.78
Stadium	65,982.6	-14.58	63,728.6	-17.50	64,305.6	-16.75
Jegi-dong	81,311.1	-7.78	78,525.1	-10.94	74,327.4	-15.70
Dongmyo	31,464.8	-8.57	31,336.0	-8.94	29,403.9	-14.56
Dobongsan	41,823.5	-6.98	41,824.9	-6.97	38,630.8	-14.08
Jangam	7,457.6	-9.94	7,336.9	-11.40	7,166.3	-13.46
Children’s Grand Park	61,769.9	-7.09	62,089.5	-6.60	57,770.8	-13.10
Magok	3,646.4	-7.30	3,585.1	-8.86	3,447.0	-12.37
Myeongdong	163,398.3	-5.96	160,340.8	-7.72	152,588.4	-12.19
Bokjeong	23,933.5	-5.36	24,290.6	-3.94	22,446.2	-11.24
Hanyang Univ.	51,641.0	-10.56	50,823.4	-11.98	51,317.4	-11.12
Cheongyangni	128,715.3	-5.88	126,761.2	-7.31	121,660.8	-11.04
…	…	…	…	…	…	…
Hangnyeoul	15,928.9	47.33	10,460	-3.25	15,959.8	47.61
Sum	20,299,748.3	**-3.17**	20,411,404.1	**-2.65**	19,832,785.5	**-5.39**

[Appendix B] Sensitivity analysis between the urban railway passengers and rainfall intensity

Station	**Less than 1mm**	**1mm~5mm**		**5 mm ~10 mm**	
	passenger	**passenger**	**Reduction ratio(%)**	**passenger**	**Reduction ratio(%)**
[1] Yeouinaru	44,541.9	42,780.8	-3.95	42,050.5	-5.59
[2] Ttukseom Resort	42,055.3	40,300.2	-4.17	39,574.1	-5.90
[3] Stadium	77,243.1	71,697.9	-7.18	69,869.9	-9.55
[4] Jegi-dong	88,168.2	85,418.2	-3.12	82,734.3	-6.16
[5] Dongmyo	34,413.1	35,039.4	1.82	33,319.5	-3.18
[6] Dobongsan	44,960.4	43,205.1	-3.90	42,102.7	-6.36
[7] Jangam	8,280.9	7,895.9	-4.65	7,860.5	-5.08
[8] Children’s Grand Park	66,480.0	63,312.0	-4.77	58,590.3	-11.87
[9] Magok	3,993.4	3,940.6	0.18	3,643.0	-7.38
[10] Myeongdong	173,761.3	173,369.7	-0.23	168,717.4	-2.90
Average	21,118,821.4	21,082,416.2	0.53	20,589,430.4	-1.84
[1] Hangnyeoul	10,812.0	10,618.7	-1.79	13,006.0	20.29
[2] Sinseol-dong	14,660.1	15,678.9	6.95	14,605.0	-0.38
[3] Dorimcheon	4,661.9	4,877,875	4.63	4,750.6	1.90
[4] Samsung	292,916.8	299,579.7	2.27	294,401.8	0.51
[5] Sujin	21,597.3	22,128.79	2.46	22,281.4	3.17
[6] Dogok	37,286.0	37,933.0	1.74	37,020.9	-0.71
[7] Songpa	28,086.5	28,762.2	2.41	28,388.9	1.08
[8] Gasan Digital Complex	184,319.8	186,244.2	1.04	181,779.6	-1.38
[9] Gangnam	482,931.1	500,013.7	3.54	493,907.8	2.27
[10] Yeoksam	247,416	248,602.0	0.48	248,142.5	0.29

Station	**10mm ~25mm**		**25 mm~50mm**		**More than 50mm**	
	passenger	**Reduction ratio(%)**	**passenger**	**Reduction ratio(%)**	**passenger**	**Reduction ratio(%)**
[1] Yeouinaru	38,672.5	-13.18	37,378.8	-16.08	34,958.1	-21.52
[2] Ttukseom Resort	37,105.7	-11.77	36,074.3	-14.22	34,158.7	-18.78
[3] Stadium	65,982.6	-14.58	63,728.6	-17.50	64,305.6	-16.75
[4] Jegi-dong	81,311.1	-7.78	78,525.1	-10.94	74,327.4	-15.70
[5] Dongmyo	31,464.8	-8.57	31,336.0	-8.94	29,403.9	-14.56
[6] Dobongsan	41,823.5	-6.98	41,824.9	-6.97	38,630.8	-14.08
[7] Jangam	7,457.6	-9.94	7,336.9	-11.40	7,166.3	-13.46
[8] Children’s Grand Park	61,769.9	-7.09	62,089.5	-6.60	57,770.8	-13.10
[9] Magok	3,646.4	-7.30	3,585.1	-8.86	3,447.0	-12.37
[10] Myeongdong	163,398.3	-5.96	160,340.8	-7.72	152,588.4	-12.19
Average	20,299,748.3	-3.17	20,411,404.1	-2.65	19,832,785.5	-5.39
[1] Hangnyeoul	15,928.9	47.33	10,460	-3.25	15,959.8	47.61

[2] Sinseol-dong	14,345.3	-2.15	14,919.4	1.77	15,338.5	4.63
[3] Dorimcheon	4,624.2	-0.81	4,967.6	6.56	4,790.1	2.75
[4] Samsung	290,964.4	-0.67	302,618.3	3.31	291,192.3	-0.59
[5] Sujin	21,692.9	0.44	21,235.7	-1.67	21,429.1	-0.78
[6] Dogok	36,558.4	-1.95	37,056.2	-0.62	36,779.2	-1.36
[7] Songpa	27,931.9	-0.55	28,459.6	1.33	27,643.1	-1.58
[8] Gasan Digital Complex	184,758.5	0.24	186,835.5	1.36	180,528.9	-2.06
[9] Gangnam	463,939.4	-3.93	473,892.0	-1.87	471.975.9	-2.27
[10] Yeoksam	245,328.5	-0.84	250,368.7	1.19	241,304.7	-2.47

FACTORS AFFECTING THE SEVERITY OF MOTORCYCLES ACCIDENTS AND CASUALTIES IN THAILAND BY USING PROBIT AND LOGIT MODEL

Santosh BARAL [1], Kunnawee KANITPONG [2],
[1,2] Thailand Accident Research Center, Asian Institute of Technology,
P.O. Box 4, Klong Luang, Bangkok, 12120, Thailand
a E-mail: baralsantosh5@gmail.com
b E-mail: kanitpon@ait.ac.th

ABSTRACT

This paper attempts to provide an additional insight into the factors that significantly influence the motorcycle accident severity in Thailand by using ordered probit, binary orbit and binary logit model. We used the data from two sources: Department of Highways (HAIMS) and Road Accident Victims Protection Co. Ltd (Eclaim), each of which depicts different factors involved in the accident. This study reveals several factors that could lead to severe motorcycle accidents and casualties: during late night and late morning, during weekend and holiday season, collision with truck, driving under influence, crash at curve, motorcycle to vehicle collision esp. head-on types, age above 40 years old, pillion passengers and asphalt pavement. Our findings reveal that the chances of being fatal in motorcycle accidents are higher in motorcycle-truck collision than motorcycle-other vehicles collision. Also, the likelihood of fatality of pillion passenger is higher than rider.

***Keywords**: Motorcycle, accident severity, ordered probit, binary probit/logit, Thailand*

2. INTRODUCTION

Motorcycle has been a very popular vehicle type used in Thailand. According to the statistical data from the Department of Land Transport (DLT), there are more than 18 million registered motorcycles in Thailand or about 60% of all registered vehicles are motorcycles. During 2002-2011, the number of motorcycles has been rapidly growing as reported by the DLT that the number of new motorcycle registration is more than 1.8 million vehicles per year. The ratio of population to motorcycle is 4 to 1, which is considered as the third highest rank among ASEAN countries, following Malaysia and Vietnam.

There are many reasons contributing to the popularity of motorcycles such as convenience and agility, capability to access to destination, low amount of fuel used, maintenance cost, and relatively low price of motorcycle itself. According to the Royal Thai Police, motorcycles are found to be the highest risk group of vehicle types to have accidents. During 2008 to 2010, the number of motorcycle injuries was about 70-80% of all accidents, and this figure tends to increase each year. The statistical data from the Ministry of Public Health revealed that during such a period of time, the number of fatalities from motorcycle accidents was as high as 80% of the total fatalities from road injuries in Thailand (Ichikawa *et a*l., 2003; Swaddiwudhipong *et al*., 1994). It was believed that the primary causes of fatalities from motorcycle injuries were speed, drunkenness, violation of traffic laws, careless ride, and lack of skill control during turning or lowering speed.

2. LITERATURE REVIEW

Most previous research have identified the relationships between motorcycle accident severity and explanatory variables of interest like age, gender, alcohol use, helmet use etc. Savolainen and Mannering (2007) estimates the probabilistic models of motorcyclists' injury severities in single and multiple vehicle crash which shows that the increasing motorcyclist age is associated with more severe injuries. Similar result was found in other research that the likelihood of fatality and disabling injury in single vehicle crash increases with increasing motorcycle rider's age (Shankhar and Mannering, 1996; Quddus *et al*., 2002; Pai and Saleh, 2007; Nunn, 2011). However, some studies show that the younger (less than 20 years old) and inexperienced motorcyclists are associated with high motorcycle crash severity (Oluwadiya et al., 2009; Lin *et al*., 2003). Also, Rutter and Quine (1996) examined the effect of the age, gender and driving experience on motorcycle accident severity and found that there is a higher casualty rate among middle-aged riders compared to those who are inexperienced. Youth drivers behave less safely than older drivers .The motorcyclist less than 30 years old and more than 50 years old have greater probabilities of injury whatever the level is (Lapparent, 2005). With respect to gender, women are found to have a higher probability of more severe injury relative to men (Quddus *et al*., 2002) and women motorcyclists between 30 to 50 years old driving powerful motorcycle are most exposed to risk of injury (Lapparent, 2005).In contrast, (Preusser *et al*., 1995; NHTSA, 2007) found that male motorcyclist tend to be associated with a higher degree of crash severity. Therefore, the contrasting findings of the previous studies on the effect of age and gender in motorcycle accident severity warrants further investigation on this matter.

Road type and geometry along with roadside installations, pavement surface conditions, lighting and visibility conditions, and manner of crashes (such as run-off road, collision with stationary object or other) constitute another group of risk factors (Vlahogianni *et al*., 2012). Intersection crashes are more likely to result in no injury whereas crashes that occur on vertical and horizontal curves are significantly more likely to result in serious injury or fatal (Clarke *et al*., 2007; Savolainen and Mannering, 2007). Also, research shows that motorcycle collision with roadside or fixed objects were found to have higher fatality or serious injury risk (Quddus *et al*., 2002; Savolainen and Mannering, 2007; Shaheed and Gkritza 2014; Keng, 2005; Lin *et al*., 2003; Daniello, 2011).

Furthermore, extensive research has been conducted on investigating the role of alcohol in motorcycle crash. The influence of alcohol was proved to be most outstanding factor in Thailand (Kasantikul *et al.*, 2005). The study revealed that alcohol accidents were distinctly different from non-alcohol crashes and alcohol accidents are frequent on weekends. Lin and Krauss (2009) suggests that motorcycle riders are more likely to drink and ride compared to other motor-vehicle drivers. Similarly, for single-vehicle motorcycle crashes with riders under the influence of alcohol are more likely to result fatal or major injury (Shaheed and Gkritza, 2014).

Only few previous research on motorcycle accident severity have examined the effect of time of day, days of week and season. Savolainen and Mannering (2007) found that April and July have greater probability of fatality in motorcycle accident. Furthermore, another study by Kasantikul *et a*l. (2005) concluded that driving under the influence related crashes are most likely to occur on weekends, at night in Thailand. Also, during the night time and due to poor visibility, there is a significant increase in the probabilities of severe or fatal crash (Lapparent, 2005; Savolainen and Mannering, 2007; Walker, 2005).

The nature of motorcycle use and the engine size of the motorcycle may be quite different in developed and developing countries. For e.g., in developing countries like Thailand, Vietnam, Phillipines, etc. motorcycle riders use the vehicle every day for their regular work, while in the west countries, the motorcycles are used more in weekend for recreational travel. Hence, the result for time of the accident, day of the week and season from previous studies may not be significant predictor of accident in the context of Thailand. In addition, a large proportion of motorcycles in developing countries are scooters with a smaller engine capacity, and the characteristics of the crash rate, crash type, and injury severity and pattern of such motorcycle seem to differ from those for big motorcycles (Salatka *et al*., 1990). Though several studies show that the motorcycle crash severity depends upon the motorcycle size, unfortunately, very few studies have attempted to investigate the small sized motorcycle to determine if the factors affecting are same or not. Some other factors (e.g., seating position, other vehicle involved in the accident, collision types, pavement types and etc.) that may affect accident severity are often overlooked in the literature.

3. METHODOLOGY

3.1 Data Set

Data from two sources: Department of Highways (HAIMS) and Road Accident Victims Protection Co. Ltd (Eclaim) were used in the analysis. Each of which depicts different factors involved in the accident. The levels of injury categorized in both sources are also different as shown in Table 1. In HAIMS database, the typical ordinal variables are categorized from least severe level to most severe level. Accidents data from the years 2008 to 2012 was obtained from HAIMS. A database of 18,463 accidents involving motorcycle was extracted from the data and used for the study. For these accidents, 5,526 (30%) are classified as PDO only, 7,836 (42%) are classified as minor injury, 2,763 (15%) are classified as serious injury and 2,338 (13%) are classified as fatality. This data also includes the accidents considering the severity of pedestrian or other vehicle's occupants. The accident is classified in the most severe form of injury to the involved person.

Similarly, in data set of Eclaim, the levels of injury are categorized as either injured or fatal. Motorcycle accidents database contains a total number of 586,809 motorcycle casualties from the years 2010 to 2012 was taken for the analysis. The data includes the injury sustained by either motorcycle rider or passenger. For these accidents, 571,376 (97.4%) are classified as injury and 15,433 (2.6%) are classified as fatality.

Table 2 Definition of dependent variables with respect to injury level

Data sources	Level	Definition	Dependent Variable
HAIMS	0	PDO	There is no bodily harm to the person from the crash- property damage only
	1	Minor Injury	Injury which is not of any threat to the life of the person or his way of living.
	2	Serious Injury	Injury which is a threat to the life of the person and his way of living.
	3	Fatality	An injury sustained in the crash that resulted in death immediately or post-accident.
Eclaim	0	Injury	Injury which is either a threat or not to the life of the person or his way of living.
	1	Fatality	An injury sustained in the crash that resulted in death immediately or post-accident.

3.2 Model Selection

This paper attempts to provide an additional insight into the factors that significantly influence the motorcycle accident severity in Thailand by using ordered probit model, binary orbit and binary logit model. The data from HAIMS is ordinal in nature and they are best analyzed using ordered probit models because they require no assumptions regarding the ordinality of the dependent variable, which in this case is the severity score. Quddus *et* *al*. (2002) utilized ordered probit models to analyze motorcycle damage and injury severity resulting from crashes. Kockelman and Kweon (2002) describes the use of ordered probit models to examine the risk of different injury levels sustained under all crash types, two-vehicle crashes, and single-vehicle crashes. Likewise, the severity of driver at multiple locations such as roadway sections, intersections, toll plazas are identified by Abdel-Aty (2003), using the ordered probit models. Due to a special property, i.e. the ordered probit model discerns unequal differences between ordinal categories in the dependent variable, it captures the qualitative differences between injury severity levels, given a unit change in the explanatory variables (Khattak and Targa, 2004; Duncan *et al*., 1998; O'Donnell and Connor, 1996). Some researcher used multinomial logit model in their study to deal with injury severity levels (Chang and Mannering, 1999; Lee and Mannering, 2002), however, these models require more number of parameter estimates and neglects the data ordinarily. By reviewing the previous studies, and because of its relative simple approach to recognize the index of various response variables, the ordered probit model was chosen to analyze the HAIMS dataset. The general form of the model is:

$$y_i{}^* = \mathbf{x}i\ \boldsymbol{\beta} + \varepsilon_i \qquad (1)$$

where, $y_i{}^*$ is a latent, unobservable and continuous dependent variable;

$\mathbf{x}_i$ is a row vector of observed non-random explanatory variables;

$\boldsymbol{\beta}$ is a vector of unknown parameter;

ε_i is the random error term; which is assumed to be normally distributed.

The ordered probit model can be derived from a measurement model in which a latent variable $y_i{}^*$ ranging from $-\infty$ to $+\infty$ is mapped to an observed ordinal variable y. The observed and coded discrete variable y_i is determined from the model as follows:

$$y_i = m \text{ if } \tau_{m-1} \leq y^* < \tau_m \text{ for } m = 1 \text{ to } M \qquad (2)$$

where, the threshold values τ' are unknown parameters to be estimated. The extreme categories, 1 and M, are defined by open-ended intervals with $\tau_0 = -\infty$ and $\tau M = \infty$.

Accident severity (dependent variable) in Eclaim database has two categories, fatal and injured. Therefore, binary logit and binary probit model are applied in order to examine the contribution of several variables to accident severity. Binary logit or probit model has been broadly used by many researchers in their study. For instances, Simoncic (2001) applied binary logit model to overcome injury severity of collisions between a pedestrian, bicycle or motorcycle and a car. Furthermore, (for e.g. Factor *et al*. 2008; Obeng, 2007; Pai, 2009; Simoncic, 2001) successfully used binary logit/probit models to overcome the severity levels, which are categorized as less and high injury. Haque *et al*. (2009) identified time factors, road features and driver-vehicle characteristics that contribute to the fault of motorcyclist in crashes at specific locations by applying binary logit model. In these models, which are applied for predicting the injury, the crash severity is a binomial distribution. So, the response variable Yi for the ith observation can take one of two values: $Y_i = 0$ or 1, where $Y_i=1$ presents the first state such as fatality and $Y_i= 0$ presents the other state: injury. The

probability of Y_i is denoted by $\pi_i = Pr(Y_i{=}1)$ The logit transformation of the probability of a π_i crash being injured is given by
$\text{Logit}(\pi i) = \log [\frac{\pi i}{1-\pi i}]$ (3)
And, the logit transformation to the predictor is
$\text{Logit}(\pi_i) = \beta X_i$
(4)
From (3) and (4), logit model can be presented as
$\text{Log} [\frac{\pi i}{1-\pi i}] = \beta X_i$
(5)
Hence, from (5), the probability of a π_i crash being injured is obtained as
$\pi_i = Pr(Y_i{=}1) = [\frac{\exp(\beta Xi)}{1-\exp(\beta Xi)}]$
where, X_i is a vector of explanatory variable such as time of day, day of week, types of collision, other vehicle involved and etc, which may have influences on crash severity. Besides, β is the coefficient regression vector of the independent variables, presenting how each independent variable affects the fatality.

Binary probit models are similar to binary logit models except the error distribution. In the binary logit models, the errors are assumed to have a standard logistic distribution with mean 0 and variance $\frac{\pi}{3}$, while the errors in binary probit models have an assumption that the error distribution has mean 0 and variance 1. The probit transformation of the probability πi is given by
$\text{Probit}(\pi_i) = \Theta^{-1}(\pi_i)$ (6)
And, the logit transformation to the predictor is,
$\text{Probit}(\pi_i) = \beta X_i$
(7)
From (6) and (7), probit models can be presented as
$\Theta^{-1}(\pi_i) = \beta X_i$ (8)
Hence, from (8) the probability of a πi crash being injured is obtained as
$\pi_i = Pr(Y_i{=}1) = \Theta(\pi_i)$
where, Θ is the cumulative distribution function of standard normal distribution.

The description of the study variables from both data sources are shown in Table 2 and Table 3.

Table 3 Description of the study variables from HAIMS data source

Variable	Description of Variable
SUN	If accident on Sunday = 1, 0 otherwise
MON	If accident on Monday = 1, 0 otherwise
TUE	If accident on Tuesday = 1, 0 otherwise
WED	If accident on Wednesday = 1, 0 otherwise
THU	If accident on Wednesday = 1, 0 otherwise
FRI	If accident on Friday = 1, 0 otherwise
SAT	If accident on Saturday = 1, 0 otherwise
JAN	If accident in January = 1, 0 otherwise

FEB	If accident in February = 1, 0 otherwise
MAR	If accident in March = 1, 0 otherwise
APR	If accident in April = 1, 0 otherwise
MAY	If accident in May = 1, 0 otherwise
JUN	If accident in June= 1, 0 otherwise
JUL	If accident in July= 1, 0 otherwise
AUG	If accident in August = 1, 0 otherwise
SEP	If accident in September = 1, 0 otherwise
OCT	If accident in October = 1, 0 otherwise
NOV	If accident in November = 1, 0 otherwise
DEC	If accident in December = 1, 0 otherwise
0 - 4	If accident happened during 0:00am to 3 :59am = 1, 0 otherwise
4 - 8	If accident happened during 4 :00 am to7: 59am = 1, 0 otherwise
8 - 12	If accident happened during 8 :00am to 11:59am= 1, 0 otherwise
12 - 16	If accident happened during 12:00noon to3:59pm=1, 0 otherwise
16 - 20	If accident happened during 4 :00pm to 7 :59pm = 1, 0 otherwise
20 - 24	If accident happened during 8 :00pm to11 :59pm =1, 0 otherwise
STRGHT	if accident on straight section =1, 0 otherwise
CURVE	if accident on normal curve = 1, 0 otherwise
INTSC	if accident on intersection = 1, 0 otherwise
U-TURN	if accident on U-turn with no auxiliary lane = 1, 0 otherwise
ACCESS	if accident on access point = 1, 0 otherwise
SPEED	If accident cause is due to speeding = 1, 0 otherwise
NO_STOP	If accident cause is due to no stop at intersection = 1, 0 otherwise
VIOLATE	If accident cause is due to violating traffic signal=1, 0 otherwise
DUI	If accident cause is due to driver under influence = 1, 0 otherwise
MC	If other vehicle is motorcycle= 1, 0 otherwise
CAR	If other vehicle is passenger car = 1, 0 otherwise
PICK UP	If other vehicle is pick-up = 1, 0 otherwise
BUS	If other vehicle is bus/Coach = 1, 0 otherwise
TRUCK	If other vehicle is truck = 1, 0 otherwise
HEAD	If the crash type is head on collision=1, 0 otherwise
RIGHT	If the crash type is right angle= 1, 0 otherwise
REAR	If the crash type is rear End = 1, 0 otherwise
SIDE	If the crash type is side Swipe = 1, 0 otherwise
FIXED	If the crash type is fixed object crash = 1, 0 otherwise
SINGLE	If the crash type is single vehicle crash=1, 0 otherwise
OTHER	If the crash is others types = 1, 0 otherwise
CONC	If the road surface is concrete = 1, 0 otherwise
NIGHT	If accident occur at night = 1, 0 otherwise

Table 4 Description of the study variables from Eclaim data source

Variables	**Description of variables**
SUN	If accident on Sunday = 1, 0 otherwise
MON	If accident on Monday = 1, 0 otherwise
TUE	If accident on Tuesday = 1, 0 otherwise
WED	If accident on Wednesday = 1, 0 otherwise
THU	If accident on Wednesday =1, 0 otherwise
FRI	If accident on Friday = 1, 0 otherwise
SAT	If accident on Saturday = 1, 0 otherwise
JAN	If accident in January = 1, 0 otherwise
FEB	If accident in February = 1, 0 otherwise
MAR	If accident in March = 1, 0 otherwise
APR	If accident in April = 1, 0 otherwise
MAY	If accident in May = 1, 0 otherwise
JUN	If accident in June= 1, 0 otherwise
JUL	If accident in July= 1, 0 otherwise

AUG	If accident in August = 1, 0 otherwise
SEP	If accident in September = 1, 0 otherwise
OCT	If accident in October = 1, 0 otherwise
NOV	If accident in November = 1, 0 otherwise
DEC	If accident in December = 1, 0 otherwise
0 TO 4	If accident happened during 0 :00 am to 3 :59 am =1, 0 otherwise
4 TO 8	If accident happened during 4 :00 am to7: 59 am = 1, 0 otherwise
8 TO 12	If accident happened during 8 :00 am to 11:59 am = 1, 0 otherwise
12 TO 16	If accident happened during 12 :00 noon to 3:59 pm = 1, 0 otherwise
16 TO 20	If accident happened during 4 :00 pm to 7 :59 pm = 1, 0 otherwise
20 TO 24	If accident happened during 8 :00 pm to 11 :59 pm =1, 0 otherwise
SINGLE	If the crash type is single vehicle crash=1, 0 otherwise
OV	If the collision with other vehicle=1, 0 otherwise
FIXED	If the crash type is fixed object crash = 1, 0 otherwise
DRIVER	If the casualty is driver = 1, 0 otherwise
MC	If other vehicle is motorcycle= 1, 0 otherwise
CAR	If other vehicle is passenger car/pick up = 1, 0 otherwise
VAN	If other vehicle is personal van= 1, 0 otherwise
BUS	If other vehicle is public bus/van = 1, 0 otherwise
TRUCK	If other vehicle is truck= 1, 0 otherwise
OTHERS	If vehicle is other type = 1, 0 otherwise
MALE	If gender is male = 1, 0 otherwise
AGE<20	If age is less than 20=1, 0 otherwise
AGE20-29	If age is 20 -29 =1, 0 otherwise
AGE30-39	If age is 30 -39 =1, 0 otherwise
AGE40-49	If age is 40 -49 =1, 0 otherwise
AGE50-59	If age is 50 -59 =1, 0 otherwise
AGE60-69	If age is 60 -69 =1, 0 otherwise
AGE70-79	If age is more than 70 = 1, 0 otherwise
AGE_C	Age is taken as continuous variable

4. ANALYSIS RESULTS

The estimation results are shown in Table 4 and Table 5 for all models from HAIMS and Eclaim data sources respectively. In order to determine whether the candidate variables are significant or not, several iterations were carried out with changing the reference variables. Model 1 to 7 are the results of HAIMS data analysis, whereas model 8 to model 16 are the results of Eclaim data analysis. The findings from models are interpreted in the following section.

Effects of time of day, days of week and season are presented in the model 1 to 5 and model 8 to 15. Based on the results in Table 4, relative to the reference time period, more severe accidents occur in the early morning (midnight to 3:59 am) followed by evening (4:00 pm to 7:59 pm). Result from Table 5 also shows that the severity of motorcycle casualties is higher during early morning and late night (8:00 pm to 11:59 pm) and lower during late morning time (8:00 am to 11:59 am). These findings are consistent to the other studies (for e.g. Rifaat and Chin, 2005; Quddus *et al.*, 2002). Low visibility and late night drowsiness delay the driver’s reaction at the impending collision with other vehicles or roadside objects. Therefore the collision impact is high due to high speed (Rifaat and Chin, 2005) resulting severe injury or fatality.

Table 5 shows that the likelihood of fatality is high in weekend than in weekdays, which also supports the findings from previous studies. Motorcyclists who ride on the weekend are more likely to commit offenses than those who ride during weekdays. Likewise, seasonal effects were measured using monthly dummy variables. The result of the models from both data sources indicates that the seasonal effect is one of the significant factors in increasing the severity of motorcycle crashes and severity of the casualties. The accident severity is significantly high during holiday seasons (Songkran and New Year) in Thailand which are in the months of April, December and January

Roadway type and geometry also constitute another risk factor and hence several types of motorcycle accident location were taken in the model. The accident severity at the curve was found to be strongly significant in severe or fatal crash as seen in Model 1 to model 7. Results of past studies summarized that insufficient sight distance, poor visibility due to horizontal or vertical curvature or darkness have been associated with an increase in motorcycle injury severity (Clarke et al, 2007; Savolainen and Mannering, 2007; Chang, 2005).

Our study also accounts for the second higher accident severity at Junction (U-turn and access point). Seva *et al.* (2013) found that junction type was significant in motorcycle accidents in the Philippines. Inattention of the automobile driver and motorcycle being overlooked easily at junction may attribute to this problem. Chang (2005) concluded that if the accident occurs at an intersection, the likelihood of no injury is significantly increased. Model 1 to 7 show that the severity of accidents associated with pavement types. Asphalt type accounts for more accident severity than concrete. The reason could be the better reflectivity of concrete pavement than asphalt during night time.

As for the type of collision, the result of the model from HAIMS shows that the severity of the motorcycle crash is high when collided with vehicle followed by fixed objects, and is low if it is single vehicle crash with no collision. This result is similar to the result of Eclaim, which explains that the likelihood of fatality is more in head-on collision than single vehicle collision. These findings are also same with Savolainen and Mannering (2007), where the author made a conclusion that head-on and right angle collision type has high severity in multiple crash. Moreover, research in past shows that motorcycle collision with roadside or fixed objects were found to have higher fatality or serious injury risk (Quddus *et al.*, 2002; Shaheed and Gkritza, 2014; Keng, 2005; Daniello, 2011). However, such studies have only considered the single vehicle crash type to estimate the factors associate with severity level.

Dummy variable for motorcyclist age and gender were included in model 8 to 13 and model 16 to 17 to estimate the severity of motorcycle casualties. While young motorcyclists were usually expected to have an increased involvement in severe or fatal crash, it is estimated that old motorcyclist above 40 years appear to have likelihood of fatality and young motorcyclist of age below 20 are more likely to have injury only. Similarly, model 14 (probit) and model 15 (logit) were conducted taking the age as a continuous variable. The age appeared to be a significant factor and in particular, the estimated result indicates that increase in age could lead to an increase in the likelihood of fatality. The reason for this may relate to the physiological difference with older riders being susceptible to severe injury or fatality. These findings are similar to the summary of previous studies that the likelihood of fatality and disabling injury increases with increasing motorcycle rider’s age (Shankhar and Mannering, 1996; Quddus *et al*., 2002; Pai and Saleh, 2007; Nunn, 2011). A study by Savolainen and Mannering (2006) found that a 1% increase in age increases the likelihood of incapacitating injury by 4.2%. However, the findings may contradict the long held belief that young and inexperienced driver are more likely to involve in severe accident (for e.g. Ballesteros and Dischinger, 2002; Lin *et al*., 2003; Oluwadiya *et al*; 2009; Seva *et al.*, 2013). With regards to the gender, our study reveals that male motorcyclists tend to have likelihood of fatality than women, which is contrasting to the findings by Quddus *et al*. (2002). But, the result is similar to (Preusser *et al*., 1995; NHTSA, 2007) in which they found that male motorcyclists are associated with a higher degree of crash severity.

Understanding and quantifying the relationship between vehicle types and severity of motorcycle crash has been often overlooked by the previous studies. As expected, model 1 to model 7 show that motorcycle accidents involving big trucks followed by bus results in higher injury severity as the size and mass of the big truck are far greater than motorcycles and the collision has a greater impact to the motorcyclist. The result also show that the severity of truck involved motorcycle accidents are greater than passenger car. This results appears to be same in the model 8 to 17 which showing that the likelihood of fatality is high for both rider and passenger in truck involved accidents. The chance of being fatal in motorcycle- truck collision is higher than motorcycle – other vehicle collision.

With respect to the severity of motorcycle crash related to the cause of accident, the estimated coefficients are presented in Model 1 to 7. Driving under influence and no stop at intersection followed by violate the traffic signal are the significant factors for the motorcycle accident. The reason for the insignificance of speeding might be due to data misinterpretation. For e.g. if the data collection officer doesn’t know the exact cause of accident, he could be tempted to judge speeding as a cause of accident.

Another interesting finding in this study is the contribution of seating position to the severity of motorcycle casualties, which are presented in the Model 8 to 17. The coefficients of these models (model 8, 9, and 12-15) indicates that pillion passengers are more vulnerable than riders since the likelihood of fatality of passenger is higher than rider. The findings is similar from the study of Lei *et al. (*2007), where the author found that back seat occupant suffers fatal head injuries when he fall on the ground after being thrown higher than the motorcycle driver over the top of the car. Also, the reason can be attributed to the helmet wearing percentage of rider (53%) and passenger (19%) in Thailand (thaiRoads foundation, 2013).

6. CONCLUSION

The research study has identified the main factors that affect the injury severity of motorcycle accident and motorcycle casualties by analyzing the accident data obtained from HAIMS and Eclaim using ordered probit, binary probit and binary logit models. We determined the candidate variables are significant for all models with changing the reference variable that yielded a robust result. This study reveals several factors that could lead to severe motorcycle accident and casualties: late night and early mornings, crash occurred during weekend and holiday season, collision with truck followed by bus and van, driving under influence and no stop at intersection, crash at curve followed by crash at junctions, motorcycle to vehicle collision esp. head-on types followed by right angle crash, age above 40 years old, pillion passengers and asphalt pavement. Crashes were found to be less severe in weekdays, during late morning, collision with motorcycle, single vehicle crash type and etc. There is also a disturbing findings esp. speeding being significant in less severity, which might be due to data misinterpretation during data collection process.

Most of our findings are consistent with previous studies, and more importantly the significance of motorcyclist’s age above 40 years old being likelihood of fatal, provides an additional evidence to the recent aggregate data trends. It was believed that young and experienced motorcyclist would engaged in severe motorcycle accident, however, we find the contrasting result, young riders and passengers of age below 20 years old are less likely to be fatal. It is estimated that increase in the age could lead to an increase in the likelihood of fatality.

Unlike to the previous studies, this study has included additional variables like other vehicle types and seating position that could affect the injury severity of the accident. Our findings reveals that the chances of being fatal in motorcycle - truck collision is higher than motorcycle – other vehicle collision. Also, this study concludes that pillion passengers are more vulnerable than riders since the likelihood of fatality of passenger is higher than rider.

Although this study has contributed to the literature in identifying the several factors that are significant in the severity of small sized motorcycle accident, it is necessary to provide more research to verify these findings.

REFERENCES

Abdel-Aty, M. (2003). Analysis of driver injury severity levels at multiple locations using ordered probit models. *Journal of Safety Research*, 34(5), 597−603.

Ballesteros, M.F., Dischinger, P.C. (2002) Characteristics of traffic crashes in Maryland. *Accident Analysis and Prevention*, 34 (3), 279–284.

Chang, L.Y. (2005) Empirical Analysis of the Effectiveness of Mandated Motorcycle Helmet Use in Taiwan. *Journal of the Eastern Asia Society for Transportation Studies*, 6, 3629 – 3644.

Chang L.Y, Mannering, F. (1999) Analysis of injury severity and vehicle occupancy in truck-and non-truck-involved accidents. *Accident Analysis & Prevention*, 31 (5), 579-592.

Clarke, D.D., Ward, P., Bartle, C., Truman, W. (2007). The role of motorcyclist and other driver behaviour in two types of serious accident in the UK. *Accident Analysis and Prevention*, 39(5), 974–981.

Daniello, A., Gabler, H.C. (2011) Fatality risk in motorcycle collisions with roadside objects in the United States. *Accident Analysis and Prevention*, 43(3), 1167-70.

Duncan, C., Khattak, A., Council, F. (1998) Applying the ordered probit model toinjury severity in truck-passenger car rear-end collisions. *Transportation Research Record*, 1635, 63–71.

Factor, R., Mahalel, D., Yair, G. (2008) Inter-group differences in road-traffic crash involvement. *Accident Analysis & Prevention*, 40(6), 2000-2007.

Haque, M.M., Chin, H.C., and Huang, H. (2009) Modelling fault among motorcyclists involved in crashes. *Accident analysis and Prevention*, 41(2), 327-335.

Ichikawa, M., Chadbunchachai, W., Marui, E. (2003) Effects of the helmet act for motorcyclists in Thailand. *Accident Analysis and Prevention*, 35 (2), 183–189.

Kasantikul, V., Ouellet, J.V., Smith, T., Sirathranont, J., Panichabhongse, V. (2005) The role of alcohol in Thailand motorcycle crashes. *Accident Analysis and Prevention*, 37(2), 357–366.

Keng, S.H. (2005) Helmet use and motorcycle fatalities in Taiwan. *Accident Analysis and Prevention*, 37(2), 349–355.

Khattak, A., Targa, F. (2004) Injury severity and total harm in truck-involved work zone crashes. *Transportation Research Record* 1877, 106-116.

Kockelman, K., Kweon, Y.J. (2002) Driver injury severity: An application of ordered probit models. *Accident Analysis and Prevention*, 34(4), 313−321

Lapparent, M. (2005) Empirical Bayesian analysis of accident severity for motorcyclists in large French urban areas. *Accident Analysis and Prevention*, 38(2006), 260-268

Lee, J., Mannering, F. (2002) Impact of roadside features on the frequency and severity of run-off-roadway accidents: an empirical analysis. *Accident Analysis & Prevention,* 34 (2), 149-161

Lei, G., Longa, J.X., Tuna, Z.X.,Jie, S., Jiu, C.Y., Guo, C.J. (2008) Study of injuries combining computer simulation in motorcycle–car collision accidents. *Forensic Sci. Int*. 177 90–96.

Lin, M.R., Chang, S.H., Pai, L., Keyl, P.M. (2003) A longitudinal study of risk factors for motorcycle crashes among junior college students in Taiwan. *Accident Analysis and Prevention*, 35(2), 243–252.

Lin, M.R., Kraus, J.F. (2009) A review of risk factors and patterns of motorcycle injuries. *Accident Analysis and Prevention*, 41(4), 710–722.

NHTSA (2008).Traffic Safety Facts (2007).National Traffic Safety Administration, U.S. Department of Transportation, Washington, DC.

Nunn,S. (2011) Death by motorcycle: background behavioral, and situational correlates of fatal motorcycle collisions. *Journal of Forensic Sciences*, 56(2), 429–437.

O'Donnell, C. J., Connor, D. H. (1996) Predicting the severity of motor vehicle accident

Obeng, K. (2007) Some determinants of possible injuries in crashes at signalized intersections. *Journal of Safety Research*, 38(1), 103-112.

Oluwadiya, K.S., Kolawo le, I.K., Adegbehingbe, O.O., Olasinde, A.A., Agodirin, O., Uwaezuoke, S.C. (2009) Motorcycle crash characteristics in nigeria: implication for control. *Accident Analysis and Prevention*. 41(2), 294–298.

Pai, C.W., Saleh, W. (2007) An analysis of motorcyclist injury severity under various traffic control measures at three-legged junctions in the UK. *Safety Science*, 45(8), 832–847.

Pai, C.W., Saleh, W. (2009) Modelling motorcyclist injury severity by various crash types at T-junctions in the UK. *Safety Science*, 46(8), 1234-1247.

Preusser, D.F., Williams, A.F., Ulmer, R.G. (1995) Analysis of fatal motorcycle crashes:crash typing. *Accident Analysis and Prevention*, 27 (6), 845–851.

Quddus, M. A., Noland, R. B., Chin H.C. (2002) An analysis of motorcycle injury and vehicle damage severity using ordered probit models. *Journal of Safety Research*, 33(4), 445–462.

Rifaat, S. M., and Chin, H. C. (2005) Analysis of severity of single-vehicle crashes in Singapore.In: TRB 2005 Annual Meeting CD-Rom, T*ransportation Research Board,* National Research Council, Washington D.C.

Salatka, M., Arzemanian, S., Kraus, J.F., Anderson, C.L. (1990) Fatal and severe injury: scooter and moped crashes in California, 1985. *American Journal of Public Health*, 80(9), 1122–1124,

Savolainen, P., Mannering, F. (2007) Probabilistic models of motorcyclists' injury severities in single and multi-vehicle crashes. *Accident Analysis and Prevention*, 39(5), 955–963.

Seva, R.R, Flores, G.M.T., Gotohio, M.P.T., Paras, N.G.C. (2013) Logit model of motorcycle accident in Philippines considering personal and environmental factors. *International Journal for Traffic and Transport Engineering*, 3(2), 173-184.

Shaheed, M.S., Gkritza, K. (2014) A latent class analysis of single-vehicle motorcycle crash Severity outcomes. *Analytic Methods in Accident Research*, 2(2014), 30–38.

Simoncic, M. (2001) Road accidents in Slovenia involving a pedestrian, cyclist or motorcyclist and a car. *Accident Analysis and Prevention*, 33(2), 147-156.

Swaddiwudhipong,W., Nguntra, P.,Mahasakpan, P., Koonchote, S., Tantriratna, G.(1994) Epidemiologic characteristics of drivers, vehicles, pedestrians and road environments involved in road traffic injuries in rural Thailand. *The Southeast Asian Journal of Tropical Medicine and Public Health*, 25(1), 37-44.

Vlahogianni, E.I., Yannis, G., Golias, J.C. (2012) Overview of critical risk factors in powered-two-wheeler safety. *Accident Analysis and Prevention* 49(1), 12–22.

Walker, I. (2005) Psychological factors affecting the safety of vulnerable road users: A review of the literature, working paper, Department of Psychology, University of Bath

Table 5 Ordered probit model estimation results from HAIMS data source

	Model 1		**Model 2**		**Model 3**		**Model 4**		**Model 5**		**Model 6**		**Model 7**	
Variable	Coeff.	P-value	Coeff.	P-value	Coeff.	P-value	Coeff.	P-value	Coeff.	P-value	Coeff.	P-value	Coeff.	P-value
SUN	0.029	0.355	0.026	0.399	0.024	0.428	0.021	0.503	0.029	0.339				
MON	0.011	0.724	0.013	0.677	0.012	0.683	0.011	0.718	0.013	0.672				
TUE	0.011	0.718	0.012	0.704	0.011	0.728	0.007	0.819	0.010	0.749				
WED	0.003	0.931	-0.005	0.875	-0.003	0.921	-0.006	0.830	-0.003	0.924				
THU	-0.045	0.140	-0.047	0.123	-0.046	0.127	-0.046	0.134	-0.047	0.126				
FRI	0.004	0.905												
SAT			0.002	0.948	0.001	0.962	0.005	0.876	0.005	0.879				
JAN	-0.161	0.000	-0.162	0.000	-0.162	0.000	-0.148	0.000	-0.162	0.000				
FEB	-0.351	0.000	-0.351	0.000	-0.351	0.000	-0.369	0.000	-0.358	0.000				
MAR	-0.427	0.000	-0.419	0.000	-0.417	0.000	-0.434	0.000	-0.425	0.000				
APR			-0.011	0.729	-0.012	0.686	0.017	0.582	-0.009	0.765				
MAY	-0.276	0.000	-0.276	0.000	-0.274	0.000	-0.314	0.000	-0.290	0.000				
JUN	-0.340	0.000	-0.339	0.000	-0.336	0.000	-0.360	0.000	-0.341	0.000				
JUL	-0.337	0.000	-0.336	0.000	-0.332	0.000	-0.355	0.000	-0.341	0.000				
AUG	-0.325	0.000	-0.324	0.000	-0.324	0.000	-0.339	0.000	-0.329	0.000				
SEP	-0.373	0.000	-0.364	0.000	-0.364	0.000	-0.389	0.000	-0.367	0.000				
OCT	-0.303	0.000	-0.303	0.000	-0.302	0.000	-0.330	0.000	-0.309	0.000				
NOV	-0.318	0.000	-0.320	0.000	-0.317	0.000	-0.339	0.000	-0.326	0.000				
DEC	0.005	0.870												
0 - 4	0.024	0.509	0.039	0.269	0.038	0.290	0.019	0.595	0.032	0.362	0.008	0.824	0.064	0.058
4 - 8	0.036	0.219	0.042	0.151	0.044	0.129	0.036	0.211	0.043	0.140	0.011	0.695	0.055	0.105
8 - 12	-0.024	0.361	-0.033	0.215	-0.034	0.195	-0.047	0.073	-0.037	0.166	-0.028	0.287	0.002	0.965
12 - 16	-0.006	0.812	-0.013	0.623	-0.016	0.546	-0.026	0.309	-0.019	0.460	-0.005	0.852	0.027	0.440
16 - 20													0.046	0.097
20 - 24	-0.056	0.051	-0.046	0.113	-0.046	0.110	-0.044	0.127	-0.044	0.131	-0.060	0.036		
STRGT			-0.100	0.002	-0.197	0.000			-0.316	0.000			-0.344	0.000
CURVE	0.442	0.000	0.361	0.000	0.270	0.000	drop		0.150	0.055	0.465	0.000	0.143	0.003
INTSC	0.130	0.000					0.020	0.515	-0.221	0.004	0.138	0.000	-0.237	0.000
U-TURN	0.343	0.000	0.260	0.000	drop		drop		0.041	0.609	0.315	0.000		
ACCESS	0.307	0.000	0.186	0.011	0.103	0.147	0.228	0.001			0.352	0.000	drop	
SPEED			-0.234	0.000	-0.231	0.000	-0.241	0.000	-0.241	0.000			-0.249	0.000
NO_STOP	0.256	0.208					0.003	0.989	0.021	0.919	0.235	0.245	0.051	0.803
VIOLATE	0.024	0.775	-0.270	0.002	-0.284	0.001	-0.268	0.002	-0.269	0.002	0.034	0.688		
DUI	0.212	0.000	0.053	0.246	0.053	0.251					0.332	0.000	0.144	0.001
MC	-0.525	0.000	-0.569	0.000	-0.564	0.000	0.053	0.037	-0.279	0.000			-0.369	0.000
CAR	-0.696	0.000	-0.734	0.000	-0.731	0.000			-0.446	0.000	-0.307	0.000	-0.537	0.000

PICK UP	-0.296	0.000	-0.344	0.000	-0.343	0.000	0.291	0.000			0.102	0.000	-0.136	0.000
BUS	-0.349	0.000	-0.379	0.000	-0.374	0.000	0.261	0.000	-0.090	0.202	0.030	0.675		
TRUCK							0.743	0.000	0.393	0.000	0.499	0.000	0.285	0.000
HEAD			0.591	0.000	0.575	0.000	0.800	0.000	0.486	0.000			0.525	0.000
RIGHT	-0.072	0.103	0.213	0.000	0.216	0.000	0.443	0.000	0.104	0.026	-0.114	0.010	0.154	0.002
REAR	-0.350	0.000					0.165	0.000	-0.121	0.000	-0.393	0.000	-0.082	0.017
SIDE	-0.368	0.000	-0.049	0.207	-0.053	0.169	0.113	0.003	-0.152	0.001	-0.419	0.000	-0.123	0.008
FIXED	-0.312	0.000	-0.034	0.420	-0.032	0.447	0.147	0.000	-0.135	0.004	-0.334	0.000	-0.080	0.099
SINGLE	-0.397	0.000	-0.236	0.000	-0.236	0.000	0.502	0.000			0.013	0.654		
OTHER	-0.558	0.000	-0.249	0.000	-0.249	0.000			-0.332	0.000	-0.610	0.000	-0.324	0.000
CONC	-0.511	0.000	-0.483	0.000	-0.485	0.000	-0.534	0.000	-0.477	0.000	-0.519	0.000	-0.497	0.000
NIGHT	0.172	0.000	0.169	0.000	0.168	0.000	0.171	0.000	0.172	0.000	0.188	0.000	0.173	0.000
No. of obs.	18463		18463		18463		18463		18463		18463		18463	
Log likelihood	-21372.9		-21229.4		-21244		-21576.2		-21239.1		-21591.9		-21394.1	
LR chi^2	4176.87		4463.88		4434.6		3770.45		4444.72		3738.85		4134.69	
Pseudo R^2	0.089		0.0951		0.0945		0.0804		0.0947		0.0797		0.0881	

Table 6 Binary probit/logit model estimation result from Eclaim data source

	Model 8		**Model 9**		**Model 10**		**Model 11**		**Model 12**		**Model 13**		**Model 14**		**Model 15**		**Model 16**		**Model 17**	
	probit	logit	probit	logit	probit	logit	probit	logit	probit	logit	probit	logit	probit	logit	probit	logit	probit	logit	probit	logit
Variable	Coeff.	P value	Coeff.	P value	Coeff.	P value	Coeff.	P value	Coeff.	P value	Coeff.	P value	Coeff.	P value	Coeff.	P value	Coeff.	P value	Coeff.	P value
SUN	0.058	0.000	0.136	0.000	0.039	0.003	0.08	0.01	0.034	0.012	0.076	0.014								
MON	-0.004	0.767			-0.019	0.167	-0.04	0.17	-0.026	0.062	-0.054	0.089	-0.056	0.000	-0.120	0.000				
TUE	0.022	0.120	0.054	0.095	0.008	0.569	0.01	0.74					-0.033	0.020	-0.073	0.025				
WED			-0.003	0.929	-0.015	0.289	-0.05	0.14	-0.021	0.128	-0.057	0.076	-0.055	0.000	-0.132	0.000				
THU	0.003	0.836	0.012	0.699	-0.013	0.361	-0.03	0.31	-0.018	0.193	-0.039	0.224	-0.050	0.000	-0.112	0.001				
FRI	0.017	0.214	0.049	0.121					-0.004	0.777	-0.004	0.900	-0.037	0.008	-0.079	0.013				
SAT	0.032	0.019	0.075	0.016	0.015	0.256	0.03	0.36	0.010	0.450	0.022	0.483	-0.021	0.128	-0.050	0.114				
JAN					0.056	0.003	0.12	0.01	0.022	0.228	0.039	0.344	-0.006	0.771	-0.020	0.653				
FEB	-0.024	0.215	-0.045	0.300	0.035	0.067	0.08	0.08	-0.002	0.896	-0.010	0.811	-0.039	0.048	-0.089	0.049				
MAR	-0.002	0.935	-0.012	0.783	0.056	0.003	0.11	0.01	0.017	0.326	0.019	0.637	-0.015	0.421	-0.052	0.235				
APR	0.001	0.960	0.007	0.865	0.057	0.002	0.13	0.00	0.020	0.272	0.038	0.355								
MAY	-0.062	0.001	-0.132	0.002					-0.040	0.027	-0.093	0.027	-0.071	0.000	-0.160	0.000				
JUN	-0.050	0.008	-0.107	0.012	0.008	0.683	0.01	0.82	-0.028	0.120	-0.069	0.091	-0.061	0.002	-0.140	0.002				
JUL	-0.052	0.005	-0.113	0.007	0.004	0.825	0.00	0.91	-0.030	0.085	-0.077	0.057	-0.055	0.004	-0.126	0.004				
AUG	-0.048	0.011	-0.099	0.019	0.010	0.580	0.02	0.61	-0.024	0.172	-0.056	0.165	-0.053	0.006	-0.119	0.007				

SEP	-0.059	0.002	-0.126	0.003	-0.003	0.859	-0.01	0.82	-0.038	0.033	-0.090	0.027	-0.061	0.001	-0.138	0.002				
OCT	-0.023	0.207	-0.038	0.357	0.035	0.053	0.08	0.05					-0.033	0.079	-0.070	0.102				
NOV	-0.008	0.642	-0.008	0.847	0.052	0.004	0.12	0.00	0.014	0.399	0.031	0.419	-0.015	0.422	-0.028	0.497				
DEC	0.016	0.369	0.035	0.370	0.078	0.000	0.17	0.00	0.037	0.023	0.073	0.052	0.009	0.627	0.013	0.759				
0 TO 4					0.243	0.000	0.51	0.00	0.448	0.000	0.978	0.000	0.254	0.000	0.544	0.000	0.253	0.000	0.537	0.000
4 TO 8	-0.332	0.000	-0.746	0.000	-0.071	0.000	-0.19	0.00	0.122	0.000	0.250	0.000	-0.075	0.000	-0.204	0.000	-0.072	0.000	-0.197	0.000
8 TO 12	-0.555	0.000	-1.236	0.000	-0.287	0.000	-0.67	0.00	-0.092	0.000	-0.226	0.000	-0.288	0.000	-0.675	0.000	-0.289	0.000	-0.676	0.000
12 TO 16	-0.505	0.000	-1.129	0.000	-0.248	0.000	-0.58	0.00	-0.043	0.000	-0.115	0.000	-0.239	0.000	-0.567	0.000	-0.248	0.000	-0.584	0.000
16 TO 20	-0.457	0.000	-0.998	0.000	-0.201	0.000	-0.46	0.00					-0.194	0.000	-0.445	0.000	-0.205	0.000	-0.468	0.000
20 TO 24	-0.251	0.000	-0.530	0.000					0.195	0.000	0.445	0.000								
SINGLE	-0.346	0.000	-0.843	0.000					-0.546	0.000	-1.293	0.000	-0.344	0.000	-0.847	0.000	-0.345	0.000	-0.847	0.000
OV	-0.005	0.771	-0.017	0.660	0.517	0.000	1.23	0.00					0.006	0.719	0.015	0.710	-0.003	0.876	-0.012	0.757
FIXED					0.387	0.000	0.95	0.00	-0.158	0.000	-0.352	0.000								
DRIVER	-0.032	0.002	-0.062	0.008	0.003	0.772	0.02	0.42	-0.049	0.000	-0.104	0.000	-0.060	0.000	-0.131	0.000	0.002	0.810	0.018	0.444
MC					-0.250	0.000	-0.58	0.00	-0.274	0.000	-0.631	0.000								
CAR	0.333	0.000	0.740	0.000	0.147	0.000	0.32	0.00	0.129	0.000	0.279	0.000	0.312	0.000	0.696	0.000	0.323	0.000	0.718	0.000
VAN	0.497	0.000	1.092	0.000	0.321	0.000	0.69	0.00	0.295	0.000	0.635	0.000	0.451	0.000	0.997	0.000	0.496	0.000	1.085	0.000
BUS	0.701	0.000	1.485	0.000	0.522	0.000	1.08	0.00					0.679	0.000	1.447	0.000	0.696	0.000	1.476	0.000
TRUCK	1.080	0.000	2.189	0.000	0.893	0.000	1.76	0.00	0.875	0.000	1.723	0.000	1.045	0.000	2.131	0.000	1.066	0.000	2.156	0.000
OTHERS	0.348	0.000	0.771	0.000					drop		drop		0.329	0.000	0.733	0.000	0.342	0.000	0.760	0.000
MALE	0.308	0.000	0.694	0.000	0.297	0.000	0.67	0.00	0.316	0.000	0.717	0.000	0.307	0.000	0.701	0.000	0.299	0.000	0.675	0.000
AGE <20	-0.627	0.000	-1.393	0.000					-0.359	0.000	-0.824	0.000								
AGE20-29	-0.548	0.000	-1.217	0.000	-0.071	0.000	-0.17	0.00	-0.278	0.000	-0.643	0.000					-0.067	0.000	-0.163	0.000
AGE30-39	-0.501	0.000	-1.111	0.000	-0.027	0.018	-0.07	0.01	-0.231	0.000	-0.534	0.000					-0.023	0.046	-0.062	0.018
AGE40-49	-0.423	0.000	-0.926	0.000	0.050	0.000	0.11	0.00									0.054	0.000	0.120	0.000
AGE50-59	-0.370	0.000	-0.806	0.000	0.103	0.000	0.23	0.00	-0.100	0.000	-0.231	0.000					0.105	0.000	0.236	0.000
AGE60-69	-0.281	0.000	-0.600	0.000	0.194	0.000	0.44	0.00	-0.012	0.499	-0.026	0.509					0.195	0.000	0.444	0.000
AGE >70					0.307	0.000	0.69	0.00	0.094	0.000	0.206	0.000					0.307	0.000	0.687	0.000
AGE_C													0.007	0.000	0.016	0.000				
No. of obs.	586807		586807		586807		586807		586807		586807		586807		586807		586807		586807	
Log likelihood	-63434.503		-63459.077		-64304.136		-64346.026		-64025.76		-64055.207		-58129.574		-58178.239		-64354.595		-64397.563	
LR chi^2	15883.81		15834.66		14144.54		14060.76		14701.3		14642.4		12858.7		12761.37		14043.62		13957.69	
Pseudo R^2	0.1113		0.1109		0.0991		0.0985		0.103		0.1026		0.0996		0.0988		0.0984		0.0978	

OPTIMUM ASSIGNMENT OF HOUSINGS AND JOBS WITH CONSTRAINED CAPACITY CONSIDERING DISCOMFORT AND TRAVEL COSTS

Yuki MUNEMASA[1], Yudai HONMA[2] and Kotaro IMAI[3]
[1]Graduate Student, School of Eng., The University of Tokyo, Japan
munemasa@iis.u-tokyo.ac.jp
[2]Lecturer, ICUS, IIS, The University of Tokyo, Japan
[3]Professor, IIS, The University of Tokyo, Japan

ABSTRACT

In this paper, we propose a new calculation method of optimum assignment and derive the optimum distribution of housings and jobs theoretically in the urban models with constrained capacities. First, we show that a problem which incorporates commuting travel cost, working travel cost and discomfort cost caused by the density of the node will be a non-convex quadratic programming problem. By using Reformulation-Linearization Technique, we are able to derive analytically the optimum location of housings and jobs.

Specifically, we set the urban model with constrained capacity to each nodes and show that the problem of optimum assignment of all costs is equal to mathematical programming problem. It is clear that the problem is a non-convex quadratic programming problem because the matrix we introduce at the formulation does not meet semidefinite programs. Therefore, we formulate the problem to a linear programming problem with Reformulation-Linearization Technique in order to derive the optimum allocation of housings and jobs. For numerical examples, we show two optimum assignments in linear and 2D urban models and describe the meanings of parameters, α: working travel frequency, and β: discomfort parameter. This model will be a new standard model for the formation of housings and jobs distribution.

***Keywords**: distribution of housings and jobs, travel cost, discomfort cost, system optimum assignment, quadratic programming problem*

3. INTRODUCTION

The purpose of this study is to derive the optimum arrangement structure of residence and jobs in theory considering working travel cost among working region, constrained capacity of buildings and discomfort. We make a process of optimum arrangement demanding a constant estimated result in the range of the city scale using spatial interaction model and relaxation of nonconvex quadratic programming problem. Moreover, after examination of advantages and disadvantages of the urban model, we recommend the possibility to apply the optimum arrangement of residence and jobs in actual city.

The population ratio in three metropolitan areas in Japan is already surpassed 50%, and it has been estimated that the population of depopulated areas will be decrease by 61% in the next 35 years (Ministry of Land, Infrastructure, Transport and Tourism, 2011). And Japan is already an aging society, sustainable regional development is a big problem to be investigated and they study the shift to compact city as one of the techniques to solve those problems. However, the method to greatly change the urban structure needs the planning process in short and mid-term and considering the influence to people going existing cities, the method is a high degree of difficulty and the embodiment is still problem.

In this study, we handle two building types, working place *(W)* and housing place *(H)*, as elements in the city, and derive the optimum arrangement which minimizes discomfort and travel cost in it. In urban renovation or shrinking expected with depopulation, we have to consider not only amenity and travel cost, but environmental conservation, other elements of building type or unforeseen problems. However, we think that it is conceivable to approach the actual city by formulating the distribution of *W-H*.

The study of minimizing travel cost in urban cities has been carried out in recent years. A series of the research stemmed from Hamilton et al. (1983) has been achieved the development as follows: study of the urban structure with population growth (Kondo and Yoshikawa, 2012), study of optimal 3D urban form of energy saving city (Matsuhashi, 1996), study of congestion mitigation and surplus transportation (Suzuki, 2003; Ohtsuand Koshizuka,1999;MaruyamaandHarada,2003, Yokota and Muromachi,2012), study of determining joint distribution of homes and workplaces (Honma and Kurita, 2004). However, the researches above mentioned derive optimum arrangement by selecting or simulating distribution randomly in the processofcalculatingtravelcostanditisnotthesolutioninastrictsense. Above all, connection of working regions is the essential element in considering the optimum arrangement of residence and jobs. Needless to say, Ohtsu et al. (1999) and Honma et al. (2004) study the optimum arrangement considering the element partially, but they simplify the process with mean distance theory or numerical simulation. It is quite natural to come out mathematical modeling clearly considering commuting travel cost and working travel cost simultaneously after Hamilton model. In this study, we have a shy at formulation of working travel cost as quadratic form and the solution.

In addition, we propose the formulation of discomfort and travel cost of the urban model considering (a) commuting travel cost, (b) working travel cost and (c) discomfort after setting constrained capacity in this study and simulate the optimum arrangement structure of residence and jobs distribution which was not performed until now based on numerical solutions. Constrained capacity we give here means to set the maximum of the number of people in buildings. In the long term, urban city will be changed to compact city is a likely supposition, however, so much energy is required to rearrange the urban structure in the sort and mid-term. In that sense, the significant is that we are able to give existing buildings by considering constrained capacity and derive the optimum arrangement.

This paper is organized as follows. In Sec. 2, we organize the urban model and show that minimizing problem of discomfort and travel cost is to be quadratic programming problem, and we clear that it is nonconvex quadratic programming problem because distance matrix we set does not satisfy the condition of semidefinite. Then, we describe that we are able to apply nonconvex quadratic programming problem to linear programming problem using reformulation-linearization technique. Moreover, we formulate relaxed linear programming problem in order to derive the optimum solutions. Specifically, we derive the optimum solution according to linearize executable area of linear programming problem by reasonable quadratic inequalities. In Sec. 3, we analyze numerical solutions considering of discomfort, constrained capacity and distribution of residence and jobs in virtual linear cities and 2D city. The urban model we set is much simple structure model for clear understanding. At the last, we describe the possibility how to apply discomfort and travel cost of the urban model in order to derive the optimum arrangement of residence and jobs to actual city, and the significance (Sec. 4).

2. FORMULATION

First, we formulate discomfort and travel cost of urban model in this study and disclose that minimizing problem of both of them is to be nonconvex quadratic programming problem.

2.1 Urban Model

Let us consider an urban city which contains of working place *(W)* consisting of the building nodes I $(1 \leqslant i \leqslant I)$ and residence place *(H)* consisting of the building node J $(1 \leqslant j \leqslant J)$, and assume that only two building types exist in the urban city in order to make formulation much more concise. Moreover, proposal urban model is independent; the total number of people moving *W-H* is T (= constant number) and there is no in flow and out flow of people between other cities.

We assume that there is two travel type in urban city, (i) commuting travel of *W-H* and (ii) working travel of *W-W’* and (iii) discomfort due to density of the node. At this time, our purpose of this study is to derive optimum arrangement which minimizing discomfort and travel cost in the urban city. On that account,

$$T = \sum_{i=1}^{I}\sum_{j=1}^{J} t_{ij}^{\mathrm{h}} \quad (1 \leqslant i \leqslant I,\ 1 \leqslant j \leqslant J), \tag{1}$$

$$w_i = \sum_{j=1}^{J} t_{ij}^{\mathrm{h}} \quad (1 \leqslant j \leqslant J), \tag{2}$$

$$h_j = \sum_{i=1}^{I} t_{ij}^{\mathrm{h}} \quad (1 \leqslant i \leqslant I), \tag{3}$$

where t^h_{ij} is a commuting number from i to j, w_i is a working number of people at node i and h_j is a residence number of people at node j. Furthermore, we assume the following inequalities to provide the idea of constrained capacity mentioned in Sec. 1,

$$0 \leq w_i \leq W_i, \tag{4}$$
$$0 \leq h_j \leq H_j, \tag{5}$$

where W_i and H_j is each capacity at the node. When we derive commuting travel cost, commuting travel is a regular trip and we set the commuting distance between i and j as d^h_{ij},

$$[\text{Commuting Travel Cost}] = 2 \times \sum_{i=1}^{I}\sum_{j=1}^{J} t_{ij}^{\mathrm{h}} \cdot d_{ij}^{\mathrm{h}}. \tag{6}$$

In the next place, we derive working travel cost. We define $t^w_{ii'}$ as the total number of people moving among working regions and α as movement frequency among them, so

$$t_{ii'}^{\mathrm{w}} := \alpha \cdot \frac{w_i \cdot w_{i'}}{T}, \tag{7}$$

In formula (7), we quote the way of spatial interaction model, however $t^w_{ii'}$ is free from decrement by the distance. We set $d^w_{ii'}$ as the distance of node $i - i'$ of working regions, working travel cost is,

$$\begin{aligned}[\text{Working Travel Cost}] &= \sum_{i=1}^{I}\sum_{i'=1}^{I} t_{ii'}^{\mathrm{w}} \cdot d_{ii'}^{\mathrm{w}} &(8)\\ &= \sum_{i=1}^{I}\sum_{i'=1}^{I} w_i \cdot w_{i'} \cdot \frac{\alpha}{T} \cdot d_{ii'}^{\mathrm{w}}. &(9)\end{aligned}$$

At the last, we introduce discomfort causing the density of population. We set ρ_i and ρ_j is a density of each node,

$$\rho_i := \frac{w_i}{W_i} \quad (1 \leqslant i \leqslant I), \tag{10}$$

$$\rho_j := \frac{h_j}{H_j} \quad (1 \leqslant j \leqslant J), \tag{11}$$

so, the formulation of discomfort is,

$$[\text{Discomfort}] = \sum_{i=1}^{I} \beta_{\text{w}} \cdot \rho_i \cdot w_i + \sum_{j=1}^{J} \beta_{\text{h}} \cdot \rho_j \cdot h_j, \tag{12}$$

where β_w, β_h is the discomfort value of each nodes i and j. A conceptual diagram of the urban model and movement form is shown below (Figure1).

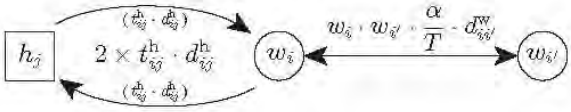
h_j
$(t^{\text{h}}_{ij} \cdot d^{\text{h}}_{ij})$
$2 \times t^{\text{h}}_{ij} \cdot d^{\text{h}}_{ij}$
$(t^{\text{h}}_{ij} \cdot d^{\text{h}}_{ij})$
w_i
$w_i \cdot w_{i'} \cdot \frac{\alpha}{T} \cdot d^{\text{w}}_{ii'}$
$w_{i'}$

Figure 1: The urban model and movement form

2.2 Formulation as Quadratic Programming Problem

For the purpose of this study is to derive optimum arrangement which minimizing discomfort, formula (12) and travel cost, formula (6) and (9) under constrain equations formula (1)–(5), we introduce $(I+J+I\times J)^{th}$ variable vector x, $(I+J+I\times J)^{th}$ constant vector and $(I+J+I\times J)\times(I+J+I\times J)$ square matrix Q. However, each factors are,

$$x_k = \begin{cases} w_k & (1 \leqslant k \leqslant I\,) \\ h_{k-I} & (I+1 \leqslant k \leqslant I+J\,) \\ t^{\text{h}}_{ij} & (\text{otherwise}) \end{cases}, \tag{13}$$

$$c_k = \begin{cases} 0 & (1 \leqslant k \leqslant I\,) \\ 0 & (I+1 \leqslant k \leqslant I+J\,) \\ d^{\text{h}}_{ij} & (\text{otherwise}) \end{cases}, \tag{14}$$

$$Q_{kl} = \begin{cases} \frac{\alpha}{T} \cdot d^{\text{w}}_{kl} + \delta_{kl} \frac{\beta_{\text{w}}}{W_k} & (1 \leqslant k \leqslant I,\ 1 \leqslant l \leqslant I\,) \\ \frac{\beta_{\text{h}}}{H_k} & (I+1 \leqslant k = l \leqslant I+J\,) \\ 0 & (\text{otherwise}) \end{cases}. \tag{15}$$

And as a result, formula (6), (9) and (12) are to be,

$$(6) = 2 \times \sum_{i=1}^{I} \sum_{j=1}^{J} t^{\text{h}}_{ij} \cdot d^{\text{h}}_{ij} = 2\boldsymbol{c}^{\top}\boldsymbol{x}\,, \tag{16}$$

$$\begin{aligned}(9) + (12) = &\sum_{i=1}^{I} \sum_{i'=1}^{I} w_i \cdot w_{i'} \cdot \frac{\alpha}{T} \cdot d^{\text{w}}_{ii'} \\ &+ \sum_{i=1}^{I} \beta_{\text{w}} \cdot \rho_i \cdot w_i + \sum_{j=1}^{J} \beta_{\text{h}} \cdot \rho_j \cdot h_j = \boldsymbol{x}^{\top}\boldsymbol{Q}\boldsymbol{x}\,,\end{aligned} \tag{17}$$

$$f(\boldsymbol{x}) = \boldsymbol{x}^\top Q\boldsymbol{x} + 2\boldsymbol{c}^\top \boldsymbol{x}\,. \tag{18}$$

Formula (18) is clearly quadratic programming problem of linear constraint. Here, square matrix *Q* was a symmetrical matrix and semidefinite, formula (18) will be convex quadratic programming problem and the solutions are well known such as quasi Newton method (Fujitaetal., 1998) or conjugate gradient method (Togawa, 1997), however, matrix *Q* introducing formula (15) is distance matrix and it does not satisfy semidefinite condition generally, and minimizing problem of discomfort and travel cost of urban city in this study is nonconvex quadratic programming problem.

2.3 Derivation of Optimum Solution with RLT

We relax nonconvex quadratic programming problem using RLT and propose the calculation method of derivation optimum solution in urban model.

First of all, we think a quadratic programming problem including nonconvex one;

$$\left|\begin{array}{ll} \text{Minimize} & f(\boldsymbol{x}) = \boldsymbol{x}^T Q\boldsymbol{x} + 2\boldsymbol{c}^T\boldsymbol{x} \\ \text{subject to} & \boldsymbol{A}\boldsymbol{x} \le \boldsymbol{b}, \quad \boldsymbol{P}\boldsymbol{x} = \boldsymbol{q} \end{array}\right. , \tag{19}$$

and, we introduce new variable $Y_{ij}=x_ix_j$ $(1\leqslant i\leqslant j\leqslant n)$, and set executable area of problem (19) as *D* and its convex hull as *coD*. Moreover, we define $\langle Q,Y\rangle$ as inner product of matrixes, so we can introduce new problem as follows;

$$\left|\begin{array}{ll} \text{Minimize} & g(\boldsymbol{Y},\boldsymbol{x}) = \langle \boldsymbol{Q},\boldsymbol{Y}\rangle + 2\boldsymbol{c}^T\boldsymbol{x} \\ \text{subject to} & (\boldsymbol{Y},\boldsymbol{x}) \in co\mathcal{D} \end{array}\right. . \tag{20}$$

Here, Sherali (1995, 2012, 2013) prove that if the optimal solution of problem (20) exists and it is to be (Y^*, x^*), so objective function of the problem will be linear. Asaresult, (Y^*, x^*), is end point of *coD* and objective function is equal of problem (19) because optimal solution exists as $Y=x^*x^*$. Furthermore, in the relaxation of nonconvex quadratic programming problem,Ya-jima (1999) show the lemma as follow;

if $(\boldsymbol{Y},\boldsymbol{x}) \in [\mathcal{D}]^2_L$, then $\boldsymbol{x} \in \mathcal{D}$,
specially if $\boldsymbol{x}$ is the end of set $\mathcal{D}$, then $\boldsymbol{Y} = \boldsymbol{x}\boldsymbol{x}^*$.

In brief, if (Y^*, x^*) is the optimal solution of the problem, $g(Y^*, x^*)$ is to be the lower bound value of quadratic programming problem (19), and at the same time $f(x^*)$ has upper bound value because of $x^*\in D$, and more if x^* is the end of set *D*, then the value is the optimum solution of problem (19).

2.4 Optimum Solution of Proposal Model

The preceding section demonstrates that we are able to get the optimum solution in nonconvex quadratic programming problem. In this subsection, we apply it to optimum arrangement of residence and jobs which minimizing discomfort and travel cost, $f(x)$, in formula (18). Minimization problem of the urban model proposed in 2.2 is,

$$\left|\begin{array}{ll} \text{Minimize} & f(\boldsymbol{x}) = \boldsymbol{x}^\top \boldsymbol{Q}\boldsymbol{x} + 2\boldsymbol{c}^\top \boldsymbol{x} \\ \text{subject to} & 0 < w_i \leq W_i \\ & 0 < h_j \leq H_j \\ & T = \sum_{i=1}^{I}\sum_{j=1}^{J} t_{ij}^{\mathrm{h}} \\ & w_i = \sum_{j=1}^{J} t_{ij}^{\mathrm{h}} \\ & h_j = \sum_{i=1}^{I} t_{ij}^{\mathrm{h}} \end{array}\right. . \tag{21}$$

The problem (21) suits the condition of formula (19), so reformulation-linearization technique introduced in 2.3 is realized. Therefore, we are able to derive the optimum arrangement of residence and jobs in the urban model using the method of preceding section. In numerical examples described later in Sec.3, we guarantee precision of the solution we get by calculating the gap, even if the case of $f(x^*) \neq g(Y^*,x^*)$,

$$\text{gap} := \frac{f(\boldsymbol{x}^*) - g(\boldsymbol{Y}^*, \boldsymbol{x}^*)}{f(\boldsymbol{x}^*)}. \tag{22}$$

3. NUMERICAL EXAMPLES

In this section, we attempt to derive optimum arrangement of virtual urban models with the proposal method in Sec.2. It includes (i)“*H-W-H*” linear city and (ii)“*H-W-H*” 2D city.

To solve the problem, we use the following computer, CPU; Intel (R) Core (TM) i7-3770K (3.50GHz), RAM; 32.0GB and software, IBMCPLEX12.6.

3.1 Optimum Arrangement of Residence and Jobs

We derive the distribution of residence and jobs while changing the values of T, α and β in the urban model (i) and (ii).

(i)“*H-W-H*” linear city

We set the linear urban model as; I=10 in W, J=10 in H, constrained capacity = 1.00, and T=5.5 (Figure2). When we change the parameter α (Figure2 (a)-(c)), working nodes get together in one and change the parameter β, working nodes spread and working place density is to be average due to rising of the discomfort cost. In spite of rising the cost of working travel and discomfort, housings nodes which close to working place nodes have the number of people to constrained capacity due to commuting travel cost.

(ii)"*H-W-H*"2D city We set the 2D urban model as; I=9 in W, J=40 in H, constrained capacity in W=1.00, constrained capacity in H=0.25, and T=5.5 (Figure3). When we rise the parameter α, the center of W has the number of people of the capacity, however, percentage of discomfort cost in total costs is high when we change β from 0.50 to 1.50 so nodes of W is to be average. Moreover,we rise α and β together, the model shows final state distribution of housings and jobs.

3.2 Specific Characters of *T*, α and β on Optimum Arrangement

In preceding section, we show that optimum arrangements fluctuate while changing T, α and β in each linear city and 2D city. In this section, we describe the specific character of them in the distribution of residence and jobs.

The formula (6) and (9) have distance element but informula (12), there is not. The unit of travel cost is "Number of People" × "distance" and so the unit of β is "distance". The character of β introduced calculating discomfort cost is "distance" shows that we can regard the cost of node itself as distance, and it is reasonable by the distribution we show in 4.1.

In addition, it is expected that information society evolves and population decline in near future, so α will rise and β will down in the urban city in Japan. There is some possibility of recommending the policy of reconstruction of the city with the method and numerical examples we propose in this research.

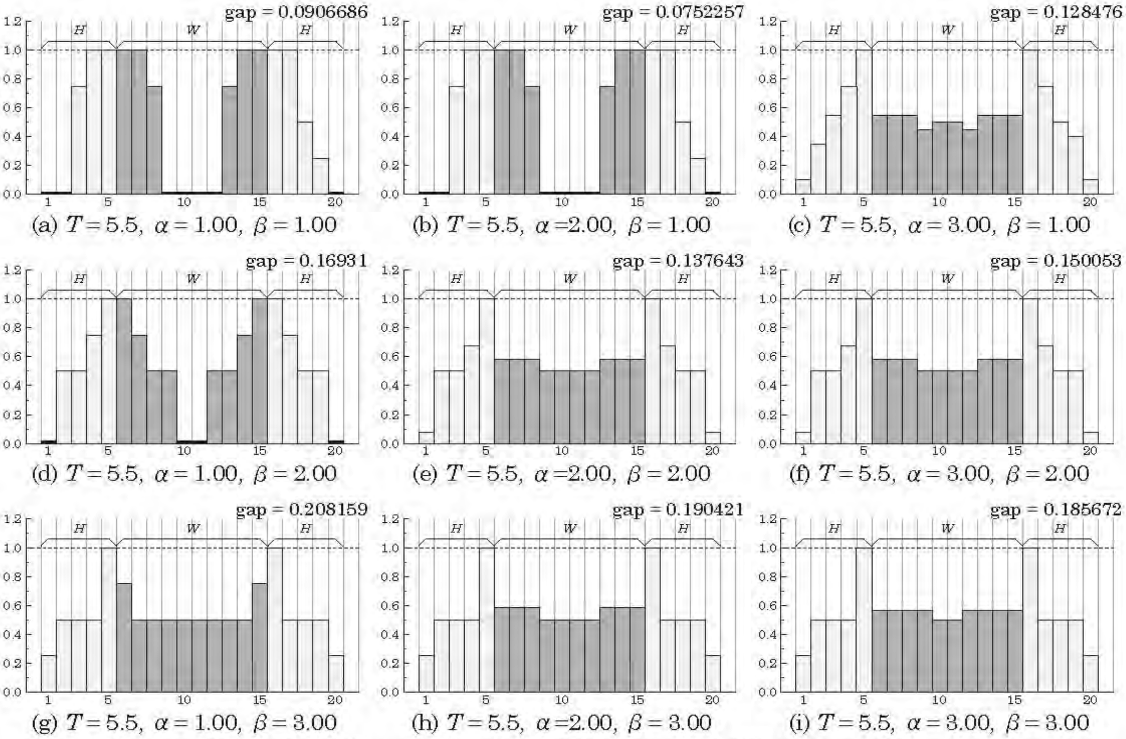

(a) $T = 5.5,\ \alpha = 1.00,\ \beta = 1.00$ (b) $T = 5.5,\ \alpha = 2.00,\ \beta = 1.00$ (c) $T = 5.5,\ \alpha = 3.00,\ \beta = 1.00$

(d) $T = 5.5,\ \alpha = 1.00,\ \beta = 2.00$ (e) $T = 5.5,\ \alpha = 2.00,\ \beta = 2.00$ (f) $T = 5.5,\ \alpha = 3.00,\ \beta = 2.00$

(g) $T = 5.5,\ \alpha = 1.00,\ \beta = 3.00$ (h) $T = 5.5,\ \alpha = 2.00,\ \beta = 3.00$ (i) $T = 5.5,\ \alpha = 3.00,\ \beta = 3.00$

Figure 2 Optimum Assignment of Housings and Jobs in linear City

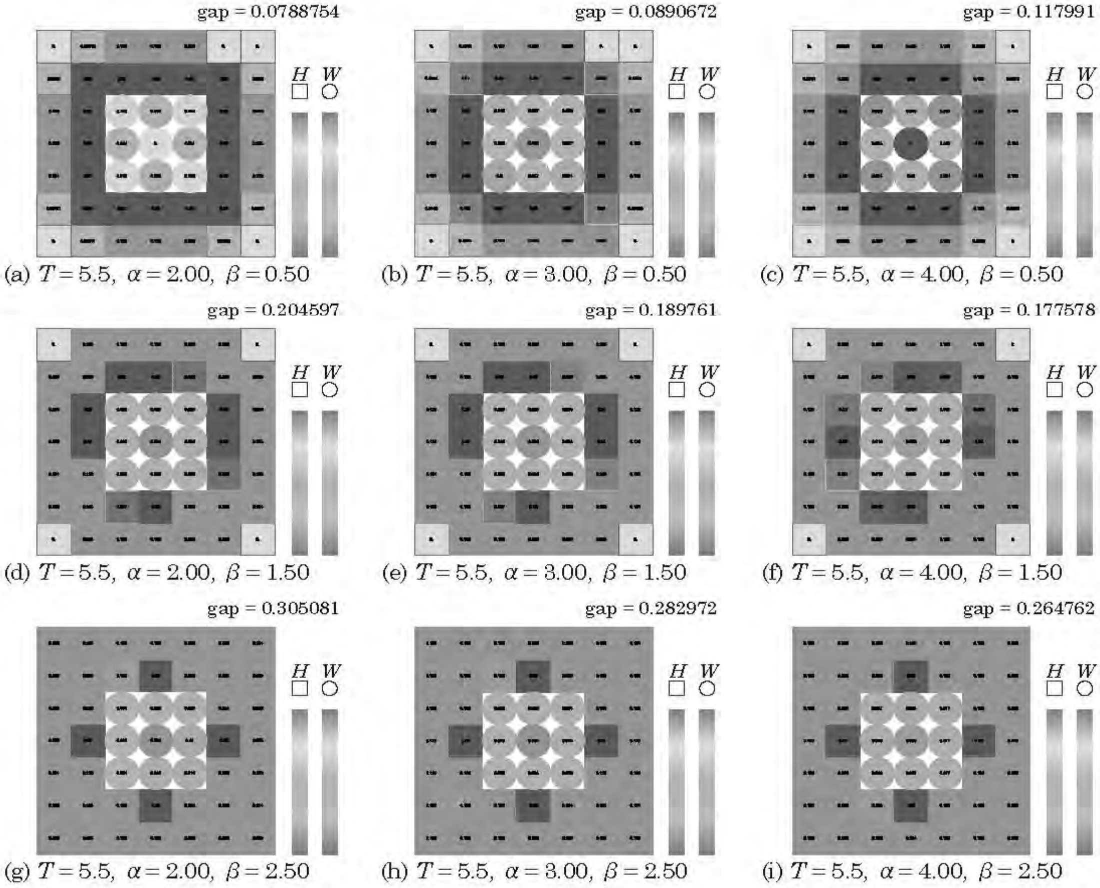
gap = 0.0788754
gap = 0.0890672
gap = 0.117991
gap = 0.204597
gap = 0.189761
gap = 0.177578
gap = 0.305081
gap = 0.282972
gap = 0.264762
H W
□ ○

(a) $T = 5.5,\ \alpha = 2.00,\ \beta = 0.50$ (b) $T = 5.5,\ \alpha = 3.00,\ \beta = 0.50$ (c) $T = 5.5,\ \alpha = 4.00,\ \beta = 0.50$

(d) $T = 5.5,\ \alpha = 2.00,\ \beta = 1.50$ (e) $T = 5.5,\ \alpha = 3.00,\ \beta = 1.50$ (f) $T = 5.5,\ \alpha = 4.00,\ \beta = 1.50$

(g) $T = 5.5,\ \alpha = 2.00,\ \beta = 2.50$ (h) $T = 5.5,\ \alpha = 3.00,\ \beta = 2.50$ (i) $T = 5.5,\ \alpha = 4.00,\ \beta = 2.50$

Figure 3: Optimum Assignment of Housing and Jobs in 2D City

4. CONCLUSION

In this study, we clarify that minimizing problem of discomfort calculated from population density and travel cost as a total of commuting travel and working travel in urban city consisting or working place and residence is non convex quadratic problem, and propose a new method of deriving optimum solution using RLT. In particular, we relax nonconvex quadratic problem as linear programming problem incorporated with spatial interaction model and relaxation of nonconvex quadratic problem, and as a result, we derive the optimum arrangement distribution of residence and jobs. Furthermore, we point out qualitative characteristics of T, α and β, we get the knowledge that the method is effective to time development of optimum arrangement of residence and jobs. Due to combine of linear urban model and two dimensional urban model, we can construct complex urban model, and we consider that it enables us to derive the optimum arrangement conforming to more realistic urban city.

We get the optimum solutions without slight errors, and they show the gap as follow, 0.128474-0.305086. We consider the reason why the method makes gap is that the domain $[D]^{L}{}_{2}$ is evidently larger than the area D at the time of using RLT. There are other ways of relaxation technique like Semidefinite Programming Problem (SDP) known as a type of convex optimization (Kojima and Waki, 2004), so we consider that SDP relaxation enable us to improve the formulation of minimizing problem of discomfort and travel cost and adapt the virtual urban model to actual urban city. This is the research task from now on.

REFERENCES

Ministry of Land, Infrastructure, Transport and Tourism, 2011. Long-Term Prospects of the Country, *Report of Ministry of Land, Infrastructure, Transport and Tourism*, p.7. (In Japanese)

Hamilton, B.W., 1982. Wasteful commuting, *Journal of political Economy*, 90, pp.1035-1053.

Kondo, T. and Yoshikawa, T., 2012. Study on Three-Dimensional Urban Form which Minimizes Travel cost: Assuming introduction of hierarchical districts and transportation, *Journal of Architectural Institute of Japan*, Vol.77, No.675, pp.1087-1093. (In Japanese)

Matsuhashi, K., 1996. A Study on Optimal 3D Urban Form of Energy-Saving City – From a Viewpoint of Trips -, *Journal of the City Planning Institute of Japan*, 31,pp.43-48. (In Japanese)

Suzuki, T., 2003. A Commutation Flow Model and the Effect of Workers Decentralization Using the Joint Distribution of Home and Workplace Location, *Journal of The Japan Society of Industrial and Applied Mathematics*, Vol.13, No.3, pp.403-415. (In Japanese)

Ohtsu, S. and Koshizuka, T., 1999. An Optimum Distribution of Home and Workplace Minimizing a Total Cost of Transportation in a City, *Journal of the City Planning Institute of Japan*,34, pp. 775-780. (In Japanese)

Maruyama, T. and Harada, N., 2003. Optimal Job-Housing Location Patter Considering Congestion in Network and Its Empirical Study, *Journal of the City Planning Institute of Japan,* 38 (3), pp. 517-522. (In Japanese)

Yokota, Y. and Muromachi, Y., 2012. Reducing Railway Excess Commuting in Tokyo Metropolitan Area by Residential Relocation, *Journal of the City Planning Institute of Japan,* 47 (3). Pp. 853-858. (In Japanese)

Honma, Y. and Kurita, O., 2004. Determining Joint Distributions of Homes and Workplaces Based on the Random Utility Theory, *Journal of the City Planning Institute of Japan*, 39, pp. 769-774. (In Japanese)

Fujita, H., Konno, H. and Tanabe, K., 1998. *Optimization Problem,* Iwanami Shoten, Tokyo. (In Japanese)

Togawa, H., 1977. *Conjugate Gradient Method,* KYOIKU-SHUPPAN, Tokyo. (In Japanese)

Sherali, H. D. and Tuncbilek, C. H., 1995. A Reformulation-Convexification Approach for Solving Nonconvex Quadratic programming Problems, *Journal of Global Optimization,* 7(1), pp. 1-31.

Sherali, H. D. and Admas, W.P., 2013. *A Reformulation-Linearization Technique for Solving Discrete and Continuous Nonconvex Problems,* Springer US.

Sherali, H. D., Dalkiran, E. and Liberti, L., 2012. Reduced RLT representations for nonconvex polynomial programming problems, *Journal of Global Optimization,* Vol.52, Issue 3, pp. 447-469.

Yajima, Y., 1999. Nonconvex Quadratic Programming Problems and Combinatorial Optimization, *Communications of the Operations Research Society of Japan*, Vol.44, No. 5, pp. 237-242. (In Japanese)

IBM Corporation, IBM ILOG CPLEX Optimizer 12.6, http://www-01.ibm.com/software/commerce/optimization/cplex-optimizer/, 2014/11/7.

Kojima, M. and Waki, H., 2004. Semidefinite Programming Relaxation for Polynomial Optimization Problem, *Systems Control and Information,* 48(12), pp.477-482. (In Japanese)

FACTORS INFLUENCING RED LIGHT RUNNING BEHAVIOR: A STUDY OF SOCIO-ECONOMIC CHARACTERISTICS AND GEOMETRY OF INTERSECTIONS

Auearree JENSUPAKARN [a], Kunnawee KANITPONG [b],
Piyapong JIWATTANAKULPAISARN [c]
[a,b] Thailand Accident Research Center, Asian Institute of Technology,
P.O. Box 4, Klong Luang, Bangkok, 12120, Thailand
[a] E-mail: a.jensupakarn@gmail.com
[b] E-mail: kanitpon@ait.ac.th
[c]ThaiRoads Foundation, Ladprao Soi 3, Jatujak, Bangkok, Thailand;
E-mail: piyapong.j@gmail.com

ABSTRACT

In Thailand, red light running is considered as one of the most dangerous behaviors at intersections. Red light running behavior is caused by the failure to obey the traffic control signal. However the drivers who are running through red lights constitute a major portion of intersection crashes, little research study has been done to evaluate the contributing factors influencing the red light violation behavior. This study aims to determine the factors influencing the red light running behavior including road and traffic condition, traffic control signal, and geometry of intersection. Trained observers and video cameras were used to record the red light running behavior at 33 intersections in Nakhon Ratchasima, the largest province in the northeastern region of Thailand. In addition, the socio-economic characteristics of red light runners were obtained from self-reported survey. The Binary Logistic Regression and the Multiple Linear Regression model were used to determine the characteristics of red light runners and the factors influencing rates of red light running respectively. The result from this study can help to understand the characteristics of red light runners, and factors affecting them to run red lights.

***Keywords**: Red Light Running, Traffic Violation, Driver Characteristics, Road Safety, Injury Prevention, Thailand*

1. INTRODUCTION

Red light violations are now a problem in many countries, especially in developing countries. A principal contributing factor in motor-vehicle crashes in Thailand and other countries is failure of drivers to obey traffic control devices. In Thailand, red light running is considered as one of the most dangerous behaviors on roadways. According to the Royal Thai Police's Database in 2011, there were 1,702 red light running crashes which accounted for 2.79% of all accidents caused by drivers. As illustrated in Figure 1, though the number of accident caused by red light running is less than the others, it is still considered as a serious problem. Most of these crashes occur at intersection, where one or more drivers decide to disobey a traffic signal, usually end up with the seriously crashes which resulting in severe injuries and fatalities.

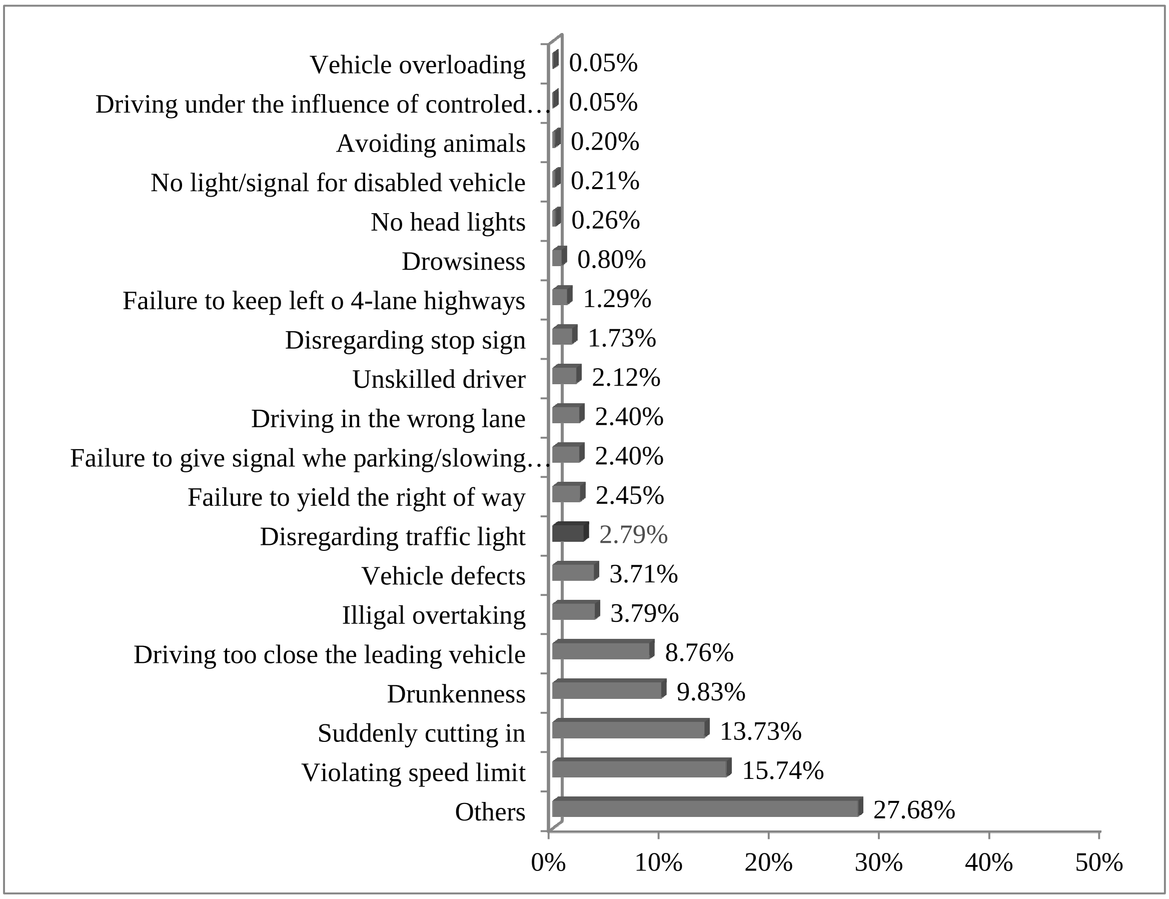

Figure 1: Proportion of traffic accidents caused by the drivers (The Royal Thai Police, 2011)

Thai Traffic Police Official reported more than 100,000 red light runners were issued a fine ticket over the past two months after the red light cameras were operating (December 30, 2008). That means, on average, the number of red light runner is around 2,000 motorists per day. These numbers obtained from red light camera at only 30 intersections from more than 1,500 intersections around Bangkok; moreover, the red light camera in each intersection was installed in one approach only. Though the number of red light runners dropped to 800-900 motorists per day (Thai Traffic Police Official, April 2012), it is better if the number of red light runners dropped to zero.

Red light running is a complex problem that could result from various causes. Some drivers run red lights because they are in a hurry or they are sometimes too impatient to wait for the signal to turn green. Other drivers are simply annoyed at red lights and they just do not want to wait. In many countries, especially Thailand, the yellow light has come to symbolize "hurry up" instead of "slow down". This driver's behavior is now becoming to a habit; if drivers have run red light at one time, it is likely that they will do it again if they have a chance.

Running a red light can cause the adverse effects for everyone involved. For instance, it can result in someone's death or injury, damaging the vehicle, and getting a ticket from the police. One of the most dangerous effects that running a red light could have is death. A car that runs a red light is liable to come in the path of the traffic that has the green light. Many drivers tend not to look right and left while crossing the intersection when they have the green light. This means, that a person running a red light is driving into a potential car that is coming violently at high speed from either side. A collision between the two cars could result in serious injuries and even death.

However, the drivers who are running through red lights constitute a major portion of intersection crashes, little is known about their characteristics or the other contributing factors influencing the number of red light violations e.g. vehicle characteristics and geometry of intersections. Therefore, this study aims to determine the factors those are influencing to the number of red light running including: driver factors, vehicle factors, and geometry of intersection factors. In addition, the importance of this study is to provide the data that may help understand who the red light runners are and what factors affecting them to run red lights. Furthermore, this study could lead to the improvement of implemented policies to dealing with running a red light through an intersection in order to reduce the number of red light runners.

The main objectives of this study are to:

1. Determine the characteristics of motorcycle drivers who run red lights by observation.
2. Determine the socio-economic characteristics of red light runners by using secondary data of self-reported survey.
3. Determine the intersection factors influencing rates of red light running by observation.

2. LITERATURE REVIEW

Based on the findings from previous studies, the factors affecting to the number of red light running at an intersection can be divided into four categories: driver characteristics, physical conditions of intersection, traffic condition, and driving environment. These findings are presented in below section.

Kraus and Quiroga (2004) reported on red light running trends in Texas and found that older age groups accounted for a relatively small portion of red light running crashes compared to the young age group. C.Y. David Yang and Wassim G. Najm (2006) presented the results of the relationship between red light runners and their related factors from an analysis of about 47,000 red light violation records collected from 11 intersections in the City of Sacramento, California, by red light photo enforcement cameras between May 1999 and June 2003. Three groups of factor were considered in the study: various driver, intersection, and environmental factors. They suggested that younger drivers under 30 years of age are more likely to run red lights than drivers in other age groups. Another studies also reported in the same way that young drivers are more likely to run the red lights compare to other age groups (Porter and Berry, 2001) and red light runners tend to be drivers under 30 years old (Retting *et al.*, 1999 and Retting and Williams, 1996). Gender of driver also found as a contributing factor. Retting *et al.* (1999) reported that the red light runners are more likely than non-runners to be male.

Many research studies have considered the occupancy in a vehicle as a factor contributing to drivers' behavior. Porter and Berry (2001) concluded that passengers reduced drivers' tendencies to run red lights. 25.6 percent of drivers reported being likely to run a red light however, this percentage drops sharply when there are passengers in the vehicle. Moreover, Porter (1999) has reported that passengers decrease red light running probability especially child passengers.

Survey results from The Richmond Metro Poll (1999) also pointed out that red light running was related to other risk behaviors. Drivers who reported that they always wear seat belts were also more likely to have reported that they never ran red lights (54%). Driving record was proved to be one factors influencing to running the red lights. The studies found that the drivers with poor driving records (Retting and Williams, 1996) such as driving with suspended or revoked driver's license (Retting *et al.*, 1999) or driver who have been ticketed (Porter, 1999) have a higher tendency to run the red lights. There are another driver's characteristics influencing to red light running such as ethnicity, occupation, alcohol consumption, and frustration.

In a study done by Elmitiny *et al.* (2010), a field data collection was conducted at a high-speed signalized intersection, using video-based system with three cameras. The objective of their study was to know how the probabilities of a stop or go decision and of red light running are associated with the traffic parameters. The results were obtained from the classification analysis, as the distance from the intersection increase, the probability of a stop decision increases while the probability of go decision decreases. In 1985, Chang et al. has concluded about the probability of a vehicle stopping for a traffic light; probability decreases as the distance from vehicle to the intersection decreases. Moreover, Chang *et al.* (1985) was found that the width of intersection is another one factor affecting to stop and go decision of drivers; most of drivers tend to stop for traffic lights more at wider intersections than at narrower intersections.

Approaching speed was found as contributing factor to drivers' decision. The probability of a driver stopping for a traffic light decreases as the approach speed to the intersection increases (Chang *et al.*, 1985). Elmitiny *et al.* (2010) found that if operating speeds are lower than 50.55 mph, drivers are more likely to stop for a traffic light. Yang and Najm (2006) also reported that about 56% of the red light runners were driving at or below the posted speed limit.

Furthermore, the signal timing, especially yellow timing, has some effect on drivers' decision. From the study done by Retting *et al.* (2008), the objective was to evaluate the incremental effects on red light running of first lengthening yellow signal timing, followed by the introduction of red light cameras. Results showed that yellow timing changes reduced red light violations by 36%. The yellow signal timing should be adequate; otherwise, it could increases probability of running the red lights. The result from a study done by Brewer *et al.* (2002) shows that the frequency of red light running increases when the yellow interval is less than 3.5 seconds. And the result of Elmitiny *et al.* (2010) also shows that when the yellow time larger than 4.3 seconds, the red light running violations can occur.

When considering the previously studies about factors affecting to the red light running, the traffic conditions such as time pressure or approach traffic volume can be affects to drivers' behavior. A large number of drivers tend to speed up to beat the yellow light which followed by the red light because of wanting to save time (Porter and Berry, 2001). When considering the approach traffic volume factor, higher traffic volumes could lead more red light running rates. The reason was reported by Elmitiny *et al.* (2010); an intersection with higher traffic volumes, drivers would have more chances to be in a following position in the traffic flow at the onset of yellow, therefore the red light running rate would increase.

Many studies found that time of day and day of week are affecting to drivers' behavior to stop for the traffic lights. The number of red light running tends to increase during the morning and evening peak hours compared to other times of the day (Retting *et al.*, 1998). At nighttime red light running were more than at daytime due to high possibility of drivers to have high blood alcohol concentrations (Harb *et al.*, 2007). When considering the day of week factor, many researchers reported that there are more red light violations during the weekdays compared to weekends.

3. METHODOLOGY

The study area is in Nakhon Ratchasima, the biggest province of Thailand. It is located in the northeast of Thailand. The study was conducted at the 33 intersections in both rural and urban areas of the province. Potential intersections were identified and selected according to the following criteria: signalized, at-grade, four-legged, standard geometry layout (i.e. approximately 90-degree angle for each approach), properly functioning traffic signal, pre-timed signal operation, allow left-turning on red, not turn into flashing signal throughout the observation periods, and clearly visible stop line and/or zebra crossing. The selected intersections were observed on weekdays and weekends and the data were collected for one hour at different time periods: peak, off-peak, and nighttime.

3.1 Model Selection for the Analysis of Characteristics of Motorcycle Drivers

The first objective is focused on the characteristics of motorcycle drivers who ran the red lights. Their gender, estimated age, helmet wearing status, number of pillion passenger, and type of motorcycle they used were recorded. The data would be used for analyze the driver characteristics factors influencing the red light running behavior by using Binary Logistic Regression Method. The model is suit to the analysis that the alternative of a problem are discrete. Discrete choice model is classified to several sub models according to the assumption of the error term. Logit model, a form of discrete choice model, assumes the distribution of the error as the gumble distribution. The model is widely used in several studies. Also, in this study, the characteristics of motorcycle drivers who run the red light are described via Binary Logistic Regression Model.

$$Y = e^{\beta_0 + \beta_1 x_1 + \beta_2 x_2 + \cdots + \beta_n x_n} \quad (1)$$

"Y" is a dependent variable which represents the decision of motorcycle driver when they when see the changing of traffic light from green to yellow or from yellow to red at the intersection. A driver has two choices: stop behind the stop line or violate the traffic light. "X_1, X_2, …, X_n" are the independent variables include; gender, estimated age, helmet wearing behavior, number of pillion passenger and type of motorcycle (as shown in Table 1). These variables would affect to the dependent variable "Y" which is the decision of motorcycle drivers.

Table :. Study variables from observation survey for Binary Logistic Regression Model

Variable type	Explanatory variable	Description of Variable	Average
Dependent	Driving behavior	1 = run the red light, otherwise 0	0.4
Independent	gender	1 = male driver, otherwise 0	0.8
	y_age	1 = driver age below 20, otherwise 0	0.3
	m_age	1 = driver age between 20-50, otherwise 0	0.6
	o_age	1 = driver age more than 50, otherwise 0	0.1
	hm	1 = driver wears a helmet, otherwise 0	0.4
	psg0	1 = drive with no pillion passenger, otherwise 0	0.7
	mc_type	1 = driver with automatic gear motorcycle, otherwise 0	0.4

For both of red light and yellow light runners' data, the highest Pearson correlation was found between young aged drivers and middle aged drivers with the coefficient of -0.888 and -0.844 respectively. Another one was found between no passenger and one passenger with the coefficient of -0.977 for red light runners and -0.839 for yellow light runners. Therefore, one of each variable for all of correlation will be excluded from the model.

3.2 Model Selection for the Analysis of Socio-Economic Characteristics of Red Light Runner

The second emphasizes is collecting the secondary data from self-reported survey in 2010 (thaiROADS Foundation, 2010). Questionnaire was providing the information about a frequency of violating behavior of each respondent and their socio-economic characteristics. The data would be used for analyze the socio-economic characteristics of drivers that affecting the red light running behavior. Secondary information gathered from the previous study— Self-Reported Survey on driver socio-economic characteristics, driver behaviors, and driver attitudes. (ThaiROADS Foundation, 2010). The data about personal data and characteristics collected are used for analyze the relationship between drivers' violation behavior and their socioeconomic characteristics by using Binary Logistic Regression model.

"Y" is a dependent variable which represents the red light running behavior. "X_1, X_2, …, X_n" are independent variables include; gender, age, education level, occupation, vehicle types, driving license, helmet/safety belt wearing, and attitudes on risk behavior as shown in Table 2 and Table 3 separated for the motorcycle users and personal car users respectively.

Table 2. Study variables from secondary data source (thaiROADS) of motorcycle users for Binary Logistic Regression Model

Variable type	Explanatory variable	Description of Variable	Average
Dependent	Driving behavior (scenario1)	1 = run the red light, otherwise 0	0.4
	Driving behavior (scenario2)	1 = run the red light, otherwise 0	0.2
Independent	age	age of driver	29.3
	gender	1 = male driver, otherwise 0	0.5
	edu_1	1 = primary school or lower, otherwise 0	0.2
	edu_2	1 = high school/GED, otherwise 0	0.5
	edu_3	1 = bachelor degree or higher, otherwise 0	0.4
	ocp_1	1 = agriculturist, otherwise 0	0.1
	ocp_2	1 = employee, otherwise 0	0.3
	ocp_3	1 = proprietor/trader, otherwise 0	0.2
	ocp_4	1 = government/state enterprise officer, otherwise 0	0.1
	ocp_5	1 = student, otherwise 0	0.4
	licen	1 = driver has driving license, otherwise 0	0.7
	helmet	1 = driver wears the helmet, otherwise 0	0.6
	risk	1 (low) – 3 (high) the risk of being caught by police	2.2

Table 3: Study variables from secondary data source (thaiROADS) of personal car users for Binary Logistic Regression Model

Variable type	Explanatory variable	Description of Variable	Average
Dependent	Driving behavior (scenario1)	1 = run the red light, otherwise 0	0.4
	Driving behavior (scenario2)	1 = run the red light, otherwise 0	0.1
Independent	age	age of driver	31.7
	gender	1 = male driver, otherwise 0	0.7
	edu_1	1 = primary school or lower, otherwise 0	0.1
	edu_2	1 = high school/GED, otherwise 0	0.3
	edu_3	1 = bachelor degree or higher, otherwise 0	0.5
	ocp_1	1 = agriculturist, otherwise 0	0.1
	ocp_2	1 = employee, otherwise 0	0.3
	ocp_3	1 = proprietor/trader, otherwise 0	0.3
	ocp_4	1 = government/state enterprise officer, otherwise 0	0.2
	ocp_5	1 = student, otherwise 0	0.2
	car_1	1 = driver usually drive a passenger car, otherwise 0	0.4
	car_2	1 = driver usually drive a pick-up, otherwise 0	0.6
	car_3	1 = driver usually drive a van, otherwise 0	0.0
	licen	1 = driver has driving license, otherwise 0	0.8
	belt	1 = driver fasten the seatbelt, otherwise 0	0.7
	risk	1 (low) – 3 (high) the risk of being caught by police	2.2

The highest Pearson correlation for motorcycle driver analysis was found between high school/GED and bachelor degree or higher which the correlation coefficient of -0.712. For passenger vehicle analysis was found the correlation between high school/GED and bachelor degree or higher with the coefficient of -0.752 and another one was found between passenger car and pickup with the coefficient of -0.952.

3.3 Model Selection for the Analysis of Intersection Factors Influencing Rates of Red Light Running

The third one is the characteristics of intersection that may influence the red light running rates. The physical conditions (i.e. geometry, traffic signal conditions, etc.) of each intersection were recorded and used for analyze the relationship between rate of red light running and their contributing factors related to the physical conditions of intersection by using the Multiple Linear Regression Method. Multiple Linear Regression (MLR) is a method used to model the linear relationship between a dependent variable (Y) and one or more independent variables (X_i). The model will explains how the independent variables affect to the dependent variable.

$$Y = b_0 + b_1 x_{i,1} + b_2 x_{i,2} + b_k x_{i,k} + e_i \qquad (2)$$

where

* k is total number of independent variables

"Y" is a dependent variable which is the rates of red light running. "Xi" is predictors which are the general characteristics of intersection: Cycle length, Yellow time, Signal phasing, Operating speed, Traffic volume, Number of lane, Lane width, Median width, Available of auxiliary lane, Presence of police booth and Illumination at intersection (in night time). as shown in Table 4.

Table 4: Study variables from observation survey for Multiple Linear Regression Model

Variable type	Explanatory variable	Description of Variable	Average
Dependent	Rate of Red Light Running	number of red light running per analysis hourly volume	3.7
Independent	th	1 = data collected in through direction, otherwise 0	0.5
	mi	1 = data collected on minor road, otherwise 0	0.5
	wd	1 = data collected from weekday, otherwise 0	0.5
	peak	1 = data collected in peak hour, otherwise 0	0.2
	night	1 = data collected at nighttime, otherwise 0	0.3
	vol	1 = analysis hourly volume, otherwise 0	390.1
	nol	1 = number of travelling lane, otherwise 0	2.6
	lw	width of lane	4.6
	iw	width of intersection	11.5
	med	1 = available of median, otherwise 0	0.3
	mw	width of median	1.8
	isd	intersection sight distance	11.2
	sinst	1 = normal pole, otherwise 0	0.4
	sdisp	1 = normal (no countdown), otherwise 0	0.4
	ph	number of phase	2.7
	cl	length of cycle time	117.7
	yt	length of yellow interval	3.2
	locat	1 = intersection located in urban area, otherwise 0	0.6
	spd	approaching speed (kph)	48.2
	ads	1 = available of advanced warning sign, otherwise 0	0.4
	add	distance of advanced warning sign to stop line	71.7
	pave	1 = asphalt, otherwise 0	0.8
	lux	illumination at nighttime	12.2
	rn	level of pavement roughness, 1(smooth) - 5(severe)	2.2

The highest Pearson correlation was found between: number of lane and auxiliary lane, number of lane and approaching speed, crossing lane width and number of crossing lane, intersection sight distance and auxiliary lane, intersection sight distance and location of intersection, location and type of signal operation, location and number of phase, location and cycle length, number of phase and cycle length, presence of police and cycle length, advanced warning sign and advanced warning sign distance.

4. MODEL RESULTS

4.1 Explanation of Statistical Test for the Red Light Runners' Characteristics

In this section, the data were analyzed by using the Binary Logistic Regression Model. This model will analyze the significance of independent variables (drivers' characteristics) that affecting to red light running behaviors. The statistical results are presented in Tables 5.

Table 5: Model estimation result of motorcycle drivers' characteristics affecting red light running behavior

Independent Variables	Model 1		Model 2		Model 3	
	Coef.	P>|Z|	Coef.	P>|Z|	Coef.	P>|Z|
gender	1.113	***	1.235	***	1.151	***
o_age[i]	-2.251	***	-2.074	***	-2.401	***
hm	-1.481	***	-1.349	***		
psg0[ii]	0.958	***			1.100	***
mc_type	-1.120	***				
Constant	-0.940	0.000	-0.823	0.000	-2.091	0.000
Summary of Statistics:						
Observations	4257		4257		4257	
Log Likelihood	-2272.8251		-2493.8441		-2583.1661	

i comparison group is young aged driver

ii comparison group is driver with two pillion passengers

- Not relevant; *** Significant at 1% level; ** Significant at 5% level; * Significant at 10% level.

Gender of driver was found that it has a positive effect to the dependent variable. It means male drivers tend to run the red light if compared with female drivers because males are generally feel confident themselves and also like challenges. Especially for the critical time when the light changes from yellow to red, males are more likely to speed up to beat with the oncoming red light than females. Retting *et al.* (1999) concluded that Red light runners are more likely than non-runners to be male.

Age of driver is also the most significant to the model. The results show that old aged drivers tend to stop than run a red light compared with the young aged drivers. It might be because of their perception abilities (i.e. visualization is not clear, take more times to perceive and react, etc.). Thus, old aged drivers do not feel confident themselves enough to run a red light. This finding is consistent with the previous studies done by Kraus and Quiroga (2004); Porter and Berry (2001); Retting *et al.* (1999); Retting and Williams (1996).

Helmet use is one of driver behavior which was included in the model. Drivers who wear the helmet tend to stop for a red light.

Drivers with no pillion passenger are more likely to run the red light than those who travelling with their pillion passengers. Passengers decrease red light running likelihood, particularly child passengers (Porter and Berry, 2001; Porter, 1999). Because when driver travelling alone, they feel like no need to take care of someone. If they face the situation of oncoming red light, the might decide to drive through the intersection with no other concerning. On the other hand, if drivers travelling with someone, they may think more about the other lives that depending on their decisions and their behaviors. So, driver could recognize that they have to take more responsibility to their pillion passenger and they might decide to stop for a red light.

A type of motorcycle has a negative effect to the model. It means the drivers who drive the automatic gear motorcycle tend to stop more than the drivers who drive the manual gear motorcycle. The reason is because of the accelerating rate of each type. The manual transmission motorcycle is normally has more power than the automatic one in terms of accelerating rate. Drivers who drive the manual motorcycle might have more ability to accelerate. So, they might be confident themselves to drive through the intersection before onset of red light.

4.2 Explanation of Statistical Test for Socio-Economic Characteristics of Motorcycle Red Light Runners

As shown in Table 6 and Table 7, Binary Logistic Regression Model was used to analyze the socio-economic characteristics affecting to behavior of running the red lights of motorcycle drivers. Significant variables are come in both directions; negative and positive which are described below.

Table 6: Model estimation result of motorcycle drivers who ran the red lights and their socio-economic characteristics (Scenario 1)

Independent Variables	Model 1		Model 2		Model 3		Model 4	
	Coef.	P>|Z|	Coef.	P>|Z|	Coef.	P>|Z|	Coef.	P>|Z|
age	-0.005	***	-0.005	***	-0.005	***	-0.005	***
gender	0.518	***	0.522	***	0.537	***	0.539	***
edu_1	0.002	0.956			-0.018	0.542		
ocp_1	0.050	0.224			0.045	0.276		
ocp_3	0.099	***	0.103	***	0.102	***	0.105	***
ocp_4	-0.054	0.143			-0.047	0.204		
ocp_5	0.127	***	0.131	***	0.113	***	0.119	***
licen	0.162	***	0.157	***				
helmet	-0.123	***	-0.125	***				
risk	-0.073	***	-0.073	***				
Constant	-0.514	0.000	-0.522	0.000	-0.650	0.000	-0.656	0.000
Summary of Statistics:								
Observations	45,806		45,806		45,806		45,806	
Log likelihood	-30139.396		-30141.931		-30195.403		-30197.177	

- Not relevant; *** Significant at 1% level; ** Significant at 5% level; * Significant at 10% level.

Table 7: Model estimation result of motorcycle drivers who ran the red lights and their socio-economic characteristics (Scenario 2)

Independent Variables	Model 1		Model 2		Model 3		Model 4	
	Coef.	P>|Z|	Coef.	P>|Z|	Coef.	P>|Z|	Coef.	P>|Z|
age	-0.008	***	-0.009	***	-0.009	***	-0.009	***
gender	0.438	***	0.437	***	0.452	***	0.455	***
edu_1	0.164	***	0.161	***	0.154	***	0.166	***
ocp_1	-0.023	0.685			-0.018	0.743		
ocp_3	0.071	*	0.076	**	0.077	*	0.098	***
ocp_4	-0.087	*	-0.083	0.107	-0.084	0.107		
ocp_5	0.087	**	0.090	**	0.086	**	0.104	***
licen	0.106	***	0.107	***				
helmet	-0.135	***	-0.135	***				
risk	-0.079	***	-0.079	***				
Constant	-1.611	0.000	-1.613	0.000	-1.792	0.000	-1.805	0.000
Summary of Statistics:								
Observations	45,806		45,806		45,806		45,806	
Log likelihood	-19288.606		-19288.688		-19316.231		-19317.543	

- Not relevant; *** Significant at 1% level; ** Significant at 5% level; * Significant at 10% level.

Gender of driver was found that it has a positive effect to the model. It means male drivers tend to run the red lights than the females. Drivers with low education level were found that they are more likely to run the red light compared with drivers with bachelor degree or higher. For the occupations, drivers who are a proprietor or trader and drivers who are a student tend to run the red light in compared with drivers who are an employee. The driving license also has the positive effect to the model which means that drivers who have driving license are more likely to run the red light. The reasons should be because of the drivers who have no driving license do not want to being caught by doing something illegally because they might get more fines due to their illegal behavior and also be charged for drive with no driving license.

Age of driver has the negative effects to the model. It means the lower age of driver, the higher possibility to run the red lights. Drivers who usually wear the helmet are more likely to stop for the red lights than those who rarely wear the helmet. Drivers' attitude towards risk of being caught when they violate the traffic signal inversely affects to the possibility of running the red light. It means if drivers define that they have less risk of being caught; they will have less concerning about the police.

4.3 Explanation of Statistical Test for Socio-Economic Characteristics of Passenger Vehicle Red Light Runners

Binary Logistic Regression Model was used to analyze the socio-economic characteristics affecting to behavior of running the red lights of passenger vehicle drivers as shown in Table 8 and Table 9.

Table 8: Model estimation result of personal car drivers who ran the red lights and their socio-economic characteristics (Scenario 1)

Independent Variables	Model 1		Model 2		Model 3		Model 4	
	Coef.	P>|Z|	Coef.	P>|Z|	Coef.	P>|Z|	Coef.	P>|Z|
age	-0.013	***	-0.013	***	-0.015	***		
gender	0.351	***	0.366	***	0.359	***		
edu_1	0.178	***	0.188	***	0.182	***	0.116	***
ocp_1	-0.293	***	-0.253	***			-0.304	***
ocp_3	-0.129	***	-0.131	***	0.001	0.976	-0.193	***
ocp_4	-0.281	***	-0.288	***			-0.388	***
ocp_5	-0.123	***	-0.112	***	-0.013	0.635	-0.013	0.625
car_1	0.120	***	0.105	***	0.104	***		
licen	0.185	***			0.185	***		
belt	-0.494	***			-0.494	***		
risk	-0.211	***			-0.209	***		
Constant	0.390	0.000	-0.271	0.000	0.327	0.000	-0.377	0.000
Summary of Statistics:								
Observations	45,724		45,724		45,724		45,724	
Log likelihood	-29519.633		-29964.207		-29570.84		-30181.432	

- Not relevant; *** Significant at 1% level; ** Significant at 5% level; * Significant at 10% level.

Table 9: Model estimation result of personal car drivers who ran the red lights and their socio-economic characteristics (Scenario 2)

Independent Variables	Model 1		Model 2		Model 3		Model 4	
	Coef.	P>|Z|	Coef.	P>|Z|	Coef.	P>|Z|	Coef.	P>|Z|
age	-0.016	***	-0.016	***	-0.018	***		
gender	0.244	***	0.244	***	0.256	***		
edu_1	0.607	***	0.607	***	0.632	***	0.503	***
ocp_1	-0.444	***	-0.444	***	-0.406	***	-0.503	***
ocp_3	-0.217	***	-0.217	***	-0.223	***	-0.294	***
ocp_4	-0.277	***	-0.277	***	-0.287	***	-0.385	***
ocp_5	-0.136	***	-0.135	***	-0.088	**	0.060	0.125
car_1	0.188	***	0.188	***	0.168	***		
licen	-0.001	0.985						
belt	-0.393	***	-0.393	***				
risk	-0.286	***	-0.286	***				
Constant	-0.789	0.000	-0.790	0.000	-1.613	0.000	-1.905	0.000
Summary of Statistics:								
Observations	45,724		45,724		45,724		45,724	
Log likelihood	-16432.7		-16432.7		-16655.084		-16758.328	

- Not relevant; *** Significant at 1% level; ** Significant at 5% level; * Significant at 10% level.

Gender of driver was found as a positive effect variable. It means male drivers have more red light running frequency than females. Education level also affecting to red light running behavior; drivers with low education level (primary school or lower) are more likely to run the red light than the drivers with bachelor degree or higher. Drivers who drive the passenger car tend to run the red light more than drivers who drive the van.

Negative effects of independent variables were found in the model. Young drivers tend to run the red light than old drivers. For an occupation, agriculturists, proprietor or traders, and government/state enterprise officers are found to be more likely to stop for the red light compared with the employees. The reason should be because most of employee drivers have fixed-time working schedule so that they want to save time in a rush hour. Drivers who often use the safety belt tend to stop for the red lights than the drivers who never used. Red light runners are less likely to wear safety belts (Retting and Williams, 1996), same as our finding. The attitude towards the risk of being caught when they violate the traffic signal also has a negative effect to the model. If driver think that there is less risk, they will have more possibility to run the red lights.

4.4 Explanation of Statistical Test for Factors Influencing Rates of Red Light Running

As shown in Table 10, Multiple Linear Regression Model was used to analyze the factors influencing the rates of red light running. The results of analysis from four model show that nine variables are significant in negative and positive effects.

Table 10: Model estimation result of factors influencing rates of red light running

Independent Variables	Model 1		Model 2		Model 3		Model 4	
	Coef.	P>|Z|	Coef.	P>|Z|	Coef.	P>|Z|	Coef.	P>|Z|
wd	0.396				0.383			
peak	0.589				0.450			
night	4.877	***	4.857	***	4.974	***		
mi	-0.254				-0.289		-0.621	
th	0.367				0.367		0.367	
vol	-0.003	***	-0.002	***	-0.002	***	-0.006	***
nol	-0.191						0.064	
lw	0.502	**	0.558	***			0.491	**
mw	-0.004						0.028	
isd	0.040	**	0.034	**			0.034	*
sinst	-1.211	**	-1.222	***			-1.277	**
sdisp	0.210						0.211	
cl	0.006						0.005	
yt	-0.609	*	-0.716	**			-0.652	*
add	-0.004	**	-0.003	*			-0.005	**
pave	-0.521						-0.394	
lux	0.092	***	0.079	***			0.115	***
rn	-0.024	*	-0.025	*			-0.022	*
Constant	2.814	0.152	1.984	0.144	2.566	0.000	5.660	0.007
Summary of Statistics:								
Observations	792		792		792		792	
R-squared	0.2621		0.2539		0.2090		0.1443	
Adjusted R-	0.2440		0.2463		0.2030		0.1266	

squared

- Not relevant; *** Significant at 1% level; ** Significant at 5% level; * Significant at 10% level.

Nighttime, illumination, traffic volume are the most significant. Nighttime red light runners were more likely than daytime runners to have high blood alcohol concentrations. (Harb *et al.*, 2007). In compared with daytime, nighttime tend to have more red light running because traffic volume is quite low and drivers do not want to wait for long time so that they might decide to run the red light. The significance of traffic volume support that less traffic volume will lead to high rates of running the red light. The intersections where there is high level of illumination at nighttime tend to have more rates of red light running. It is because of driver can see the objects including the other vehicles clearly at bright intersection, so they can confident more.

Lane width was significant to the model; the wider width of lane, the more rates of red light running. If the intersection sight distance is so clear, the rates of red light will tend to increase because driver can see the other approaching vehicles clearly, so they can ensure that no vehicle comes before they reach the intersection and they might decide to violate the traffic light. The intersection which there is an advanced warning sign to warn the driver before they reach the intersection is more likely to have lower rates of red light running. However, if the advance warning sign is located at too close to the intersection, the rates tend to increase.

For traffic signal conditions, types of signal installation have a negative effect to the rates of red light running; if the signal has installed as an overhang pole. At intersection with short yellow interval, the rates of red light running will increase. Normally, yellow time require to give an opportunity for drivers to make a decision (i.e. stop or go), but if the yellow time is too short, drivers might not be able to stop in time and resulting in running the red light. Similar findings from past research show that the frequency of red light running increases when the yellow interval is less than 3.5 seconds (Brewer *et al*., 2002). In contrast, if the yellow timing changes (increased by about 1 second), red light violation will reduce by 36%. (Retting *et al.*, 2008).

5. CONCLUSION

This study identified factors that influencing to red light running behaviors. The contributing factor for driver characteristics affecting to red light running behavior is estimated in this study. Most of red light runners are males. Old aged drivers tend to stop than run a red light compared with the younger drivers. Drivers who wear the helmet tend to stop for a red light. Drivers who travel alone are more likely to run the red light. Most of drivers who ran the red light use a manual gear motorcycle.

The socio-economic characteristics of red light runners were obtained from self-reported survey. The study revealed that, for motorcycle drivers, most of red light runners are males and lower age of driver, higher possibility to run the red lights. Compared to the drivers with high education level (bachelor degree or higher), low education level drivers (primary school or lower) more likely to run the red light. Driver who is a proprietor or trader and a student tend to run the red light in compared with driver who is an employee. Most of red light runners has driving license. Driver who usually wear the helmet are more likely to stop for the red lights than those who rarely wear the helmet. Drivers' attitude towards risk of being caught when they violate the traffic signal has an inverse effect to the possibility of running the red light; the lower risk, the higher probability to run the red light. For passenger vehicle, most of red light runners are males and young aged drivers. Driver with low education level has high possibility to run the red light. Most of red light running is caused by passenger car drivers in compared with van. Agriculturists, proprietor or traders, and government/state enterprise officers are found to be more likely to stop for the red light compared with the employees. Drivers who often use the safety belt tend to stop for the red lights than the drivers who never used. The driver's attitude towards the risk of being caught when they violate the traffic signal is low, the probability to run red light is high.

Likewise, models were used to determine the factors influencing rates of red light running, the estimated results shows that : for rates of red light running, traffic volume is less, rates of red light running is high. Most of red light running occurred during nighttime. Intersections with high illumination at nighttime have high rates of red light running. Wider lane width, higher rates of red light running. Rates of red light running increase when the intersection sight distance is so clear. The distance of advanced warning sign decrease, the rates of red light running increase. For traffic signal conditions, at intersection with short yellow interval, the rates of red light running will increase.

REFERENCES

Brewer, M. A., Bonneson, J., Zimmerman, K. (2002). Engineering Countermeasures to Red-

Light-Running. *Proceeding of the ITE 2002 Spring Conference and Exhibit (CD-ROM).*

Washington, DC: Institute of Transportation Engineers.

Chang, M.-S., Messer, C. J., and Santiago, A. J. (1985). Timing Traffic Signal Change Intervals Based on Driver Behavior. Transportation Research Record 1027, 20-30. Transportation Research Board, Washington, DC.

Eccles, K. A., and McGee H. W. (July 2001). *A History of the Yellow and All-Red Intervals for*

Traffic Signals. Washington, DC: Institute of Transportation Engineers.

Elmitiny, N., Yan, X., Radwan, E., Russo, C., and Nashar, D. (2010). Classification Analysis of Driver's Stop/Go Decision and Red-Light Running Violation. *Accident Analysis and Prevention, 42, 101-111.*

Federal Highway Administration (FHWA). (2003). *Making Intersections Safer: A Toolbox of Engineering Countermeasures to Reduce Red-Light Running*. Washington DC: U.S. Department of Transportation.

Harb, R., Radwan, E., and Yan, X. (2007). Larger Size Vehicles (LSVs) Contribution to Red Light Running, Based on a Driving Simulator Experiment. *Transportation Research Part F, 10,* 229-241.

Insurance Institute for Highway Safety (2007). Red Light Cameras in Philadelphia all but Eliminate Violations. *Status Report, 42(1), Jan. 27*.

Kamyab, A., McDonald, T., and Stribiak, J. J. (2002). The Scope and Impact of Red Light Running in Iowa. Preprint CD-ROM of the 81st Annual Meeting of the Transportation Research Board, Washington, DC.

Kamyab, A., McDonald, T., Stribiak, J. J., and Storm, B. (December 2000). Red Light Running in Iowa: The Scope, Impact, and Possible Implications. Ames IA: Center for Transportation Research and Education, Iowa State University.

Kraus, E. and Quiroga, C. (2004). Red Light Running Trends in Texas. *Preprint CD-ROM of*

the 83rd Annual Meeting of the Transportation Research Board, Washington, DC.

Liu, B. S. (2007). Association of Intersection Approach Speed with Driver Characteristics, Vehicle Type and Traffic Conditions Comparing Urban and Suburban Areas. *Accident Analysis and Prevention, 39(2), 216-223.*

Lum, K. M. and Wong, Y. D. (2003). Impacts of Red Light Camera on Violation Characteristics. *Journal of Transportation Engineering, November/December,* 648-656.

McGee, H. W. (2002). Safety Impact of Red Light Camera Enforcement Program. *Proceeding*

of the ITE 2002 Spring Conference and Exhibit (CD-ROM). Washington, DC: Institute of Transportation Engineers.

National Highway Traffic Safety Administration (NHTSA). (2006). Analysis of Red Light Violation Data Collected from Intersections Equipped with Red Light Photo Enforcement Cameras. Washington DC: U.S. Department of Transportation.

Papaioannou, P. (2007). Driver Behaviour, Dilemma Zone and Safety Effects at Urban Signalised Intersections in Greece. Accident Analysis and Prevention, 39, 147-158.

Porter, B. E. and Berry, T. D. (2001). A Nationwide Survey of Self-Reported Red Light Running: Measuring Prevalence, Predictors, and Perceived Consequences. Accident Analysis and Prevention, 33, 735-741.

Porter, B. E. and Berry, T. D. (1999). A Nationwide Survey of Red Light Running:

Measuring Driver Behaviors for the "Stop Red Light Running" Program. *FHWA, U.S. Department of Transportation.*

Porter, B. E. and England, K. J. (2000). Predicting Red-Light Running Behavior: A Traffic

Safety Study in Three Urban Settings. *Journal of Safety Research, 31(1),* 1-8.

Porter, B. E., Johnson, K. L., and Bland, J.F. (2013). Turning Off the Cameras: Red Light Running Characteristics and Rates After Photo Enforcement Legislation Expired. Accident Analysis and Prevention, 50, 1104-1111.

Retting, R. A., Ferguson, S. A., Farmer, C. M. (2008). Reducing Red Light Running Through Longer Yellow Signal Timing and Red Light Camera Enforcement: Results of a Field Investigation. Accident Analysis and Prevention, 40(1), 327-333.

Retting, R. A. and Williams, A. F. (1996). Characteristics of Red Light Violators: Results of a

Field Investigation. *Journal of Safety Research, 27(1),* 9-15.

Retting, R. A., Williams, A. F., Farmer, C. M., and Feldman, A. F. (1999a). Evaluation of Red Light Camera Enforcement in Oxnard, California. Accident Analysis and Prevention, 31, 169-174.

Retting, R. A., Williams, A. F., Farmer, C. M., and Feldman, A. F. (1999b). Evaluation of Red

Light Camera Enforcement in Fairfax, Virginia. *ITE Journal, Vol. 69, No. 8,* 30-34.

Retting, R. A., Williams, A. F., and Greene, M. A. (1998). Red-Light Running and Sensible Countermeasures: Summary of Research Findings. Transportation Research Record 1640, 23-26. Transportation Research Board, Washington, DC.

Romano, E., Tippetts, S., and Voas, R. (2005). Fatal Red Light Crashes: The Role of Race and Ethnicity. Accident Analysis and Prevention, 37, 453-460.

Royal Thai Police (RP). (2011). Statistic of Traffic Accident by Road Crashes. Available from http://statistic.police.go.th/traff_main.htm.

Ruby, D. E. and Hobeika, A. G. (2003). Assessment of Red Light Running Cameras in Fairfax

County, Virginia. *Transportation Quarterly, Vol. 57, No. 3,* 33-48.

Schattler, K. L., Hill, C., and Datta, T. K. (2002). Clearance Interval Design and Red Light Violations. *Proceeding of the ITE 2002 Spring Conference and Exhibit (CD-ROM).* Washington, DC: Institute of Transportation Engineers.

Shinar, D. (1998). Aggressive Driving: the Contribution of the Drivers and the Situation. Transportation Research Part F: Traffic Psychology and Behavior, 1(2), 137-160

THE OPTIMUM TRAFFIC VOLUME SURVEY LOCATIONS FOR THE TRAVEL DEMAND ANALYSIS IN KOREA

Seong-min KANG[1], Choong-shik LEE[2], Cheol PARK[3]
and Hyun-myung KIM[4]
[1] Researcher/Transportation Planning Lab, Dept. of Transportation Eng.
College of Engineering, The MyongJi University, South Korea
goodksm0508@gmail.com
[2] Researcher, The MyongJi University, South Korea
[3] Researcher, The MyongJi University, South Korea
[4] Ph.D, Director, The MyongJi University, South Korea

ABSTRACT

A traffic counts data has been widely used as baseline data for the transportation planning analysis and the transportation engineering part. Recently, it also is used for transportation planning to analyze traffic demand and calibrate traffic network. However, the current traffic volume survey locations had been located in based on the class of roads, which was more suitable for maintenance and management of roads. Because of this, there are two problems to analyze the travel demand. First, the current traffic volume survey locations have spatial bias on certain areas. This makes hard to get traffic volume and its spatial distribution. Second, some survey locations have a huge number of intra-zonal traffic volumes. To verify the travel demand between region, traffic survey locations should be located in cordon line which is boundary between adjacent zones. Due to short of average trip length at zone which has heavy intra-zonal traffics, the locations are not appropriate to analyze traffic demand between zones.

For these reasons, this study proposed criteria which determine to traffic volume survey locations for travel demand analysis and identified the adequacy of the current traffic volume survey locations

***Keywords**: Traffic counts, Traffic volume survey location, Spatial bias, Intra-zonal traffic volume, Cordon line, Determination location theory, GIS spatial analysis*

1. INTRODUCTION

A traffic counts data have been widely used as baseline data for the transportation planning analysis and the transportation engineering part. In the field of transportation engineering, a traffic counts data can be used to analyze traffic flow or develop strategy for transportation management throughout all processes. In the field of transportation planning, a traffic counts data which check the total amount of demand play a key role that validates and establishes the forecasting model. Also, these data can be used to estimate and validate traffic volume of origin to destination. Especially, traffic volume of cordon line and screen line is one of the most important basic materials across transportation planning.

However, traffic volume survey is being done only part of location because of limited budget. So, the current traffic volume survey locations had been positioned based on the class of roads. The positions are not optimal location in terms of traffic planning. As a result, Korea Institute of Civil engineering and building Technology(KICT) was used to determine traffic volume survey location through class of road. They didn't include necessary considerations to check the traffic pattern, but just they are focused on collecting the total amount of traffic volume.

Intra-zonal traffic volume ratio of the current traffic volume survey locations; 6,885 separated the grade of roads can be calculated. The highest Intra-zonal traffic volume ratio means including location of lots of intra-zonal traffic volumes that can't be explained by traffic volume of origin to destination.

Therefore, traffic survey locations should be located in cordon lines, which does not include intra-zonal traffic volume and screen line is necessary for supporting traffic volume survey. This study proposed criteria which determine to traffic volume survey locations for travel demand analysis and identified the adequacy of the current traffic volume survey locations.

2. LITERATURE REVIEW

Lee. & Lee.(2003) claimed to need a study about Appropriate positions and the number, Because O-D estimation varies depending on location and the number of traffic volume survey location.

A study of Yang. & Zhou(1998) is representative for determining traffic volume survey location on abroad. This paper is a leading role of the related study. The study proposed 4 roles Related to link traffic volume survey location based on maximum relative error and suggested integer programming model and heuristic algorithm to determine link that meet these 4 rules. Presented 4 rules are as follows by Yang et al.

Rule 1 (O-D covering rule): the traffic counting points on a road network should be located so that a certain portion of trips between any O-D pair will be observed.

Rule 2 (maximal flow fraction rule): for a particular O-D pair, the traffic counting points on a road network should be located at the links so that the flow fraction between this O-D pair out of flows on these links is as large as possible.

Rule 3 (maximal flow-intercepting rule): under a certain number of links to be observed, The chosen links should intercept as many flows as possible.

Rule 4 (link independence rule): the traffic counting points should be located on the network so that the resultant traffic counts on all chosen links are not linearly dependent.

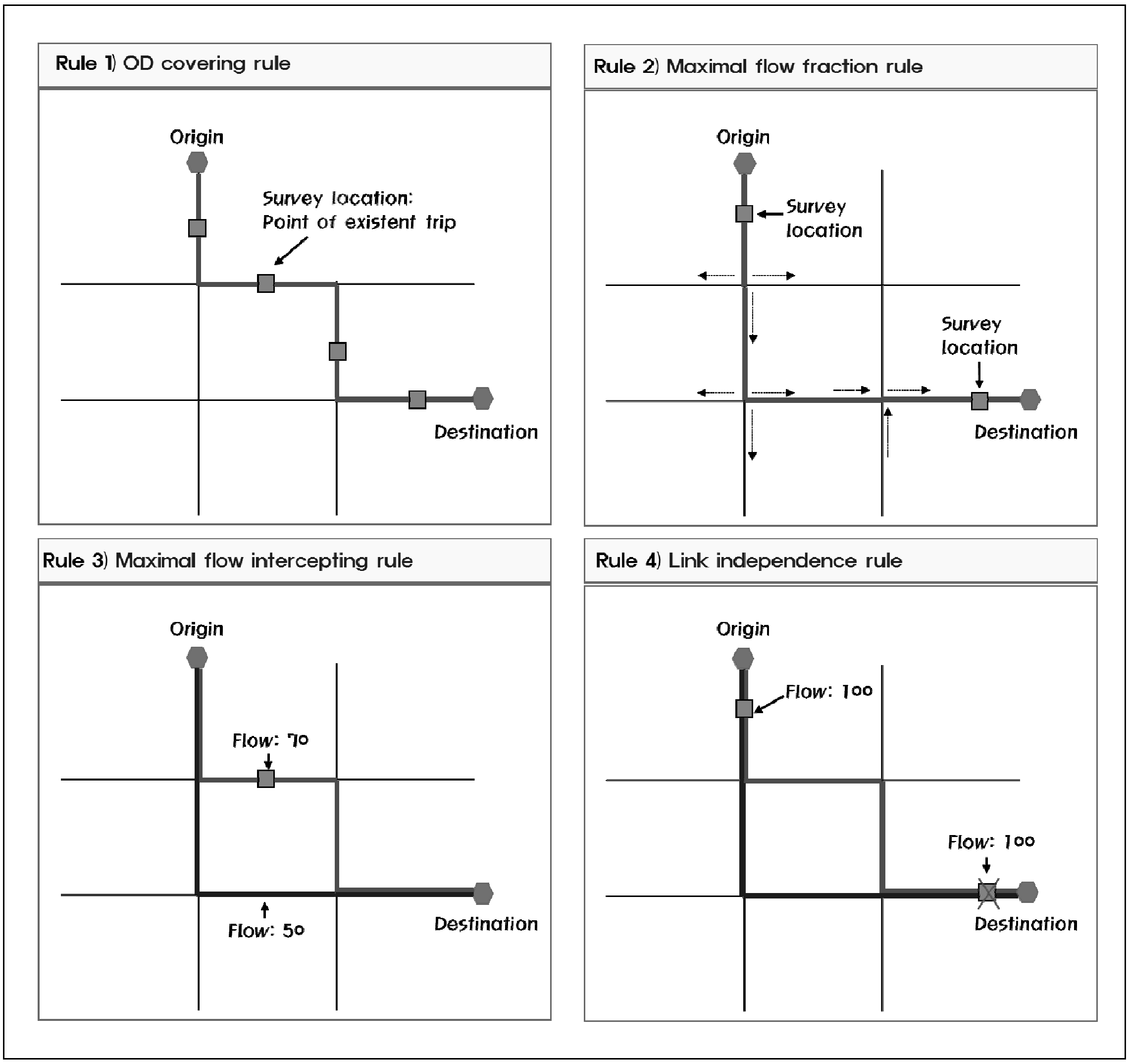
Rule 1) OD covering rule
Origin
Survey location:
Point of existent trip
Destination
Rule 2) Maximal flow fraction rule
Origin
Survey location
Survey location
Destination
Rule 3) Maximal flow intercepting rule
Origin
Flow: 70
Flow: 50
Destination
Rule 4) Link independence rule
Origin
Flow: 100
Flow: 100
Destination

Figure 1: 4 rules of determining traffic volume survey location (Yang et al, 1998)

Baek et al.(1998) applied the way that establish Surrounding each unit zone and observe traffic volume at link across cordon line in order to estimate optimal location.

As study result, link traffic volume of cordon line satisfied 4 rules of link observation location by Yang, and analyzed.

3. DETERMINATION TRAFFIC VOLUME SURVEY LOCATION THEORY

3.1 Establishing criteria of determination

A traffic volume survey location can be used to estimate about O-D estimated value. The criteria deduct reasonable and reliable value so that it can be admitted as true value. As shown we've just seen, various criteria should be considered for travel demand analysis for determination. In this study, the most important criteria are established as follow.

1) Traffic volume survey should be selected for link which pass cordon and screen line.

In case of cordon line, it doesn't need to consider passing traffic volume because it doesn't include Intra-zonal traffic volume. In case of (2+1) screen line in Korea, also it doesn't include Intra-zonal traffic volume because it is established according to boundary of zone. Therefore, if Traffic volume survey can consist of link which pass cordon and screen line, a necessary data perfectly can be established for validation of Departure and arrival traffic volume.

2) Locations that pass through a lot of traffic volume of origin to destination should be selected.

If traffic volume of cordon and screen line can't get caught, it is required to survey for traffic volume at position where a lot of flow volume is captured.

3) Locations where pass through a lot of pairs of origin and destination should be selected.

Locations where can verify the trip pattern should be selected for travel demand analysis. From study of Yang et al.(1998) and Baek(1998), locations where pass a lot of pairs of origin and destination should be selected.

4) At least one path about every pair of origin and destination should be caught by a traffic volume survey location.

This criterion is one of requirements of traffic volume survey location for verification of origin and destination's traffic volume. If traffic volume doesn't completely captured anywhere in a traffic volume survey locations, verification is not possible.

5) The last considerable is road grade.

Because regional traffic trip of origin and destination usually is likely to use higher road grade, if other conditions are similar, it should be include a lot of high-grade road in the survey. Therefore this study will be applied to the result to the secondary criteria of determination of location.

3.2 The adequacy of the current traffic volume survey locations

Analyzing should be identified the adequacy of the current traffic volume survey locations. First, cordon-screen line of traffic volume survey location under the zone system can be checked as shown in Fig.2.

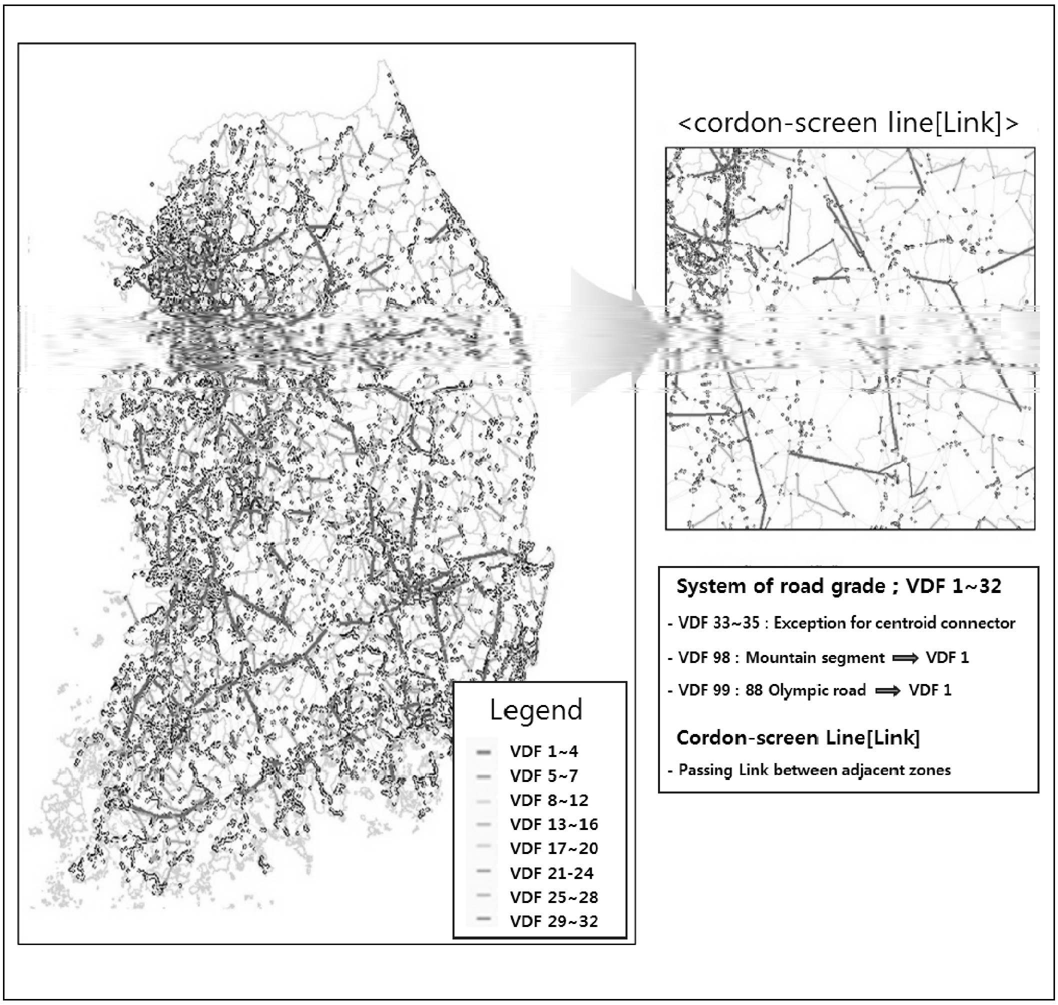
<cordon-screen line[Link]>
System of road grade ; VDF 1~32
- VDF 33~35 : Exception for centroid connector
- VDF 98 : Mountain segment ⟹ VDF 1
- VDF 99 : 88 Olympic road ⟹ VDF 1
Cordon-screen Line[Link]
- Passing Link between adjacent zones
Legend
VDF 1~4
VDF 5~7
VDF 8~12
VDF 13~16
VDF 17~20
VDF 21-24
VDF 25~28
VDF 29~32

Figure 2: Cordon-screen line by system of road grade

The number of location passing through the cordon and screen line is 5,193. The portion of urban is high among the entire survey locations. After verifying location of cordon-screen line, verifying adequacy of the current traffic survey locations. The next step in the present analysis of spatial distribution is whether the current traffic volume survey locations is how much is located in cordon-screen line. To examine the spatial distribution, the amount of locations and portion are considered as table 1.

As a result, urban road has a high percentage in case of cordon-screen line, but rural road has a high percentage in case of the current survey location. (cordon-screen line : urban 76.22%, rural 23.78% / the current survey location : urban 41.58%, rural 58.42%)

Table 1: Cordon-screen line and current survey location

VDF	**Road property**			**Cordon-screen line**		**Current survey location**	
	Road Type	**Lanes**	**Urban/ Rural**	**Count**	**Ratio**	**Count**	**Ratio**
1	Expressway	Below two-lane	Urban	201	3.87%	364	5.31%
2			Rural	99	1.91%	258	3.76%
3		Above three-lane	Urban	194	3.74%	337	4.92%
4			Rural	5	0.10%	22	0.32%
5	Urban Expressway	Below two-lane	Urban	35	0.67%	2	0.03%
7		Above three-lane		62	1.19%	0	0.00%
9	Multi-lane Highway	one-lane	Urban	278	5.35%	297	4.33%
10			Rural	309	5.95%	674	9.83%
11		Above two-lane	Urban	52	1.00%	73	1.06%
12			Rural	20	0.39%	50	0.73%
13		one-lane	Urban	394	7.59%	422	6.16%
14			Rural	357	6.87%	1,082	15.78%
15		Above two-lane	Urban	236	4.54%	297	4.33%
16			Rural	69	1.33%	317	4.62%
17		one-lane	Urban	128	2.46%	149	2.17%
18			Rural	102	1.96%	422	6.16%
19		Above two-lane	Urban	176	3.39%	164	2.39%
20			Rural	34	0.65%	199	2.90%
21		one-lane	Urban	149	2.87%	151	2.20%
22			Rural	86	1.66%	388	5.66%
23		Above two-lane	Urban	480	9.24%	327	4.77%
24			Rural	51	0.98%	342	4.99%
25		one-lane	Urban	123	2.37%	36	0.53%
26			Rural	28	0.54%	79	1.15%
27		Above two-lane	Urban	679	13.08%	168	2.45%
28			Rural	34	0.65%	136	1.98%
29		one-lane	Urban	177	3.41%	18	0.26%
30			Rural	23	0.44%	15	0.22%
31		Above two-lane	Urban	594	11.44%	45	0.66%
32			Rural	18	0.35%	21	0.31%
Total			Urban	**3,958**	**76.22%**	**2,850**	**41.58%**
			Rural	**1,235**	**23.78%**	**4,005**	**58.42%**
			Total	**5,193**	**100%**	**6,855**	**100%**

Second, this study compared to regional location of cordon-screen line and the current survey location to examine the spatial bias of the current survey location.

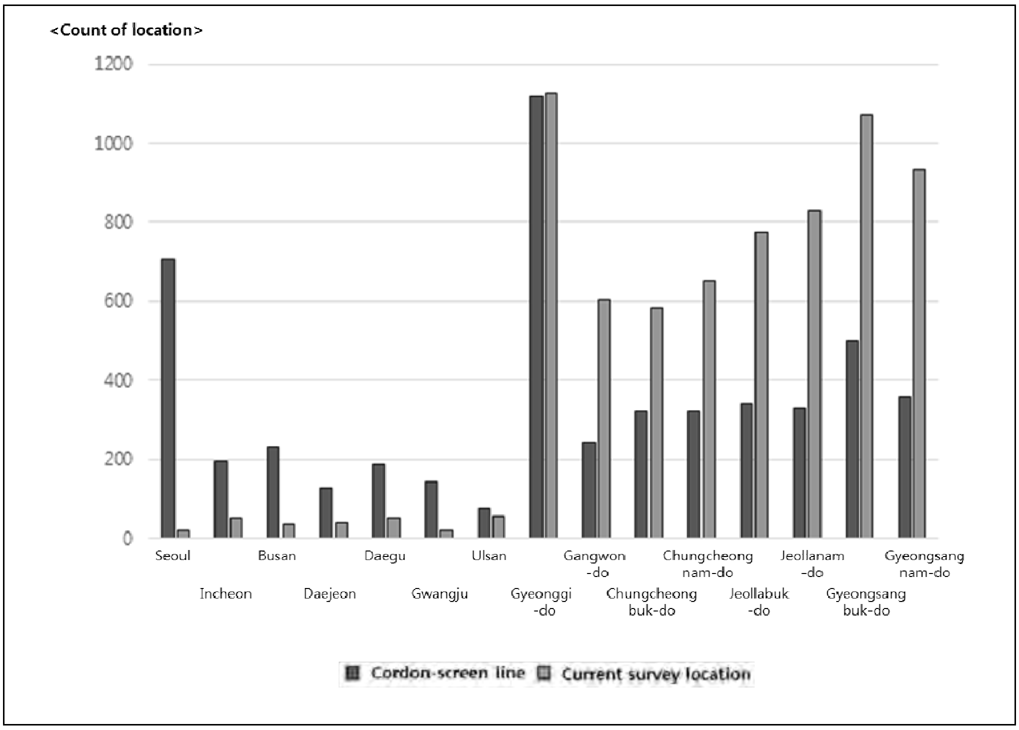

Figure 3: Estimated to the amount of matched locations

When comparing the traffic volume survey location and cordon-screen line, survey location id biased among regions. More important analysis is how much the current survey location consistent with cordon-screen line. Only 1,389 point is matched with cordon-screen line and current location. This result is about 20% for current 6,855 points. Reviewing the 1,389 locations by region, total number of matched locations is small. Also regional bias can be confirmed as Figure 3.

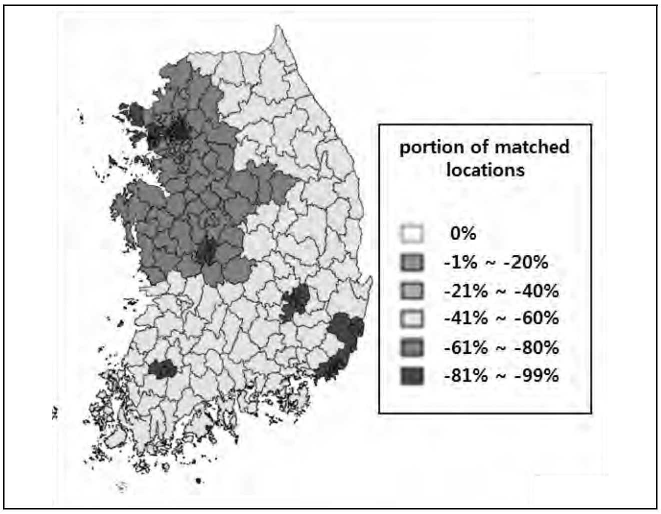

Figure 4: Estimated to portion of matched locations

4. CONCLUSIONS

This study established the most important criteria for travel demand analysis and identified the adequacy of the current traffic volume survey locations. To identify the adequacy of the current traffic volume survey locations, this study compared to cordon-screen line and the current survey location by region and road grade. The current survey locations partly were covering the cordon-screen lines. However, Locations are selected on unnecessary road or biased among regions. A lack of location that total amount is smaller than the cordon-screen line need to complement to traffic volume survey location.

This study will rearrange to locations using navigation data. This study may help to analyze travel demand by surveying on appropriate location.

REFERENCES

Yang. H, Jing Zhou,1998. *Optimal traffic counting locations for O/D estimation*, Transpn, Res, 25B, pp.315~363

Baek Seung-Kirl, Lim Kang-Won, Lee Seung-jae , 1998. *Zone Cordon line as Optimal Traffic Counting Locations for O-D Estimation*, Korea Planners Association, Vol.33 No.6[1998], pp.189~198

Lee Seung-Jae, Lee Hun-Ju, 2003. *Selection of the Optimal Location of Traffic Counting Points for the OD Travel Demand Estimation*, Journal of Korean Society of Transportation, Vol.21 No.1[2003], pp.53~63

SITE SELECTION OF POTENTIAL RAILWAY ROUTE FOR SUPPORTING DAWEI DEEP-SEA PORT CASE STUDY: TAMBON BAN KAO AMPHOE MUEANG OF KANCHANABURI PROVINCE

Rattanawadee DUTSADEESUNTORNSAKUN[1], Sathaporn MONPRAPUSSORN[2] and Sutatip CHAVANAVESSKUL[2]
[1] Department of Geography, Srinakharinwirot University, Thailand
rattanawadeeduts@gmail.com
[2], Department of Geography, Srinakharinwirot University, Thailand

ABSTRACT

The objective of this study is finding the potential areas for building railway route to support Dawei deep-sea port from the Ban Kao railway station at amphoe Mueang, Kanchanaburi province, Thailand. The criteria of site selection are road network, fault, soil, slope, land use, population density, forests and water resources. Method analysis with rating scale, weighting scale and dividing potential area. Result of study was divided 3 potential areas as the low potential area 8,955 square kilometers at Ban Huay Nam Khaw, Ban Pu Noi, Ban Tha Poh, Ban Tor Mai Dang, Ban Nong Ban Kao and Ban Takhian Ngam; the moderate potential area 45,913 square kilometers at Ban Tha Thung Na, Ban Huay Nam Khaw, Ban Pu Nam Ron, Ban Kao, Ban Thung Sala and the high potential area 62,149 square kilometers at Ban Lum Thahan, Ban Pra Tu Dan, Ban Sam Nong and Ban Lum Sai.

Keywords: *decision support, site selection, railway route*

2. INTRODUCTION

According the Asian Economic Communit is promoting, Thailand is located a heat of South East Asian. The Thailand logistics is important for economic in Asian region in term of supporting and employment creation. The deep-sea port project is promoted to support the logistic system in Southeast Asia region. Thailand is high potential to be gateway of the region,, be able the route of goods pass through North India to Middle East via Dawei deep-sea port of Myanmar. Ban Kao sub district (Tombon Ban Kao), located in Kanchanaburi Province, is boarder area where the shorten route to the Deep-Sea Dawei part by train. The traditional transportation spends 16-17 day by train, pass Malacca Strait that facing with pirate hijack. Hence the new railway is developed to get rid of those problems.

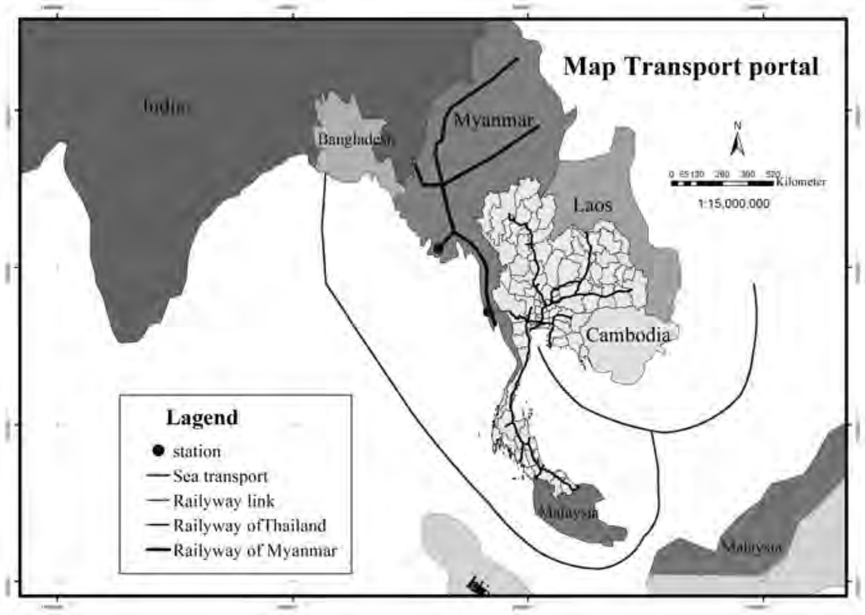
Map Transport portal
India
Myanmar
Bangladesh
Laos
Cambodia
Malaysia
Malaysia
N
Kilometer
1:15,000,000
Lagend
● station
Sea transport
Railyway link
Railyway of Thailand
Railyway of Myanmar

Figure 1: Traditional logistic system of Southeast Asian region.

The aim of research

The objective for this research is finding the potential area for railway construction, routing from Ban Kao sub district to the border of Thailand (called Ban Phu Nam Ron).

The importance of research

The propose new railway is highly potential route which provides an effectiveness of logistic, reduces the transport time period from 16-18 days to 7-8 days.

Scope of Research

This research focusing in the potential area for railway construction using spatial analysis and physical parameters. The construction area focus only between Ban Kao train station and border of Thailand, that has the shortest route to the Dewai deep-sea project.

However, Ban Phu Nam Ron barrier near the Dawei deep-sea port project possible. The distance from the border with Thailand to the Dawei deep-sea port only 160 kilometers.

Literature review

According The 11th National Economic and Social Development Plan (2012-2016) under the develop the country’s infrastructure and logistics systems chapter;

> *“… 1) Encourage development of multimodal transportation by advancing energy efficient forms of transportation.*

Infrastructure and multimodal transportation management systems should be developed that integrate roads, railways, and water and air transport for both domestic and international uses. This will improve efficiency and meet international standards for speed, safety, and punctuality, and it will support regional economic cooperation. Effective distribution systems for goods should be built to reduce the overall cost of logistics.

2) *Increase the efficiency of logistics management by developing professional human resources. Business networks for transport and logistics should be created throughout the supply chain. Laws and regulations should be amended to foster innovative research and development in the logistics field. To make trade more efficient and facilitate it, upgrade the National Single Window system, distribution centers, and cross-border trade. The efficiency of transport management systems should be improved. The strategic role played by major airports and seaports should be defined in order to reduce transportation costs and increase the nation's competitiveness in the long run*
3) *Improve railway transport by upgrading the present railway system and the links between road and railway networks to increase safety. Dual-track rail lines along major routes should be added. Locomotives and rolling stock should be provided and railway-signaling systems should be upgraded to increase efficiency for transportation of passengers and goods. A high speed railway should be developed to link major regional cities and ASEAN countries. The management structure of the State Railway of Thailand should be changed to improve efficiency and promote better services and operation*

This research used spatial technique called overlay analysis as the main analysis function. Overlay analysis is stated as

"*Geographic Information Systems (GIS) model selected aspects of reality. Overlay analysis is one of the spatial GIS operations. Overlay analysis integrates spatial data with attribute data. (Attributes are information about each map feature.) Overlay analysis does this by combining information from one GIS layer with another GIS layer to derive or infer an attribute for one of the layers. At its simplest, overlay analysis can be a visual operation, but analytical operations require one or more data layers to be joined physically. This overlay, or spatial join, can integrate data of different types, such as soils, vegetation, land ownership, jurisdictions, etc. with assessor's parcels. Results of overlay analysis rely on the spatial accuracy of the GIS layers. If the layers don't line up well, then the attributes inferred by the overlay may be incorrect. That is, the results are only as good as the GIS data used for the analysis.*"

Related research

Artid Intara (2549). The development of rail transport in the Northeast of Thailand, staring from Surin province to connect the lower part of area with another part of area. Result in an increasing of the business. Moreover the government is promoting a dual-track. and high-speed railway transport to link those area to neighboring countries.

Farkas (2009). His research focused in the route selection and assessment of the impact of building a metro station that the route selected for subway station construction in downtown area. His method used the assessment criteria technique with the GIS. Those criteria were used in his study was 1) geological structure (ground) the appropriateness of the ecosystem. 2) population density characteristics metro engineering. 3)construction costs. 4) mechanical characteristics and determine the cost of construction of the metro. The effect on the outcome of the vote.

Jeong, et al (2012) The research focused in to determine the location of the railway construction inthe countryside, using several spatial criteria through decision-making process technique called Multi-criteria evaluation (MCA) with Simple additive weighting (SAW). Three criteria are only physical environmental. . Result showed the satisfies classification which the economy screening can find suitable areas with the highest total score on four grounds

Malczewski (1999) Research focused in use of Multiple Criteria Decision Analysis to assess the geographical conditions and created maps using those criteria on the basis of the method. Multi-criterria Decision Analysis (MCDA) and evaluation criteria to selected thesuitable area. MCDA evaluate criteria weighting using Analytical Hierarchy Process (AHP). The identification and analysis based on hierarchy involving seven factors of land use gradient, industrial, forest, roads, hydrology and geology.

Safian (2012) Research focus in the evaluated the location of an office building in Malaysia by applying analytic hierarchy process with GIS. In a study using the five factors. The ability and ease of access to transport and the distance from the parking location, the commercial area of trade and the flow of vehicles. The results showed that the building suitable for most office buildings.

Carver (2009) Research focus in geographic information systems (GIS) are effective in the decision-making process. To evaluate various alternatives on the basis of several criteria for evaluation of multiple criteria is a common way of finding the impact of external factors. While GIS can bring environmental and economic development.

This study selected a suitable location. Based on reviews, that the most research technique showed in the use of GIS with multi-decision criteria. The decision by the Overly Analysis for the potential to lay the tracks. As a way to accept the decision that has many options and applied spatial well.

Methodology

The criteria applied in this research came from government sectors. All criteria are weighted by ranking technique, the rank came from previous research and experts. For instance, the research of Napong Surongkarat and Tonlavid Sathapanajaru found that road criteria have the difference priority depend on the buffer distances as500 meter = 4 high potential area, and 2000 meter = 1 lowest potential. For soil criteria, the research of Farkas divided soil into 2 groups as group1: 33, 33B, 44B, 47B, 48B, 48C, 48D, 56B = 3 high potential area and group2: 17, 20, 29, 31B, 31C, 31D, 44C, 47C, 48C D, 55B, 56C, 62 C = 1 lowest potential area, population density 93.19 - 146.4 persons / sq km = 4 high potential area and 13.40 - 40.00 persons / sq km = 1 lowest potential area. Malczewski use factor land use agricultural lands = 3 high potential area and Basin, ore mine and digging wells = 1 lowest potential area. The state railway of Thailand use 2 factor slop 0 – 5.3 % = 4 high potential area and 23.8 - 80% =1 lowest potential area, fault factor distance buffer from fault 9 kilometer = 4 high potential area and 1 kilometer= 1 lowest potential area. The GIS data of Tambon Ban Kao Amphoe Mueang of Kanchanaburi Province .This data 9 layers 1. Road 2. Soil 3. Fault Line 4. Slope 5. Land Use 6. Population Density 7. Water 8. Woodland 9. Administrative district;

Factor	stratification data	rank
Road	2000 meter	1
	1500 meter	2
	1000 meter	3
	500 meter	4
Fault	1 kilometer	1
	3 kilometer	2
	6 kilometer	3
	9 kilometer	4
Soil	Soil group; 17, 20, 29, 31B, 31C, 31D, 44C, 47C, 48C D, 55B, 56C, 62 C	1
	Soil group; 52B, 52C	2
	Soil group; 33, 33B, 44B, 47B, 48B, 48C, 48D, 56B	3
Slop	23.8 - 80%	1
	13.8 – 23.8 %	2
	5.3 – 13.8 %	3
	0 – 5.3 %	4

Factor	stratification data	rank
Land use	Basin, ore mine and digging wells	1
	Natural sources	2
	Building	3
	agricultural lands	4
Population Density	13.40 - 40.00 persons / sq km	1
	66.60 - 93.18 persons / sq km	2
	93.19 - 146.4 persons / sq km	3

Union analysis technique applied for analysis. Result from union analysis, the potential area is come out as the potential area for railway construction map. The following chart shows overall method for this research.

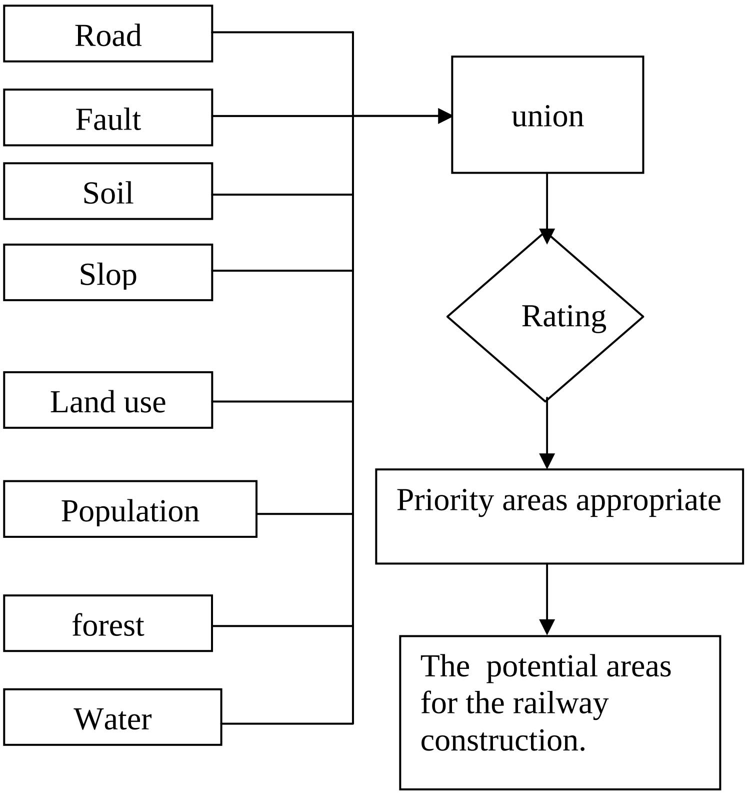
Road
Fault
Soil
Slop
Land use
Population
forest
Water
union
Rating
Priority areas appropriate
The potential areas for the railway construction.

Figure 2: Chart

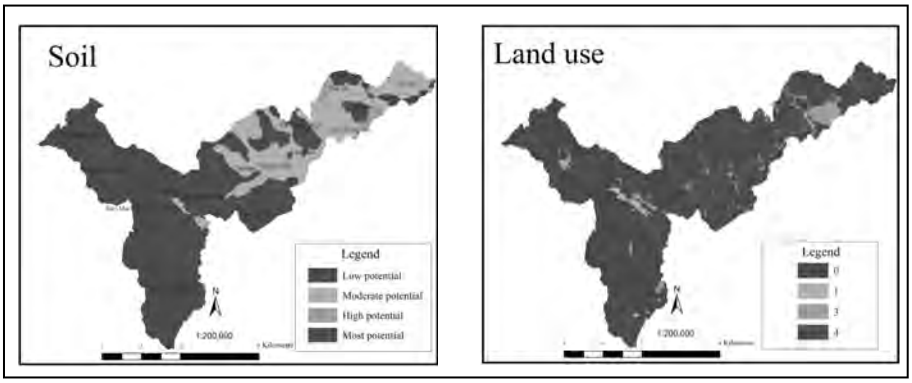
Soil
Legend
Low potential
Moderate potential
High potential
Most potential
N
1:200,000
Kilometers
Land use
Legend
0
1
3
4
N
1:200,000
Kilometers

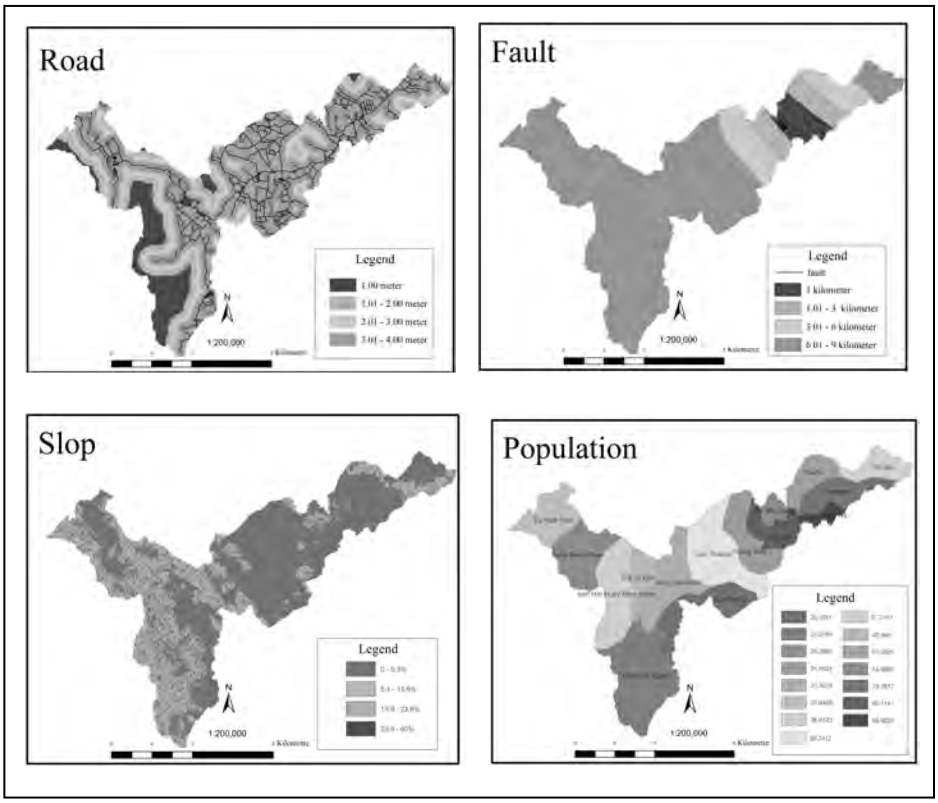
Road
Legend
1.00 meter
1.01 - 2.00 meter
2.01 - 3.00 meter
3.01 - 4.00 meter
1:200,000
Kilometer
Fault
Legend
fault
1 kilometer
1.01 - 3 kilometer
3.01 - 6 kilometer
6.01 - 9 kilometer
1:200,000
Slop
Legend
0 - 5.3%
5.4 - 13.9%
13.9 - 23.8%
23.9 - 40%
1:200,000
Population
Legend
1:200,000

Figure 3: Factor Map

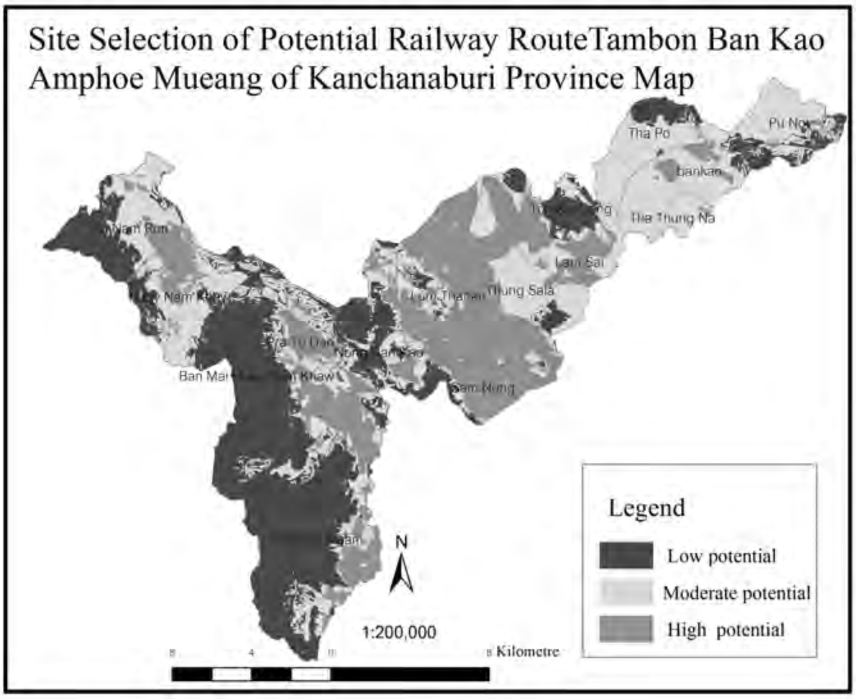
Site Selection of Potential Railway RouteTambon Ban Kao Amphoe Mueang of Kanchanaburi Province Map
Tha Po
Pu Noi
bankao
Tha Thung Na
Lam Sai
Thung Sala
Nam Run
Ban Mai
N
1:200,000
8 4 0 8 Kilometre
Legend
Low potential
Moderate potential
High potential

Figure 4: Site Selection of Potential Railway Route for Supporting Dawei Deep-Sea Port Case study: Tambon Ban Kao Amphoe Mueang of Kanchanaburi Province Map

Results

The results of the potential railway route construction, for Supporting Dawei Deep-Sea Port, are divided into 3 classes as follows the low potential area 8,955 square kilometers located at Ban Huay Nam Khaw, Ban Pu Noi, Ban Tha Poh, Ban Tor Mai Dang, Ban Nong Ban Kao and Ban Takhian Ngam. Moderate potential area 45,913 square kilometers located at Ban Tha Thung Na, Ban Huay Nam Khaw, Ban Pu Nam Ron, Ban Kao, Ban Thung Sala and the high potential area 62,149 square kilometers located at Ban Lum Thahan, Ban Pra Tu Dan, Ban Sam Nong and Ban Lum Sai.

Discussions

According this research is primitive research for potential area of railway construction, to more effective result the more criteria such as soil, fault, landuse population, road, slop and Dawei railway station location will be apply for further research.

REFERENCES

Andras, F., 2009. *Route/Site Selection of Urban Transportation Facilities: An Integrated GIS/MCDM Approach*. Budapes, Hungary

Anzhelika, A., Fahui, W., and Chester, W., 2015. *Urban land uses, socio-demographic attributes and commuting: A multilevel modeling approach.* Los Angeles, USA.

Edie, E., Mohd, S., and Abdul, H., 2012. *Combining AHP with GIS in the evaluation of locational characteristics quality for purpose-built offices in Malaysia. aspen 2nd campus.* Selangor, Malaysia.

Jacek, M., 1999. *GIS-based multi-criteria decision analysis: a survey of the literature.* John Wiley& Sons Inc., New York.

Stephen, J. C., 2007. *International Journal of Geographical Information Systems*

NUMERICAL EVALUATION OF ROAD DISCONNECTION RISK FOCUSING ON ROAD COLLAPSING AFTER A LARGE EARTHQUAKE IN CHIGASAKI CITY, KANAGAWA

Yuto TOKUMITSU[1], Shoko KUDO[2], Ryoko SERA[3], Takaaki KATO[4]
[1]Master Course Student, Dept. of Urban Eng.,
The University of Tokyo, Japan
tokumity@iis.u-tokyo.ac.jp
[2]Sewerage Works Department, Tokyo Metropolitan Government, Japan
[3]Geosearch Co., Ltd, Research Development Center, Japan
[4]Associate Professor, ICUS, IIS, The University of Tokyo, Japan

ABSTRACT

Securing a sufficient road network and its traffic functions after a large earthquake is essential for handling post-earthquake situations and preventing further damage. Although many causes can be involved in road disconnection, road blockage by collapsed buildings is currently the only cause backed with legal consideration. Road blockage may not be the only significant cause, and it can be suggested that road collapsing is another major cause for road disconnection other than blockage by collapsed buildings. This study aims to numerically evaluate the risk of road disconnection by focusing on road collapsing.

Numerical evaluations of the risk of road collapsing in Chigasaki City, Kanagawa Prefecture, Japan, were done by developing a model that expresses the behavior of underground cavities caused by aging city infrastructure and applying it to the city's road network. Comparing the risks of road collapsing to risks of blockage by collapsed buildings, current calculations conclude that considering road collapsing is as important as including collapsed buildings. Furthermore, it can be said that preventing roads from collapsing is necessary to maintain traffic functions for daily use. Therefore, this study suggests to create maintenance plans to secure traffic functions after a large earthquake and to relate disaster mitigation plans with city maintenance plans.

Keywords: *earthquake, road collapsing, underground cavity, road maintenance, model analysis*

1. INTRODUCTION

Traffic functions provided by road networks are necessary for everyday life, but are also essential when dealing with disasters and mitigating or preventing further damage. Passage of fire trucks, transportation of the injured is just examples of disaster handling actions that require a sufficiently functioning road network. The absence of such network leads to an increase in the amount of damage and loss caused by earthquakes.

The Japanese government is fully aware of the importance of securing a sufficient road network, and provides several laws aiding projects to secure traffic functions. Yet, these laws only focus on preventing road blockage by collapsed buildings, even though many causes of function loss are involved. In this study, road collapsing caused by underground cavities is suggested as another significant cause in the loss of traffic functions. Through the construction of a model to express the behavior of underground cavities and application to an actual road network in Chigasaki City, this paper aims to solidly suggest underground cavities are as significant as collapsed buildings in the loss of traffic functions.

2. MODEL CONSTRUCTION

In order to compare the risks of collapsed buildings to the risks of road collapsing, models were created to numerically express the possibilities of functional loss by the causes.

2.1 Model of Road Blockage by Collapsed Buildings

In the evaluation of risk of road blockage by collapsed buildings, the process shown in figure 1 below was used.

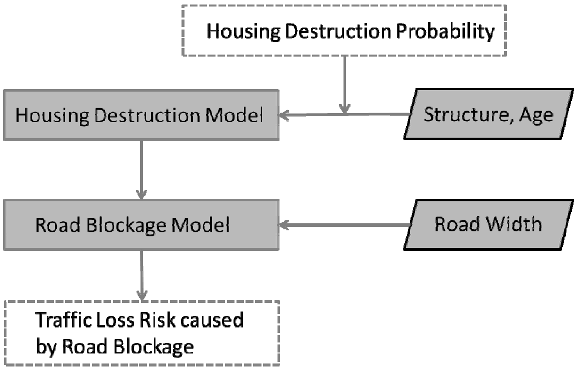
Housing Destruction Probability
Housing Destruction Model
Structure, Age
Road Blockage Model
Road Width
Traffic Loss Risk caused by Road Blockage

Figure 1: Evaluation process of Road Blockage Risk

The housing destruction probability is provided by the probability curve included in “Damage Estimations of Tokyo caused by Nankai Trough

Quake” by the Tokyo Disaster Prevention Council. In this paper, the probabilities of seismic intensity 6.5 is assumed and used from figure 2.

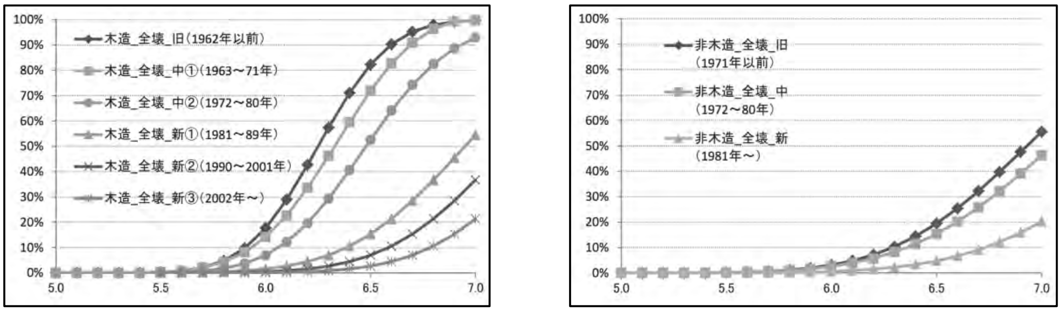

Figure 2: Destruction Probability Curve
(Left: Wooden, Right: Non-wooden)

Destruction in this case is defined as completely unusable for shelter, and in order to evaluate the risk of road blockage, probability of a structure completely collapsing into debris is needed. To do this, the following equation is used to calculate the probability of collapsing from the probability of destruction.

$$y = 1 - (1 - x)^{1/4.5} \quad (1)$$

y: probability of collapse x: probability of destruction

In this study, the spread of debris produced by a collapsed building follows the Omnidirectional Debris Flow Model, but assumes the debris to spread over within a distance half of the building’s height and not equal. Road blockage is defined as having less than 4 meters of road width that is not occupied by this debris, and the probability of a road link becoming blocked is as the following equation.

$$\text{Probability of a Road becoming Blocked} = 1 - \prod_{i=1}^{n}(1 - P_i) \quad (2)$$

n: Number of possible road blockage point
P_i: Possibility of road blockage at that point

2.2 Model of Road Collapsing

To evaluate the risk of traffic function loss due to road collapsing, a simulation model expressing the behavior of underground cavities was constructed and used to calculate the probability of a road collapsing.

In order to simplify, all underground cavities are assumed to be produced by cracks in underground sewage pipes. The model constructed in this study assumes that an underground cavity grows according to the process illustrated in figure 3.

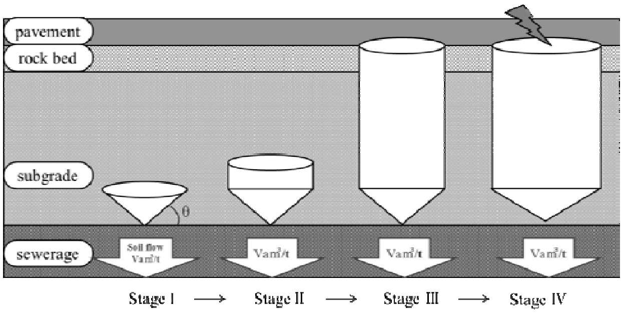
pavement
rock bed
subgrade
sewerage
θ
Soil flow
Vam³/t
Vam³/t
Vam³/t
Vam³/t
Stage I → Stage II → Stage III → Stage IV

Figure 3: Steps in the growth of an underground cavity(Side view)
Observed from above, growth of the diameters of the cavity is expressed as the diagram in figure 4.

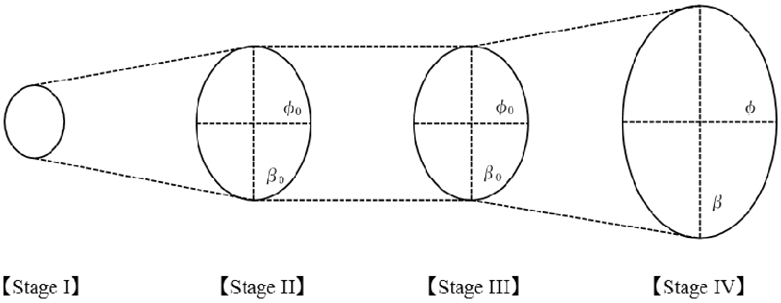
ϕ0
β0
ϕ0
β0
ϕ
β
【Stage I】
【Stage II】
【Stage III】
【Stage IV】

Figure 4: Steps in the growth of an underground cavity (Above view)

When a crack occurs in a sewerage pipe, sediment continuously flows. The amount of sediment flowing can be expressed as a constant V_a m^3/i, in which i is one step in the simulation. The cavity grows in a cone-shape until the small diameter reaches ϕ_0 meters and the height h_c meters, and from there it grows upward in a cylindrical shape maintaining its diameters. After reaching the pavement, the cavity grows horizontally until the pavement gives way and collapses.

The height of the cavity and the time for growth in each stage can be written as the following equations.

【Stage I】

$$T_a = \frac{h_c \cdot \frac{\phi_0}{2} \cdot \frac{\beta_0}{2} \cdot \pi}{3 \cdot V_a}\ [T] \tag{3}$$

T_a: time the cavity stays in stage I β_0: large diameter corresponding to ϕ_0

$$h(i) = \left(\frac{\frac{\psi}{2} \cdot h_c^3}{T_a}\right)^{\frac{1}{3}} = \left(\frac{3 \cdot V_a \cdot \frac{\psi}{2} \cdot h_c^2}{\pi \cdot \frac{\phi_0}{2} \cdot \frac{\beta_0}{2}}\right)^{\frac{1}{3}} \tag{4}$$

$h(i)$: height of cavity during stage I ϕ: short diameter during stage I

【Stage II】

$$h(i) = \frac{V_a \cdot (i - T_a)}{\pi \cdot \frac{\phi_0}{2} \cdot \frac{\beta_0}{2}} + h_c \tag{5}$$

$h(i)$: height of cavity during stage II

【Stage III】

$$T_b = T_a + \frac{(h_l - h_c) \cdot \pi \cdot \frac{\phi_0}{2} \cdot \frac{\beta_0}{2}}{V_a} \tag{6}$$

T_b: time the cavity takes to reach the pavement h_l: initial depth of the cavity

【Stage IV】

$$\phi(i) = \phi_0 \cdot \left(\frac{i}{T_b}\right)^{\frac{1}{2}} \tag{7}$$

$\phi(i)$: small diameter of cavity during horizontal growth

The behavior of the growth of underground cavities can be expressed as a function of $h(i)$, but to simplify the above equations (3) through (7), variables h_l, ϕ_0, β_0, h_c, V_a will be expressed as constants based on the following assumptions.

h_l: Since many sewerage pipes are placed 1.2 ~ 1.4 meters underground, the initial depth for each cavity was set by a random number within that range.

ϕ_0: Based on observational data provided by Geosearch Co. Ltd., the maximum small diameter of the cone-shape, or the minimum small diameter of the cylindrical shape, is assumed to follow the distribution given as the following table.

Small diameter ϕ_0	Percentage of occurrence (%)
0.3-0.5	0.901
0.5-0.7	2.703
0.7-0.9	16.216
0.9-1.1	16.216
1.1-1.3	14.414
1.3-1.5	19.820
1.5-1.7	9.910
1.7-1.9	4.505
1.9-2.1	8.108
2.1-2.3	5.405
2.3-2.5	1.802

Figure 5: Distribution of ϕ_0

β_0: Based on the observational data, ϕ_0 and β_0 were assumed to have a linear relationship. Therefore β_0 can be given as the following expression using ϕ_0.

$$\beta_0 = 1.164\phi_0 + 0.517 \tag{8}$$

h_c: The maximum height of the cone can be given by the following equation

$$h_c = \frac{\phi_0}{2} \cdot \tan\theta \tag{9}$$

In soil mechanics, the angle at which a pile of soil becomes stable is at 30 degrees. Therefore, angle θ is assumed at this angle.

V_a: From observational data by Geosearch, the average rate of soil flow of underground cavities was used. In this study it is assumed that this data is sufficient enough for use. Further studies to increase the accuracy of this number would lead to an increased ability of the model itself.

In addition to the growth of an underground cavity during daily circumstances, the behavior of a cavity after an earthquake can be expressed as the following figure.

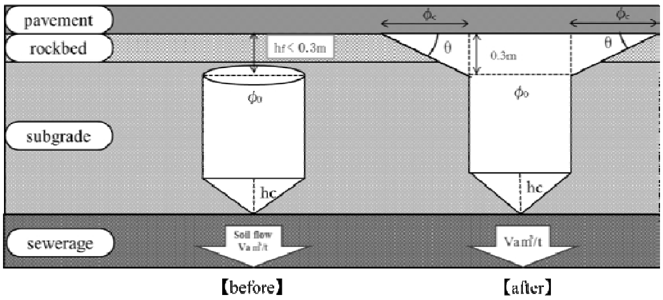

Figure 6: Behavior of underground cavity after an earthquake

It was experimentally determined that when shaken at a strong quake level, the soil close to the surface collapses to create the stable angle stated earlier. This study assumes that soil within 0.5 meters from the surface will collapse when shaken, and the small diameter of the cavity after the quake ϕ_e can be given by the following equation.

$$\phi_e = \phi_0 + 2\frac{0.3}{\tan\theta} \tag{10}$$

To calculate the probability of a road collapsing due to a large underground cavity, a probability function for the collapse of road pavement at a given small diameter was calculated using observational data from Geosearch. The function is as follows.

$$P \quad = 3.2873(\phi - 0.3)^2 \quad \text{(when } 0.3 \le \phi \le 0.69\text{)}$$

$$P \quad = -0.6038(\phi - 1.6)^2 + 1 \text{ (when } 0.69 \le \phi \le 1.6\text{)} \tag{11}$$

P: possibility of pavement collapsing ϕ: small diameter of cavity

3. SIMULATION

After constructing the model to express the behavior of underground cavities, simulation was done to determine the probabilities of a road losing functionality due to road collapsing. This was done by using observational data of Chigasaki city. To simplify calculations, simulation to determine probabilities was done using a representation model of the city road network. This model assumes a 100m road with intersection points at both ends, and possesses the average number of sewerage facilities such as manholes and supply conduits.

First, the number of observed underground cavities in Chigasaki city in a certain area that was target of analyzation by Geosearch was counted up according to the year the sewerage was planted, and paired with causes for occurrence using sewerage facility data. The categories for causes are as shown in figure 7.

Cause	**Explanation of cause**
Manhole	Used for inspection, connections with adjacent pipes can become loose
Supply-conduit	Pipes that drain sewage out of buildings, connections with adjacent pipes can become loose.
Multiple causes	Point where both manholes and supply-conduits exist
Pipe	Connections between pipes themselves can become loose.

Figure 7: Categories for the causes of underground cavities

Then, the numbers were averaged to fit the 100m simulation model as expected numbers of cavities. Through 100, 000 times of simulation using the relationship that probability equals the expected value divided by time to reach that value, probabilities for the occurrence of cavities were calculated as follows.

year of construction	**probability of cavity P_{1r} （road portion without conduits）**	**probability of cavity P_{1h} （road portion with only conduits）**	**probability of cavity P_{1j} （intersection points）**
1965 - 1969	0.0097	0.0056	0.0022
1970 - 1974	0.0022	0.0013	0.0005
1975 - 1979	0.0018	0.0015	0.0007
1980 - 1984	0.0037	0	0.0008
1985 - 1989	0.0032	0.0014	0.0003
after 1990	0	0	0

Figure 8: Probabilities of an underground cavity occurring

4. CASE STUDY IN CHIGASAKI CITY

Using the calculated probabilities, the risk of the road network of Chigasaki city losing function after a large earthquake was evaluated. This study assumes that the occurrence of a single point of road collapsing renders a road not functional. The evaluation also focuses on the main roads in the southern part of the city, where the sewerage infrastructure is relatively old.

The probability of a vehicle being able of passing through each road link was calculated using a function similar to that of (2). In this case, a road link is defined by a link connecting an intersection to the next adjacent intersection. The difference in probability of passage between road blockage and road collapsing is as the following diagram. The construction year of the sewerage pipes were based on the Chigasaki city sewerage plans. Note that the calculated value is the probability of passage considering only collapsed buildings minus the probability of passage considering only collapsed roads.

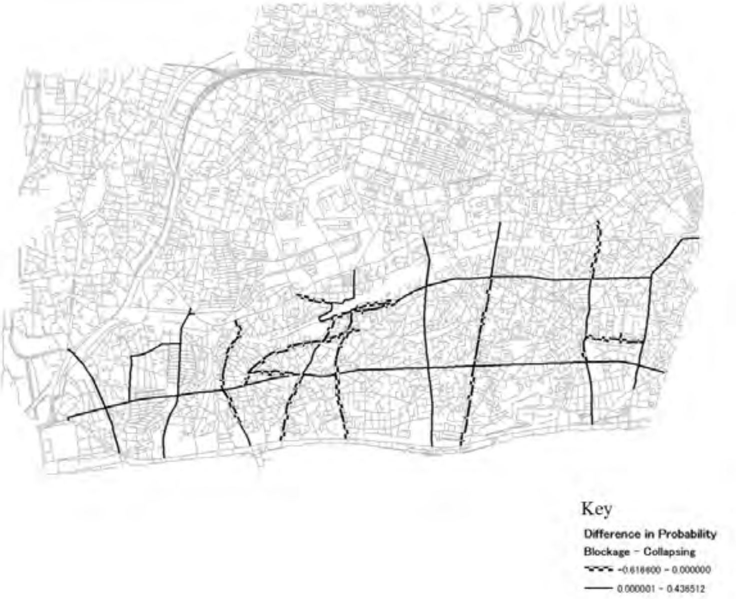

Figure 9: Difference in Probability of Passage

As it can be seen, most of the roads have a positive value, meaning that the probability of a road being functional is less when considering road collapsing. This is because many of the sewerage pipes in this area were constructed more than 30years ago, and the aging of these facilities has increased the risk of underground facilities.

To further evaluate the road network functions, several routes were set connecting a fire station to a point in the network seen as important. 3 fire stations and 3 intersections were each paired and the probability of arrival was calculated. The results are as figure 10.

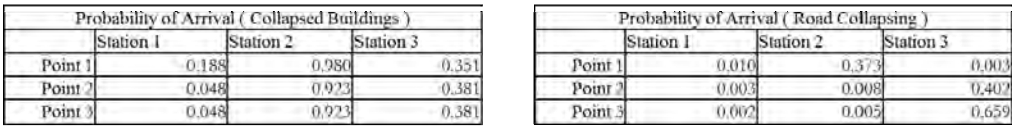

Probability of Arrival (Collapsed Buildings)			
	Station 1	Station 2	Station 3
Point 1	0.188	0.980	0.351
Point 2	0.048	0.923	0.381
Point 3	0.048	0.923	0.381

Probability of Arrival (Road Collapsing)			
	Station 1	Station 2	Station 3
Point 1	0.010	0.373	0.003
Point 2	0.003	0.008	0.402
Point 3	0.002	0.005	0.659

Figure 10: Probability of arrival for each route

Similar to the evaluation shown in figure 9, for most of the routes road collapsing has a more significant effect on the probability of arrival than that of collapsed buildings. This shows that road collapsing is as a significant cause of loss of traffic function as collapsed buildings.

5. CONCLUSION

Looking at the given results from the case study in Chigasaki city, it can be concluded that the risk of road blockage by collapsed roads are as significant as the risk of road blockage by collapsed buildings. The difference in handling the two risks are that while buildings may take several decades until they can be fully renewed, infrastructure can be renewed through regular maintenance plans.

Reinforcing buildings to withstand large quakes is a large project on its own, but in the case of sewerage it is only necessary to include the objectives for disaster mitigation in regular maintenance plans. By doing this, renewing the facilities and improving the functionality of roads can be done at the same time. However, because the renewal of pipes constructed more than 30 years ago is an urgent matter, disaster mitigation plans that include the improvement of sewerage should be made at first as emergency procedures to ensure time to create the regular maintenance plans. After the emergency procedures are done and the plans are made, it could be possible to maintain resilient infrastructure at a higher level.

Yet, the accuracy of the evaluation method used in this study has many areas in which it can be improved. Though this study assumed that a road lost its function when at least one road collapsing occurred, possibilities exist in which roads have enough width to maintain function even after several road collapsing. Other assumptions such as the rate at which soil flows should be improved, for it is an country wide average. Also, when considering emergency maintenance plans, roads with old structures built along them should have a priority on improving the buildings first before starting on the sewerage.

Altogether, this study presents a method to analyze the risk of traffic function loss considering factors other than collapsed buildings, and suggests the inclusion of mitigation plans in regular maintenance plans.

REFERENCES

Many references made to internal documents provided by Geosearch.

(To be published) Ryoko Sera and Yuki Horiuchi. Model Experimentation Report on the Effects of an Earthquake on the Expansion of Underground Cavities. To be presented at *Geotechnical Engineering Society 50th Geotechnical Engineering Research Presentation.*

Chigasaki city. 2012. Chigasaki City Public Plumbing Pipes and Facilities Long-life Realization Plans

IMAGE PROCESSING TECHNIQUES FOR VEHICLE AND PEDESTRIAN SAFETY EVALUATION

Jinwoo PARK[1] and Wonho SUH[2]
[1] Research Assistant, Hanyang University, Korea
[2] Assistant Professor, Hanyang University, Korea
wonhosuh@hanyang.ac.kr

ABSTRACT

With the advancement of recent image processing technologies numerous imaging applications have been developed to collect traffic information. In this study, image processing technology is applied to roadway safety to detect and measure the conflict between pedestrians and vehicular traffic. By using an image processing technique, pedestrian and vehicular movements are detected and the distance between these two are calculated to detect conflicts between them. In this study, Machine Learning techniques within MATLAB program are utilized to facilitate more accurate and efficient detection. It is assumed that the intersection is accident-prone if conflicts between pedestrian and vehicular traffic appear more frequently than other intersections. This approach is expected to identify accident-prone intersections without actually experiencing crashes; therefore, this would potentially reduce social costs associated with traffic accidents.

***Keywords**: image processing, vehicle detecting, traffic safety, pedestrian safety*

1. INTRODUCTION

Pedestrians are vulnerable road users. When they are involved in collisions with vehicles, there are considerably higher chances of being severely or fatally injured, while a large number of collisions between vehicles are property damage only. Surrogate safety measures has been developed as a complementary method to improve pedestrian safety and offer more in depth analysis than relying on historic accident data alone. There is a growing effort to use recent image processing technologies for a conflict analysis between vehicles and pedestrians. In this study, vehicle tracking and pedestrian tracking technologies currently developed and used are reviewed.

2. VEHICLE TRACKING

2.1. 3D Model-based Tracking

Model-based tracking utilizes a priori knowledge of typical objects. For a vehicle tracking, vehicles in an image captured from a video are tracked. These methods recognize vehicles. However, this method tends to fail when there is an occlusion for the target object. Also, this tracking method is limited in recognizing all the vehicle types on the roadway.

2.2 Region-based Tracking

Region -based tracking method is to identify connected regions of the image associated with each target vehicle. Regions are usually acquired from background subtraction. Also, this method utilizes Kalman filters to process available information from the image including motion, size, color, shape, texture, and centroid. It is known that this tracking method is computationally efficient and the detection accuracy is generally good in free-flowing traffic conditions. However, if traffic is congested – when background images do not change over a short period of time and vehicles partially occlude one another, this method tends to have problems, since separating individual vehicles are becoming challenging. Sometimes, such vehicles are identified as one vehicle, resulting in low detection rates.

2.3 Contour-based Tracking

Contour-based tracking method uses the boundary curves of the moving object. For example, this method tracks pedestrians by identifying the contour of a pedestrian’s head. This method is known to have more efficient description of objects than region-based methods. However, this method still shares the weakness of region-based tracking when traffic condition is congested.

2.4 Feature-based Tracking

Feature-based tracking does not track object as a whole in image processing. Instead, this method tracks unique features. There features can be points or lines of the object which are distinct from other objects. When the target object is partially occluded, some of the distinctive features of the moving object remain visible and detectable, resulting in successful tracking. The advantage of this method over other tracking methods is that the same algorithm can be applied for tracking in different lighting or traffic conditions. For example, this method utilizes window corners or bumper edges during the day when the entire object is visible. During the night, this method uses tail lights, since other features are not detectable in night time lighting conditions. Currently, this method is advanced and computational efficient allowing this method to be used in real time processing. An example of vehicle tracking is provided in Figure 1.

1. PEDESTRIAN TRACKING

To identify conflicts between vehicles and pedestrians, all movements of vehicular and pedestrian traffic need to be tracked from video frames. Especially, this is challenging since pedestrians sometimes move in group and change directions, while vehicular movements are somewhat predictable. To overcome the issues and increase the accuracy of tracking, there are three tracking methods which are currently popular; tracking by detection, tracking using flow, and tracking with probability.

Tracking by detection method detects objects using background modeling and subtraction with the current image or deformable templates. Tracking using flow is similar to feature based tracking. This method is popular in traffic monitoring and pedestrian counting. Tracking with probability uses a Bayesian tracking framework. This method also utilizes other filers and methods, such as particle filters, Markov chain, and Monte Carlo methods. An example of pedestrian tracking is provided in Figure 2. Also, Figure 3 presents an example of vehicle and pedestrian tracking in an intersection.

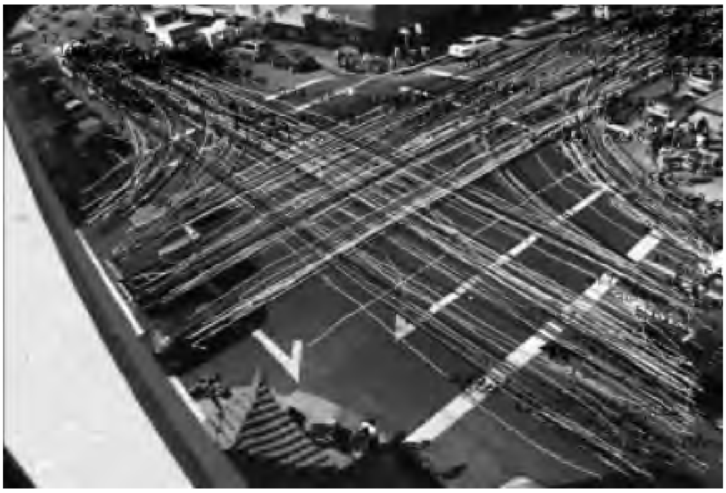

Figure 1: Vehicle tracking (Ismail, Sayed, and Saunier, 2010)

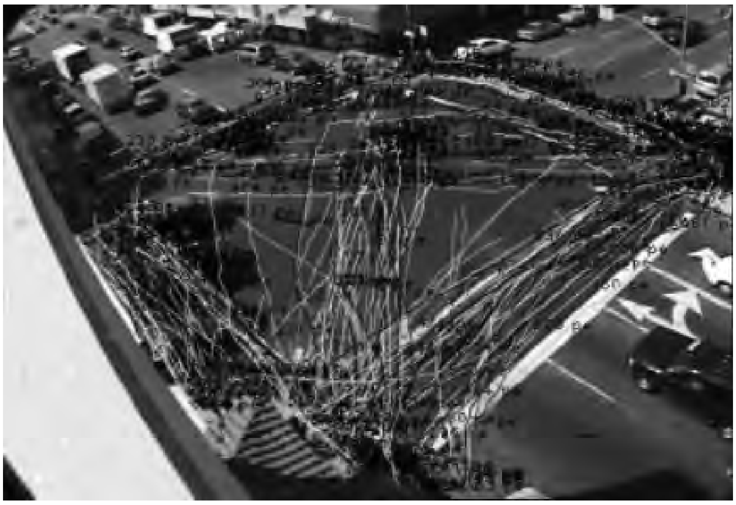

Figure 2: Pedestrian tracking (Ismail, Sayed, and Saunier, 2010)

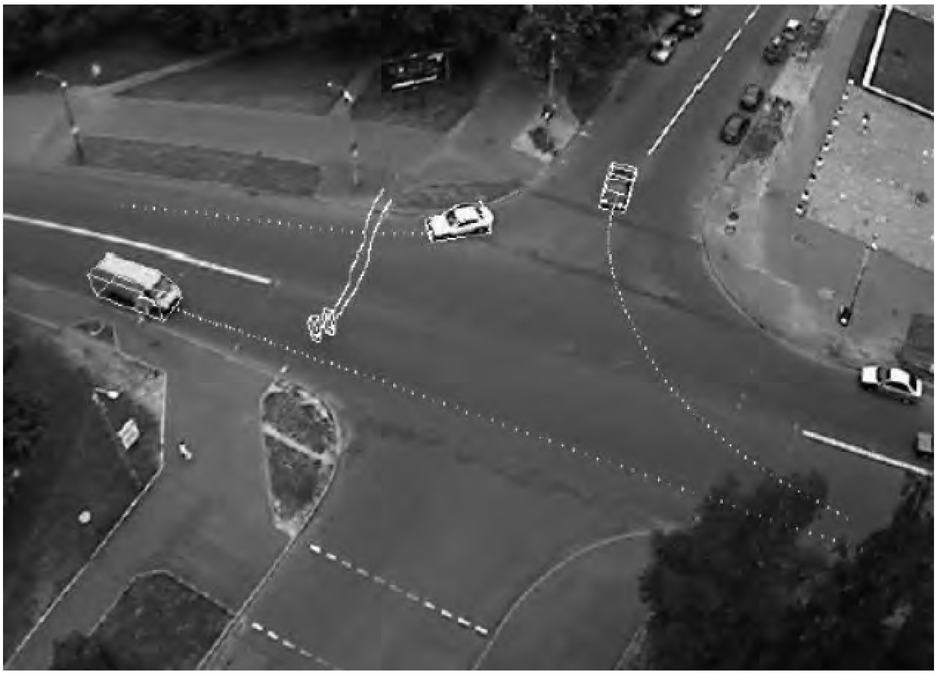

Figure 3: Vehicle and pedestrians tracking (Laureshyn, 2014)

3. CALCULATING CONFICTS

To calculate conflicts between vehicular and pedestrian traffic, potential accident-prone conditions need to be identified. These conditions are illustrated in Figures 4, 5, and 6. Based on the calculated time gap between the vehicle and pedestrian, conflict data can be obtained.

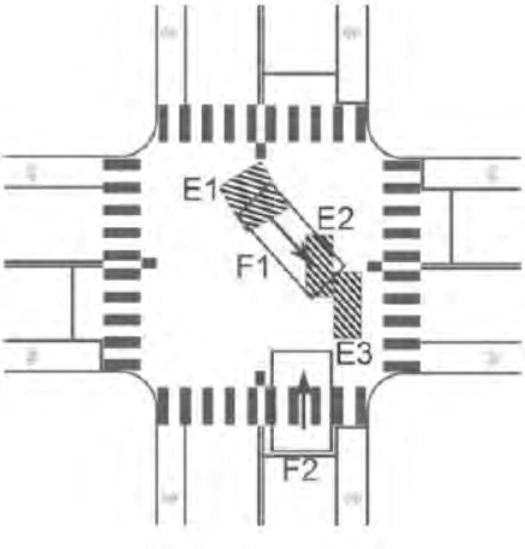

Figure 4: Left turning vehicle conflict example (Madsen, 2014)

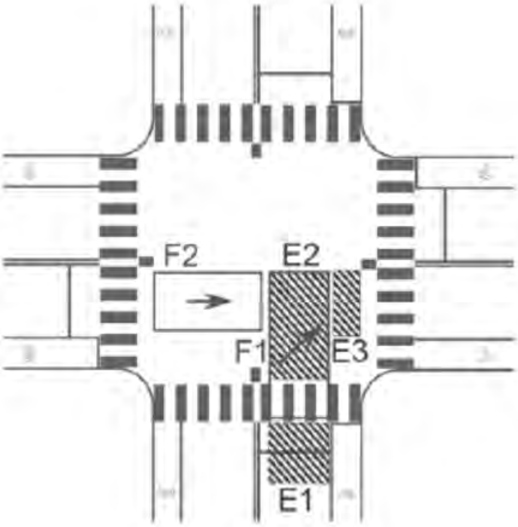
F2
E2
F1
E3
E1

Figure 5: Thru moving vehicle conflict example (Madsen, 2014)

2. PRELIMINARY RESUTLS AND FUTURE WORKS

The research team is in a process of developing vehicle and pedestrian tracking method. The team was successfully tracked vehicles in a video collected from an intersection in Seoul, Korea (Figure 6). The team is planning to continue to develop the tracking algorithm and calculate the conflicts between vehicular and pedestrian traffic. The team is utilizing MATLAB Machine Learning techniques to reduce the detection error and increase the efficiency of the program.

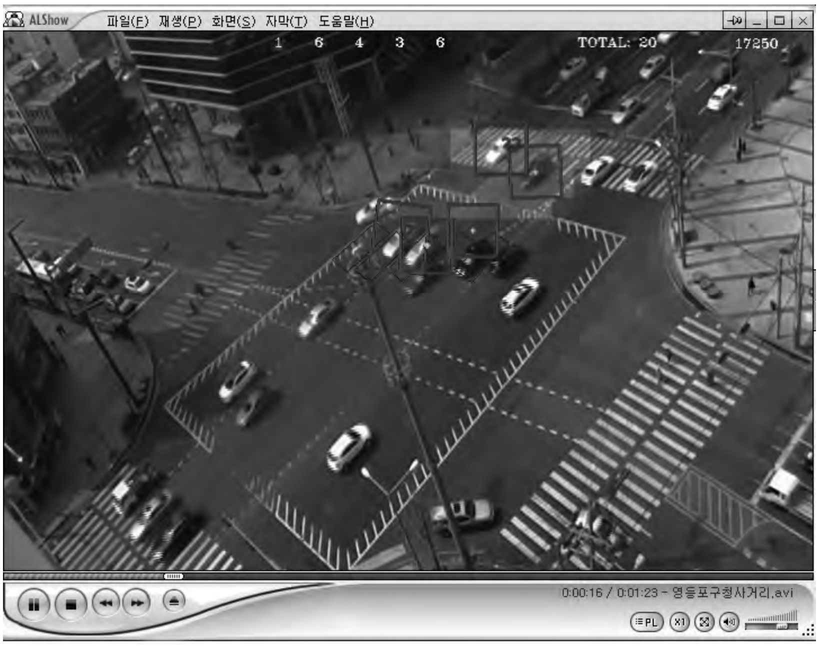
ALShow
파일(F)
재생(P)
화면(S)
자막(T)
도움말(H)
1 6 4 3 6
TOTAL: 20
17250
0:00:16 / 0:01:23 - 영등포구청사거리.avi
PL
X1

Figure 6: Vehicle tracking program snapshot

REFERENCES

Ismail, K., Sayed, T., and Saunier, N. 2010. Automated analysis of pedestrian-vehicle conflicts: Context for before-and-after studies. *Transportation Research Record: Journal of the Transportation Research Board*, 2198, 52–64.

Laureshyn, A., 2014. Superpixel based road user tracker, Workshop on the Comparison of Surrogate Measures of Safety Extracted from Video Data, Transportation Research Board 93rd Annual Meeting.

Madsen T., 2014. Automatic Detection of Conflicts At Signalized Intersections, Workshop on the Comparison of Surrogate Measures of Safety Extracted from Video Data, Transportation Research Board 93rd Annual Meeting

AGEING EFFECT INDUCED BY PARTICLE MOVEMENT

Koji TANAKA[1] , Ikuo TOWHATA[2] ,and Shigeru GOTO[3]
[1]Master Course Student, Department of Civil Engineering,
The University of Tokyo, Japan
k.tanaka@geot.t.u-tokyo.ac.jp
[2]Visiting Professor, Kanto Gakuin University, Japan
[3]Visiting Researcher, Waseda University, Japan

ABSTRACT

During the 2011 Great East Japan earthquake, there were many liquefaction damage sites around the Tokyo Bay. One of the typical damaged sites is Urayasu City, which is now suffering from land price decline and reduction of population. On the other hand, according to the design codes of each structure, they do not take "ageing effect" into consideration. Ageing effect is a phenomenon by which the liquefaction resistance of sandy ground increases with time. Thus, we cannot properly evaluate the liquefaction resistance in current methods. By properly evaluating the increment of liquefaction resistance by the ageing effect, the risk of future liquefaction will be more appropriately assessed and the above-mentioned social problems will be mitigated.

Several phenomena, such as cementation or secondary consolidation, are considered as the mechanism of ageing effect. In this paper, by hypothesizing that particle movement within sandy ground contributes to the increment of liquefaction resistance, particle movement of sand is observed by a microscope under consolidation and shaking states. At the same time, liquefaction resistance of consolidated samples was measured by undrained cyclic triaxial tests.

In conclusion, the relationship between the number of moving particles and the liquefaction resistance was obtained. In addition, different movement of sand particles was observed in consolidation and shaking states.

Keywords: *ageing effect, liquefaction*

3. **BACKGROUND**

Evaluating the liquefaction resistance of subsoil is important to make an earthquake hazard map. Currently, F_L method is often used in evaluation, by taking into consideration SPT N-value, fines content, and so on$^{1)}$. However, significant liquefaction damage was observed only in recently reclaimed ground in contrast to lack of liquefaction in more aged alluvial soil[2)]. Such liquefaction resistance improvement by ageing effect is widely observed not only in 2011 Great East Japan Earthquake, but also in previous earthquakes. Thus, the risk of liquefaction is high in relatively young reclaimed land and abandoned river bed.

Ageing effect is not taken into consideration in F_L method. This is probably the main cause of the result that all the area in Figure 1 was estimated to be liquefied before the earthquake in 2011. Although this realizes the safer design, it will also lead to the land price decline and population decrease in target areas. Therefore, to establish more accurate method for liquefaction resistance estimation, the mechanism of ageing effect is discussed in this paper.

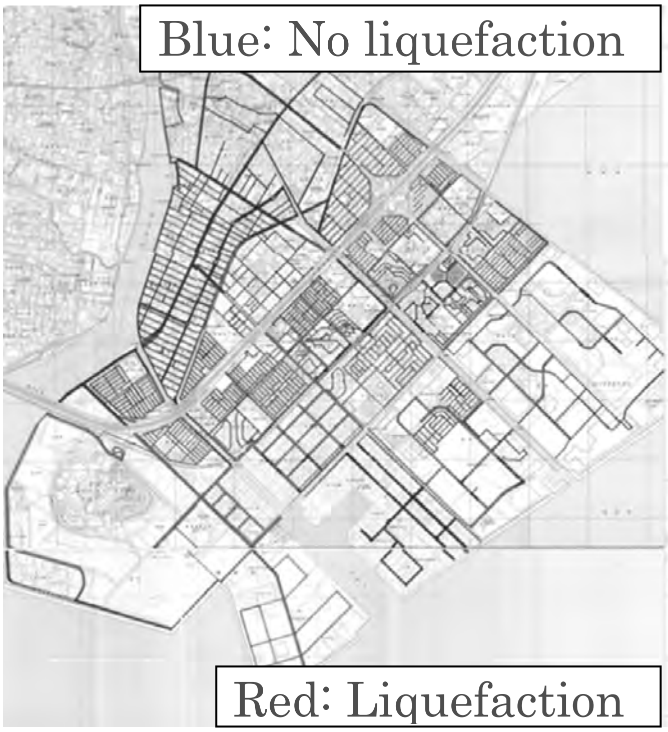

Figure 1: Liquefaction occurrence map in Urayasu City after 2011 earthquake

Several kinds of phenomena are considered to be the mechanisms of ageing effect[3)4)]. Mitchel and Solymar (1984) stated that cementation strengthens the connection between particles, which triggers the ageing effect. Goto and Towhata (2014) reported that secondary consolidation has something to do with the ageing effect. As seen above, there is something unclear remaining concerning the mechanisms of ageing effect.

Shintaku and Towhata (2014) pointed out the possibility that particle movement within sandy ground contributes to the increment of liquefaction resistance[5)], as shown in Figure 2. They conducted sand box observation test and undrained cyclic triaxial tests, and finally concluded that there is a relationship between the frequency of particle movements and the liquefaction resistance. However, they could not clarify the effect of shaking frequently happening in Japan on the particle movement and liquefaction resistance.

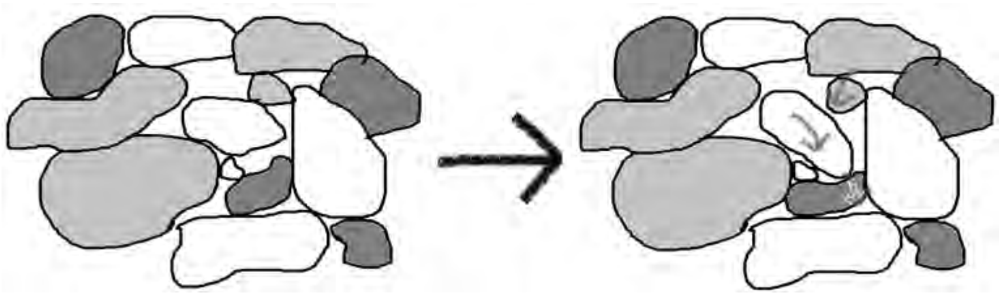

Figure 2: Image of particle movement

2. METHODOLOGY

2.1 Sand box observation

Two kinds of sand were prepared with the same mean diameter (D_{50}) and different uniformity coeffecients (U_c). Here are the table showing the physical properties and the figure showing the grain size distribution curves of the sands (Figure 3).

Table 1: Physical character of samples

Name	**e_{max}**	**e_{min}**	**$D_{50(mm)}$**	**U_c**	**FC(%)**
#6	1.023	0.638	356	1.5	0
S1	0.907	0.480	365	4.0	5.4

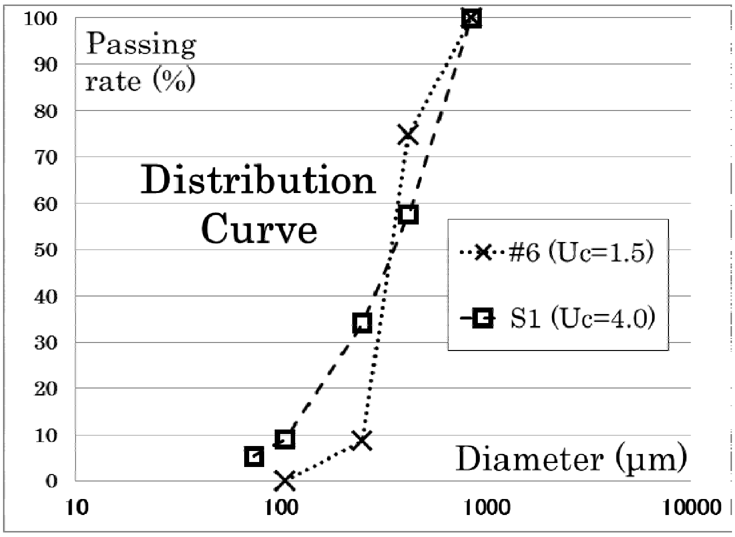

Figure 3: Grain size distribution curves of samples

These samples are set in the cuboid sand box with 6cm × 20cm bottom and 10cm height. They are fully saturated by pluviation method, and 25kPa pressure is applied. The cross section of the samples is shot by microscope at the same intervals through one side of the sand box made by acrylic plate. Pictures obtained each day are compared, and the number of moving particles are counted. In addition, this sand box is set on the shaking table, and 20 sinusoidal shaking waves were applied to it at 5 seconds intervals. The maximum acceleration of one wave is 75 Gal, the frequency is 5 Hz, and the duration is 3 seconds, which reproduces the relatively small but frequent earthquakes in Japan. In a similar way as mentioned above, the pictures before and after shaking are compared, and the number of moving particles was counted.

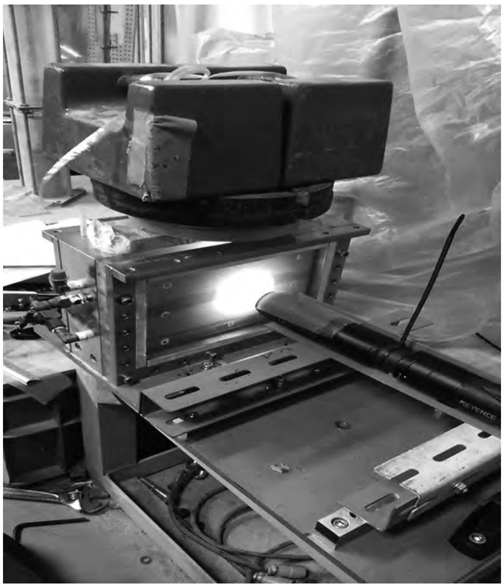

Figure 4: Sand box observation

2.2 Undrained cyclic triaxial test

S1 samples with 5cm diameter, 10 cm height, and about 60% relative density are prepared with different consolidation terms (1day, 4day, and 64 day). After the consolidation, undrained cyclic triaxial test is conducted. It is reasonable to assume that the same kind of particle movement as in the sand box observation occurs in the triaxial samples during the consolidation period.

3. RESULTS AND DISCUSSION

3.1 Sand box observation

Figures 5 and 6 show the results of sand box observation in static setting. The vertical axis stands for the accumulated number of moving particles per 1 square centimeter within the observation area. The horizontal axis indicates the elapsed time with logarithmic scale.

When the sand box is set statically, a larger number of particles moved in S1 case, with a well graded sample. Besides, a greater number of particles moved in low relative density case in each material. Firstly, smaller particles were more likely to move with well graded sample. Second, loosen sand has more space for particles to move. These two would be the reason of this result. Thus, particle movement is observed in local areas, not overall movement. This phenomenon is called “void filling” in the following pages.

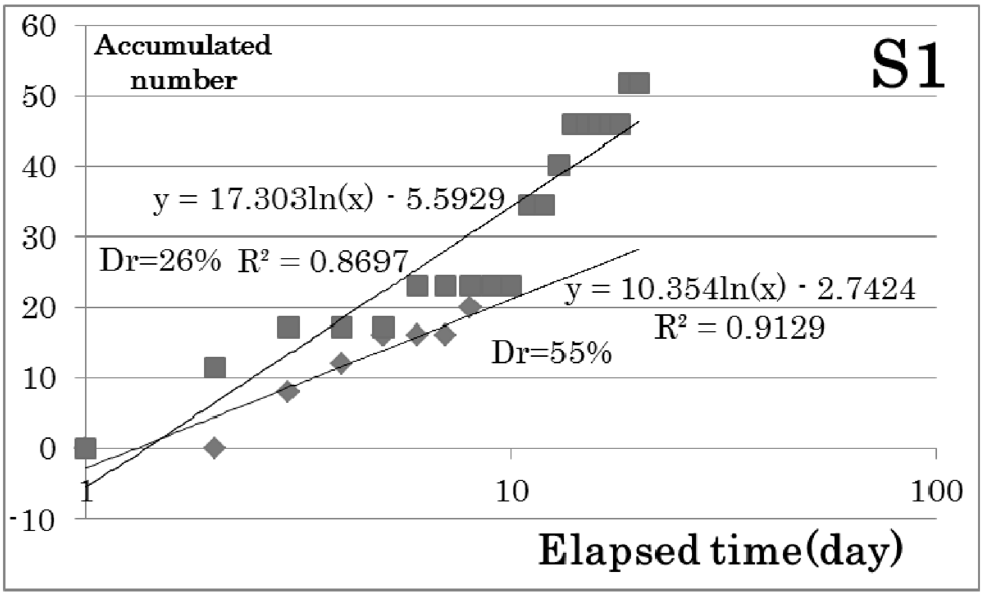

Figure 5: The relationship between elapsed time and accumulated number of moving particles (S1)

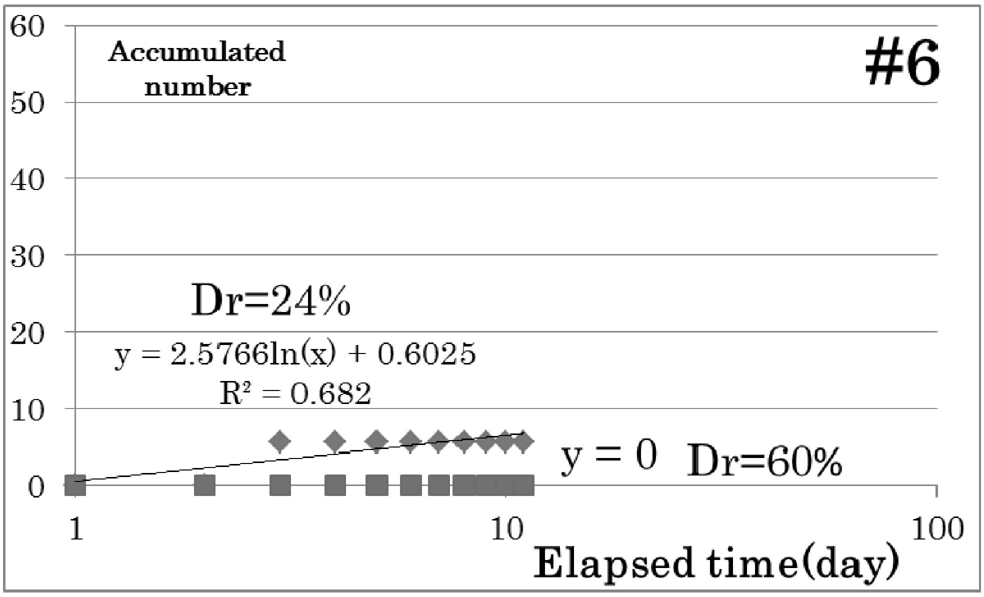

Figure 6: The relationship between elapsed time and accumulated number of moving particles (#6)

On the other hand, when the sinusoidal wave is applied to the sand box, overall structure of the sample changed in loose sand case. In place of counting the number, the pictures taken before and after shaking were analyzed by PTV (Particle Trace Velocimetry), and the arrow figures were obtained as shown in Figure 7.

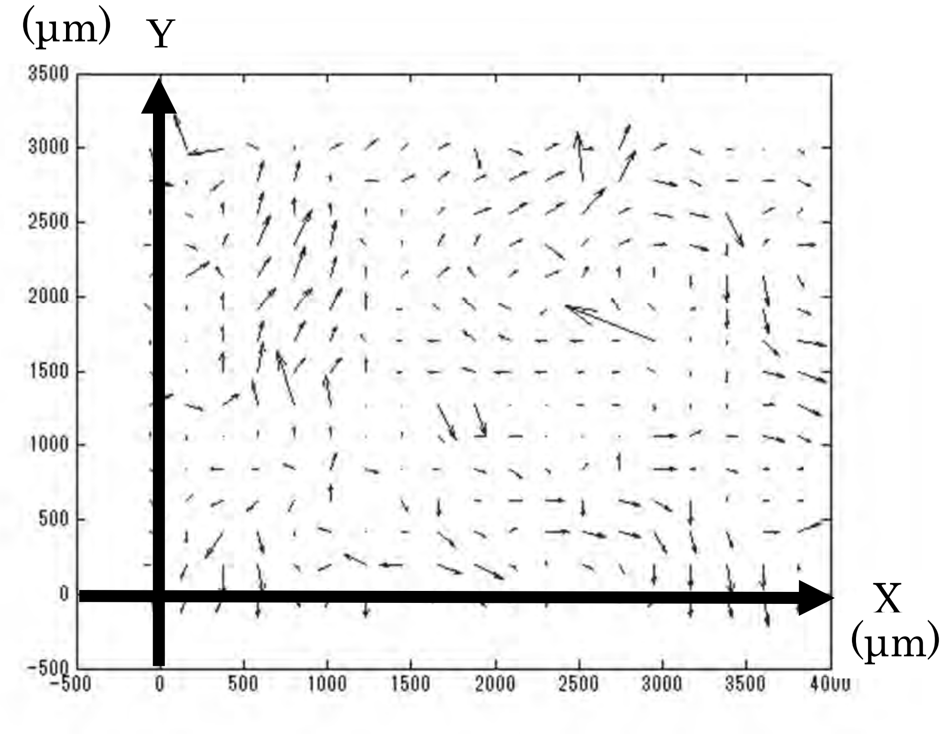

Figure 7 : Result of PTV analysis (#6, Dr=24%)

Since one particle movement was judged in relation to surrounding ones, it was difficult to say whether counting the number of moving particles was valid. This phenomenon is called “structural change”, and is distinguished from “void filling”. In denser sand, structural change was not observed.

The actual observed distance is increased 10 times for better outlook. Random movement of the particles is observed. The average element of each direction is +0.41(μm) for X direction and +0.69 (μm) for Y direction, and the average length of the arrows is 10.2 (μm).

Since there is no evidence of overall displacement or height change during observation, structural change is not considered to be triggered by the volume change caused by negative dilatancy. However, observation of whole cross section would be necessary since the target of this test is only the one local point of cross section.

3.2 Undrained cyclic triaxial test

Figure 8 shows the result of undrained cyclic triaxial tests. The relationship between the stress ratio and the number of cycles when the double amplitude reached 5% is obtained. While the liquefaction resistance of samples with 1 day and 4 days consolidation is almost the same, the increment of the resistance was observed in 64 days consolidation case. When the data are compared by the stress ratio, the resistance of 64 days sample became 1.50 times greater than those of 1 day and 4 days sample.

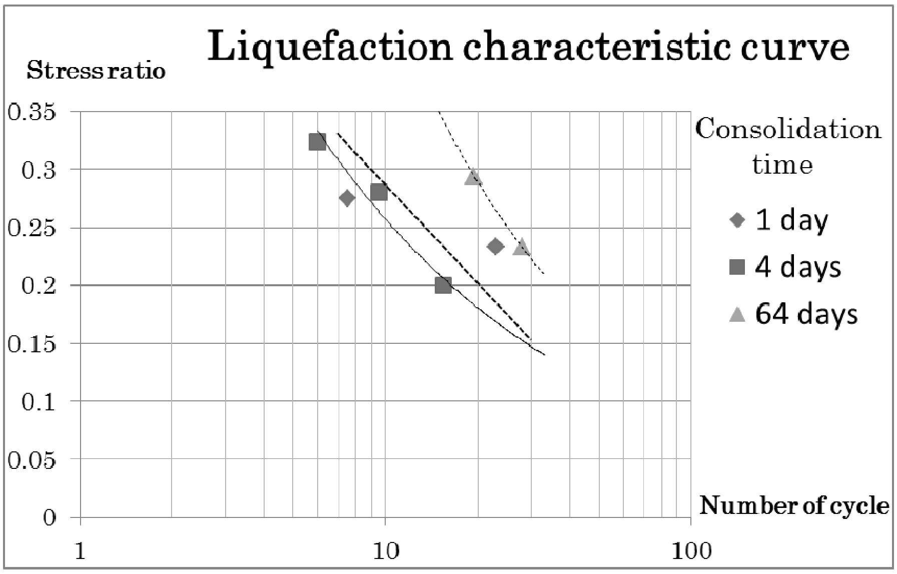

Figure 8: Liquefaction characteristic curve

Shintaku and Towhata (2014) [5)] obtained the same kind of graph as Figures 5 and 6 by using the same samples as this test with Dr around 60%. Then, it was concluded that the frequency of void filling in case S1 is about 8 times greater than that in case #6. It is also reported by him that the liquefaction resistance of #6 sample in 64 days consolidation was 1.07 times larger than that in 1 day case.

By combining these information and the result obtained in this test, the relationship between the increment ratio of liquefaction resistance and the frequency of void filling is obtained as shown in Figure 9.

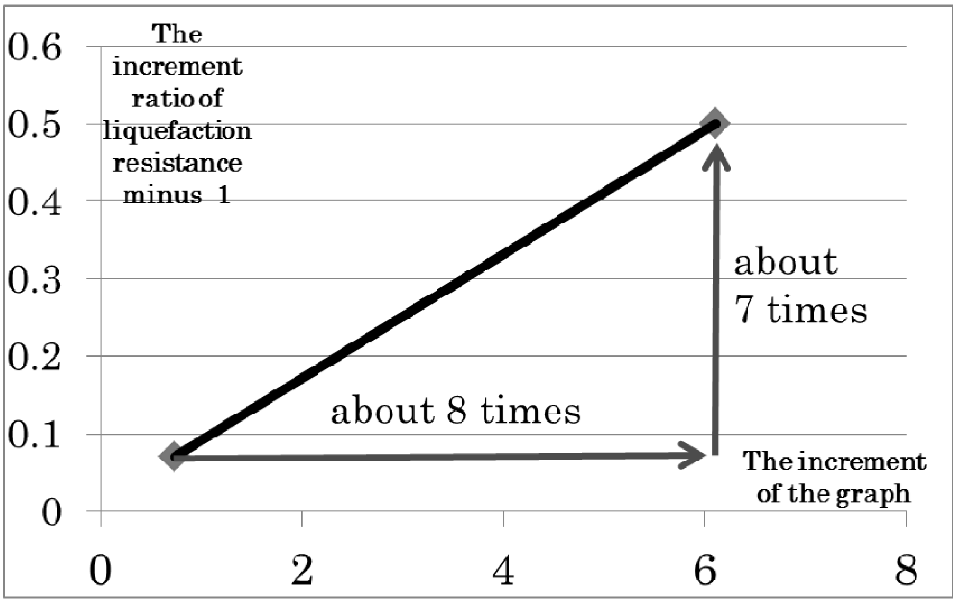

Figure 9: Relationship between the increment ratio of liquefaction resistance and the frequency of void filling

4. CONCLUSION

In this study, to indicate the mechanism of ageing effect from the viewpoint of particle movement, sand box observation and undrained cyclic triaxial tests were conducted. As a result, following two points were shown.

- Different mode of particle movement was observed with and without shaking. This might be because of the different effect of static load and shaking on the sand ground.
- There is a correlation between the increment ratio of liquefaction resistance and the frequency of void filling.
- Particle movement is more frequently observed in looser and better graded sand.

REFERENCES

Japan Road Association 2012 : *Specifications for highway bridges*（V: seismic design part）

Ikuo Towhata, Yuichi Taguchi, Toshihiko Hayashida, Yuki Hamada, Shogo Aoyama, Shigeru Goto, 2014. : *About the phenomenon that liquefaction resistance of sand ground increasese as time passes* , journal of geotechnical engineering, Vol. 10 (submitted)

Mitchell, J. K. and Solymar, Z. V., 1984: *Time-Dependent Strength Gain in Freshly Deposited or Densified Sand*, Journal of ASCE, GT11, Vol.110, pp.1559-1576

Shigeru Goto, Ikuo Towhata, 2014 : *the liquefaction characteristic of sand sample in ageing effect condition by repeatedly sheared in drained condition or consolidation in high- temperature environment*, journal of geotechnical engineering, Vol.9, No.4, 707-719

Yuki Shintaku, Towhata Ikuo, 2014 : *Test on the relationship between particle movement and ageing effect from the viewpoint of liquefaction resistance of sand*, Proc. 49th Japan National Conference on Geotechnical Engineering

AN ANALYSIS OF NETWORK THROUGHPUTS FOR DIFFERENT ORIGIN-DESTINATION PATTERNS

Koki SATSUKAWA[1], Kentaro WADA[2]
[1] Graduate student, Dept. of Civil Engineering,
The University of Tokyo, Japan
kouki@iis.u-tokyo.ac.jp
[2] Ph.D., Doctor of Information Science, Institute of Industrial Science,
The University of Tokyo, Japan

ABSTRACT

A recent study revealed the existence of the Macroscopic Fundamental Diagram (MFD) that links average density and average flow within an area. MFD describes network performance and traffic state at an aggregate level. It has also been shown that the spatial distribution of link density in a network (congestion pattern)) is one of the key components in defining the shape of an MFD. However, the effect of congestion patterns on MFD has not been clarified. In this paper, we analyze macroscopic network performance by taking into consideration congestion patterns. More specifically, we derive the network throughput analytically by solving the dynamic user equilibrium (DUE) problem, which describes the congestion pattern based on the user's route choice. And as an application of this theory, we examine several example networks and clarify the effects of the difference of the OD structure.

Keywords: *macroscopic fundamental diagram, network throughput, dynamic user equilibrium, many-to-one network, one-to-many network*

4. INTRODUCTION

Recently, Daganzo (2007) has proposed a Macroscopic Fundamental Diagram (MFD) that links average density (or accumulation) and average flow (or throughput) within an area; it describes network performance and traffic states at an aggregate level. This concept would be useful for establishing a robust traffic control policy because we can simply understand the traffic state of an area and control parameters can be flexibly adjusted on the basis of this real time information.

Geroliminis and Sun (2010) have shown that the spatial distribution of link density in a network is one of the key components in defining the shape of an MFD. However, almost all empirical studies have only analyzed the correlation between the frequency distribution of link density and MFD. Therefore, the effect of spatial patterns of link density on MFD has not been clarified. To understand this effect, Daganzo et al. (2011) theoretically analyzed the dynamics of traffic flow on a simple network with two interconnected rings. They revealed that network throughput decreases because of the heterogeneity of densities between two rings. It is, however, difficult to extend the model to investigate the effect of congestion patterns in more general networks.

The purpose of this study is to analyze macroscopic network performance by taking into consideration general congestion patterns in a network. To achieve this, we use a new method, proposed by Wada and Satsukawa (2015) and Satsukawa and Wada (2015), for deriving throughputs based on a dynamic traffic assignment model with many-to-one and one-to-many origin–destination (OD) demands. Specifically, for a given congestion pattern, we consider the dynamic user equilibrium (DUE) problem, which describes the congestion pattern based on the user's route choice. Therefore, by solving this problem, we can connect and clarify the relationship between the macroscopic network performance and the microscopic congestion pattern. This enables us to analyze the effects of the topology of congested links and route choice on throughput.

The organization of the paper is as follows. In the next section, we briefly review the DUE assignment. In section3, we derive the throughput analytically by solving DUE problem. In section4, we examine several example networks and clarify the effects of the difference of the OD structure. Finally, we summarize the results.

2. PRELIMINARIES: DYNAMIC USER EQUILIBRIUM

2.1 Networks and Notation

This paper considers general networks with one-to-many and many-to-one OD (origin-destination) demands. A network consists of a set of nodes N, a set of links L, and a set of OD pairs W. A node-link incidence matrix $\mathbf{A}^*$ (N × L matrix) represents the structure of a network. And we define an irreducible incidence matrix $\mathbf{A}$ by eliminating an arbitrary row of $\mathbf{A}^*$. We call the node corresponding to the elimination "reference node". In this paper, we choose the unique origin node in a network with one-to-many pattern, and the unique destination node in a network with many-to-one pattern as reference node. We also define a matrix $\mathbf{A}_{-}$, which is obtained by replacing all the +1 elements with 0 of A. For each link, we employ a First-In-First-Out (FIFO) principle and model traffic flow dynamics by a point queue model: it is assumed that each link (i, j) is consists of a free-flow section with constant travel time m_{ij} and a bottleneck section with constant capacity μ_{ij}. Then, the link travel time for a user entering the link at time *t* is given by

$$c_{ij}(t) = m_{ij} + \frac{x_{ij}(t + m_{ij})}{\mu_{ij}} \tag{1}$$

$$\text{where } x_{ij}(t) = A_{ij}(t) - D_{ij}(t) \tag{2}$$

where $x_{ij}(t)$ is the amount of traffic in the queue at time *t*, $A_{ij}(t), D_{ij}(t)$ are the cumulative inflow and outflow of the link by time *t*.

2.2 Decomposed Property of Dynamic User Equilibrium assignment

The dynamic user equilibrium (DUE) is defined as the state that no user can reduce his/her travel time by changing his/her route. Under the DUE state, the users who arrive their destination at the same time have the same arrival time at any node that is commonly passed through on the way to their destination (Kuwahara and Akamatsu, 1993). Based on this property, we can determine the equilibrium arrival time at each node uniquely for every arrival time at the destination. This implies that the DUE assignment with many-to-one OD pattern can be decomposed with respect to the arrival time at the destination. Hence, we can obtain the equilibrium pattern for whole time periods by successively applying the same procedure at the order of the arrival-time.

2.2.1 Formulation and Equilibrium Solutions on Saturated Many-to-One Networks

The DUE assignment on a many-to-one network can be decomposed with respect to the destination arrival-time *u*. In the following, we formulate the problem of obtaining equilibrium pattern for users, which arrive at destination at time *u*. In the decomposed formulation of DUE with destination arrival-time *u*, two types of variables, (y^u_{ij}, τ^u_i) play a central roll. τ^u_i is the earliest arrival time at node *i* for users arriving at destination at time *u*; y^u_{ij} is the link inflow rate with respect to *u*. In addition, we denote the cumulative OD demands whose arriving at destination from origin *o* until time *u* by $Q_{od}(u)$. Using these variables, the decomposed DUE assignment with respect to *u* is formulated as the following three conditions. The first condition is the link travel time function given by

$$c^u_{ij} = c^{u=0}_{ij} + \int_0^u c^u_{ij}\, du \quad \forall u. \tag{3}$$

$$\text{where} \quad \dot{c}^u_{ij} = \frac{dc^u_{ij}}{ds} = \begin{cases} y^u_{ij} / \mu_{ij} - \dot{\tau}^u_i & \text{if } x_{ij}(\tau^u_i + m_{ij}) > 0 \\ 0 & \text{if } x_{ij}(\tau^u_i + m_{ij}) = 0 \end{cases} \tag{4}$$

Second is the flow conservation condition given by

$$\sum_i y^u_{ik} - \sum_j y^u_{kj} + \dot{Q}^u_{kd} = 0 \quad \forall k, k \neq d, \forall u. \tag{5}$$

$$\text{where} \quad \dot{Q}^u_{kd} = \frac{dQ_{kd}(u)}{du}. \tag{6}$$

Third is the user's route choice condition

$$\begin{cases} y^u_{ij}\{c^u_{ij} + \tau^u_i - \tau^u_j\} = 0 \\ c^u_{ij} + \tau^u_i - \tau^u_j \geq 0, \quad y^u_{ij} \geq 0 \end{cases} \quad \forall ij \in L, \quad \forall u. \tag{7}$$

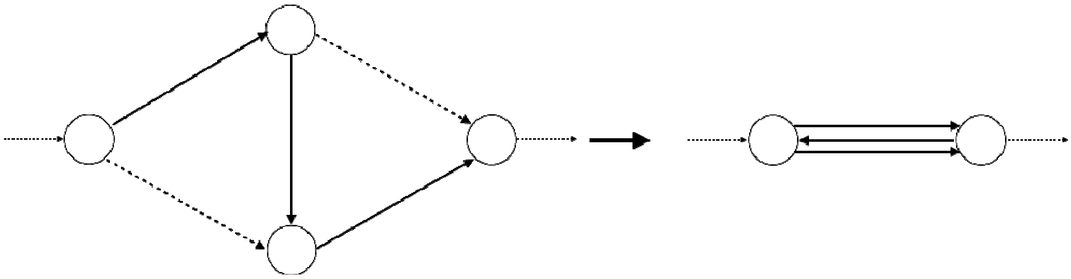

The DUE assignment is formulated as a complementarity or variational inequality problem and we cannot solve analytically. Therefore, to obtain analytical solution, we confine our analysis to “saturated networks”, which satisfy the following two conditions: (1) all links in a network have positive inflows (i.e., $y_{ij}^{u} > 0$), and (2) all links have queues (i.e., $x_{ij}(t) > 0$). In a saturated network, the decomposed DUE assignment results in a system of linear equations, and thus we can obtain an analytical solution (Akamats, 2000; Akamatsu and Heydecker, 2003b). In addition, we can apply the same methodology to a non-saturated network by constructing a saturated network, which is called “reduced network” (Akamatsu and Heydecker, 2003a). This network is a saturated network constructed by appropriately removing links, which have no flow or no queue (Figure 1). Hereafter, we proceed to a discussion on a reduced network.

Now, let us derive an analytical solution of the DUE assignment with respect to the destination arrival-time *u*. The complementarily conditions of link travel time (4) and user’s route choice (7) result in the following two equality conditions:

Figure 1: Example of constructing reduced network, Dotted: non saturated, Bold: saturated

$$\dot{c}_{ij}^{u} = y_{ij}^{u} / \mu_{ij} - \dot{\tau}_{i}^{u} \quad \forall ij. \tag{8}$$

$$\dot{c}_{ij}^{u} + \dot{\tau}_{i}^{u} - \dot{\tau}_{j}^{u} = 0 \quad \forall ij. \tag{9}$$

By substituting equation (9) into equation (8), we derive

$$\begin{aligned} y_{ij}^{u} &= \mu_{ij}\dot{\tau}_{j}^{u} \quad \forall ij \\ \Leftrightarrow \mathbf{y}^{u} &= -(\mathbf{M}\mathbf{A}_{-}^{T})\dot{\tau}^{u} \end{aligned} \tag{10}$$

$$\text{where} \quad \mathbf{M} = \begin{bmatrix} \ddots & & 0 \\ & \mu_{ij} & \\ 0 & & \ddots \end{bmatrix}. \tag{11}$$

By substituting this equation into flow conservation condition (5), we see that the DUE solution $\dot{\tau}_{k}^{u}$ is governed by

$$\dot{\mathbf{Q}}^{u} = -(\mathbf{A}\mathbf{M}\mathbf{A}_{-}^{T})\dot{\tau}^{u}. \tag{12}$$

However, if there are links, which connect to a reference node, inflows of those links disappear because of eliminating an arbitrary row of $\mathbf{A}^{*}$ (i.e., a flow conservation condition is no longer satisfied in the saturated network). We can solve this problem by treating these inflows as outflows from a network. Specifically, by using a column vector δ, which components are capacities of those links, equation (12) is revised by

$$\dot{\mathbf{Q}}^{u} - \delta = -(\mathbf{AMA}_{-}^{T})\dot{\tau}^{u}. \tag{13}$$

In addition, we can represent this equation as a block matrix by distinguishing pure origin nodes, which has no incoming link (denoted by *p*), origin nodes (denoted by *o*) and transient nodes (denoted by *i*).

$$\dot{\mathbf{Q}}^{u} = \begin{bmatrix} \dot{\mathbf{Q}}^{p} \\ \dot{\mathbf{Q}}^{o} \\ 0 \end{bmatrix} = -\begin{bmatrix} \mathbf{A}_{p} \\ \mathbf{A}_{o} \\ \mathbf{A}_{i} \end{bmatrix} \mathbf{M} \begin{bmatrix} 0 & \mathbf{A}_{o} & \mathbf{A}_{i} \end{bmatrix} \begin{bmatrix} \dot{\tau}_{p}^{u} \\ \dot{\tau}_{o}^{u} \\ \dot{\tau}_{i}^{u} \end{bmatrix} + \begin{bmatrix} \delta_{p} \\ \delta_{o} \\ \delta_{i} \end{bmatrix}. \tag{14}$$

2.2.2 Formulation and Equilibrium Solutions on Saturated One-to-Many Networks

As with the many-to-one OD pattern, the DUE assignment on a one-to-many network can be decomposed with respect to the origin departure-time *s*. In the decomposed formulation with origin departure time *s*, two types of variables, (y_{ij}^{s}, τ_{i}^{s}) play a central roll. τ_{i}^{s} is the earliest arrival time at node *i* for users departing from origin at time *s*; y_{ij}^{s} is the link inflow rate with respect to *s*. In addition, we denote the cumulative OD demands whose departing from origin to destination *d* until time *s* by $Q_{od}(s)$. By using these variables, we can derive the DUE solution,

$$\dot{\mathbf{Q}}^{s} + \delta = (\mathbf{AMA}_{-}^{T})\dot{\tau}^{s}. \tag{15}$$

Similarly with many-to-one OD pattern, we can represent this equation as a block matrix by distinguishing destination nodes (denoted by *d*) and transit nodes (denoted by *i*).

$$\dot{\mathbf{Q}}^{s} = \begin{bmatrix} 0 \\ \dot{\mathbf{Q}}^{d} \end{bmatrix} = \begin{bmatrix} \mathbf{A}_{i} \\ \mathbf{A}_{d} \end{bmatrix} \mathbf{M} \begin{bmatrix} \mathbf{A}_{i-} & \mathbf{A}_{d-} \end{bmatrix} \begin{bmatrix} \dot{\tau}_{i}^{s} \\ \dot{\tau}_{d}^{s} \end{bmatrix} - \begin{bmatrix} \delta_{i} \\ \delta_{d} \end{bmatrix}. \tag{16}$$

3. MACROSCOPIC NETWORK PERFORMANCE

In this section, we analyze the macroscopic network performance under the DUE state. Firstly, we briefly review the concept of Macroscopic Fundamental Diagram (MFD) and Network Exit Flow (NEF) proposed in Daganzo(2007). Secondly, we mathematically describe the throughputs by using the microscopic variables used in the formulation of DUE. Finally, we derive an analytical formula of the throughputs by solving an inverse problem of the DUE formulation.

3.1 Macroscopic Fundamental Diagram and Network Exit Flow

Recently, Daganzo (2007) has proposed a macroscopic traffic modeling approach. This approach is based on the following hypothesis: if traffic demands to a network system change slowly compared with the travel time across the network, then the system can be described as near steady-state. Under this state, the network throughput should be approximated by Network Exit Flow (NEF) $G(n(t))$, which is a function of the vehicle accumulation $n(t)$ on the network.

However, it is difficult to measure the throughput practically. Therefore, we employ the MFD that links average density *k* and average flow *q* within an area as an alternative of NEF. We can derive the relationship between NEF and MFD when the average distance travelled by exiting vehicles is *d* and the total length of the network is *l*: $G(n(t)) = (l/d)q(k)$. Consequently, MFD is the result of a scale transformation of NEF. Hereafter, we deal with the NEF (throughput) to analyze the macroscopic network performance.

3.2 Formulations and Analytical Solution of the Throughputs

3.2.1 Throughput with Many-to-One OD pattern

Let us describe the throughput under the DUE state. First, we describe the relationship between microscopic variables used in the formulation of DUE and macroscopic traffic state variables. Define $A_o(t)$, $D_o(t)$, $n_o(t)$ as the cumulative number of vehicles to have arrived and left a network distinguished by origin *o*. These macroscopic variables is represented by

$$A_o(t) \equiv Q_{od}(t + C_o^*(t)) \quad \forall o \tag{17}$$

$$D_o(t) \equiv Q_{od}(t) \quad \forall o \tag{18}$$

$$n_o(t) \equiv A_o(t) - D_o(t) \quad \forall o \tag{19}$$

where $C_o^*(t)$ is the equilibrium trip time of vehicles which depart a origin *o* at time *t*. If these variables are differentiable, the dynamics of the vehicle accumulation is given by

$$\left.\frac{dn_o(t)}{dt}\right|_{t=\tau_o^u} = \frac{dA_o(\tau_o^u)}{dt} - \frac{dD_o(\tau_o^u)}{dt} = \left(\frac{\dot{Q}_{od}^u}{\dot{\tau}_o^u} - \frac{dQ_{od}(\tau_o^u)}{d\tau_o^u}\right). \tag{20}$$

Using these variables, we derive the analytical formulation of throughput under a steady state. We define this as the state, which satisfies the following two conditions: (1) the vehicle accumulation in a network and the each of the OD demand are constant, and (2) a congestion pattern is unchangeable. These conditions can be expressed as the following two conditions. First condition is that the vehicle accumulation is constant. From equation (20), this condition is given by

$$\frac{\dot{Q}_{od}^u}{\dot{\tau}_o^u} = \frac{dQ_{od}(\tau_o^u)}{d\tau_o^u}. \tag{21}$$

And second condition is that each OD demands is constant. This condition is given by,

$$\dot{Q}_{od}^u = \frac{dQ_{od}(\tau_o^u)}{d\tau_o^u}. \tag{22}$$

Substituting (22) into (21), we can derive the following periodic boundary condition given by,

$$\dot{\tau}_o^u = 1. \tag{23}$$

This condition implies that $\dot{\mathbf{Q}}^s$ represent both of the inflow and outflow rate, also the throughput itself. We denote this throughput in the congestion pattern $\mathbf{x}$ as $\mathbf{G}_{\mathbf{x}}$, to distinguish from the inflow and outflow rate.

Therefore, the formulation of the throughput in a network with many-to-one OD pattern can be described by,

$$\tilde{\mathbf{G}}_{\mathbf{x}} - \delta = -(\mathbf{AMA}_{-}^{T})\dot{\tau}^{u} \tag{24}$$

Define $\tilde{\mathbf{G}}_{\mathbf{x}}$ as a vector whose transit-node components are 0: $\tilde{\mathbf{G}}_{\mathbf{x}} \equiv \left[\mathbf{G}_{\mathbf{x}} \,|\, 0\right]^{T}$. Finally, by solving this formulation, we can derive following analytical throughput.

$$\mathbf{G}_{\mathbf{x}} = \begin{bmatrix} \mathbf{G}_{\mathbf{x}}^{p} \\ \mathbf{G}_{\mathbf{x}}^{o} \end{bmatrix} = \begin{bmatrix} -\mathbf{V}_{po}\mathbf{1} + \mathbf{V}_{pi}(\mathbf{V}_{ii})^{-1}[\mathbf{V}_{io}\mathbf{1} - \delta_{i}] - \delta_{p} \\ -\mathbf{V}_{oo}\mathbf{1} + \mathbf{V}_{oi}(\mathbf{V}_{ii})^{-1}[\mathbf{V}_{io}\mathbf{1} - \delta_{i}] - \delta_{o} \end{bmatrix}. \tag{25}$$

where $\mathbf{V}_{ab} \equiv \mathbf{A}_{a}\mathbf{MA}_{b-}^{T} \quad (a,b \in \{p,o,i\})$

This implies that the macroscopic network performance is characterized by the structure of congested links. By using this equation, we can derive macroscopic network performance, which takes into consideration the network topology. In addition, we can represent the throughput by elements from equation (24).

$$\begin{aligned} \left[\mathbf{G}_{\mathbf{x}}^{p}\right]_{p} &= \sum\nolimits_{l} \mu_{pl}\dot{\tau}_{l}^{u} \\ \left[\mathbf{G}_{\mathbf{x}}^{o}\right]_{o} &= \sum\nolimits_{l} \mu_{ol}\dot{\tau}_{l}^{u} - \sum\nolimits_{l} \mu_{lo} \end{aligned}. \tag{26}$$

Equation (26) means the flow conservation condition in the reduced network. Specifically, the first terms of these equations represent the outflow, and the second term represents the inflow from the origin nodes in the reduced network respectively. Note that this equation includes the variable $\dot{\tau}_{l}^{u}$, which characterizes the equilibrium solution in the DUE state; e.g., the effects of the route choice. This variable represents the state of the congested flow pattern in downstream of node *l*. It implies that this throughput has been influenced by the downstream states of a group of origin nodes (the whole of network).

3.2.2 Throughput under One-to-Many OD pattern

As with the many-to-one OD pattern, we derive the analytical formulation of throughput in a network with one-to-many OD pattern. We can derive a periodic boundary condition in the same way.

$$\dot{\tau}_{d}^{s} = 1. \tag{27}$$

This equation has the same meaning to many-to-one pattern. Then, formulation of the throughput in a one-to-many network can be described by,

$$\tilde{\mathbf{G}}_{\mathbf{x}} + \delta = (\mathbf{AMA}_{-}^{T})\dot{\tau}^{u}. \tag{28}$$

From these equations, we can derive following analytical throughput.

$$\begin{gathered} \mathbf{G}_{\mathbf{x}} = \mathbf{V}_{dd}\mathbf{1} - \mathbf{V}_{di}(\mathbf{V}_{ii})^{-1}[\mathbf{V}_{id}\mathbf{1} - \delta_{i}] - \delta_{d}. \\ \text{where} \quad \mathbf{V}_{ab} \equiv \mathbf{A}_{a}\mathbf{MA}_{b-}^{T} \quad (a,b \in \{i,d\}) \end{gathered} \tag{29}$$

To analyze this solution, let us describe the throughput by elements.

$$\left[\mathbf{G}_{\mathbf{x}}\right]_{d} = \sum\nolimits_{k} \mu_{kd} - \sum\nolimits_{k} \mu_{dk}\dot{\tau}_{k}^{s}. \tag{30}$$

We can recognize that this equation is also the flow conservation condition in the reduced network.

4. ANALYSIS OF EXAMPLE NETWORKS

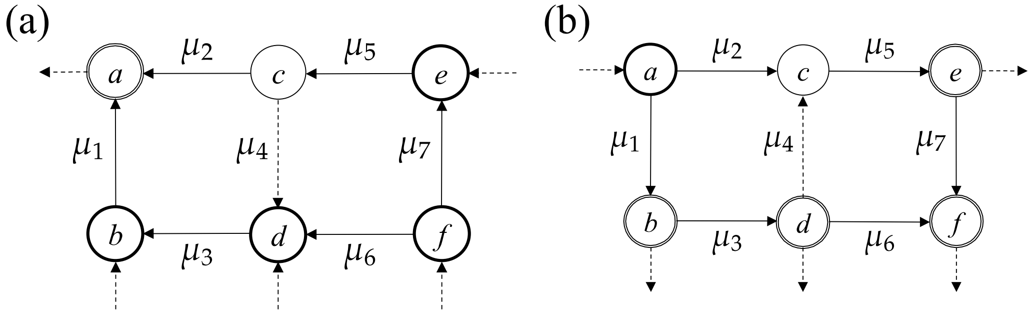

In this section, we apply the analyses in section 3 to networks, which have symmetrical OD demands and link connection. We then analyze the difference of the throughput with respect to the OD structure. Figure 3 shows the symmetrical networks. In these networks, each link has a capacity $\mu_{ij}\ (ij \in L)$.

4.1 Examples that Networks have the Same Throughputs

Consider the network shown in Figure 2(a), where nodes *b, d, e* and *f* are origins; node *a* is the only destination. Links except link 4 are saturated and link 4 is not saturated. The matrixes in equation (26) for this network are given by

$$\mathbf{V}_{po} = \begin{bmatrix} 0 & -\mu_6 & -\mu_7 \end{bmatrix}. \tag{31}$$

$$\mathbf{V}_{oo} = \begin{bmatrix} \mu_3 & 0 & 0 \\ -\mu_3 & \mu_5+\mu_6 & 0 \\ 0 & -\mu_5 & \mu_7 \end{bmatrix}. \tag{32}$$

$$\delta_o = \begin{bmatrix} \mu_1 \\ \mu_2 \\ 0 \end{bmatrix}. \tag{33}$$

By using these matrixes, the throughputs distinguished by origin nodes and the network throughput become

$$\begin{bmatrix} \mathbf{G}_{\mathbf{x}}^{b} \\ \mathbf{G}_{\mathbf{x}}^{d} \\ \mathbf{G}_{\mathbf{x}}^{e} \\ \mathbf{G}_{\mathbf{x}}^{f} \end{bmatrix} = \begin{bmatrix} \mu_1-\mu_3 \\ \mu_2+\mu_3-\mu_5-\mu_6 \\ \mu_5-\mu_7 \\ \mu_6+\mu_7 \end{bmatrix} \tag{34}$$

$$\mathbf{G}_{\mathbf{x}} = \mu_1+\mu_2\,. \tag{35}$$

Figure 2: Example networks, (a) One-to-many OD (b) Many-to-one OD

Double line: origin, Bold line: destination

We can easily find that the network throughput is consistent with the sum of inflow link capacities to the destination.

Similarly, we can derive the throughput of the network in Figure 2(b), where node *a* is the only origin; nodes *b*, *d*, *e* and *f* are destinations. The matrixes in equation (30) for this network are given by

$$\mathbf{V}_{dd} = \begin{bmatrix} \mu_1 & -\mu_3 & 0 & 0 \\ 0 & \mu_2+\mu_3 & -\mu_5 & -\mu_6 \\ 0 & 0 & \mu_5 & -\mu_7 \\ 0 & 0 & 0 & \mu_6+\mu_7 \end{bmatrix}. \tag{36}$$

Substituting these equations into (30), we derive

$$\begin{bmatrix} \mathbf{G}_{\mathbf{x}}^{b} \\ \mathbf{G}_{\mathbf{x}}^{d} \\ \mathbf{G}_{\mathbf{x}}^{e} \\ \mathbf{G}_{\mathbf{x}}^{f} \end{bmatrix} = \begin{bmatrix} \mu_1-\mu_3 \\ \mu_2+\mu_3-\mu_5-\mu_6 \\ \mu_5-\mu_7 \\ \mu_6+\mu_7 \end{bmatrix}. \tag{37}$$

$$\mathbf{G}_{\mathbf{x}} = \mu_1+\mu_2\,. \tag{38}$$

By comparing (35) and (38), we can easily find that the throughputs are the same. This is because there are no route choice effects of the DUE state in these networks, which do not have transit nodes. In other words, the second terms of the equation (25), (29) disappear. In this case, the throughputs only depend on the structure of congested links to the destination node(s). Therefore, the throughputs in these symmetric networks become the sum of the inflow link capacities to the destination node(s).

4.2 Examples that Networks have the Different Throughputs

We now consider the networks where link 4 becomes congested. Let us derive the throughputs with many-to-one OD pattern at first. The matrixes in equation (26) for this network are given by

$$\mathbf{V}_{po} = \begin{bmatrix} 0 & -\mu_6 & -\mu_7 \end{bmatrix},\ \mathbf{V}_{ii} = \begin{bmatrix} \mu_5 \end{bmatrix}\ \mathbf{V}_{io} = \begin{bmatrix} 0 & -\mu_4 & 0 \end{bmatrix} \tag{39}$$

$$\mathbf{V}_{oo} = \begin{bmatrix} \mu_3 & 0 & 0 \\ -\mu_3 & \mu_4+\mu_6 & 0 \\ 0 & 0 & \mu_7 \end{bmatrix}\ \mathbf{V}_{oi} = \begin{bmatrix} 0 \\ 0 \\ -\mu_5 \end{bmatrix} \delta_o = \begin{bmatrix} \mu_1 \\ 0 \\ 0 \end{bmatrix} \delta_i = \begin{bmatrix} \mu_2 \end{bmatrix} \tag{40}$$

Substituting these equations into equation (26), we can derive the throughputs.

$$\begin{bmatrix} \mathbf{G}_{\mathbf{x}}^{b} \\ \mathbf{G}_{\mathbf{x}}^{d} \\ \mathbf{G}_{\mathbf{x}}^{e} \\ \mathbf{G}_{\mathbf{x}}^{f} \end{bmatrix} = \begin{bmatrix} \mu_1-\mu_3 \\ \mu_3-\mu_4-\mu_6 \\ \mu_2+\mu_4-\mu_7 \\ \mu_6+\mu_7 \end{bmatrix}. \tag{41}$$

$$\mathbf{G}_{\mathbf{x}} = \mu_1+\mu_1\,. \tag{42}$$

The network throughputs do not change at all regardless of the changes of origin throughputs.

Then, we derive the throughput with one-to-many OD pattern in the same way. The matrixes in equation (30) for this network are given by

$$\mathbf{V}_{dd} = \begin{bmatrix} \mu_1 & -\mu_3 & 0 & 0 \\ 0 & \mu_3 & 0 & -\mu_6 \\ 0 & 0 & \mu_5 & -\mu_7 \\ 0 & 0 & 0 & \mu_6+\mu_7 \end{bmatrix}, \quad \mathbf{V}_{di} = \begin{bmatrix} 0 \\ -\mu_4 \\ 0 \\ 0 \end{bmatrix}. \tag{43}$$

$$\mathbf{V}_{ii} = \begin{bmatrix} \mu_2+\mu_4 \end{bmatrix}, \ \mathbf{V}_{id} = \begin{bmatrix} 0 & -\mu_5 & 0 & 0 \end{bmatrix} \tag{44}$$

Substituting these equations into equation (30), we can derive the throughputs.

$$\begin{bmatrix} \mathbf{G}_{\mathbf{x}}^{b} \\ \mathbf{G}_{\mathbf{x}}^{d} \\ \mathbf{G}_{\mathbf{x}}^{e} \\ \mathbf{G}_{\mathbf{x}}^{f} \end{bmatrix} = \begin{bmatrix} \mu_1-\mu_3 \\ \mu_3-\mu_6-\dfrac{\mu_4\mu_5}{\mu_2+\mu_4} \\ \mu_5-\mu_7 \\ \mu_6+\mu_7 \end{bmatrix}. \tag{45}$$

$$\mathbf{G}_{\mathbf{x}} = \mu_1+\mu_5-\frac{\mu_4\mu_5}{\mu_2+\mu_4}. \tag{46}$$

By comparing the equations (37) and (45), we can find that the throughput from node *d* have changed and the network throughput may decrease. This is because the second term of the equation (30) has changed by the route choice effects of the DUE state. The equilibrium DUE solution at a node is affected by flows to destinations which are downstream of the node. Therefore, at the upstream node *d* of node *c*, we derive the throughput affected by the effect of route choice in the DUE state.

From these results, we find that the throughputs of the symmetric networks are not always symmetric and become different. This difference is interpreted as the following. In the many-to-one network, all vehicles go to the same destination regardless of the difference of their origins. Therefore, the throughput results in just the sum of inflow link capacities to the destination and not influenced by the other links strongly. On the other hand, in the one-to-many network, some vehicles may use an upstream destination node as just a transit node to go to a downstream destination node. In this case, such vehicles interrupt vehicles, which go to upstream destination nodes. Then, the throughput in one-to-many network becomes less than the simple summation of inflow link capacities.

5. CONCLUSION

In this paper, we derived the network throughputs with taking into consideration of the effect of network topology and route choice. In addition, we analyzed the difference of the throughputs with respect to the OD structure. Our simple analysis in example networks showed that even if the networks have the symmetrical congestion patterns, the throughputs become different due to the route choice effects. We can expect this kind of asymmetry result in general. Therefore, we should extend our analysis to more general sensitivity analysis: sensitivity to the changes of link capacity or the link state. In addition, in one-to-many network, we find the throughputs may decrease with congestion by the effect of the route choice. These results imply that network throughput in one-to-many network is more sensitive to the user's route choice than that in many-to-one network, and the key components for analyzing the characteristics of throughputs are inherent in one-to-many network congestion pattern. Toward this direction, we should explore the key congestion pattern with one-to-many OD pattern for deciding the capacity of a network.

REFERENCES

Kuwahara, M. and Akamatsu, T., (1993) Dynamic equilibrium assignment with queues for one-to-many OD pattern. *Proceedings of The 12th International Symposium on Transportation and Traffic Theory*, pp. 185-204.

Akamatsu, T., (2000) A dynamic traffic equilibrium assignment paradox. *Transportation Research Part B: Methodological*, **34**, pp. 515-531.

Akamatsu, T. and Heydecker, B., (2003a) Detecting Dynamic Traffic Assignment Capacity Paradoxes in Saturated Networks. *Transportation Science* , 37, pp. 123-138

Akamatsu, T. and Heydecker, B., (2003b) Detecting Dynamic Traffic Assignment Capacity Paradoxes: Analysis of non-saturated networks. *Working Paper*, Tohoku University(Japan)

Daganzo, C. F., (2007). Urban gridlock: Macroscopic modeling and mitigation approaches, *Transportation Research Part B: Methodological* **41**, pp. 49 – 62

Daganzo, C. F., Gayah, V. V. and Gonzales, E. J., (2011). Macroscopic relations of urban traffic variables: Bifurcations, multivaluedness and instability, *Transportation Research Part B: Methodological* **45**, pp. 278 - 288

Geroliminis, N. and Sun, J., (2011). Properties of a well-defined macroscopic fundamental diagram for urban traffic, *Transportation Research Part B: Methodological* **45**, pp. 605 – 617

Satsukawa, K. and Wada, K (2015) Macroscopic Traffic Performance under Dynamic User Equilibrium with Many-to-One Origin-Destination Patterns, Japan Society of Traffic Engineering, accepted.

Wada, K and Satsukawa, K. (2015) Network throughput under dynamic user equilibrium, *Working paper*

WATER RETAINABILITY AND BASIC PROPERTIES OF COAL BOTTOM ASH USED AS FINE AGGREGATE REPLACING MATERIAL IN CONCRETE

Noulananh LATHSOULIN[1],Pakawat SANCHAROEN[2] and
Somnuk TANGTERMSIRIKUL[1,2]
[1] School of Civil Engineering and Technology,
Sirindhorn International Institute
of Technology, Thammasat University, Thailand.
[2] Construction and Maintenance Technology Research Center,
Sirindhorn International Institute of Technology,
Thammasat University, Thailand.
Khaek_noulananh@hotmail.com

ABSTRACT

Bottom ash from coal power plant is a porous material and its particle size is comparable to that of fine aggregate used in concrete. So it is considered to be used as porous fine aggregate. However, current standard method for determining water absorption of fine aggregate cannot be used effectively with porous fine aggregate due to it is difficult to justify the saturated surface dry condition of it. Thus water retainability was determined instead. Water retainability of bottom ash was tested by proposed method which was fully submerged a few days to reach the over saturated condition before being vibrated-drained for 24 minutes. Other basic properties such as specific gravity, gradation or chemical compositions were also studied and compared with natural fine aggregate. The results showed possibility of coal bottom ash to be used as fine aggregate replacing material in concrete.

***Keywords**: porous aggregate; basic properties of bottom ash; water retainability*

1. INTRODUCTION

Presently, specific porous materials or water retaining materials have been studied for the concrete cases due to a large amount of waste materials has been dumped or used as a land-filled material and amount of natural sand is insufficient in some area. Bottom ash is used as partially replace sand, it can saves a lot of money, solve some environmental problem and may enhance in mechanical properties and durability of concrete (Andrade et. al, 2009) and (Kasemchaisiri and Tangtermsirikul 2007).

Bottom ash is a porous material that has high water retainability, coarse particle size and usually no pozzolanic effect (Andrade et. al, 2009), However, determining water absorption of fine aggregate cannot be used effectively with porous fine aggregate due to it is difficult to justify the saturated surface dry condition of it, so the water retainability was determined instead.

This is the big problem for concrete mix design in order to achieve the efficient concrete and also workability because these porous materials is the moisture content of porous aggregate is always higher than normal aggregate. Previous studies have reported that concrete mixed with bottom ash and recycled concrete-crush was very nonworkable due to a significant water demand from their porous properties (Bucholc and Ghafoori, 1996). There was a certain difficulty in determining the exact moisture properties of bottom ash (Landgren, 1994).

Water retainability has been discovered by some researchers for analysis and design of the fresh concrete properties (Kasemchaisiri and Tangtermsirikul, 2007). For concrete incorporating porous aggregate, it is appropriate to apply water retainability instead of water absorption to adjust amount of mixing water according to concrete mix proportion.

The purpose of this study is to develop of practical method to determine water retainability of porous fine aggregate based on available laboratory equipment and short testing time, In addition basic properties of bottom ash were also studied.

2. METHODOLOGY

The study was tested by using 12 types of bottom ash were tested on basic properties such as sieve analysis, specific gravity, chemical composition and water retainability.

2.1 Materials

Bottom ash was collected from Mae Moh electricity generating plant, Thailand during April to September 2014. Bottom ash on each month had different properties such as physical and chemical properties of themselves because of different percentage of coal. Main two bottom ashes with different burning process had been tested in this study. The bottom ashes with 150MW capacity and bottom ashes with 300MW capacity. Bottom ash was sieved pass sieve (No.4) prior testing.

2.2 Gradation

Bottom ash particles had to be dried in the oven before testing. Sieve analysis of bottom ash has investigated according to ASTM C136-06 standard (ASTM C136-06, 2004).

2.3 Specific gravity

There are 2 sample conditions for testing specific gravity as shown in details below (ASTM C128, 2004).

(1) Water retainability sample condition: Determine the specific gravity of bottom ash at the stage of water retainabilty, adjust the water of dried-bottom ash until reach the water retainability condition. After that, standard test method for specific gravity and absorption of fine aggregate (ASTM C128) can be applied.

(2) Dry sample condition: Standard test method for specific gravity and absorption of fine aggregate (ASTM C128) can be applied but with the use of oven-dried sample. Then bulk specific gravity at the state of water retainability can be calculated from equation (1).

$$SG_{OD} = SG_{OD}/(1+WR/100) \qquad (1)$$

Where SG_{OD} and SG_{WR} are the bulk specific gravity of bottom ash at oven-dried and water retainability conditions, respectively and WR is the water retainability of bottom ash (% by oven-dried weight of bottom ash).

2.4 Chemical composition

For chemical analysis testing according to the (ASTM E1621-94, 2004), 12 samples of bottom ash have been analyzed for chemical analysis. Bottom ashes were tested with the machine Bruker AXS, Germany, Model: S4 Pioneer Wavelength dispersive, X-Ray Fluorescence (WDXRF) Spectrometry. Voltage/Current : 60 kV / 50 mA. Conditions: Range 0.2 – 20 A (60 – 0.6 keV), total resolution 3 – 100 eV, typical measurement time 2 – 10 s per element. Program used: SPECTRA Plus software of the Bruker with the standardless Analysis.

2.5 Water retainability

Prepared the sample with the quantity required to fill the cylinder (5-6 kg) as showed in Figure 1(a). Mix the sample with the water in a container, wrap the container and immerse the sample for 3 days as showed in Fig. 1(b). Before testing, sample should be drained around 30 minutes before filling into the apparatus as showed in Figure 1(c).

Compacting sample into the cylinder pipe was separated into three layers, then hammering 30 times for each layer. Vibrate the cylinder pipe by ordinary fine aggregate sieving machine at 24 minutes. Collected the sample from the top of container and obtained the moisture content of the sample for 3 centimeter thickness. This method is called proposed test method. The water retainability of sample is the value of the moisture content from the top of the containers.

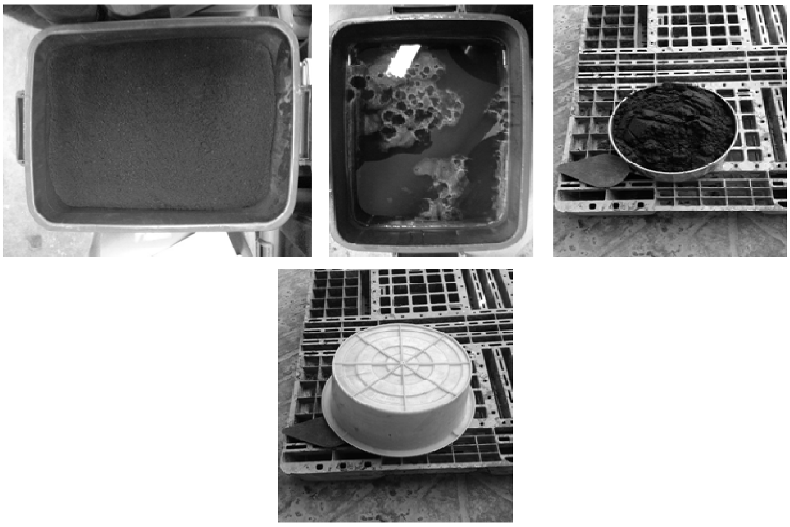

(a) (b) (c)

Figure 1: (a) Sample with specified amount of water; (b) Sample with water (fully saturated); (c) Draining water from sample with cover.

3. RESULTS AND DISCUSSION

3.1 Gradation

Figure 2 and 3 showed the gradation of all types of bottom ash used in this study. Bottom ash passing sieve no. 4 was used in this study to avoid the large particles and to maintain a gradation to be similar to that of the sand. It can be observed that gradation and fineness modulus on each month in the same burning process had nearly same values and same tendency as showed in Figure 2 and 3. The gradation of bottom ash from 150MW capacity as shown in Figure 2 had particles size bigger than bottom ash from 300MW capacity as shown in Figure3. Fineness particle of bottom ashes from 300MW capacity showed finer than limit of standard ASTM C136-06, especially No.50 and No.100 respectively. In addition, the fineness modulus of bottom ashes from 150MW capacity are coarser than bottom ashes from 300MW capacity as shown in Figure 4 .

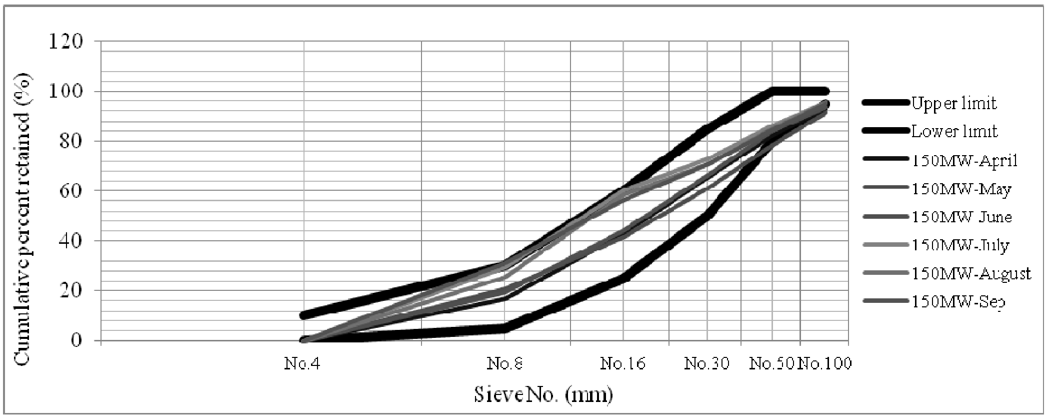

Figure 2: Gradation of bottom ash from 150MW capacity

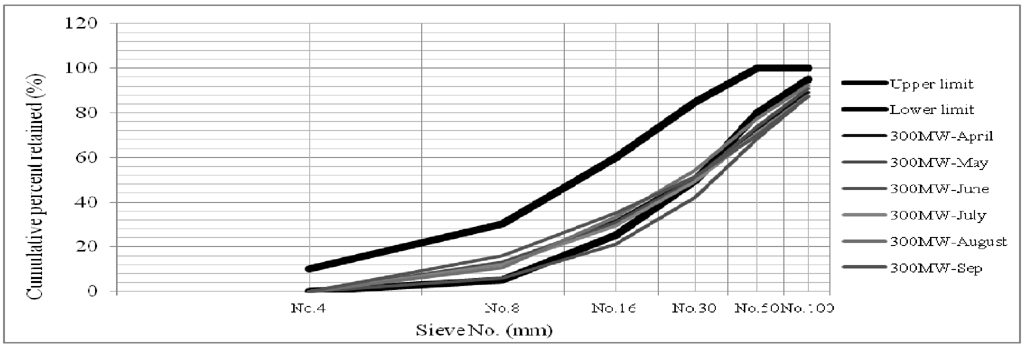

Figure 3: Gradation of bottom ash from 300MW capacity

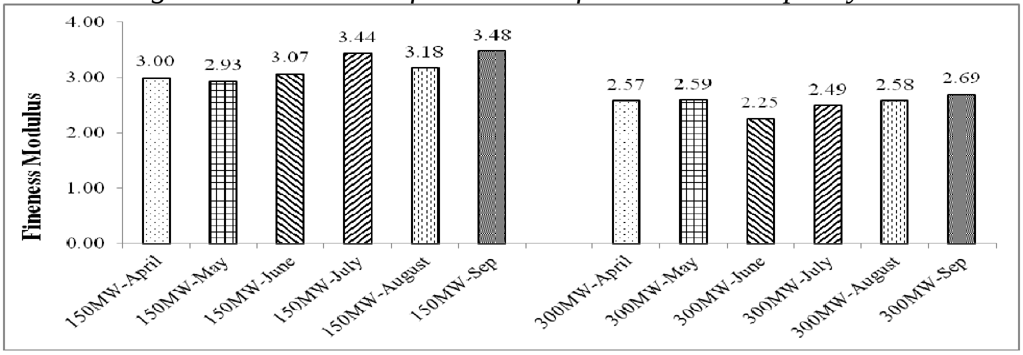

Figure 4: Fineness Modulus of bottom ash from 150MW and 300MW capacity

3.2 Specific gravity

In this study, specific gravity of bottom ashes were tested by water retainability condition. Figure 5 showed that the specific gravity of all types of bottom ash used in this study. It can be observed that specific gravity of bottom ash on each month in the same burning process had nearly same values and same tendency as showed in Figure 5. It can be observed that specific gravity of bottom ash from 150MW capacity had the value higher than bottom ash from 300MW capacity as shown in Figure 5.

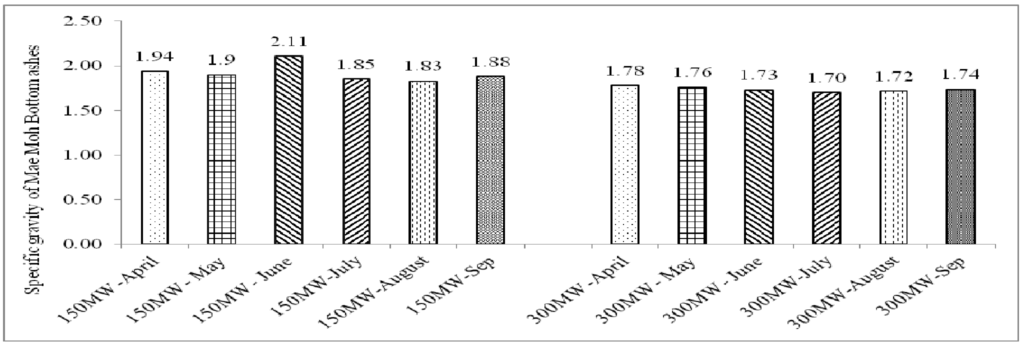

Figure 5: Specific gravity of bottom ash from 150MW and 300MW capacity

3.3 Chemical composition

Table 1 and 2, showed that the chemical composition of all types of bottom ash used in this study. It can be seen that chemical composition of bottom ash on each month in the same burning process had nearly same values of chemical substances. All types of bottom ash from 300MW capacity had Silicon dioxide higher than all types of bottom ash from

150MW capacity. In contrast, all types of bottom ash with 300MW capacity had Calcium Oxide and Sulfur trioxide lower than all types of bottom ash with 150MW capacity.

Table 1: Chemical composition of all types of bottom ash of 150MW capacity

Formula	**Concentration(%wt)**					
Name	150MW-April	150MW-May	150MW-June	150MW-July	150MW-August	150MW-Sep
SiO_2	30.13	29.50	33.26	30.12	29.61	31.73
CaO	27.78	29.50	26.95	28.11	28.03	23.45
Al_2O_3	17.84	16.43	18.14	14.58	14.68	16.49
Fe_2O_3	15.99	15.66	13.54	15.56	15.60	16.94
K_2O	2.27	2.25	2.17	2.18	2.16	2.99
MgO	2.19	1.90	1.90	1.69	1.74	1.65
SO_3	1.92	1.85	1.42	2.93	2.86	2.87
Na_2O	0.90	0.79	0.70	0.65	0.66	0.75
TiO_2	0.50	0.49	0.44	0.51	0.50	0.55
P_2O_5	0.24	0.22	0.25	0.23	0.23	0.00
MnO	0.00	0.00	0.00	0.15	0.15	0.00
BaO	0.00	0.00	0.00	0.14	0.16	0.19
LOI	0.20	1.41	1.22	3.15	3.6	2.39
Total	99.96	100.00	99.99	100.00	100.00	100.00

Table 2: Chemical composition of all types of bottom ash of 300MW capacity

Formula	**Concentration(%wt)**					
Name	300MW-April	300MW-May	300MW-June	300MW-July	300MW-August	300MW-Sep
SiO_2	35.50	35.63	35.11	37.17	33.23	32.61
CaO	21.84	21.08	21.34	17.68	21.73	20.28
Al_2O_3	17.45	18.94	19.48	21.46	17.28	17.46
Fe_2O_3	14.03	14.92	15.00	10.08	15.26	14.05
K_2O	2.38	2.55	2.64	2.46	3.01	2.58
MgO	1.78	1.76	1.81	2.38	1.72	1.69
SO_3	1.59	1.42	1.19	2.45	2.58	2.35
Na_2O	0.83	0.82	0.83	1.21	0.78	0.73
TiO_2	0.45	0.48	0.49	0.4	0.56	0.48
P_2O_5	0.16	0.18	0.16	0.17	0.17	0.17
MnO	0.00	0.00	0.00	0.00	0.00	0.14
BaO	0.00	0.00	0.00	0.00	0.16	0.15
LOI	3.98	2.22	1.93	4.52	3.52	7.30
Total	99.99	100	100	100.00	100	100.00

3.4 Water retainability

In this study, water retainability of bottom ashes were tested by proposed test method. Fig. 6 showed that water retainability of all types of bottom ash used in this study. It can be observed that water retainability of bottom ash on each month in the same burning process had a little different as showed in Fig.6. It can be also said that water retainability of bottom ash from 150MW capacity had the value lower than bottom ash from 300MW capacity as shown in fig.6. The values of specific gravity showed high values, then the values of water retainability always showed low values.

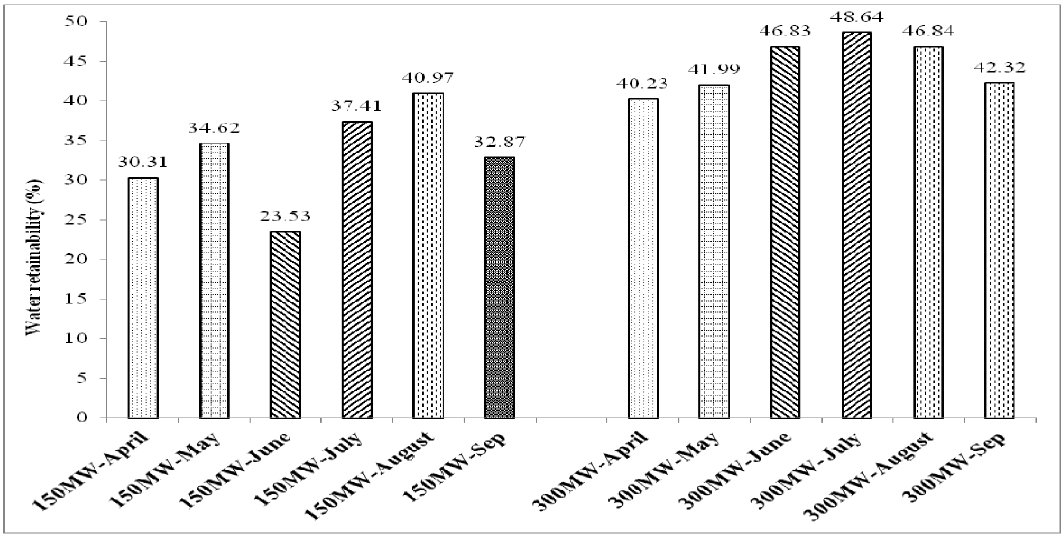

Figure 6: Water retainability of bottom ash from 150MW and 300MW capacity

4. CONCLUSION AND RECOMMENDATION

According to the results above, it can showed that basic properties and water retainability of porous aggregate was significant and necessary for concrete mix design, especially water retainability because the amount of water was very important and effective on performance of concrete.

From the experiment results, it was concluded that basic properties of bottom ash such as gradation, specific gravity, chemical composition and water retainability showed useful and appropriate values, it can also It also showed that bottom ash has the possibility to be used as fine aggregate replacing material due to its properties is comparable to that of natural fine aggregate. Moreover, high water retainabiltiy will show the benefit as internal curing material for concrete.

REFERENCES

Andrade, L. B., Rocha, J. C., & Cheriaf, M., 2009. Influence of coal bottom ash as fine aggregate on fresh properties of concrete. Construction and Building Materials, 23(2), 609-614.

Kasemchaisiri, Ratchayut, and Somnuk Tangtermsirikul., 2007. A method to determine water retainability of porous fine aggregate for design and quality control of fresh concrete. Construction and Building Materials 21.6: 1322-1334.

Andrade, L. B., J. C. Rocha, and M. Cheriaf., 2009. Influence of coal bottom ash as fine aggregate on fresh properties of concrete. Construction and Building Materials 23.2: 609-614.

Bucholc J, Ghafoori N. (1996). “Investigation of lignite-based bottom ash for structural concrete” J Mater Civ Eng, American Society of Civil Engineer; 8(3):128.

Landgren R. Unit weight, specific gravity, absorption, and surface moisture. In: Klieger Paul, Larmond Joseph F., 1994, editors. Significance of tests and properties of concrete-making materials, ASTM STP 169C. Philadelphia: American Society for Testing and Materials; p. 421.

ASTM C136-06., 2004. Standard Test Method for Sieve Analysis of Fine and Coarse Aggregates. Annual Book of ASTM Standards 04.02.

ASTM C128., 2004. Standard Test Method for Density, Relative Density (Specific Gravity), and Absorption of Fine Aggregate. Annual Book of ASTM Standards 04.02

ASTM E1621-94., 2004. Standard Guide for X-Ray Emission Spectrometric Analysis. Annual Book of ASTM Standards 04.02.

Kinaanath Hussain., (2011) “DEVELOPMENT OF A MINIMUM CURING CONCRETE BY INTERNAL CURING PROCESS “Thesis CE-MS. Sirindhorn International Institute of Technology, Thammasat University

EXPERIMENTAL STUDY ON IN-PLANE AND OUT-OF-PLANE BEHAVIOR OF MASONRY WALLETTES RETROFITTED WITH SPECIAL FIBER REINFORCED PAINT

Kenjiro YAMAMOTO[1], Muneyoshi NUMADA[2], and Kimiro MEGURO[3]
[1]Graduate Student, Department of Civil Engineering,
the University of Tokyo, Japan
k-yama@iis.u-tokyo.ac.jp
[2]Assistant Professor, ICUS, IIS, the University of Tokyo, Japan
[3]Director/Professor, ICUS, IIS, the University of Tokyo, Japan

ABSTRACT

Unreinforced masonry buildings (adobe, rubble stone, burned brick, concrete block, etc.) can be damaged easily even by low intensities of ground shaking and be collapsed very rapidly by high intensities. These buildings are common in seismic areas around the world, and have caused heavy casualties in the past earthquakes (Coburn and Spence, 2002). To improve seismic capacity of these weak structures, many methods have been developed. However, most of them are time-consuming and labor-intensive but not attractive as they don't directly increase amenity of the life of residents which slowed down the spread of these methods. In our research group, a much easier new method has been developed using SG-2000, a kind of newly developed paint. (Yamamoto, 2014). In this study we have conducted in-plane and out-of-plane tests to investigate the seismic capacity of this method using SG-2000. Based on the results, wallettes fully coated with SG-2000 have approximately 40 and 30 times larger deformation capacities in cases of in-plane and out-of-plane tests, respectively, than those of the unreinforced masonry wallette. We have also found coating only on the joints between bricks had almost the same efficacy as full coating.

Keywords: *masonry, seismic retrofitting, fiber-reinforced paint*

1. INTRODUCTION

In the last century there were more than 1,100 fatal earthquakes causing a total loss of life exceeding 1.53 million people. From a classification of earthquake deaths by cause during the 20th century, the collapse of masonry buildings is the top cause of the deaths by earthquakes in the world. Besides, much of the increased populations in developing countries will continue to be housed in this type of structure for foreseeable future (Coburn and

Spence, 2002). Therefore, retrofitting low earthquake-resistant structures is the key issue for the reduction of casualties by earthquakes. Also, seismic retrofitting ultimately reduces the costs of recuperating from an earthquake (reduces the cost of rescue and first aid activities, rubble removal, temporary residence building, and permanent residence reconstruction to re-establish normal daily life) (Yoshimura and Meguro, 2004). To retrofit these structures, many seismic retrofitting techniques have been developed so far (Bamboo band, Shotcrete, FRP and so on) (Amiraslanzadeh et al., 2012). However, these techniques need much time and labor, but not attractive for local people because they don't improve the living standards, which has delayed these techniques' spreading in developing countries. Considering these problems, a new retrofitting technique has been suggested using glass fiber reinforced paint (SG-2000). The material needed for this technique is only SG-2000, which significantly reduces the amount of time and labor for retrofitting. Also, paint is usually used to make houses look fine, and many masonry structures are coated in paint. Therefore, SG-2000 can be easily used by local people as the form of paint. The previous experiments in-plane diagonal compression tests and out-of-plane bending tests shows that wallettes partly coated with SG-2000 whose ratio of fiber is 1.5 % achieved larger deformation capacities than unretrofitted wallettes did. Also, with comparative studies, it has been suggested that the amount of paint could be reduced by coating only on the joint of bricks (Yamamoto, 2014).

In this study, in-plane diagonal compression tests and out-of-plane bending tests were conducted using wallettes fully coated with SG-2000. Also, the efficacy of coating in two separate times was investigated. Finally, the failure behavior of wallettes coated only on the joint of bricks was compared with those fully coated to evaluate how much the amount of paint to use can be reduced.

2. AXIAL TENSILE TEST OF SG-2000

Tensile tests were conducted to check deformational capacities and strength of dried SG-2000 whose fiber ratio is 1.5 %. To determine the change of its elasitic modulus, ultimate strain and tensile strength corresponding to its drying period, 3 specimens with drying period of 28days were tested under uniaxial tensile condition with constant rate deformation (2 mm/min). The nominal stress is determined using the cross section of each specimen measured before the test.

From the result, the stress-strain curve is non-linear (Figure 1). Its initial modulus of elasticity was 0.00389 GPa (Table 1). Considering its large deformation capacity, SG-2000 can improve the structure's ductility.

Table 1: Tensile test results of SG-2000

Specimen	Tensile strength (MPa)	Elongation	Initial modulus of elasticity (GPa)
1	0.613	3.71	0.00330
2	0.671	3.63	0.00453
3	0.644	2.79	0.00384
Average	0.642	3.38	0.00389

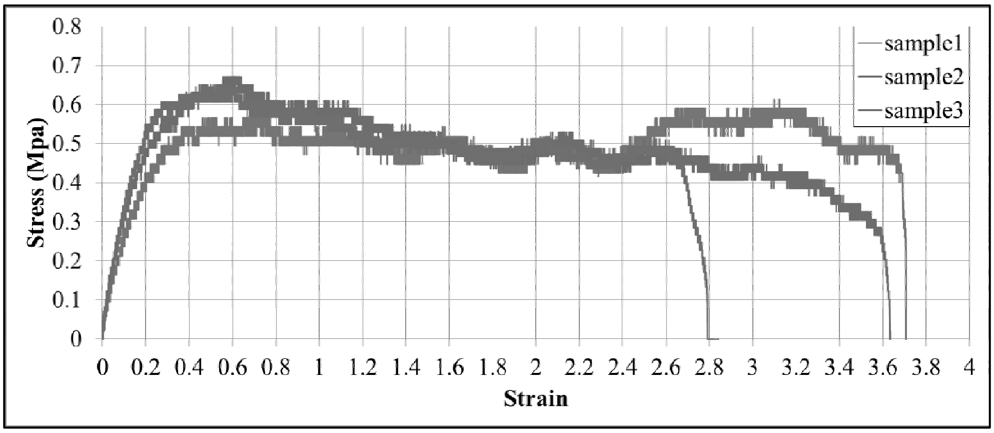

Figure 1: Stress-strain curve for SG-2000

3. IN-PLANE DIAGONAL COMPRESSION TEST

3.1 Test setup

To evaluate the seismic performance of the proposed SG-2000 retrofitting method in in-plane direction, in-plane diagonal compression tests using unreinforced masonry wallettes and those retrofitted with SG-2000 for burnt brick were conducted. The dimensions of wallettes were 277.5 × 282 × 50 mm^3, composed of 7 brick rows of 3.5 bricks each. The mortar joint thickness was 5mm with the C/W ratio 0.14.

Unreinforced specimens (URM) were tested 56 days after the construction. For reinforced specimens were also tested after the same period, but SG-2000 (1.5% ratio of fiber) was painted 28 days after their construction with the thickness in 1mm, and dried for 28 days under the same condition. To evaluate the efficiency of painting, the same amount of paint in two separate times, the specimens were also prepared that were painted 28 days after their construction with half amount of SG-2000, and painted the other half amount 14 days after that, and dried for 14 days again (Figure 2). Also, to evaluate how much paint can be reduced to make the retrofitting cost lower, the specimens that were coated only on the joints of bricks and 5mm around them were prepared (Figure 3). These retrofitted specimens were named in following convention: **A-B. A** indicates the number of times the specimens are painted; **P1**: the whole quantity of paint was used at once, **P2**: half quantity was used and the other half was used 14 days after the first painting. **B** indicates the coated area; **F**: fully coated, **J**: coated only on the joint and 5mm around the joint.

The loading rates were 0.15 mm/min for URM, and 0.25 mm/min for retrofitted specimens to reduce the time of experiment. The previous tests have shown that there is no difference in the results in between these two different loading rates.

3.2 Behavior of retrofitted masonry

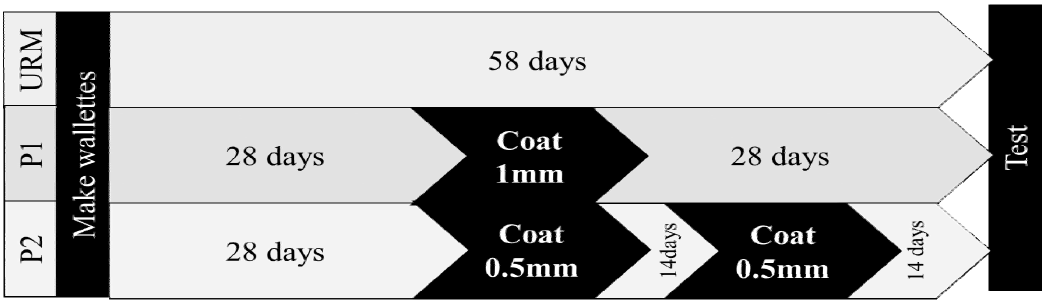

Figure 2: Curing period of each type of specimens

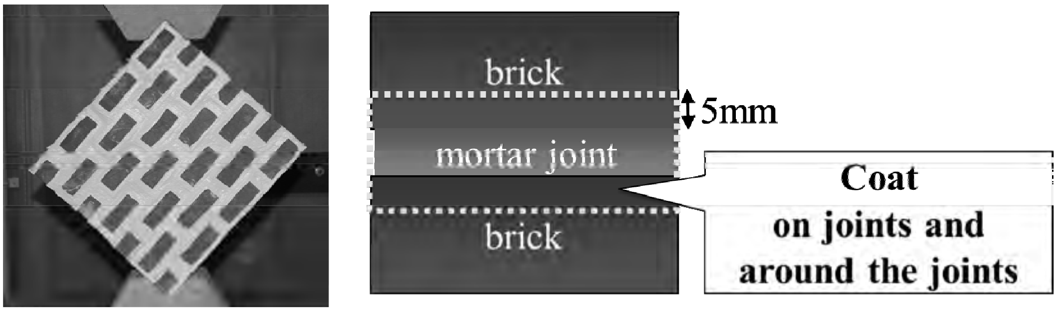

Figure 3: Coating on joints and around the joints

Figure 4 shows URM and P1-F at the end of the test, where the vertical deformations of URM and P1-F were 2mm and 80mm, respectively. Figure 5 shows the diagonal compression strength with vertical deformation for URM and P1-F. URM showed no residual strength after the specimen with compressive strength of 0.55kN made the first cracking. On the other hand, P1-F has connected bricks and produced the residual strength (3.5kN) which is higher than the strength of mortar after the mortar joint had been broken. SG-2000 also changed its crack pattern, which made the strength increase again by shifting the place to be loaded. This effect had been seen until the SG-2000 itself was torn-off. Even after stopping producing residual strength, SG-2000 barely connected bricks. From the failure pattern and the graph, it has been shown that SG-2000 does not increase the masonry structure's initial stiffness, but improves its peak strength, and deformation capacity.

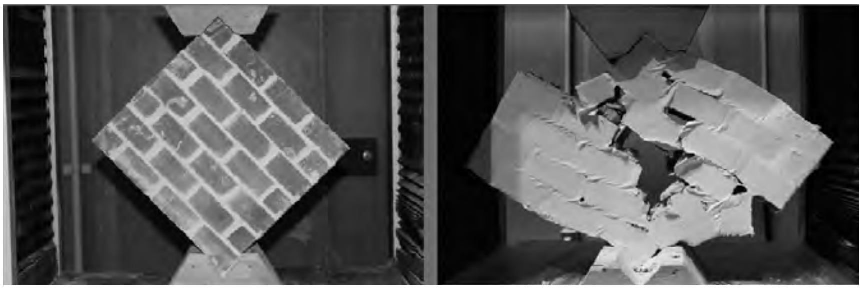

Figure 4: URM and P1-F after the tests

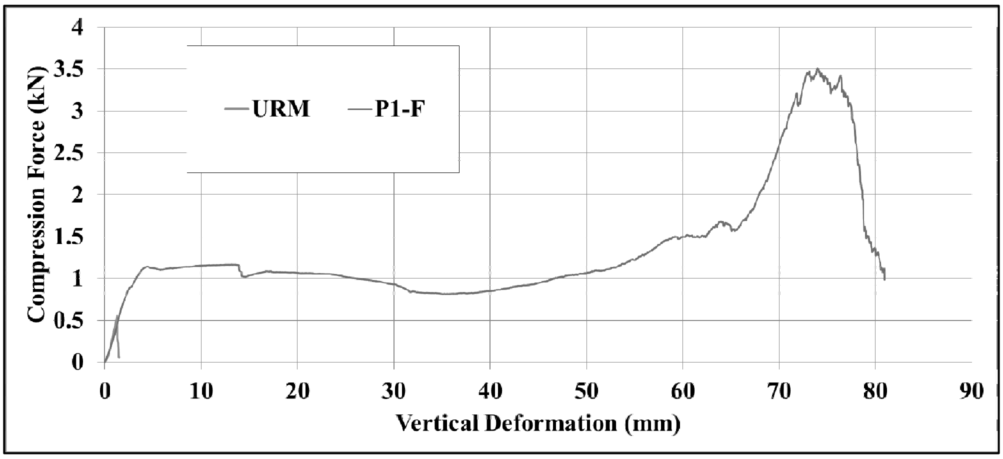

Figure 5: In-plane load-deformation curve

3.3 Efficiency of coating in two separate times

Figure 6 compares the compressive strength and the deformation capacity of P1-F and P2-F. There is not so much difference in deformation and strength between these two.

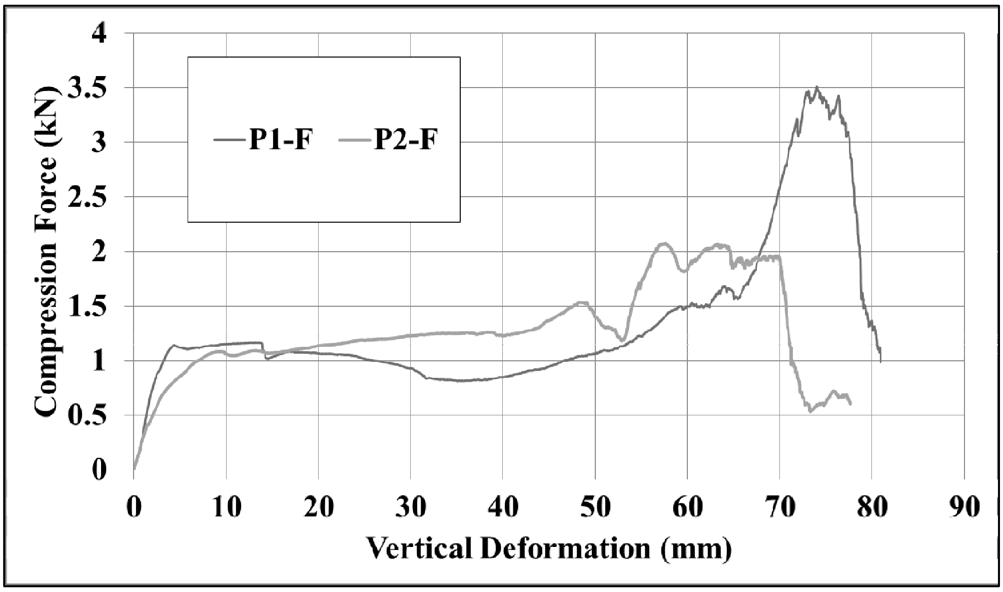

Figure 6: Comparison between P1-F and P2-F

3.4 Seismic capacity of the specimen coated only around the joint of bricks

Figure 7 compares the compressive strength and the deformation capacity of P2-F and P2-J. Some part of paint in P2-J has totally been removed (Figure 8). However, the significant difference of the performances of these two samples was not seen. This indicates that the suggested way in previous research that painting on joints was effective enough to improve the seismic capacity of masonry structure as much as full coating does, and the amount of SG-2000 can be reduced.

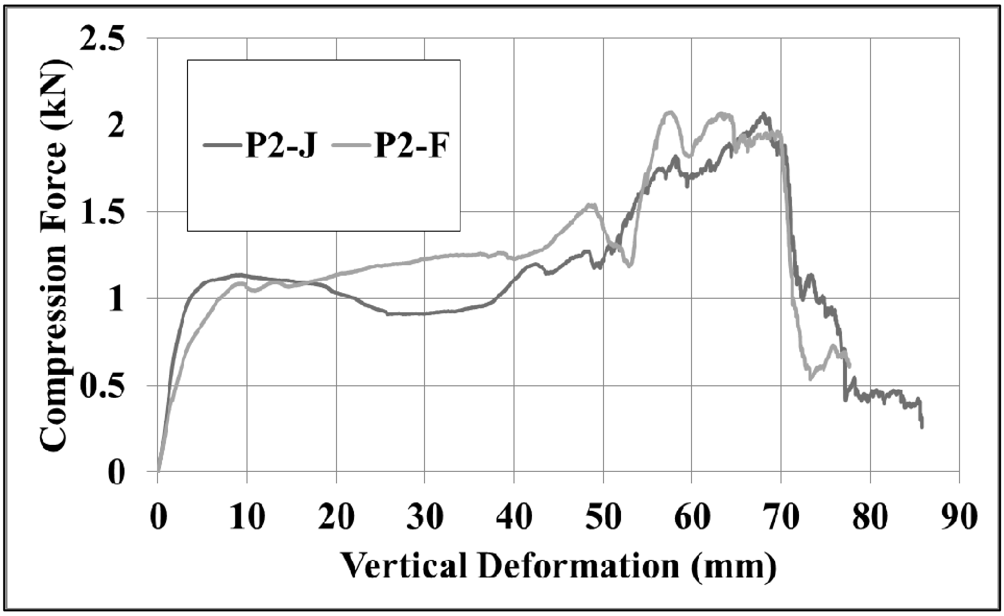

Figure 7: Comparison between P2-J and P2-F

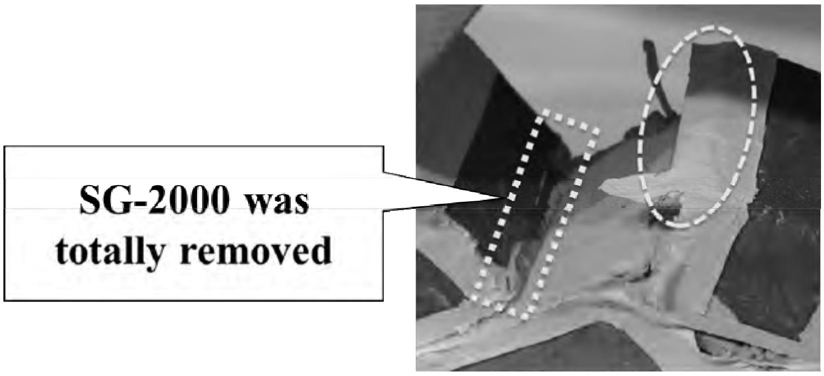

Figure 8: Total removal of SG-2000

4. OUT-OF-PLANE TEST

4.1 Test setup

To investigate the seismic performance of the proposed SG-2000 retrofitting method in out-of-plane direction, out-of-plane tests were conducted comparing unreinforced masonry wallettes and those retrofitted with SG-2000 for burnt brick. The dimensions of wallettes were 475 × 241 × 50 mm^3 , composed of 6 brick rows of 6 bricks each. The mortar joint thickness was 5mm with the C/W ratio 0.25.

Unreinforced specimens (URM) were tested 56 days after the construction. For reinforced specimens were also tested after the same period, but SG-2000 (1.5% ratio of fiber) was painted 28 days after their construction so that they have a 0.5mm layer of SG-2000 coating, and painted the same amount of paint 14 days after the first painting so that the total thickness of SG-2000 layer becomes 1mm, and dried for 14 days again. This type of retrofitted specimen was named like it has been named in the in-plane test: P2-F. The loading rate was 0.15 mm/min.

4.2 Behavior of retrofitted masonry

Figure 9 shows the out-of-plane strength with vertical deformation for URM and P2-F. URM showed no residual strength after the specimen with compressive strength of 0.34kN made the first cracking. On the other hand, P2-F has connected bricks and produced the residual strength after its initial crack has occurred on mortar joints. SG-2000 had been produced the specimens residual strength until the SG-2000 itself was torn-off. Even after stopping producing residual strength, SG-2000 barely connected bricks. From the failure pattern and the graph, it has been shown that SG-2000 does not increase the masonry structure’s initial strength, but improves deformation capacity.

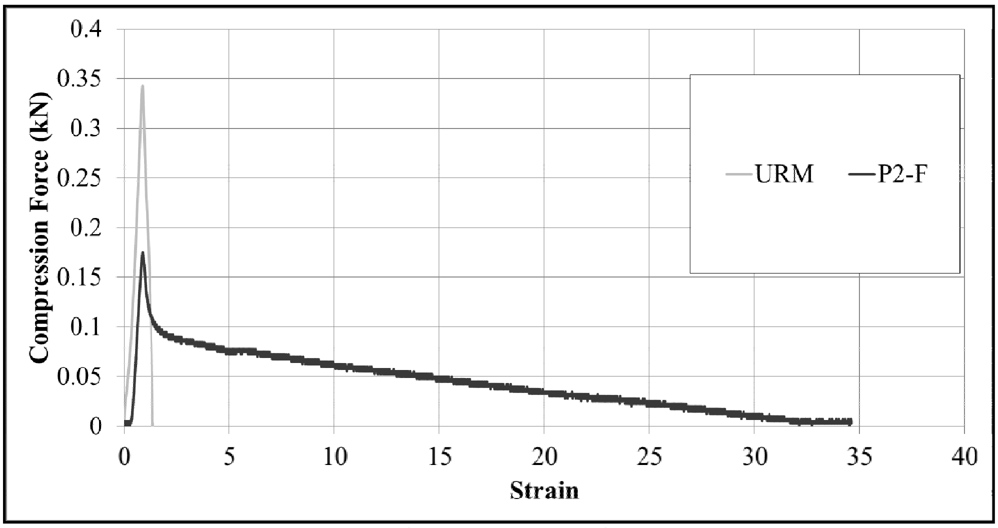

Figure 9: Out-of-plane load-deformation curve

5. CONCLUSIONS

SG-2000 retrofitting method proposed in this study is much easier to retrofit than the previous retrofitting method. The following is the discussion of Tte in-plane diagonal compression tests and out-of-plane tests that were conducted using unreinforced wallettes (URM) and wallettes coated with SG-2000.

The in-plane diagonal compression tests show that:

(i) Retrofitted one showed no difference in initial stiffness, while the increase of initial peak strength was shown. Furthermore, SG-2000 has changed its crack pattern from its initial crack, and generated residual strength after the first crack had occurred only on mortar, and improved the wallette's deformation capacity.

(ii) The retrofitted ones showed approximately 3 times larger initial strength, and produced 7 times larger residual strength than the initial strength of URM. Also, the retrofitted ones showed about 40 times larger deformation than URM.

The out-of-plane tests show that:

(i) Retrofitted one showed no difference in initial stiffness, while the increase of initial peak strength was shown. Furthermore, SG-2000 has generated residual strength after the first crack had occurred only on mortar, and improved the wallette's deformation capacity.

(ii) The retrofitted ones showed residual strength after the initial crack occurred in mortar. Also, the retrofitted ones showed about 35 times larger deformation than URM.

REFERENCES

Coburn, A., and Spence, R. 2002, *Earthquake Protection*, West Sussex: John Wiley & Sons Ltd.

Yoshimura, M., and Meguro, K., 2004. Proposal of Retrofitting Promotion System for Low Earthquake-Resistant Structures in Earthquake Prone Countries. *Proceedings on 13th World Conference on Earthquake Engineering*, Vancouver, Canada.

Amiraslanzadeh, R., Ikemoto, T., Miyajima, M., Fallahi, A., 2012. A Comparative Study on Seismic Retrofitting Methods for Unreinforced Masonry Brick Walls. *Proceedings on 15th World Conference on Earthquake Engineering*, Lisboa, Portugal.

Yamamoto, K., Numada, M., Kimiro, M., 2014, Experimental Study on Seismic Retrofitting of Masonry with Special Fiber Reinforced Paint. *Proceedings on 13th International Symposium on New Technologies for Urban Safety of Mega Cities in Asia*

KNOWLEDGE BASED IT EVACUATION FACILITY MANAGEMENT SYSTEM "COCOA"

Satoshi TAKATSU[1] and Muneyoshi NUMADA[2]
[1] Graduate Student, the University of Tokyo, Japan
s-taka@iis.u-tokyo.ac.jp
[2] Lecturer, ICUS, Institute of Industrial Science,
the University of Tokyo, Japan

ABSTRACT

It was difficult to obtain and share the disaster information for the effective initial responses during the 2011 Great East Japan Earthquake disaster.

For examples, creating a refugee roster was difficult under the conditions of the concentration of a lot of evacuees. And, a lot of inefficient operations to share the information such as the total number of evacuees in each facilities and those personal information, the needs and demands of refugees, etc. were seen in damaged areas.

It is necessary to achieve effective and smooth operations by sharing the information in the disaster headquarters and related administrations. In this study, we have developed the IT evacuation facility system "COCOA" as one of information systems that can manage and support in accordance with conditions of each evacuation facilities by sharing the information such as the needs and demands, the number of evacuees and those personal information. "COCOA" can serve and collect the various personal conditions and manage the information of all evacuation facilities.

"COCOA" can be used in many cases such as staying the evacuation facility, moving to the temporary house, condition of received administrative services and etc.

For the next huge disaster, IT system such as "COCOA" can provide the environments for sharing and managing the personal information and conditions of each evacuation facilities for effective initial responses.

Keywords: *information sharing, administration of the person, evacuation facility, refugee, development of IT system*

2. INTRODUCTION

It is very important that it is performed information sharing at the time of a disaster smoothly in performing management effectively.

For example, if Information sharing is practiced smoothly, it can do clarification and unification of the action, equalization of the supplies supply, effective placement of people, and efficiency of the work, to decrease in mistake and what not. There will be many people saved about these

Therefore I researched an information sharing method of the evacuation facility management in this study. It was difficult to obtain and share the disaster information for the effective initial responses during the 2011 Great East Japan Earthquake disaster.

The reason is no time to read manuals of the evacuation facility management. (Originally manuals did not exist.) , the placement of a volunteer and the staff was difficult, a labor shortage, the setting of the evacuation facility took a long time, the supply and demand of goods did not accord and the situation grasp of each facility is difficult because a transfer with the notebooks.

The new method that is unprecedented to improve these situation is necessary. So, I recommend the introduction of the IT system to perform the information sharing of the evacuation facility smoothly.

2. THE IT SYSTEM TO MANAGEMENT A EVACUATION FACILITY

2.1 IT system

The system which can prepare a thing for refuge beforehand is necessary.
So, I recommended the introduction of the IT system to perform evacuation facility management by using the lesson that I got by East Japan great earthquake disaster smoothly. It can improve the regime not to understand the situation if we do not go to the evacuation facility. And, it can be made by effective and average supply by performing the management of people and the management of supplies with a system. Furthermore, it can make use of a past lesson next. Therefore, it can lighten the burden on city officers and refugees.

There are the following things in the IT evacuation facility system now.

- ORANGE（Ishinomaki City）
    - Safety confirmation system at the time of the disaster
- Victim support system（Nishinomiya City）

  - System for local governments made after The Great Hanshin Earthquake
- IT support system (ISE Ltd.)
  - The system that the doctor of the evacuation facility and the doctor who are in the distant place take the communication using video call application
- Disaster needing people refuge support system (MJC Inc.)
  - Support system is that needing people evacuate smoothly and safely at the time of disaster outbreak
- Refuge guides of the whole country (first media Inc.)
  - Navigation application for disaster that we search the refuge around the present location, and a route guides the route

But, it cannot be said that these systems have utility. The reason is

1. From a problem such as a certain system having many input items, and how to use being difficult, personnel is not a usable thing now. (As for the public employee, a duty place changes in approximately three years.)
2. There are many things which are not updated in nothing more if it was made once. (The situation of the evacuation facility and the environment of the circumference change.)
3. The administration of the person is possible, but the careful management of the evacuation facility is not possible. (It is too late in the situation to think about an administration method after going to each refuge.)
4. There is the system which does not include knowledge of the evacuation facility management and does not know it whether it is utility, and we can really apply it at the time of a disaster.

So, a system with the utility that include knowledge of the disaster prevention and let you really reflect the opinion of a person concerned with the management of the evacuation facility is necessary.

2.2 IT evacuation facility management system "COCOA"

2.2.1 What is “COCOA”

In this study, I developed evacuation facility management system "COCOA" to improve a current problem. The lower image is an illustration of system constitution

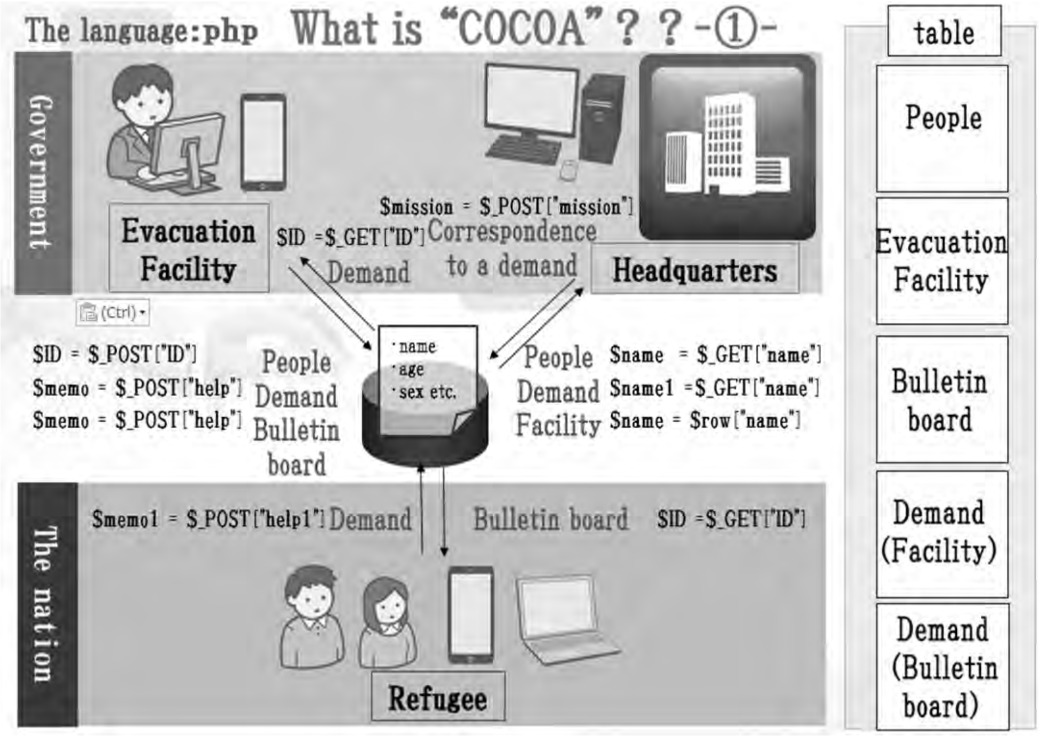

The language:php What is “COCOA” ? ? -①-

```
$mission = $_POST["mission"]
$ID =$_GET["ID"]
$ID = $_POST["ID"]
$memo = $_POST["help"]
$memo = $_POST["help"]
$name = $_GET["name"]
$name1 =$_GET["name"]
$name = $row["name"]
$memo1 = $_POST["help1"]
$ID =$_GET["ID"]
```

Government
Evacuation Facility
Correspondence to a demand
Demand
Headquarters
(Ctrl)
People
Demand
Bulletin board
·name
·age
·sex etc.
People
Demand
Facility
The nation
Demand
Bulletin board
Refugee
table
People
Evacuation Facility
Bulletin board
Demand (Facility)
Demand (Bulletin board)

The language that I used for this development is php and it is structure exchanging the information at five tables. There are the government and the page of the nation each. But, the ID of the evacuation facility uses the same thing to attach correlation. The system is such that I receive the highly confidential thing by a POST.

System in itself made anyone one that it was simple and was plain to make a usable system. For example, the item to tell on page 1 made one.

The data such as the date or the time were in the table automatically to omit trouble of the input.

The lower image is a figure of image of the utilization.

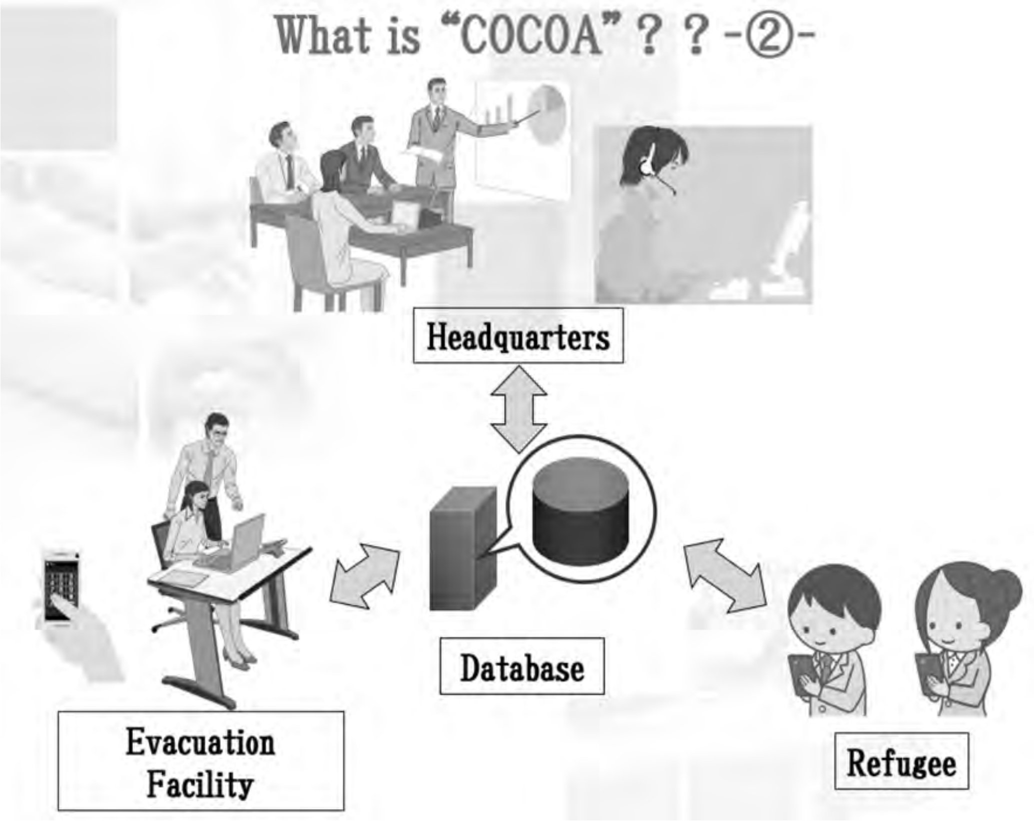

The user uses this system with a PC and a smart phone. It is performed the information sharing through a database. The user can obtain the latest information easily without moving from the place.
The headquarters can know the situation of the current evacuation facility (The number of the refugees, the demand of evacuation facility or necessary supplies) quickly and can take measures.

The manager of the evacuation facility can input refugee information quickly by bringing the information of the person in the database by ID or the name. Then, administration and the management of the person are promoted efficiency. And,

The refugees can send a demand to a refuge manager and see a bulletin board by a system. In this way of supplies are available surely, and a demand becomes easy to be reflected. The manager of the evacuation facility can do the smooth information sharing with the headquarters and the refugee by using the note of a bulletin board and the demand.

It can do the measures before the earthquake disaster are enabled by entering the facilities information (map) of the evacuation facilities and measures based on experience and it which are past into a system.

2.2.2 Real screen of "COCOA"

The lower 3 images are real screen of "COCOA".

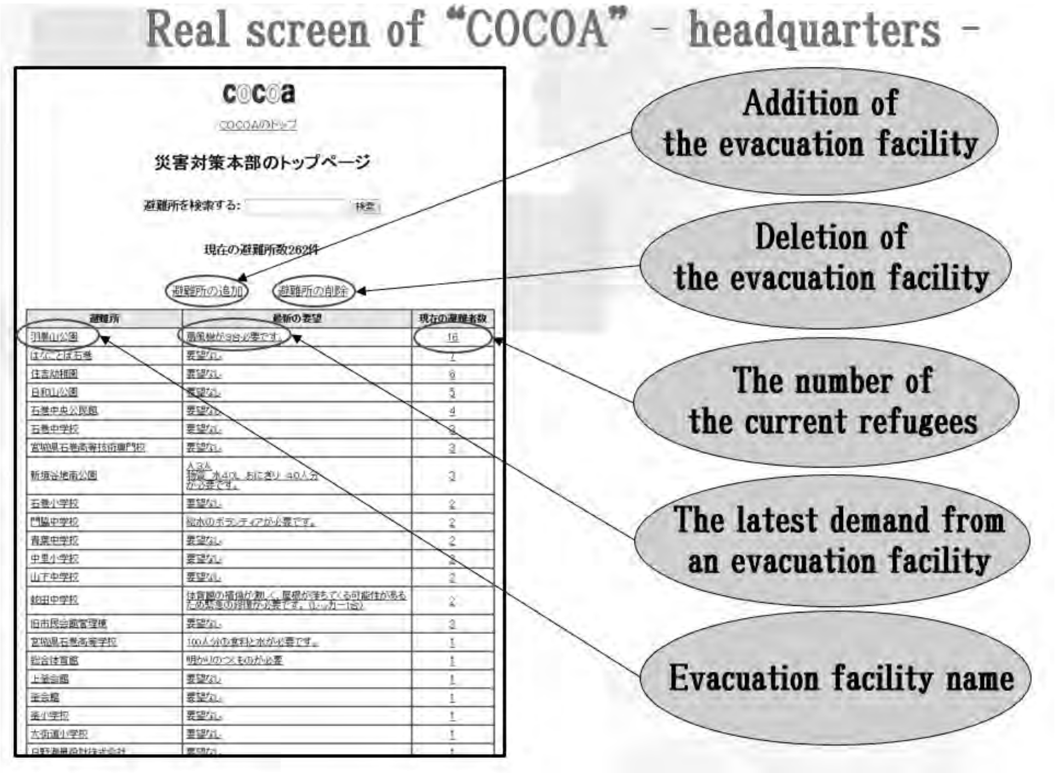
Real screen of "COCOA" - headquarters -

cocoa

COCOAのトップ

災害対策本部のトップページ

避難所を検索する: 検索

現在の避難所数262件

避難所の追加　避難所の削除

避難所	最新の要望	現在の避難者数
羽黒山公園	扇風機が3台必要です。	16
はなことば石巻	要望なし。	7
住吉幼稚園	要望なし。	6
日和山公園	要望なし。	5
石巻中央公民館	要望なし。	4
石巻中学校	要望なし。	3
宮城県石巻高等技術専門校	要望なし。	3
新境谷地南公園	人3人 物資 水40L おにぎり 40人分 が必要です。	3
石巻小学校	要望なし。	2
門脇中学校	給水のボランティアが必要です。	2
青葉中学校	要望なし。	2
中里小学校	要望なし。	2
山下中学校	要望なし。	2
蛇田中学校	体育館の損傷が激しく、屋根が落ちてくる可能性が有るため緊急の修理が必要です。(ロッカー1台)	2
旧市民会館管理棟	要望なし。	2
宮城県石巻高等学校	100人分の食料と水が必要です。	1
総合体育館	明かりのつくものが必要	1
上釜会館	要望なし。	1
釜会館	要望なし。	1
釜小学校	要望なし。	1
大街道小学校	要望なし。	1
[illegible]	要望なし。	1

Addition of the evacuation facility
Deletion of the evacuation facility
The number of the current refugees
The latest demand from an evacuation facility
Evacuation facility name

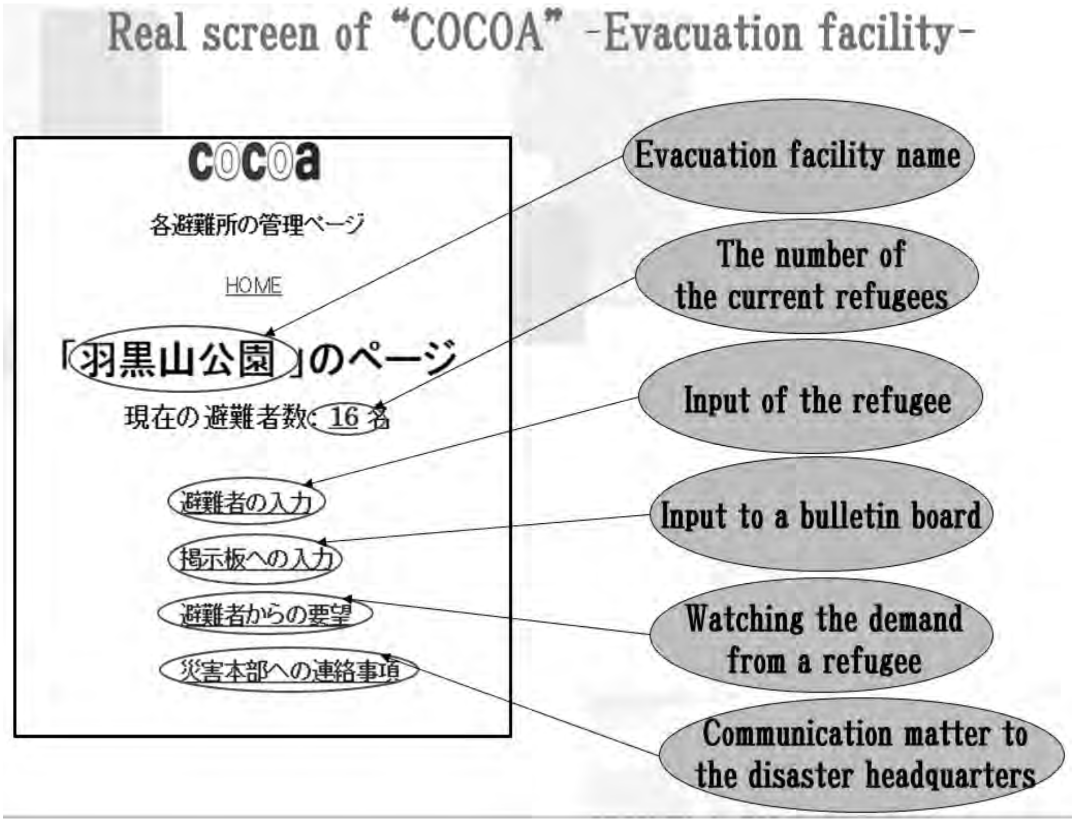
Real screen of "COCOA" -Evacuation facility-

cocoa

各避難所の管理ページ

HOME

「羽黒山公園」のページ

現在の避難者数: 16 名

避難者の入力

掲示板への入力

避難者からの要望

災害本部への連絡事項

Evacuation facility name
The number of the current refugees
Input of the refugee
Input to a bulletin board
Watching the demand from a refugee
Communication matter to the disaster headquarters

“Real screen of “COCOA” - Refugees -

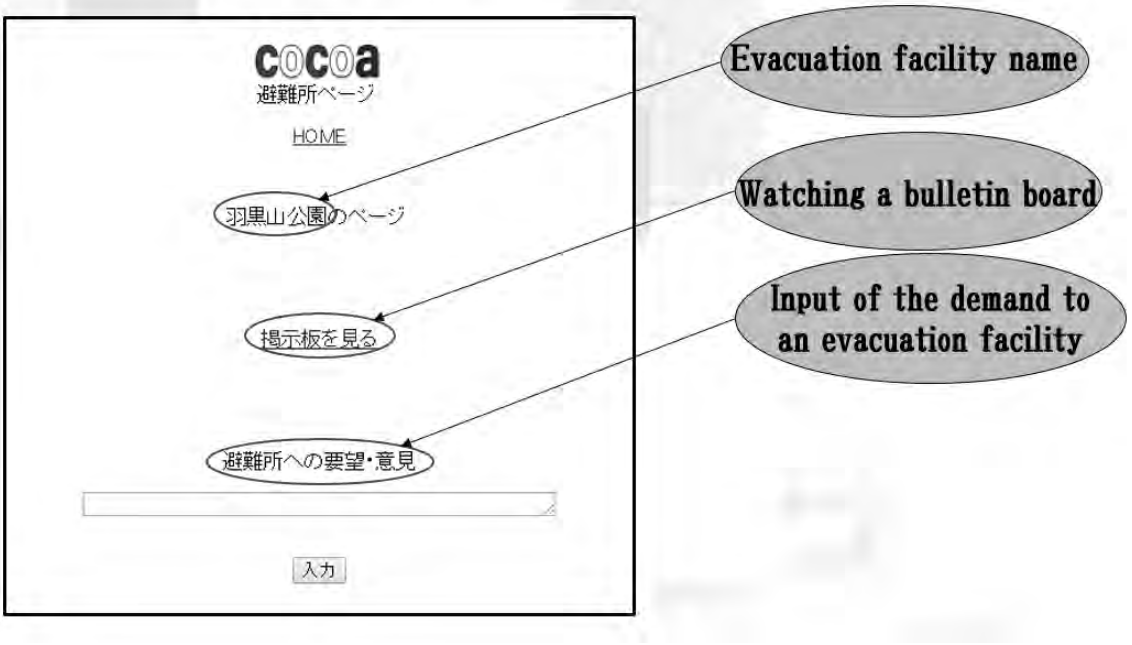
cocoa
避難所ページ
HOME
羽黒山公園のページ
掲示板を見る
避難所への要望・意見
入力
Evacuation facility name
Watching a bulletin board
Input of the demand to an evacuation facility

A basic screen is these 3 screens. The user uses the top page depending on each viewpoint.

Because the basics are simple and are made, each item becomes able to look by double click.

Items in top page of headquarters are Addition of the evacuation facility, Deletion of the evacuation facility, The number of current refugees, The latest demand from an evacuation facility and Evacuation facility name. Items in top page of an evacuation facility are Evacuation facility name, The number of the current refugees, Input of the refugee, Input to a bulletin board, Watching the demand from a refugee and Communication matter to the disaster headquarters.

Items in top page of refugees are Evacuation facility name, Watching a bulletin board and Input of the demand to an evacuation facility. I am going to make a new item to the situation sequentially from now on.

2.2.3 Effect of “COCOA”

The lower 2 images are things which is necessary for evacuation facility management. Red letter is it can manage or can anticipate improvement by using “COCOA”.

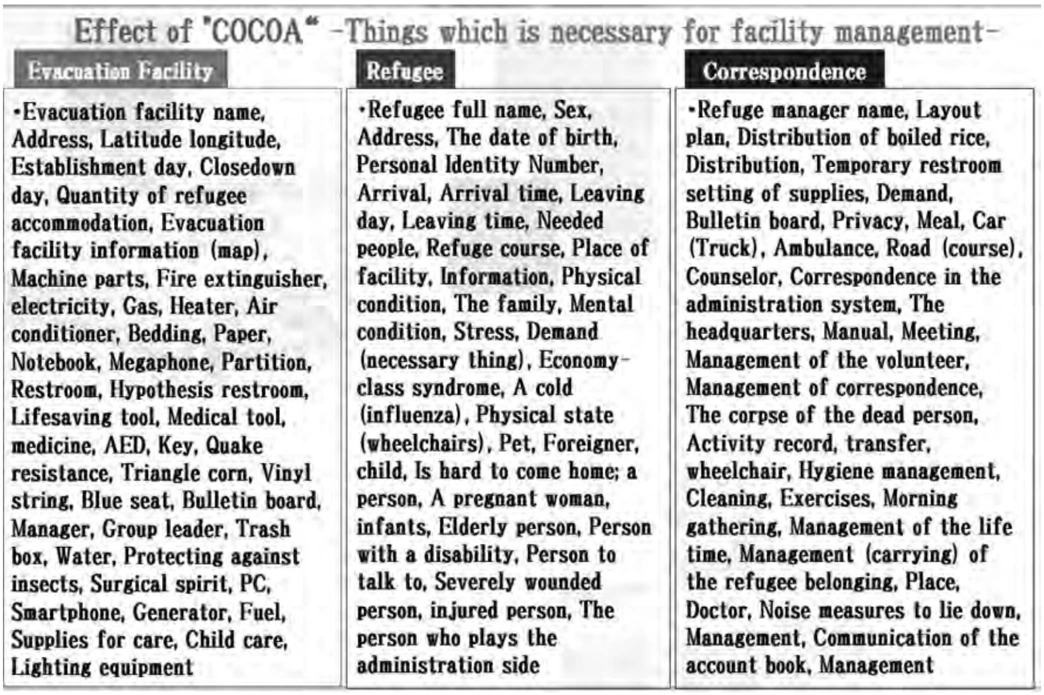

Effect of "COCOA" -Things which is necessary for facility management-

Evacuation Facility	Refugee	Correspondence
•Evacuation facility name, Address, Latitude longitude, Establishment day, Closedown day, Quantity of refugee accommodation, Evacuation facility information (map), Machine parts, Fire extinguisher, electricity, Gas, Heater, Air conditioner, Bedding, Paper, Notebook, Megaphone, Partition, Restroom, Hypothesis restroom, Lifesaving tool, Medical tool, medicine, AED, Key, Quake resistance, Triangle corn, Vinyl string, Blue seat, Bulletin board, Manager, Group leader, Trash box, Water, Protecting against insects, Surgical spirit, PC, Smartphone, Generator, Fuel, Supplies for care, Child care, Lighting equipment	•Refugee full name, Sex, Address, The date of birth, Personal Identity Number, Arrival, Arrival time, Leaving day, Leaving time, Needed people, Refuge course, Place of facility, Information, Physical condition, The family, Mental condition, Stress, Demand (necessary thing), Economy-class syndrome, A cold (influenza), Physical state (wheelchairs), Pet, Foreigner, child, Is hard to come home; a person, A pregnant woman, infants, Elderly person, Person with a disability, Person to talk to, Severely wounded person, injured person, The person who plays the administration side	•Refuge manager name, Layout plan, Distribution of boiled rice, Distribution, Temporary restroom setting of supplies, Demand, Bulletin board, Privacy, Meal, Car (Truck), Ambulance, Road (course), Counselor, Correspondence in the administration system, The headquarters, Manual, Meeting, Management of the volunteer, Management of correspondence, The corpse of the dead person, Activity record, transfer, wheelchair, Hygiene management, Cleaning, Exercises, Morning gathering, Management of the life time, Management (carrying) of the refugee belonging, Place, Doctor, Noise measures to lie down, Management, Communication of the account book, Management

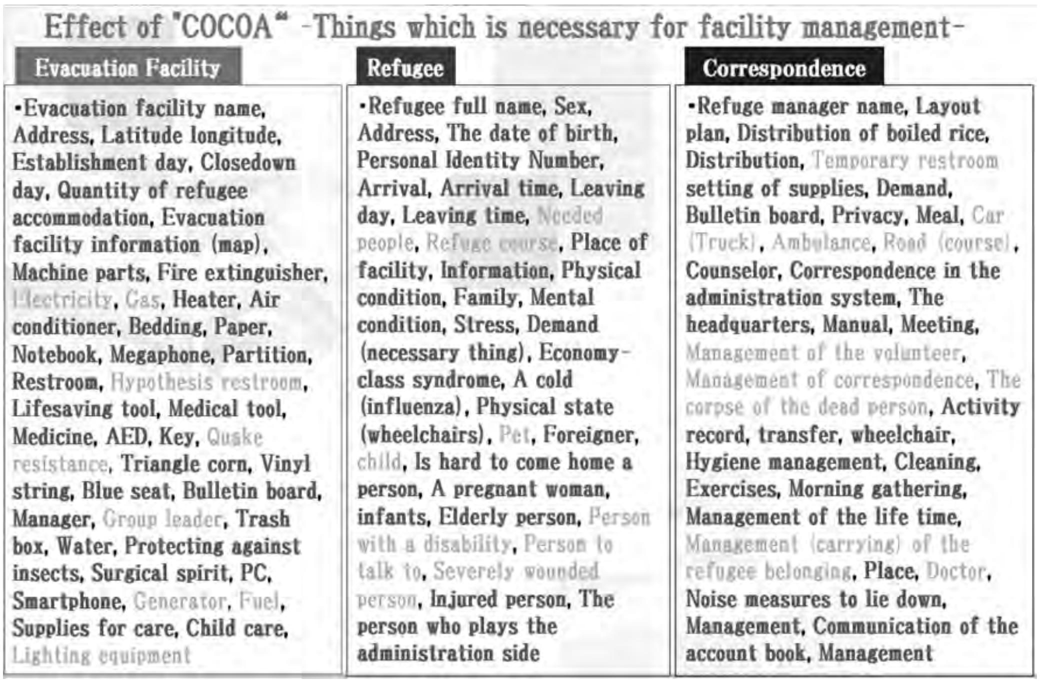

Effect of "COCOA" -Things which is necessary for facility management-

Evacuation Facility	Refugee	Correspondence
•Evacuation facility name, Address, Latitude longitude, Establishment day, Closedown day, Quantity of refugee accommodation, Evacuation facility information (map), Machine parts, Fire extinguisher, Electricity, Gas, Heater, Air conditioner, Bedding, Paper, Notebook, Megaphone, Partition, Restroom, Hypothesis restroom, Lifesaving tool, Medical tool, Medicine, AED, Key, Quake resistance, Triangle corn, Vinyl string, Blue seat, Bulletin board, Manager, Group leader, Trash box, Water, Protecting against insects, Surgical spirit, PC, Smartphone, Generator, Fuel, Supplies for care, Child care, Lighting equipment	•Refugee full name, Sex, Address, The date of birth, Personal Identity Number, Arrival, Arrival time, Leaving day, Leaving time, Needed people, Refuge course, Place of facility, Information, Physical condition, Family, Mental condition, Stress, Demand (necessary thing), Economy-class syndrome, A cold (influenza), Physical state (wheelchairs), Pet, Foreigner, child, Is hard to come home a person, A pregnant woman, infants, Elderly person, Person with a disability, Person to talk to, Severely wounded person, Injured person, The person who plays the administration side	•Refuge manager name, Layout plan, Distribution of boiled rice, Distribution, Temporary restroom setting of supplies, Demand, Bulletin board, Privacy, Meal, Car (Truck), Ambulance, Road (course), Counselor, Correspondence in the administration system, The headquarters, Manual, Meeting, Management of the volunteer, Management of correspondence, The corpse of the dead person, Activity record, transfer, wheelchair, Hygiene management, Cleaning, Exercises, Morning gathering, Management of the life time, Management (carrying) of the refugee belonging, Place, Doctor, Noise measures to lie down, Management, Communication of the account book, Management

It cannot cover all when you watch an image. But, can cover about the 80% of the things which is necessary for evacuation facility management in COCOA.

The lower image is the calculation result of system effect.

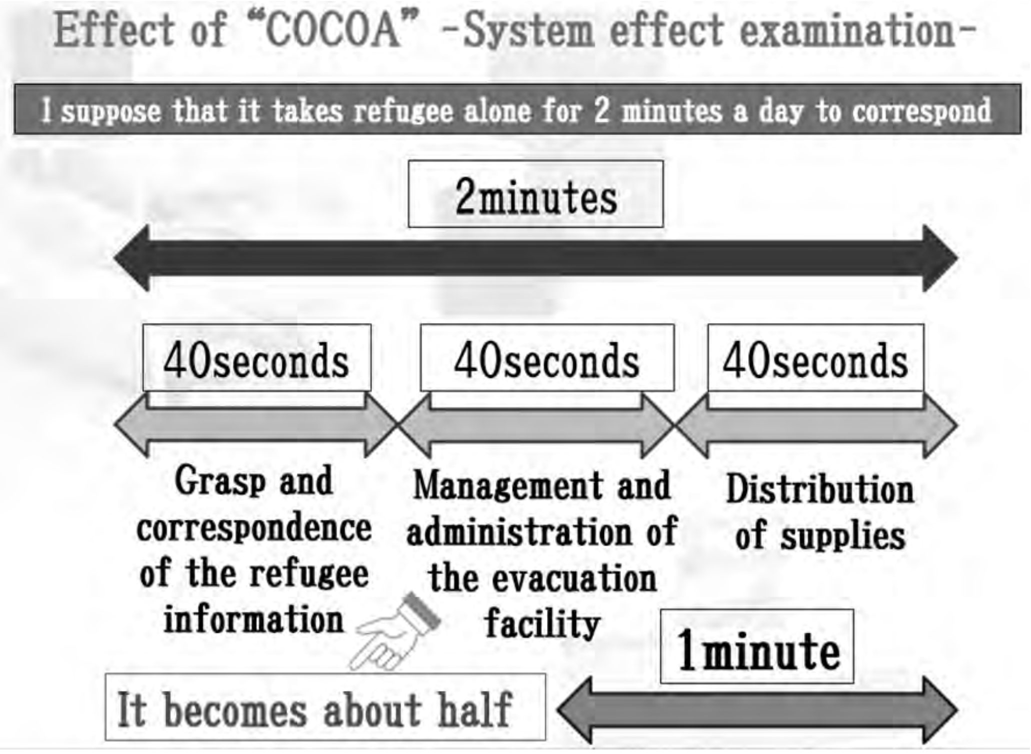
Effect of "COCOA" -System effect examination-
I suppose that it takes refugee alone for 2 minutes a day to correspond
2minutes
40seconds
40seconds
40seconds
Grasp and correspondence of the refugee information
Management and administration of the evacuation facility
Distribution of supplies
1minute
It becomes about half

I suppose that it takes refugee alone for 2 minutes a day to correspond. And, I assigned Grasp and correspondence of the refugee information, Management and administration of the evacuation facility and Distribution of supplies each with by 40 seconds.

I can anticipate the improvement of 3 items (Grasp and correspondence of the refugee information, Management and administration of the evacuation facility and Distribution of supplies) by using cocoa.

When I think that there are many parts which a person must manage directly, I suppose the time that evacuation facility management takes becomes about half by using "COCOA".

The lower image is the graph of calculation result.

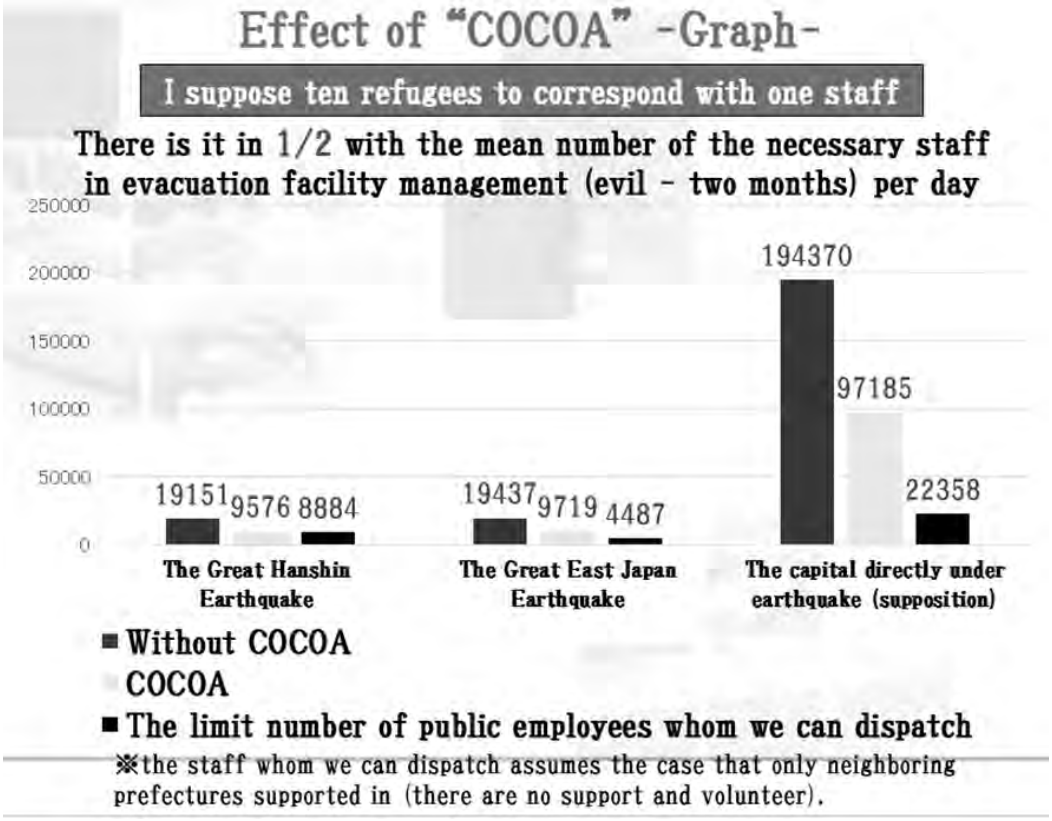

※the staff whom we can dispatch assumes the case that only neighboring prefectures supported in (there are no support and volunteer).

I suppose ten refugees to correspond with one staff. When we look in three items (The Great Hanshin Earthquake, The Great East Japan Earthquake, The capital directly under earthquake (supposition)), there is the effect of the cocoa by all earthquakes. And, there is it in 1/2 with the mean number of the necessary staff in evacuation facility management (evil - two months) per day.

When we look the limit number of public employees whom we can dispatch, we understand that the number of staffs is still insufficient.

So, it is revealed that it must make up for a labor shortage by volunteers.
But, “COCOA” can improve the current situation. And, the situation that must use the IT system even immediately includes it.

3. CONCLUSION

It is necessary to achieve smooth information sharing at the time of the disaster. When I have researched to refuge administration, there are the sudden things, and information sharing did not go well by the East Japan great earthquake disaster.

So, I recommend the information sharing method by the IT. But, a certain system cannot cover all important points of the refuge administration by it now. Therefore, I have developed knowledge based IT evacuation facility management system "COCOA". Using it to be able to share the information more smoothly. This system are characterized by a human being studying disaster prevention is concerned from the development of the program. So, we can develop a system with the utility.

But, the development such as the new systems of the volunteer is necessary because we cannot manage all "only COCOA". So, we want to develop such a system too.

In the end, the coming times need management of the information by the IT as a new way.

REFERENCES

Ishinomaki ward office, 2011. *Facility management document,* City officer, Ishinomaki, Japan.

Ishinomaki City General Affairs Department Crisis Measures Section, *ORANGE*, Ishinomaki City, Japan.

Nishinomiya City Center for Information Technology, 1997, *Victim support system*, Nishinomiya City, Japan.

ISE Ltd., *Effective working papers of the IT system in the refuges at the time of the disaster,* ISE Ltd, Japan.

MJC Inc., 2015, *Disaster needing people refuge support system*, MJC Inc., Japan.

President-director Kaichi Yamazaki, 2015, *It supports Apple Watch! Disaster prevention information "whole country refuge guide" Ver.5.3*, first media Inc., Japan.

Cabinet Office, 2011, *about a change of the number of the refuge dwellers of the East Japan great earthquake disaster*, Japan.

Orient economic online editorial department, 2014, *Latest "public employee yearly income ranking" top 500*, Japan.

Local public entity capacity management meeting for the study, 2012, *a present conditions, analyses sheet such as the number of the staffs by the reference index*, Japan

Student Report

Impressions from the Student Participants

The Joint Seminar on Civil Infrastructures was the first international conference in my life. This seminar gave me a precious opportunity to discuss with people who have different background.

In this seminar, I experienced and leaned many things that I had not done before going and taking this seminar. And, the communication with students who came from different countries was valuable for me and increased my motivation to learn. I hope to proceed with my research based on the things which I obtain in this seminar. Lastly, I want to express my gratitude to people related to this seminar. **(by Koki Satsukawa)**

The Student Seminar was the first international conference in my life that I participated in as a presenter. I learned how difficult it was to tell one's thing that I wanted to convey to audience by this seminar clearly briefly. It was different in how to make and how to convey PowerPoint and watched it by the difference of a country and the school and was very interesting for me. It was very stimulating for myself with a little overseas experience that I was able to give presentation while learning the characteristic of the country in Thailand. And, what was able to interchange with a student of Thai and Korea which could not usually interchange was very valuable and I was glad. I'm looking forward to joining Student Seminar again. **(by Satoshi Takatsu)**

This seminar was the second international conference for me, after USMCA 2014. The place we have presented was not as large as that of USMCA, and the amount of participants was very small. Therefore, I think this seminar was the best place for students who have joined international conference for the first time to practice having a presentation there. Also, it was nice place to become friends with students from other countries. For me, this experience was vital for the next USMCA 2015, held in Nepal. **(by Kenjiro Yamamoto)**

This was the first time for me to join such an international conference. Making presentation in English is a little tough for me, but this seminar was a very good chance to practice it. Through seminar, my professor and my senior students advised me about my research, and I had some chances to talk with foreign students from Thailand, Korea, and Laos. From them, I learned not only how to research and how to express the study but also foreign cultures and values. My research is on the way now, so I'll try to brush it up to achieve better results. Unfortunately, we couldn't join the field trip, but I had a very good time there. I appreciate the effort and work by everyone who organized and supported this great seminar. **(by Riko Sakata)**

Participating in the Student Seminar held at the Chulalongkorn University was a great opportunity to share my research to other students and to practice my presentation skills. Through presenting to an audience from a wide variety of fields, I was able to learn how to clearly state the contents of my research in an easy to understand flow. It was also an opportunity to learn research from a different department; being from the urban engineering department, it was especially interesting for me to learn about researches related to civil engineering. I was also able to receive valuable advice from other professors, enabling me to further improve my research. Unfortunately, due to unexpected events, we Japanese students were not able to be part of the tour. Yet, it was a valuable experience visiting Thailand and comparing the different layout of the city between Japan and Thailand. **(by Yuto Tokumitsu)**

I am honored to be able to participate The 7th International Joint Student Seminar on Civil Infrastructure in Bangkok, Thailand. It was the first time I have been and I could have many precious experiences there. All of presentations gave me so many stimulus and I was happy that I was able to exchange with participants. Needless to say, there is a sense to continue like this seminar, so I hope the seminar will be annual event. **(by Yuki Munemasa)**

Attending the join student seminar on Civil Infrastructure in Bangkok, Thailand is a great opportunity for me to propose my research and get feedback for improving my research. In this seminar, there are various kinds of researches related to civil works. Since participants with students and professors were gathered from many countries and many backgrounds as well, it was very useful for researchers who are interesting to know other researches including problems and solutions, and exchange the ideals. In this opportunity, I would like to sincerely thank organizers and attendees to meet successful seminar among the unexpected accident in Bangkok. Also I would like to thank all committees to give me for excellent presentation award. Hopefully, this activity will be continuously held as a great chance for assembling among students and professors. **(by Tanakorn Sritarapipat)**

Firstly, I would like to express my gratitude to everyone who are involved in this seminar. Thanks to those concerned, the seminar was finished successfully in spite of the bad security due to bomb explosion. It was precious experience for me to make an English presentation because I’ve never tried before. Through this seminar I was able to get to know and learn a lot of things, not only how to prepare for international conferences, but also various kinds of fields in civil engineering, or the culture like food traditionally eaten in Thailand. In addition, communication with other students motivated me to study more, and made me think that I’d like to be the one who can make good impact on others. I would like to join this seminar again if I have chance, and hope next seminar will be held in a safe place. Again, thank you for all to manage and organize this great seminar. **(by Koji Tanaka)**

The Joint Student Seminar on Civil Infrastructures provided me with a good opportunity to share my research works and practice making presentations. The other presentations were from a wide variety of fields, which gave me the chance to learn about different areas in civil engineering. I was fortunate to have the opportunity to discuss with Korean and Japanese professors about my presentation, also is a part of my thesis, and received many useful advices.

Thanks to several discussions at this seminar, I again realize the importance of communication with researchers. Lastly, I would like to express my profound gratitude and appreciation to the professors and students from the other universities as well as the staff related to this seminar. **(by Cao Nguyên Thi)**

The 7th Joint Student Seminar on Civil Infrastructures was held at the Sasa international house, Chulalongkorn University, Thailand on the 19th of August, 2015. It gave me a good opportunity and new experience in the seminar stage. In this seminar, I was presenter and shared my research project to the other presenters. All presenters had difference of interested topic and I got a lot of new knowledge from them. In addition, I have known many kindly friends and we talked about changing our culture. Finally, I am so thank you to the seminar to organize the good seminar like this. I am looking forward to join this seminar again. **(by Noulananh Lathsolulin)**

I had a great time when I attended the Joint Student Seminar on Civil Infrastructures held at the Sasa international house in Thailand. I had my presentation in English in front of many foreigners for the first time and also I was able to listen to various presentations of other foreign student. Until I am bachelor now, but it was great experience to me. Maybe this experience can be make me more strong. And, I want to thank all of people attended this seminar for giving me a chance to have wonderful memories in Thailand. I hope this Joint Student Seminar will be activated and held continuously. **(by Jinwoo PARK)**

This is my first international seminar and first visit to first presentation to people who belong to other universities. The topic of my presentation was Site Selection of Potential Railway Route for Supporting Dawei Deep-Sea Port. Case study : tambon Ban Kao Amphoe Mueang of Kanchanaburi Province in Thailand. I learned that the most important thing when presenting is to make listeners understand what you want to say. I want to make good use of these experiences and keep studying. I wish to express my gratitude to those people related to this seminar. I got a lot of stimulation from this seminar and would like to use this experience towards my future activities. **(by Rattanawadee Dutsadeesuntornsakun)**

7th Joint Student Seminar on Civil Infrastructures

Venue: Sasa International House (Room: Dipak C. Jain), Chulalongkorn University
Date: 19-20 August 2015

Page 1

Time	Topic	Name of speaker
08.00-08.30	Registration	-
08.30-08.40	Opening remarks	Dr. Yudai Honma, ICUS
08.40-09.00	Group photo & Coffee break	
Invited Professor Section (chair: Dr. Hyunmyung Kim, Myong Ji University)		
09.30-10.00	Introduction to mathematical analysis for next-generation vehicle	Keynote Japan Dr. Yudai Honma
10.00-10.30	Water leak prevention at connections of precast concrete panels with butyl rubber	Keynote Thai Dr. Withit Pansuk
10.30-11.00	Near-real time meteorological drought monitoring and early warning system for croplands in Asia	Keynote Japan Dr. Wataru Takeuchi
Student Presentation 1: Civil Engineering Section (chairs: Dr. Yudai Honma, The University of Tokyo)		
11.00-11.15	Building classification in urban area in Yangon, Myanmar using stereo high resolution images and night time light data	Tanakorn SRITARAPIPAT (Japan, UTokyo)
11.15-11.30	Experiment and simulation study on flexural behavior of reinforced concrete slab before and after fire	Nguyen Thi CAO (Thai, CU)
11.30-11.45	The key index for rational bridge maintenance by municipalities in Japan	Riko SAKATA (Japan, UTokyo)
11.45-12.00	Effect of free LIME content on mechanical properties of cement-fly ash mixtures	Adnan Nawaz (Thai, TU)
Lunch		
Student Presentation 2: Transportation Section (chairs: Dr. Wonho Suh, Hanyang University)		
13.00-13.15	The relationship between the rainfall intensity and the subway passenger ridership in the Seoul metropolitan subway system	Kyoung-seon PARK (Korea, Myong-Ji U)
13.15-13.30	Factors affecting the severity of motorcycles accidents and casualties in Thailand by using probit and logit model	Santosh BARAL (Thai, AIT)
13.30-13.45	Optimum assignment of housings and jobs with constrained capacity considering discomfort and travel costs	Yuki MUNEMASA (Japan, UTokyo)
13.45-14.00	Factors influencing red light running behavior: a study of socio-economic characteristics and geometry of intersections	Auearree JENSUPAKARN (Thai, AIT)
14.00-14.15	The optimum traffic volume survey locations for the travel demand analysis in Korea	Seong-min KANG (Korea, Myong-Ji U)
14.15-14.30	Site selection of potential railway route for supportingdawei deep-sea port. Case study : Tambon Ban Kao Amphoe mueang of Kanchanaburi province	Rattanawadee DUTSADEESUNTORNSAKUN (Thai, SWU)
14.30-14.45	Numerical evaluation of road disconnection risk focusing on road collapsing after a large earthquake in Chigasaki city, Kanagawa	Yuto TOKUMITSU (Japan, UTokyo)
14.45-15.00	Image processing techniques for vehicles and pedestrian safety evaluation	Jinwoo PARK (Korea, Hanyang U)
Coffee Break		

7th Joint Student Seminar on Civil Infrastructures

Venue: Sasa International House (Room: Dipak C. Jain), Chulalongkorn University
Date: 19-20 August 2015

Page 2

Student Presentation 3: Technical Section (chairs: Dr. Wataru Takeuchi, The University of Tokyo)		
15.30-15.45	Ageing effect induced by particle movement	Koji TANAKA (Japan, UTokyo)
15.45-16.00	An analysis of network throughputs for different origin-destination patterns	Koki SATSUKAWA (Japan, UTokyo)
16.00-16.15	Water retainability and basic properties of coal bottom ash used as fine aggregate replacing material	Noulananh LATHSOULIN (Thai, TU)
16.15-16.30	Experimental study on in-plane and out-of-plane behavior of masonry wallettes retrofitted with special fiber reinforced paint	Kenjiro YAMAMOTO (Japan, UTokyo)
16.30-16.45	Knowledge based IT evacuation facility management system "COCOA"	Satoshi TAKATSU (Japan, UTokyo)
16.45-17.15	Review comment Closing remarks	
18.00	Dinner at Sasa International House, Presentation Award Excellence Presenter Ceremony	

Thai 6 speakers (AIT 2, Chula 1, Thammasart 2, Srinakharinwirot 1)
Korea 3 speakers (Myong Ji Univ. 2, HanYang Univ 1)
Japan 8 speakers (University of Tokyo 8)
Total no. 17 speakers

***10 minute presentation and 5 minute discussion**

REPORT FROM STUDENT PARTICIPATION ON 7th JOINT STUDENT SEMINAR ON CIVIL INFRASTRUCTURE

DATE: August 19, 2015

The 7th Joint Student Seminar on Civil Infrastructure was scheduled to be consisted of an in-house seminar and a tour of several sites, but because of unexpected events, this year’s tour was unfortunately cancelled. The in-house Seminar was held at Dipak C. Jain Room, SASA International House, Chulalongkorn University, on August 19, 2015. The seminar was mainly divided into 3 parts; the lectures by invited professors, student presentations, and dinner combined with the Presentation Award Excellent Presenter Ceremony.

Sasa
INTERNATIONAL HOUSE
หอพักนานาชาติ ศศนิเวศ
BANGKOK
NEW YORK
LONDON
Sasa

Pictures of the Sasa International House

PRESENTATION SESSION

OPENING REMARKS

Before the lectures by the invited professors, Dr. Yudai Honma from the University of Tokyo gave the opening remarks to start up the seminar. He first expressed his gratitude towards all who were involved in arranging, and then offered his special thanks to each of the other professors. He then went on to emphasize that the seminar was an opportunity to share research and help each other, which will improve each of the participants' works. He ended his remarks by also mentioning that becoming accompanied with other students was as important.

INVITED PROFESSORS

Three lectures were given in the invited professors section, chaired by Dr. Hyunmyung Kim Myon from the Ji University.

First, Dr. Yudai Honma from the University of Tokyo gave his lecture titled "Introduction to mathematical analysis for next-generation vehicle". Focusing on fuel-cell powered cars as the next-generation vehicle, he introduced a method to efficiently plan the number of hydrogen stations and gasoline-hydrogen combined stations to smoothly shift from using conventional cars to using fuel-cell powered cars.

Next, Dr. Withit Pansuk from the Chulalongkorn University gave his lecture on "Water leak prevention at connections of precast concrete panels with butyl rubber". After explaining the issue on the difficulty of connecting rubber to concrete and the seeping of water into the cracks between the materials, he introduced butyl rubber, a material easy to supply which chemically bonds to concrete creating a strong connection, as a possible solution.

Last, Dr. Wataru Takeuchi from the University of Tokyo lectured on "Near-real time meteorological drought monitoring and early warning system for croplands in Asia". He lectured that by using remote sensing technology, meteorological patterns can be monitored to estimate oncoming draughts and issue warnings beforehand.

STUDENT PRESENTATIONS

15 speakers from Chulalongkorn University (Thai), Thammasart University (Thai), Srinakharinwirot University (Thai), Myonig Ji University (Korea), Han Yang University (Korea), and the University of Tokyo (Japan) presented and shared on various topics. Presentations were divided in to the Civil Engineering Section, the

Transportation Section, and the Technical Section, each chaired by Dr. Yudai Honma, Dr. Wonho Suh, and Dr. Wataru Takeuchi, respectively.

CLOSING REMARKS

To close the seminar, closing remarks were given by Dr. Hyunmyung Kim from the Myong Ji University. After explaining the history of the joint seminar, he commented that the seminar has increasingly become better and better by each seminar, and that the student presentations were well prepared and well presented. He also commented to take the experience and use it to further develop academic and international abilities.

PRESENTATION AWARD CEREMONY

In the evening after the seminar, a dinner banquet was held in which students further discussed their research as well as becoming acquainted with one another. During the banquet, 3 were announced and awarded with the Excellent Presentation Award with the professors as judges. The presenters were chosen according to criterion such as research quality, presentation abilities, and question answering. The following students were awarded with the Excellent Presentation Awards.

1. Mr. Yuto Tokumitsu, University of Tokyo (Numerical evaluation of road disconnection risk focusing on road collapsing after a large earthquake in Chigasaki city, Kanagawa)
2. Mr. Tanakorn Sritarapipat, University of Tokyo (Building classification in urban area in Yangon, Myanmar using stereo high resolution images and night time light data)
3. Mr. Yuki Munemasa, University of Tokyo (Optimum assignment of housings and jobs with constrained capacity considering discomfort and travel costs)

Excellent Presenters: (from left to right) Yuto Tokumitsu, Tanakorn Sritarapipat, Yuki Munemasa

International Center for Urban Safety Engineering
Institute of Industrial Science, The University of Tokyo
4-6-1 Komaba, Meguro-ku,
Tokyo 153-8505, Japan

Tel: +81-3-5452-6472
Fax: +81-3-5452-6476
http://icus.iis.u-tokyo.ac.jp
E-mail: icus@iis.u-tokyo.ac.jp

ISBN4-903661-74-1